



UNIVERSITY OF
BIRMINGHAM

Exploring nucleophilic nitrenoid reactivity to access complex imidazolyl heterocycles

By

Elsa Martínez Arce

A thesis submitted to the University of Birmingham
for the degree of DOCTOR OF PHILOSOPHY

School of Chemistry
College of Engineering and Physical Sciences
University of Birmingham
October 2018

UNIVERSITY OF
BIRMINGHAM

University of Birmingham Research Archive

e-theses repository

This unpublished thesis/dissertation is copyright of the author and/or third parties. The intellectual property rights of the author or third parties in respect of this work are as defined by The Copyright Designs and Patents Act 1988 or as modified by any successor legislation.

Any use made of information contained in this thesis/dissertation must be in accordance with that legislation and must be properly acknowledged. Further distribution or reproduction in any format is prohibited without the permission of the copyright holder.

Abstract

This thesis describes advances within the field of nucleophilic nitrenoids, with particular focus on the intermolecular reaction of *N*-pyridinium aminides alongside ynamides and thioynamides, in a gold-catalysed formal [3+2] cycloaddition reaction. The generality of this transformation is demonstrated with the construction of highly functionalised 5,5,6-, 5,5- and 5,6-fused imidazolyl derivatives.

Five new types of *N*-pyridinium aminides bearing a benzothiazole, benzoxazole, thiazolone, imidazolone and pyrimidinone core, have been synthesised. Their preparation, scope and limitations across a variety of ynamides in the gold-catalysed cycloaddition is discussed, along with mechanistic insights.

Thioynamides are presented as privileged ynamides for the gold-mediated annulation reaction. Their use can overcome challenging reactivity observed within some of the nitrenoid series. The prominent improvement regarding the aminide scope is shown. Preliminary investigations into an unprecedented *sulfur effect* displayed by these *N,S*-substituted alkynes and the proposed mechanistic rationale of that enhancement are discussed.

Acknowledgements

Firstly, I would like to thank my supervisor Dr Paul Davies for giving me the opportunity to join his group and to participate in his research. For all his continuous help, suggestions, recommendations, ideas and support during the last 4 years, and for showing me the high standards needed for becoming a professional scientist.

I would like to thank my AstraZeneca supervisor, Scott Lamont, for his feedback, help and suggestions during my PhD and especially, during my placement in AstraZeneca.

To the analytical facility of the University of Birmingham, especially Cécile, Louise, Chi and Peter for helping me in my research as well as for their professionalism and temperance during the latest stressful months.

I would like to thank the past members of the Davies group (Miguel, Matt Ball, Josh, Onyeka, Elli, Andy, Matt Barrett) and the present members (Mat, Ana, Paige, Laura, Peter) for becoming my Brummie family during my time in Birmingham. Thank you so much for your support, your endless patience, for the drinks after work that made those tough days a bit better, the “Exploding kittens” evenings, and for the countless number of unforgettable moments in the lab. For your generous help in all chemistry related issues -I feel extremely lucky to have met such a wonderful bunch of incredible chemists.

Sobre todo y en especial, gracias a mi familia, a mis padres y a Saray. Por todas y cada una de las conversaciones de Skype que me han dado fuerzas para seguir adelante. Por vuestro apoyo incondicional desde que decidí dedicarme a esto. Por los abrazos, cariño, alegría y sonrisas de

cada encuentro, fuera donde fuera. Por las incontables sorpresas y buenos recuerdos que me hacen sentir la persona más afortunada del mundo por teneros a mi lado.

Finally, to Mat, for your unconditional support during this long and exciting journey of the PhD. Thanks for pushing me to give the best of myself in every situation. I would have never managed to get to the end of this without you.

Table of Contents

Chapter 1:	1
1.1. Introduction to nitrenes	2
1.2. Rhodium nitrenes as nitrogen transfer reagents.....	3
1.3. Nucleophilic nitrenoids in gold catalysed reactions	9
1.3.1. Intramolecular reactions of nucleophilic nitrenoids	10
1.3.2. Intermolecular trapping of the gold carbene intermediate.....	14
1.4. Conclusions.....	26
Chapter 2:	28
2.1. <i>N</i> -Pyridinium <i>N</i> -diazinyl aminides as 1,3- <i>N,N</i> -dipoles	29
2.2. Synthesis of tri-fused imidazolyl heterocycles	33
2.2.1. Imidazole-fused benzo(heteroaryls) in medicinal and material science	34
2.3. Aims and objectives.....	36
2.4. Results and Discussion	36
2.4.1. Synthesis of <i>N</i> -pyridinium <i>N</i> -benzo(heteroaryl) aminides	36
2.4.2. Investigating the reactivity of the new nitrenoids in the [3+2] gold catalysed cycloaddition.....	38
2.4.3. Ynamides as electron-rich alkynes.....	39
2.4.4. Ynamide scope in the gold-catalysed formal [3+2] dipolar cycloaddition with <i>N</i> -pyridinium <i>N</i> -benzo(thia/oxa)zole aminides.....	44
2.4.5. Introducing variations on the nitrenoid structure	47
2.4.6. Surveying the reactivity of the functionalised aminides	50
2.4.7. Mechanistic considerations	52
2.4.8. Oxazolidinone based ynamides in the gold catalysed cycloaddition	53

2.5. Conclusions.....	57
Chapter 3:	58
3.1. Introduction.....	59
3.1.1. New approach to construct molecular complexity.....	59
3.1.2. Biological activity and physical properties of molecules containing the new heterocycles.....	60
3.2. Aims and objectives.....	63
3.3. Results and Discussion	64
3.3.1. <i>N</i> -Pyridinium <i>N</i> -thiazolone aminides: new type of nitrenoids for the gold catalysed cycloaddition	64
3.3.2. Introduction of the imidazolone core in the <i>N</i> -pyridinium aminide series	72
3.3.3. Preparation of an <i>N</i> -pyridinium <i>N</i> -pyrimidinone aminide to form new 5,6-fused imidazoles	76
3.4. Conclusions.....	78
Chapter 4:	80
4.1. Heteroatom-donor activation of the alkyne	81
4.2. Introduction to thioynamides	86
4.2. Results and Discussion	91
4.2.1. Preparation of thioynamides	91
4.2.2. Investigating the reactivity of thioynamides in the gold-catalysed formal [3+2] cycloaddition	93
4.2.3. Mechanistic proposal	96
4.2.4. Further insights on the reactivity of thioynamides.....	99
4.2.5. Study of the thioynamide scope with <i>N</i> -benzo(heteroaryl) and <i>N</i> -diazinyl aminides	102
4.2.6. Improving the reactivity of other aminides	105

4.2.5. Post catalytic transformations	109
4.4. Conclusions.....	115
Appendix	117
1. General information	118
2. Synthetic procedures and characterization data	120
2.1. Synthesis of ynamide and thioynamide precursors	120
2.2. Synthesis of ynamides.....	131
2.3. Synthesis of thioynamides	136
2.4. Synthesis of aminides from chapter 2	140
2.5. Synthesis of aminides from chapter 3 and 4	149
2.6. Cycloaddition products for chapter 2.....	157
2.7. Cycloaddition products for chapter 3.....	173
2.8. Cycloaddition products for chapter 4.....	177
2.9. Post catalysis modification products	200
3. Attempted sulfonamide deprotections	208
4. Selected NMR Spectra.....	209
5. Crystallographic Data	218
References	269

List of abbreviations

°	degree(s)
Å	angstrom(s)
*Cp	cyclopentadienyl
AuPicCl ₂	dichloro(2-pyridinecarboxylato)gold
Ac	acetyl
BrettPhos	2-(dicyclohexylphosphino)3,6-dimethoxy-2',4',6'-triisopropyl-1,1'-biphenyl
Bn	benzyl
Boc	tert-butyloxycarbonyl
C	Celsius
CAN	cerium ammonium nitrate
cod	1,5-cyclooctadiene
CuTC	copper(I) thiophene-2-carboxylate
d	doublet
DBU	1,8-diazabicyclo(5.4.0)undec-7-ene
DCB	1,2-dichlorobenzene
DCE	1,2-dichloroethane
DIPEA	<i>N,N'</i> -diisopropylethylamine
DMEDA	<i>N,N'</i> -dimethylethylenediamine
DMF	<i>N,N'</i> -dimethylformamide
DMSO	dimethyl sulfoxide
DNA	deoxyribonucleic acid
dppm	1,1-bis(diphenylphosphino)methane
dppp	1,3-bis(diphenylphosphino)propane,
DSSC	dye sensitized solar cell
DTBP	di-tert-butyl-phosphite
EI	electron ionization
eq.	equivalents
ES	electrospray
Et	ethyl
EWG	electron-withdrawing group

g	gram(s)
h	hour(s)
Hz	hertz
HRMS	high resolution mass spectrometry
IAd	1,3-bis(1-adamantyl)imidazolium
IPr	1,3-bis(2,6-Diisopropylphenyl)imidazole-2-ylidene
<i>i</i> Pr	isopropyl
IR	infrared
<i>J</i>	coupling constant
JohnPhos	(2-biphenyl)di-tert-butylphosphine
L	litre(s)
LG	leaving group
LiHMDS	lithium bis(trimethylsilyl)amide
m	metre(s)
m	multiplet
M	molar
<i>m/z</i>	mass/charge
<i>m</i> CPBA	meta-chloroperoxybenzoic acid
Me	methyl
Ms	methanesulfonyl
MS	molecular sieves
MS	mass spectrometry
mol	mole(s)
mp	melting point
NTf ₂	bis(trifluoromethanesulfonyl)imide
NBS	<i>N</i> -bromosuccinimide
<i>n</i> Bu	butyl
NIS	<i>N</i> -iodosuccinimide
NMP	<i>N</i> -methyl-2-pyrrolidone
NMR	nuclear magnetic resonance
Ns	4-nitrobenzenesulfonyl
OA	oxidative addition
OSC	organic solar cell

THP	tetrahydropyranyl
PDT	photodynamic therapy
PET	positron emission tomography
PG	protecting group
Ph	phenyl
Pic	picolinate
Piv	pivaloyl
PMB	<i>p</i> -methoxybenzyl
PMP	<i>p</i> -methoxyphenyl
Py	pyridine
q	quartet
RE	reductive elimination
RNA	ribonucleic acid
rt	room temperature
s	singlet
t	triplet
TBS	tert-butyldimethylsilyl
<i>t</i> Bu	t-butyl
BuXPhos	2-di-tert-butylphosphino-2',4',6'-triisopropylbiphenyl
TFA	trifluoroacetic acid
TIPS	triisopropylsilyl ether
TLC	thin layer chromatography
TMS	trimethylsilyl
tpa	triphenylacetate
Ts	4-toluenesulfonyl
δ	chemical shift
ν	wavenumber

Collaborations and publications of the work presented in this Thesis

Some of the results in chapter 2 have been published as part of paper *Adv. Synth. Catal.* **2017**, 359, 1837–1843 by Miguel Garzón, Elsa M. Arce, Raju Jannapu Reddy and Paul W. Davies. Miguel Garzón performed the survey of the reaction conditions for the gold-catalysed cycloaddition of ynamides with *N*-pyridinium *N*-benzo(thio/oxa)zoles. The ynamide and aminide scope shown in chapter 2 was performed by me. Imidazole **369** was prepared by Garzón and published in *Org. Lett.* **2014**, 16, 4850-4853.

Results presented in chapters 3 and 4 have not being published yet and most of them were accomplished by me. Specific contributions of the aforementioned authors are included and cited in the text and/or figures/schemes. Imidazoles **622-625** were prepared by Garzón and were published in *Adv. Synth. Catal.* **2017**, 359, 1837-1843. Caffeine based imidazole **635** was prepared by Garzón.

Dr. Loïse Male from the analytical services of the University of Birmingham obtained and solved all the X-ray crystal structures presented in this thesis.

Some aminides, ynamides or precursors prepared by other members of the Davies group that were utilised in this thesis are reported in the General information section in the Appendix.

CHAPTER 1:

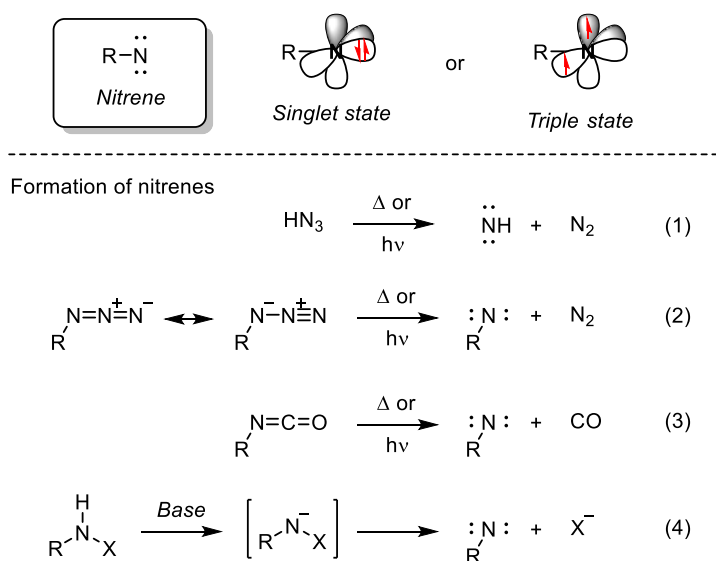
INTRODUCTION

1.1. Introduction to nitrenes

The paramount importance of nitrogen-containing molecules in living organisms, medicinal chemistry and material science has driven synthetic chemists to seek new strategies to incorporate nitrogen in complex frameworks.

Continuous efforts have been made towards the development of new transformations to incorporate nitrogen into molecules in a controllable, selective and practical manner. Possible routes to integrate nitrogen often require the use of nitrenes. These uncharged, six valence electron molecular species are highly reactive electrophiles with the ability to insert into bonds or undergo rearrangements.¹ As a result, they are one of the most utilised reagents for amination processes.

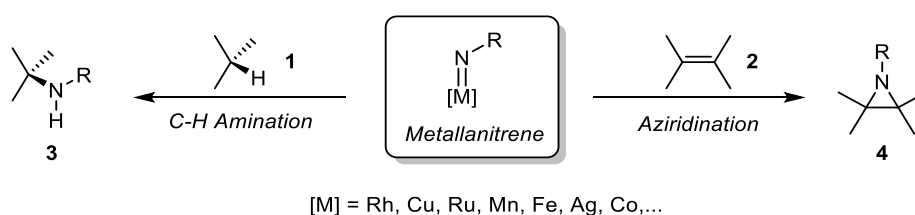
Nitrenes can be generated from thermal or photochemical decomposition of hydrazonic acids, azides and isocyanates or by α -elimination of *p*-nitrobenzenesulfonyloxy urethane (Scheme 1).



Scheme 1: Structure of nitrenes and synthetic routes for their preparation

Because of their indiscriminative reactivity, they are poor selective species and incompatible with many functionalities. In addition, their most common precursors, azides, can be hazardous to handle.

Thanks to the advent of late transition metal catalysis, more efficient methodologies for nitrene transfer processes have been achieved employing metallanitrenes as nitrene equivalents. Several transition metals have been utilised to access nitrene character and to modulate nitrene transfer reactions, such as rhodium, ruthenium and copper, with rhodium nitrenes the most widely used. In particular, the two most prominent nitrene transfer processes developed in the late sixties making use of metallanitrenes were C-H amination and aziridination (Scheme 2).^{1b}

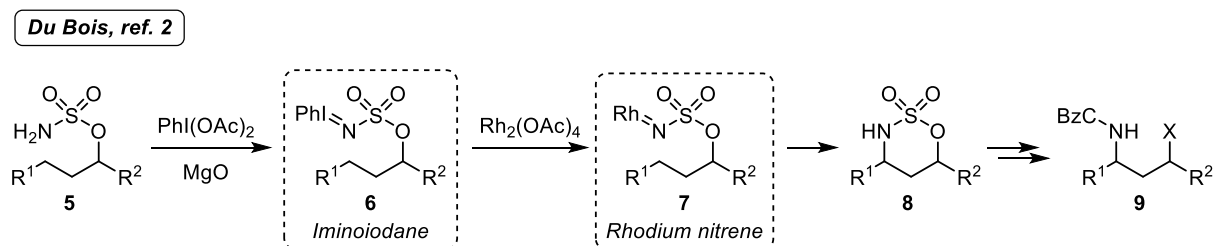


Scheme 2: Use of metallanitrenes in C-H amination and aziridination processes

1.2. Rhodium nitrenes as nitrogen transfer reagents

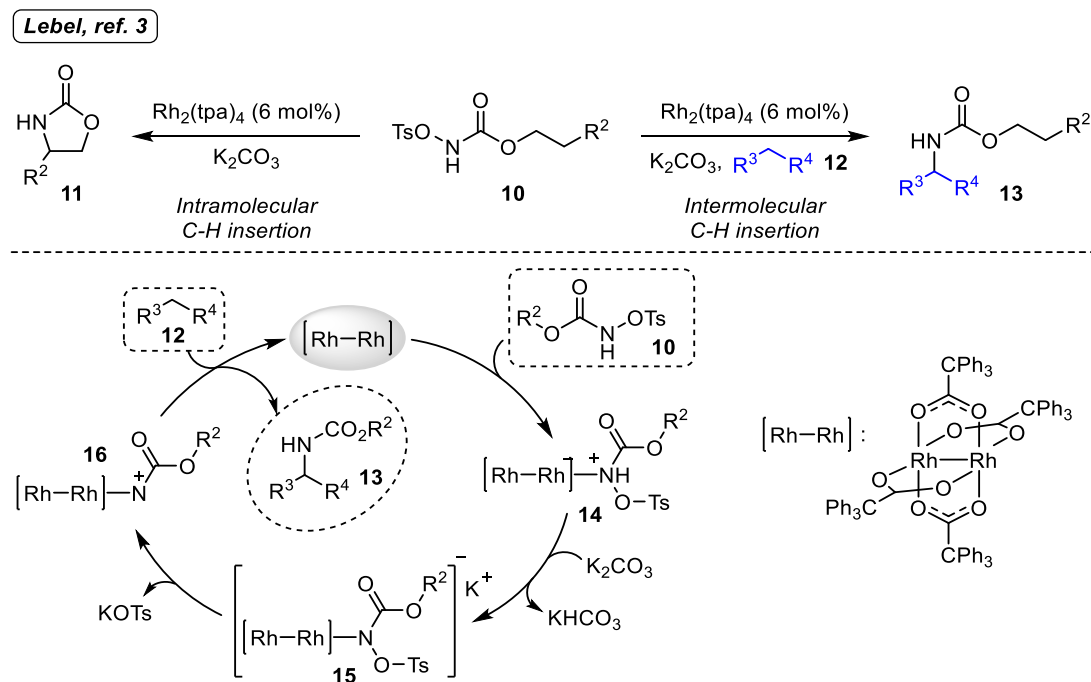
Substantial progress has been achieved by the use of rhodium nitrenes in nitrene transfer processes. The advantage of these metallated species compared to nitrenes relies on the more controllable formation and evolution of the nitrene character, which is formed *in situ*. A common method employs iminoiodane intermediates, which can be generated in an array of ways frequently from the reaction of sulfamate esters or tosyl carbamates with hypervalent iodine oxidants.

Du Bois and co-workers² pioneered this field investigating the rhodium catalysed intramolecular C-H amination of sulfamate esters **5** to form oxathiazinanes **8** (Scheme 3). These poly-heteroaromatic products were then converted into a wide array of benzyl chloroformate protected amines **9** by ring-opening reactions.



Scheme 3: Formation of rhodium metal nitrenes employing sulfamate esters and their application in the formation of oxathiazinanes pioneered by Du Bois

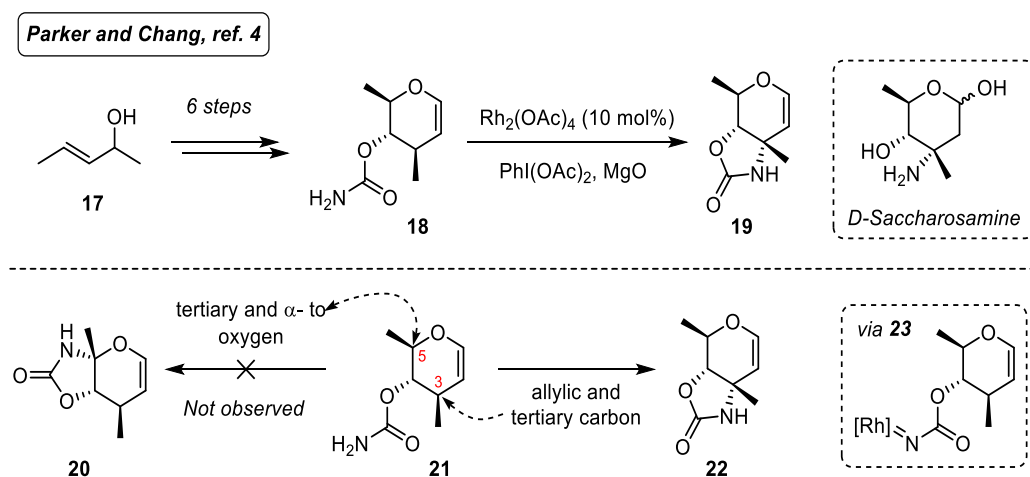
N-Tosyl carbamates **10** have also been extensively utilised as a source of nitrene (Scheme 4). Lebel and co-workers³ reported an intra- and the first inter-molecular example of rhodium nitrene C-H insertion using carbamates.



Scheme 4: Rhodium nitrene formation from tosyl-carbamates reported by Lebel

In this case, the leaving ability of the substituents on carbamate is critical. The authors carried out a series of control experiments which demonstrated that coordination of the rhodium dimer to the carbamate (**14**) occurs prior to deprotonation to form the active species (**16**). Subsequent C-H insertion and elimination of the catalyst delivers oxazolidinone **11** or Troc-protected amines **13**.

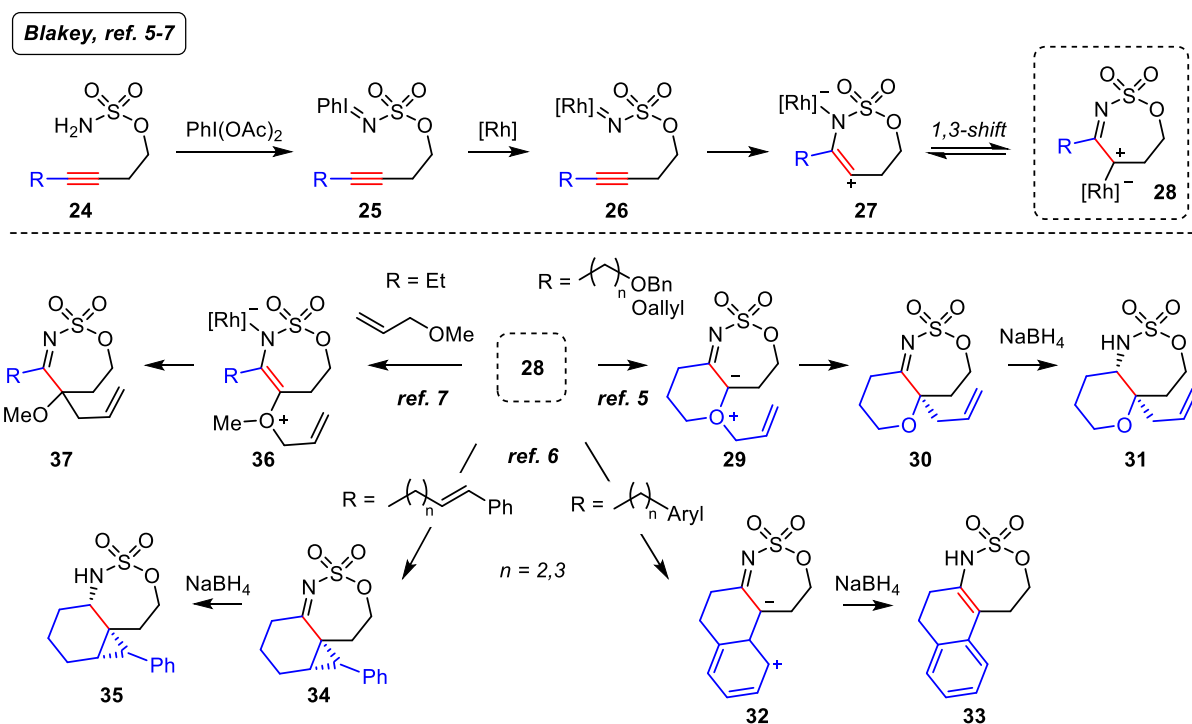
Similarly, Parker and Chang⁴ developed a synthetic route towards carbamate protected glycals **19** (Scheme 5). The crucial step involved a chemoselective intramolecular insertion into an allylic position *via* a rhodium nitrene **23**. Insertion into the allylic position was preferential over a possible side-reaction where insertion would occur in the oxygen-substituted tertiary carbon leading to **20**. Yet the latter was not observed. In this way, a modular preparation of naturally occurring trideoxyhexoses was established.



Scheme 5: Preparation of trideoxyhexoses through a rhodium nitrene intermediate reported by Parker and Chang

Blakey's group accomplished a metallonitrene/alkyne metathesis reaction using sulfamate esters **24** (Scheme 6). The reaction of **24** with (diacetoxyiodo)benzene delivered intermediate **25**, which was reacted with a rhodium catalyst to form metallonitrene **26**. The latter receives nucleophilic attack from the pendant alkyne forming **27**. Subsequently, 1,3-Rh shift from

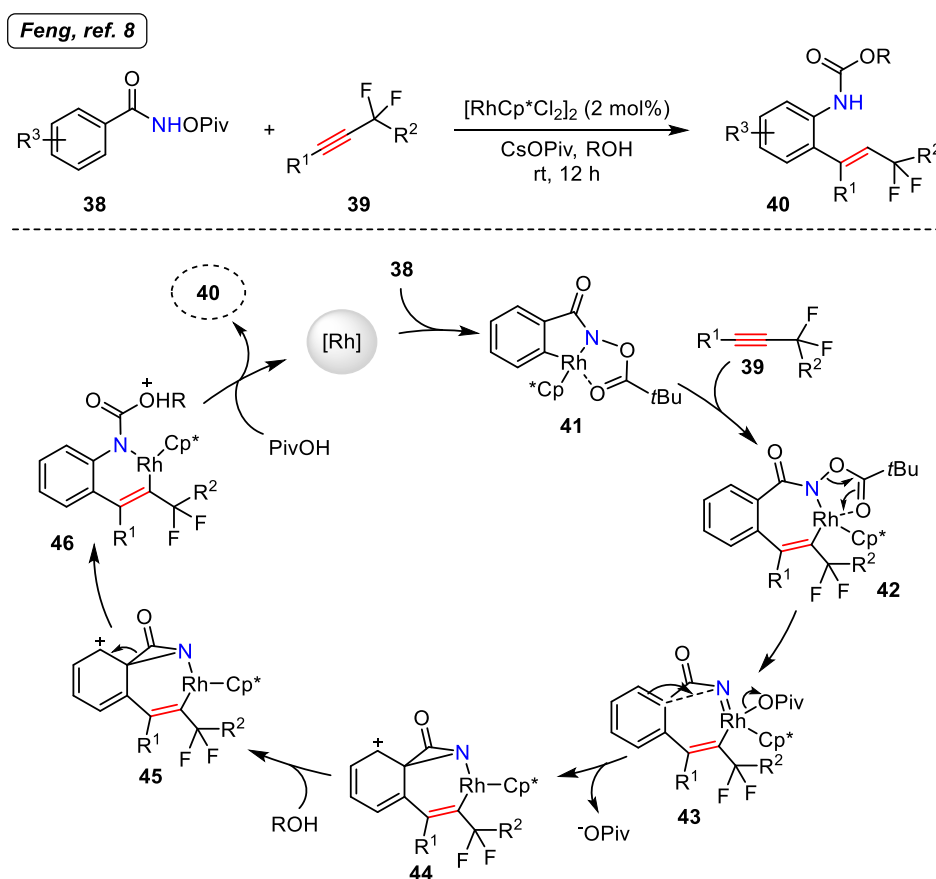
rhodacycle **27** delivered α -imino rhodium carbenoid **28**. The authors demonstrated that depending on the pendant nucleophiles attached to the alkyne, a wide range of processes could be triggered. For instance, intermediate **28** can collapse forming an oxonium ylide **29**, which after rearrangement and stereoselective reduction provides access to bicyclic sulfamates **31**.⁵



Scheme 6: Intramolecular α -imino rhodium carbenoid trapping reported by Blakey

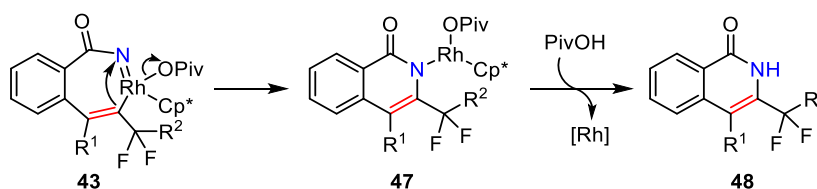
The cascade reaction can also be terminated by a Friedel-Crafts or cyclopropanation reactions when tethered aryls (**28** to **33**) or olefins (**28** to **35**), respectively, are attached to the alkyne.⁶ Final sodium borohydrate reduction provides tri-fused sulfamates. The authors further explored the potential of α -imino rhodium carbenoid **28** to diversify the cascade reaction by the addition of external allyl ethers (**28** to **37**). Trapping of intermediate **28** with an enol ether forms intermediate **36**, which after allyl group migration gives access to oxathiazepine derivatives **37** that could be then further modified.⁷

In 2017 Feng and co-workers⁸ reported the formation of a rhodium(V) nitrenoid in the synthesis of difluorinated 2-alkenyl aniline derivatives **40** (Scheme 7). Anilines **40** were formed by hydroarylation of *gem*-difluoromethylene alkynes **39** with *N*-pivaloxy arylamides **38**. Coordination of the amide to the rhodium(III) catalyst generates rhodacycle **41** by *ortho* C-H bond cleavage. Alkyne **39** then is regioselectively inserted into rhodacycle **41**. OPiv group migration of intermediate **42** to the rhodium atom triggers the formation of rhodium(V) nitrenoid **43**, which undergoes arene dearomatization onto the nitrogen. The additional participation of an external alcohol attacking the carbonyl regenerates the aromaticity (**45-46**). Eventually, protodemetalation furnishes **40** and releases the catalytic species.



Scheme 7: Rhodium(III)-catalysed hydroarylation of α,α -difluoromethylene alkynes with *N*-pivaloxy arylamides as source of nitrene

From intermediate **43**, there is also possible a distinct reaction pathway consisting on alkene group migration (Scheme 8). The presence of the fluorinated substituents on the alkene hampers this side-reaction due to the different polarity induced by the fluorine atoms to the Csp^2 carbon. As a result, product **48** was only seen as a minor by-product.

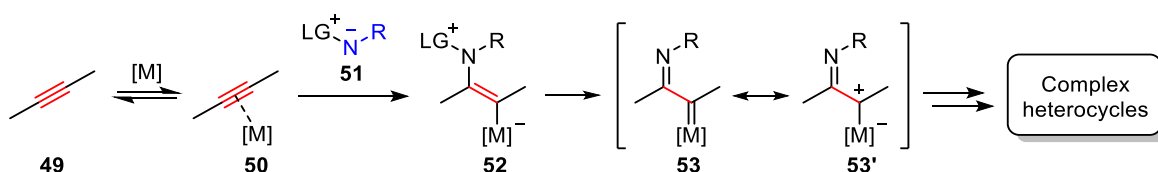


Scheme 8: Competing alkene migration side reaction leading to isoquinolone derived 41

Despite the powerful applications of metallanitrenes, the aforementioned methodologies require the use of stoichiometric amounts of external oxidants, pre-functionalization of the substrates and poor functional group compatibility as well as the use of sacrificial species. More efficient and atom economical routes for amination processes are desirable and alternative species for nitrene transfer transformations are gradually being introduced in the field.

The resurgence of π -acid catalysis represented a vast improvement towards the development of new strategies for C-N bond formation. In particular, interest was directed towards exploring and further developing the potential of α -imino metal carbenes as versatile intermediates. The formation of the latter can be envisioned from a presumed nucleophilic attack of a nitrogen containing species **51** to a π -acid activated alkyne **50**, delivering an α -vinyl metal carbenoid **52** (Scheme 9). Subsequent elimination of the leaving group attached to the nitrogen atom would form an analogous α -imino metal carbene/carbenoid (**53-53'**) to that obtained with rhodium nitrenes. The electrophilic metallated centre could then be trapped by various intra- or intermolecular pathways to access *N*-containing heterocycles.

The overall transformation can be seen as a nitrogen transfer process where **51** behaves as a *nucleophilic nitrene equivalent*, or a *nucleophilic nitrenoid*. At that point, the term *nitrenoid* was utilised to refer to those species, which display nitrene character along the reaction course, yet not being actual electrophilic nitrenes.



Scheme 9: General reactivity profile of nucleophilic nitrenoids

The advantage of these nitrene equivalents relies on their stability and selectivity, as the desired nitrene character solely arises by the reaction of the nitrogen containing species with a π -acid activated alkyne. Hence, the formation of the α -imino metal carbene intermediate is achieved in a more controllable manner than with rhodium nitrenes.

1.3. Nucleophilic nitrenoids in gold catalysed reactions

The unique ability of gold(I) and gold(III) complexes to activate carbon-carbon π -systems such as alkenes, alkynes or allenes^{1a, 9} towards nucleophilic attack, as demonstrated by the numerous gold-mediated cycloaddition, cyclisation and cycloisomerisation processes reported in the literature, have conferred gold catalysts a privileged position among the synthetic community.¹⁰

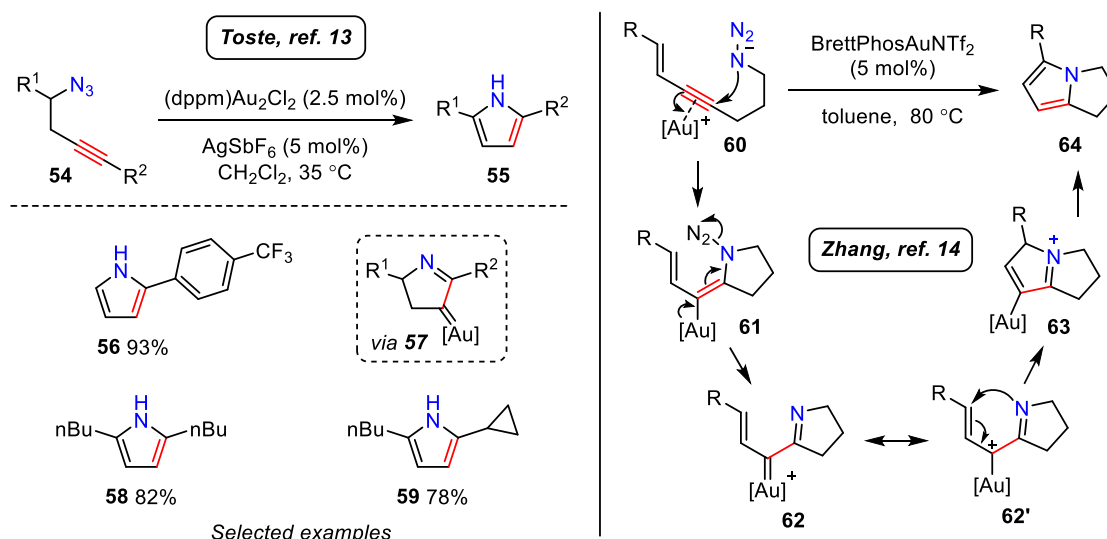
The high carbophilicity, low oxophilicity –tolerating oxygen, water and alcohols– in addition to showing scarce propensity to undergo redox processes due to the high oxidation potential between gold(I) and gold(III), make these complexes ideal mediators for constructing molecular complexity in an atom economical manner.^{10c, 10d, 11}

Compared to other transition metals, gold complexes allow for very mild reaction conditions and superb functional group tolerance, as it has been demonstrated in the application of gold-catalysed late stage transformations in many natural product syntheses.¹²

The unique features of gold-complexes have been exploited in the nitrenoid field for the generation of α -imino gold carbenes in an efficient and stereocontrolled manner. Many transformations have been developed in the last decade in which the gold carbene intermediate is trapped through a pendant nucleophile or by an external agent as it is shown in the following sections.

1.3.1. Intramolecular reactions of nucleophilic nitrenoids

Gold catalysed intramolecular nitrene transfer reactions involving nitrenoids were pioneered by Toste and co-workers in 2005.¹³ Homopropargyl azides **54** were utilised for the preparation of substituted pyrroles **55** via an annulation reaction with the pendant alkyne fragment (Scheme 10-left).

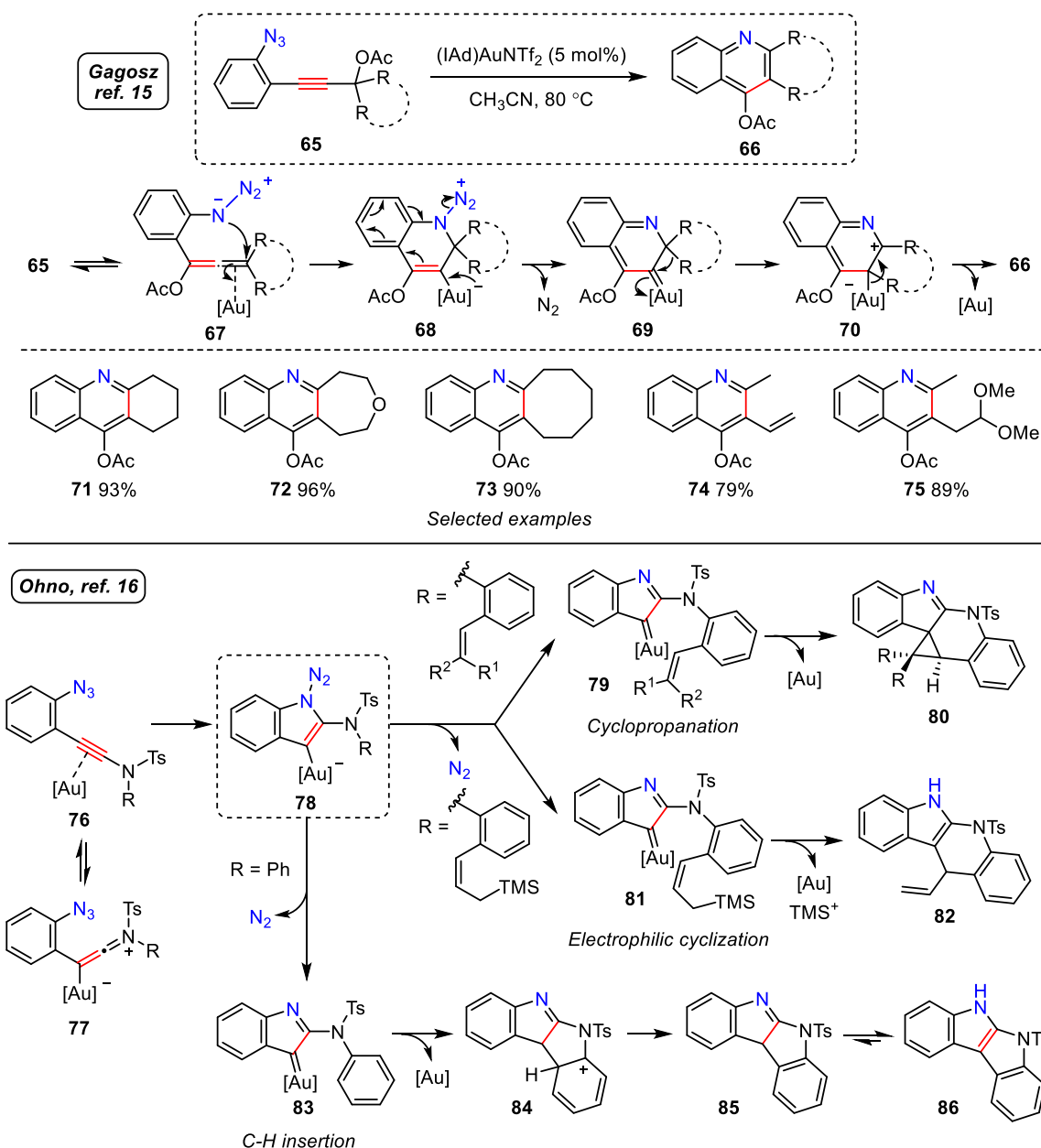


Scheme 10: Initial work in intramolecular nitrene transfer process utilising nucleophilic nitrenoids. Left: Intramolecular annulation reaction reported by Toste; Right: Gold-catalysed cyclisation reported by Zhang

Similarly Zhang and co-workers¹⁴ in 2012 employed azido 1,3-enynes **60** to prepare pyrrolizine derivatives **64** (Scheme 10-right). Coordination of the gold catalyst to the π -system (**60**) followed by an *5-exo-dig* cyclisation on the biased alkyne forms α -imino gold carbenoid **61**. Extrusion of nitrogen delivers α -imino gold carbene **62-62'**. The latter undergoes 4- π electrocyclic ring closure (**63**) followed by gold elimination giving substituted pyrrole **64**.

α -Imino gold carbenes generated from alkynyl arylazides were investigated separately by Gagosz and co-workers¹⁵ and Ohno and co-workers¹⁶ (Scheme 11). In Gagosz's method the nucleophilic attack takes place onto an allene intermediate (**67**) due to a 3,3-acyloxy shift in alkynyl azide **65**. Gold coordination triggers nucleophilic attack from the pendant azide onto the more distant double bond forming intermediate **68**. Subsequent extrusion of nitrogen and 1,2-shift from the R group forms intermediate **70**, which upon gold elimination, delivers quinoline **66**.

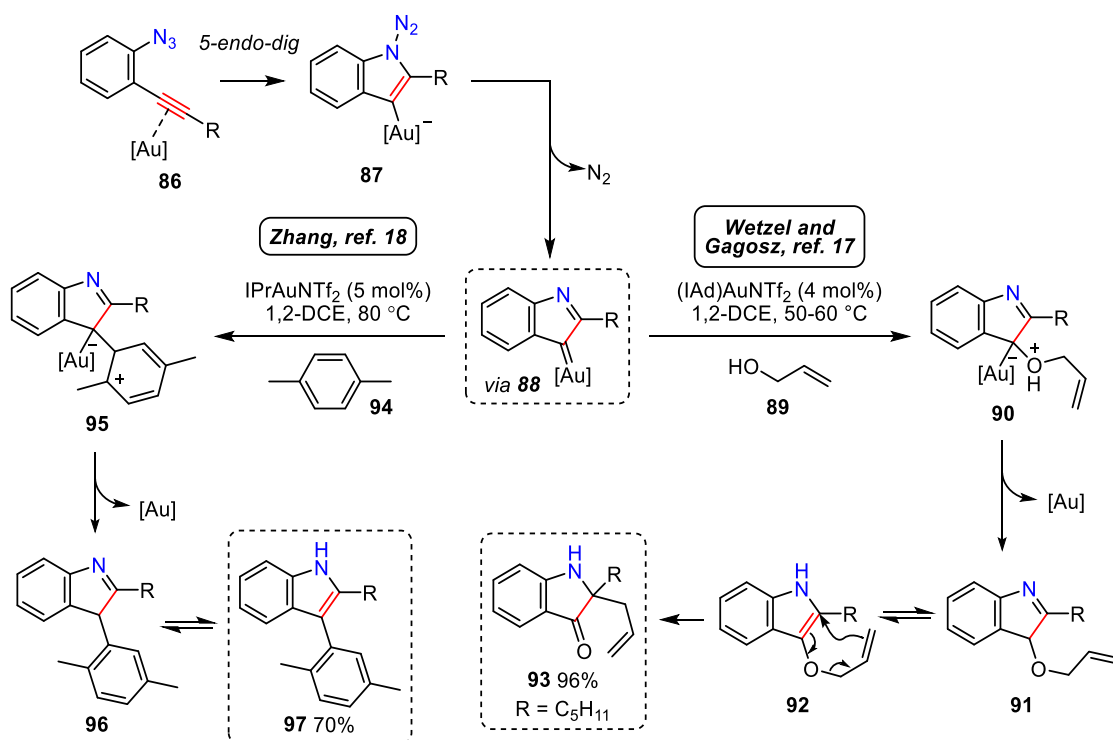
Ohno reported a gold catalysed cascade reaction of alkynyl arylazides *via* the generation of a keteniminium intermediate **77**, which receives the intramolecular attack of the azide. Upon extrusion of molecular nitrogen in intermediate **78**, the authors proposed several reaction pathways depending on the substituents on the R group. For instance, a C-H insertion reaction when R is an aryl group, ultimately delivering 5-tosyl-5,6-dihydroindolo[2,3-*b*]indole (**83** to **86**) upon rearomatization of intermediate **84**. In the presence of a pendant alkene, gold carbenoid **78** could also undergo a cyclopropanation reaction delivering 1*H*-cyclopropa[*c*]indolo[2,3-*b*]quinoline **80**. Otherwise, arylazides bearing an allylsilane moiety could evolve *via* electrophilic cyclisation; elimination of TMS followed by gold extrusion provides quinolone derivative **82**.



Scheme 11: Alkynyl arylazides in intramolecular nitrogen transfer processes. Top and middle: Gagosz' general reaction and scope; Bottom: Ohno's proposed mechanism for α -imino gold carbene formation

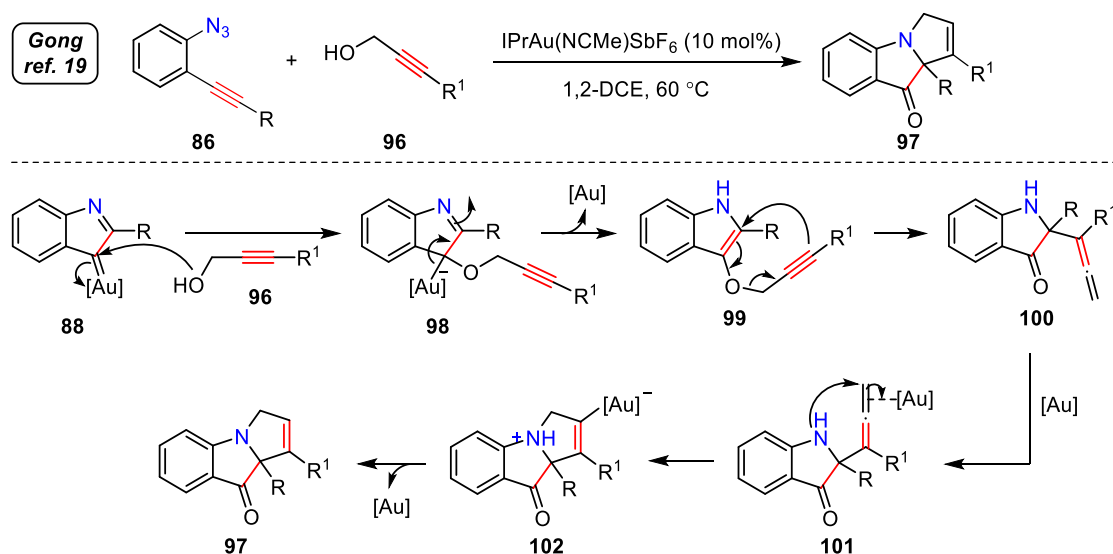
The α -imino gold carbene intermediate generated from alkynyl arylazides can also be trapped intermolecularly by the addition of external nucleophiles. Wetzel and Gagosz¹⁷ (Scheme 12-right) reacted intermediate **88** generated from alkynyl azide **86** with a range of allylic alcohols **89**. After the deprotonation and gold elimination of **90**, intermediate **91** tautomerises and subsequently undergoes a Claisen rearrangement delivering 3-indolidinones **93**.

Similarly, Zhang and co-workers¹⁸ (Scheme 12-left) reported the formation of 3-heteroaryl indoles **97** by the reaction of α -imino gold carbene **88** with numerous C-nucleophiles such as **94**. Upon elimination of the gold complex in intermediate **95**, and tautomerization, the corresponding 3-aryl indole derivative **97** is formed.



Scheme 12: Intermolecular trapping of the α -imino gold carbene generated from alkynyl azides

Gong and co-workers¹⁹ made use of propargylic alcohols **96** to access pyrroloindolone derivatives **97** (Scheme 13). The reaction proceeds *via* the formation of α -imino gold carbene **88** from the corresponding alkynyl arylazide **86**. Propargylic alcohol **96** attacks the gold carbene centre delivering intermediate **98**. After gold extrusion, intermediate **99** undergoes Saucy-Marbet rearrangement (**99-100**). Subsequent intramolecular amination catalysed by gold forms intermediate **101**, which after gold elimination provides pyrroloindolone **97** and the catalyst is regenerated.



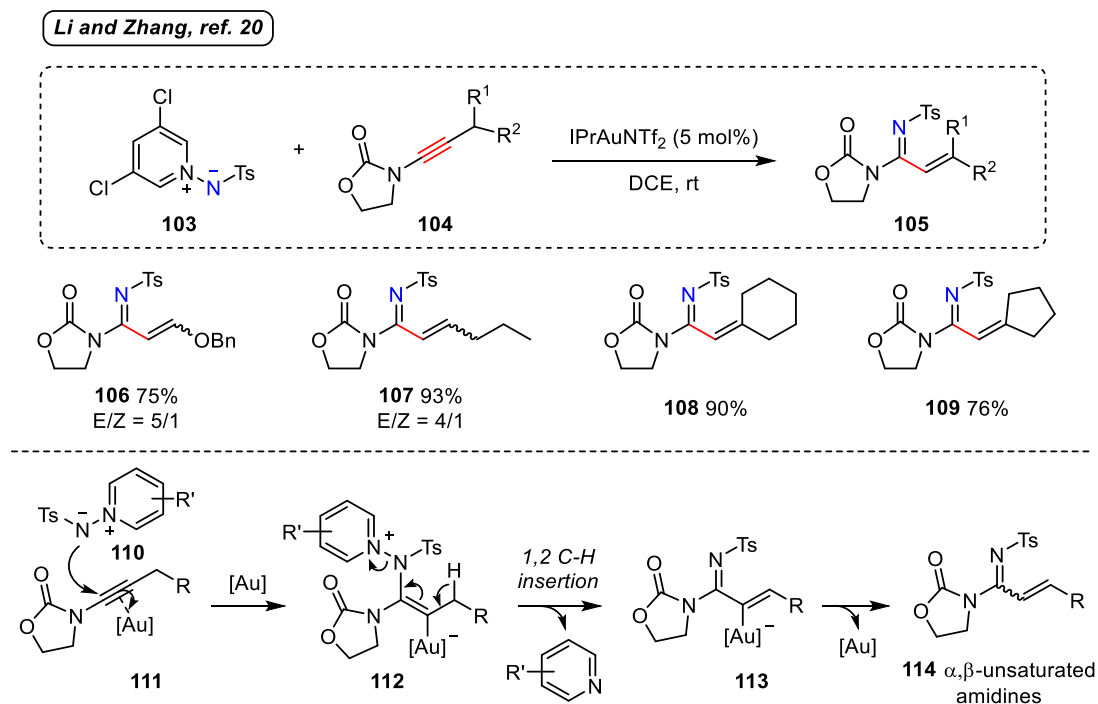
Scheme 13: Proposed mechanism by Gong to form pyrroloindolones via a gold carbene

1.3.2. Intermolecular trapping of the gold carbene intermediate

While the development of the nitrenoid field commenced with intramolecular nitrene transfer processes, intermolecular strategies arose rapidly. Thereafter the group of Zhang and Davies consecutively reported the first intermolecular versions in which *N*-pyridinium aminides acted as a source of nitrene.

Capitalising on the 1,2-C-H insertion that carbenes commonly undergo, Li and Zhang²⁰ designed a convenient methodology for the preparation of α,β -unsaturated amidines (**105**) (Scheme 14). Oxazolidonyl ynamides **104** proved more effective than acyclic sulfonamides as electron-rich π -systems and *N*-aminopyridinium aminide **103** exhibited superior oxidant character among those tested.

Noticeably, the transformation led to an inseparable mixture of *E/Z* stereoisomers, yet the *E*-configuration for the C-N bond was consistently favoured and was eventually confirmed by X-ray diffraction studies.

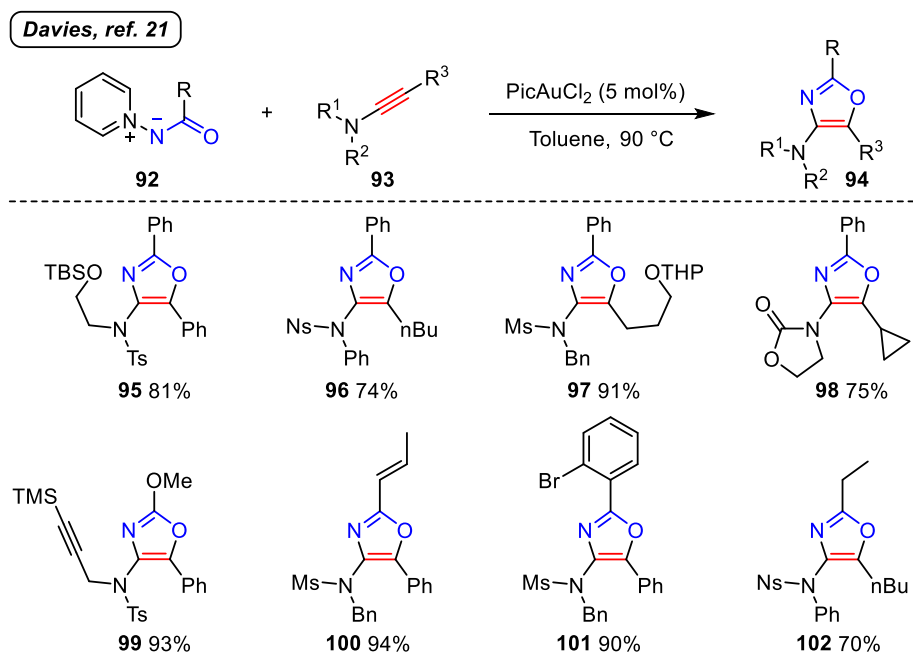


Scheme 14: Intermolecular nitrene transfer onto ynamides from *N*-pyridinium *N*-tosyl aminides

Davies and co-workers²¹ reported that *N*-pyridinium *N*-acyl aminides **115** behave as *N*-acyl nitrene equivalents in a gold-catalysed formal [3+2] dipolar cycloaddition with ynamides **116** to form tri-substituted oxazoles (Scheme 15).

The transformation tolerated a wide range of substitution patterns in position 2 and 4, such as phenyl, alkyl and alkenyl groups. The substituents introduced on the sulfonamide moiety ranged from protected alcohols, alkynyl, benzyl and phenyl groups, among others.

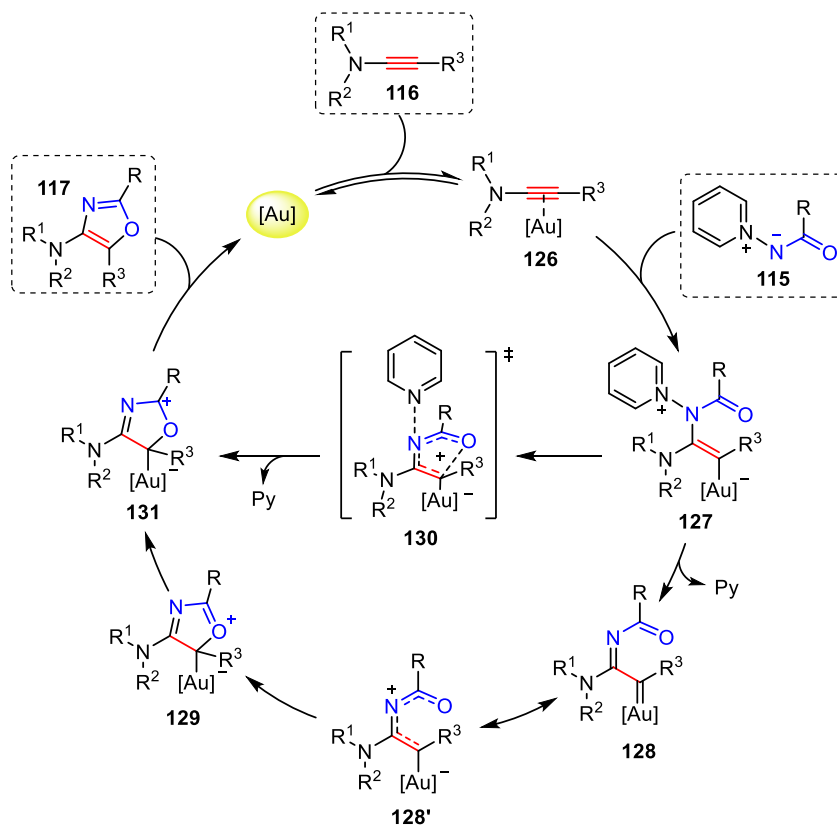
Cyclisation of the α -imino gold carbene was preferred over other undesired side-reactions or possible intramolecular processes such as aza-Claisen rearrangements, 1,2-C-H insertions or intramolecular redox reactions. The transformation proved general with a range of valuable functionalities, such as allyl, *tert*-butyldimethylsilyl, trimethylsilyl and bromobenzenes with defined regioselectivity confirmed by X-ray crystallography data.



Scheme 15: *N*-Pyridinium *N*-acyl aminides in the gold catalysed cycloaddition with ynamides reported by Davies and co-workers

The proposed mechanism commences with regiospecific intermolecular attack of aminide **115** onto the carbon adjacent to the nitrogen of the gold-activated ynamide **126** forming **127** (Scheme 16). Subsequent pyridine elimination delivers gold carbene/carbenoid **128-128**, which can be trapped by the oxygen of the acyl group forming **129**. Otherwise, intermediate **127** can evolve by 4- π electrocyclicalisation *via* **130**. Elimination of the gold complex from **131** provides oxazole **117** and regenerates the catalyst.

The potential of this methodology to construct tri-substituted oxazoles was further demonstrated thanks to the versatility offered by ynamides and *N*-pyridinium *N*-acyl aminides as building blocks (Figure 1). The development of robust synthetic routes to access the precursors –aminides from acyl chlorides, carboxylic acids, esters, isocyanates or isothiocyanates and ynamides from terminal alkynes or 2,2-dichloroenamides– in an efficient and modular manner, in addition to the introduction of wider substitution patterns on the oxazole skeleton are the main breakthroughs of the follow-up investigation.²²



Scheme 16: Proposed mechanism for the formation of substituted oxazoles reported by Davies

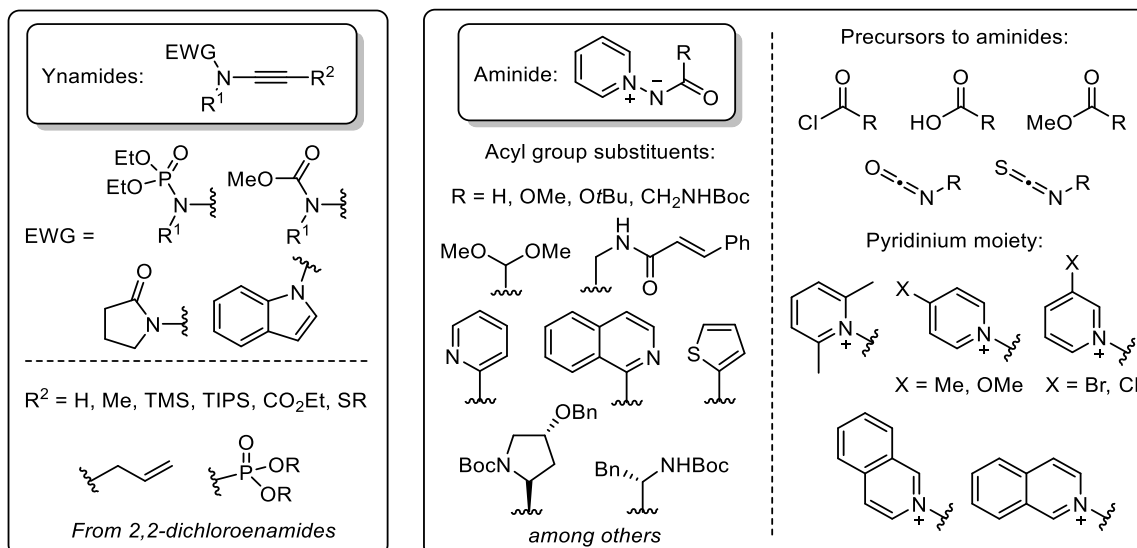
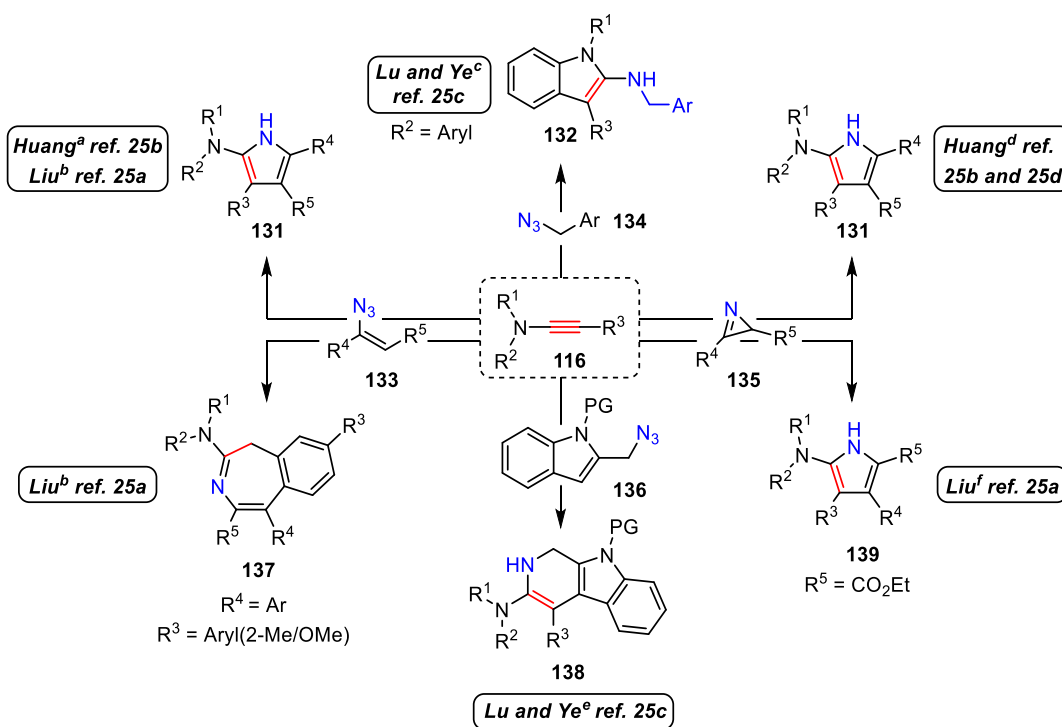


Figure 1: Exploiting the potential of aminides and ynamides in the gold-catalysed formal [3+2] cycloaddition reported by Davies to synthesise highly functionalised oxazoles

A related study utilising *N*-pyridinium *N*-aryl aminides and ynamides was reported in 2015 by Garzón and Davies to access substituted imidazoles.²⁴ That work is discussed in chapter 2 as introduction and background of the results presented throughout that chapter.

Since 2015, various groups have reported the use of ynamides in gold-catalysed intermolecular cycloadditions with azides (**133**, **134**, **136**) and azirines (**135**) as nucleophilic nitrene equivalents to generate pyrroles (**131**, **139**), indoles (**132**), pyridoindolamines (**138**) and benzoazepines (**137**) (Scheme 17).²⁵

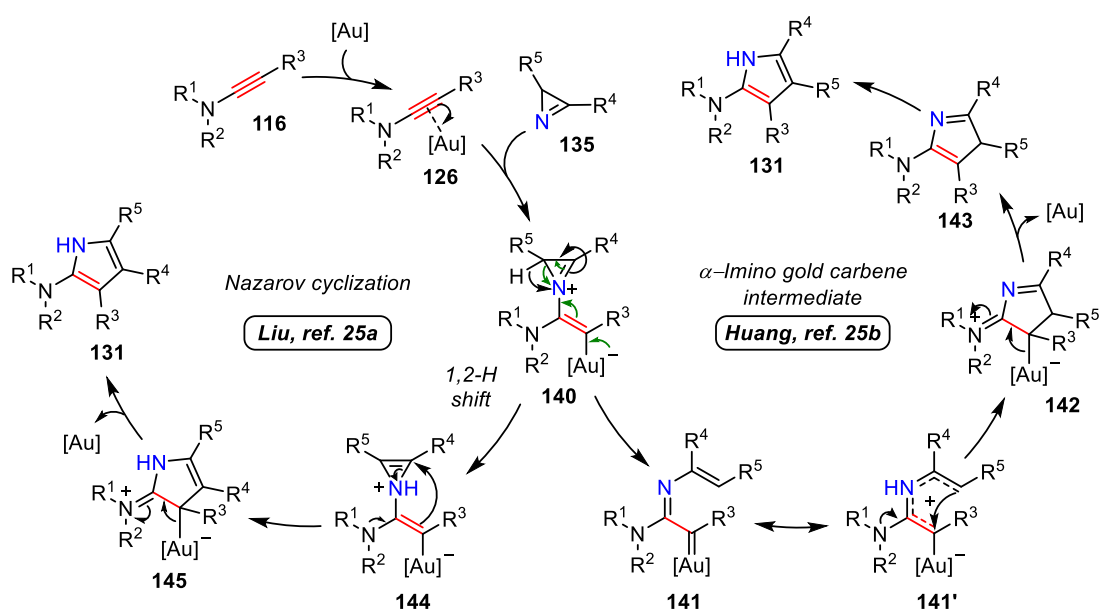


Scheme 17: Gold catalysed intermolecular transformations of azides and azirines with ynamides. ^a Using JohnPhosAu(NCMe)SbF₆ (3 mol%), 1,2-DCE at 60 °C; ^b Using IPrAuNTf₂ (5 mol%), MS 4Å, CH₃NO₂ at 80 °C; ^c Using IPrAuNTf₂ (5 mol%), MS 4Å, 1,2-DCE at rt; ^d Using JohnPhosAu(NCMe)SbF₆ (3 mol%), CH₂Cl₂ at rt; ^e Using IPrAuNTf₂ (5 mol%), MS 4Å, 1,2-DCE at 60 °C; ^f Using AuClPPh₃/AgNTf₂ (5 mol%), 1,2-DCE at rt

The regiocontrol in the attack of the nitrenoid to the π -activated system is the main challenge of intermolecular reactions involving nitrenoids. As demonstrated with the examples discussed thus far, ynamides have been utilised as convenient alkyne surrogates. An

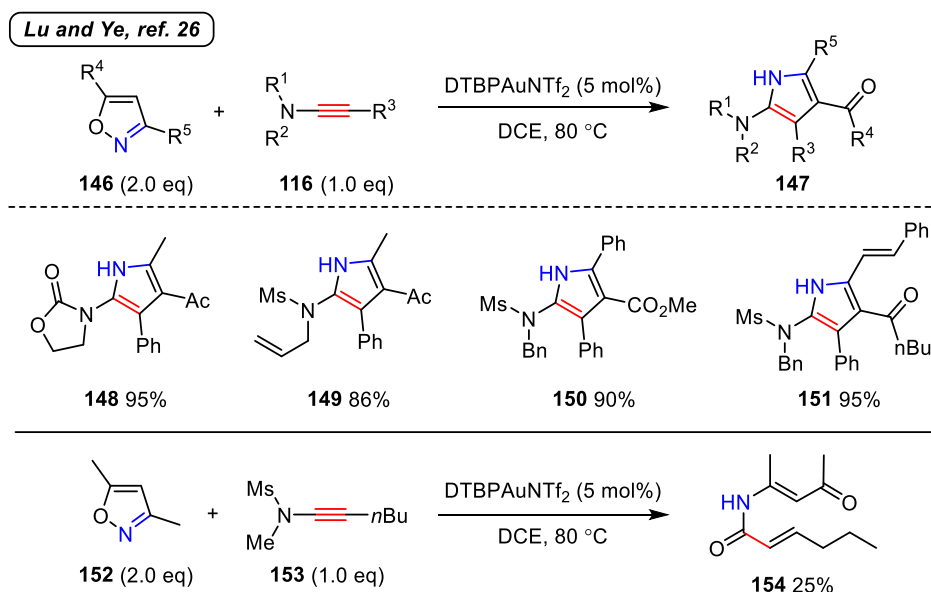
advantageous feature of ynamides is the presence of a nitrogen adjacent to the π -system. The lone pair of the nitrogen can be delocalised in the triple bond resulting in a more electrophilic α -*sp*-C and a more nucleophilic β -*sp*-C, if compared to a normal alkyne. Consequently, ynamides provide exquisite regiocontrol in nucleophilic additions to triple bonds.²³ Further discussion of the ynamide features and preparation can be found in section 2.4.3.

There is a debate in the field about whether the previous transformations involve the generation of a carbene species or a gold cationic intermediate. Huang^{25b} claimed the participation of a α -imino gold carbene by designing an ynamide bearing a benzyl group on the C-terminus which underwent 1,2-C-H insertion (Scheme 18-right). On the other hand, Liu and co-workers^{25a} proposed a gold-driven ring opening of the azirine, followed by Nazarov cyclisation as the most feasible reaction pathway (Scheme 18-left). With these insights highlighting the potential of intermolecular nitrene transfer processes, the nitrenoid field rapidly expanded.



Scheme 18: Synthesis of pyrroles through Nazarov cyclisation and via α -imino gold carbene intermediate reported by Liu and Huang, respectively

The generality of the ynamide approach was further showcased by Lu and Ye²⁶ with the preparation of 2-aminopyrroles (**147**) from isoxazoles **146** as a new type of nitrenoid (Scheme 19). The key α -imino gold carbene intermediate is generated upon *N*-nucleophilic attack onto a gold activated ynamide followed by ring opening of the isoxazole core.

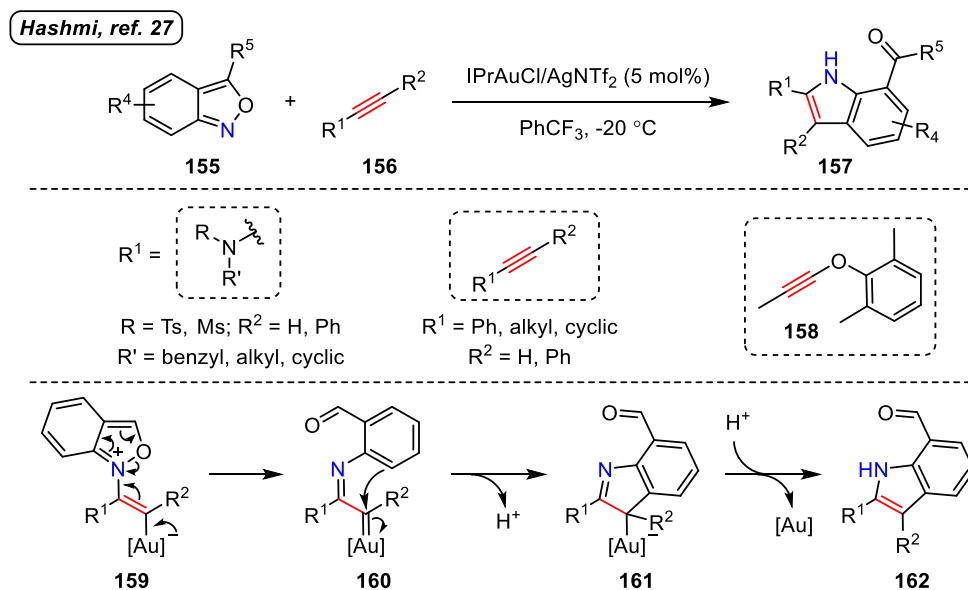


Scheme 19: Top: General reaction for the synthesis of aminopyrroles and selected examples employing sensitive ynamides. Bottom: C-H insertion onto the carbene intermediate leading to amide 133

The reaction proved general and tolerated many functionalities (**148-151**). Particularly interesting were those substituents prone to undergo other rearrangements, such as an *N*-allyl ynamide, where cyclisation was preferential affording the desired pyrrole derivative **149** in high yield. The carbene assistance was demonstrated making use of alkyl ynamide **153** to promote a 1,2-C-H insertion onto the electrophilic metallated centre, forming α,β -unsaturated amide **154**.

Structurally resembling isoxazoles, benzoisoxazoles (**155**), also known as anthranils, have exhibited analogous nucleophilic features in gold mediated processes with electron-rich alkynes. An unprecedented gold-catalysed C-H annulation reported by Hashmi²⁷ in 2016

employed benzoisoxazoles as nitrene equivalents, to access 7-acylindolyl derivatives **157** via an α -imino gold carbene (**160**) (Scheme 20). Carbene **160** is intramolecularly trapped by an *ortho*-C-H insertion from the benzene ring, which upon protodeauration delivers arylindole **162**.

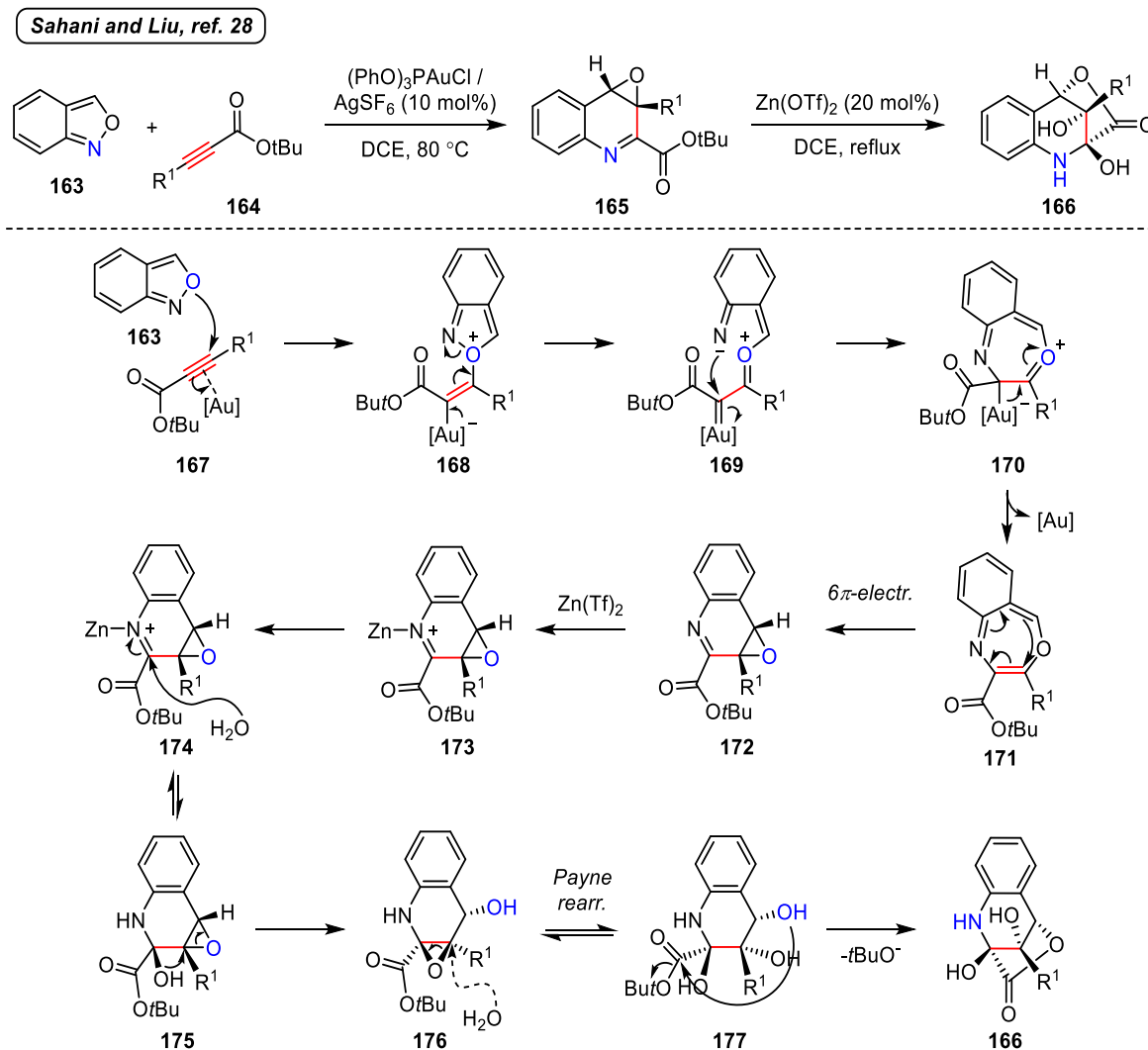


Scheme 20: Top: Intermolecular gold-catalysed annulation to form 7-acylindolyl heterocycles reported by Hashmi. Middle: scope of the alkyne partner. Bottom: proposed mechanism

While terminal ynamides proved ideal for this transformation, fully substituted ones also afforded the desired acylindolyl derivative. However, substituted ynamides were limited to aryl groups on the C-terminus since alkyl groups underwent competing C-H insertion pathways.²⁰ Alkynyl ethers also exhibited suitable electrophilic features able to drive the process as exemplified utilising **158**. Terminal and internal alkynes were also employed in this transformation, yet harsher reaction conditions and the use of Brønsted acids were required to achieve significant conversion.

Sahani and Liu²⁸ took advantage of the isoxazole functionality in a [4+2] gold catalysed annulation/cyclisation cascade to form quinolone oxides **165** (Scheme 21). Further reaction of

the resulting bicyclic system with a Zn^{II} species triggered the stereoselective formation of tetrahydroquinolines **166** in a one-pot sequential process. Alkynoates and alkynones functioned well as electronically biased π -systems in both steps.

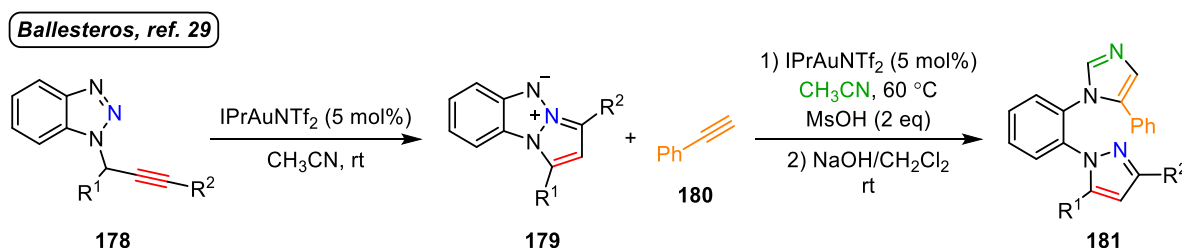


Scheme 21: Quinolone oxide synthesis by a [4+2] gold catalysed annulation/cyclisation cascade reaction and proposed mechanism reported by Sahani and Liu

The proposed mechanism involves the formation of an oxo-carbene **169** which cyclises by the intramolecular attack of the exocyclic nitrogen giving **170**. Extrusion of the gold complex (**171**), followed by a 6- π electrocyclic reaction furnishes **172** and re-establishes the aromaticity of the benzenoid system. Addition of zinc triflate forms iminium intermediate

173. Water then attacks from the face opposite to the epoxide delivering intermediate **175**, which undergoes a Payne rearrangement. Hydrolysis of **177** and ring closing generates tricyclic **166** stereoselectively.

While investigating 1-propargyl-1*H*-benzotriazoles **179** under gold catalysis, Ballesteros and co-workers²⁹ envisioned the potential of the resulting 5-*endo-dig* cyclisation products (triazapentalanes **179**) as a source of nitrene due to their electronic resemblance to azides (Scheme 22).

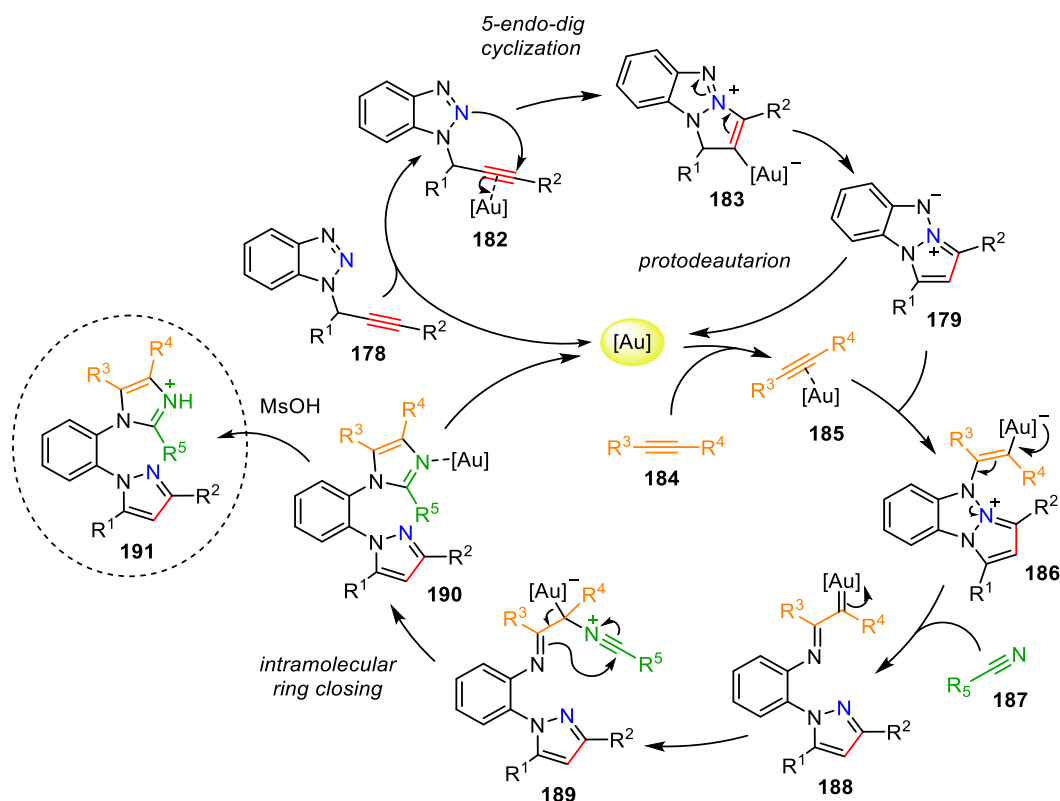


Scheme 22: Three-component gold-catalysed synthesis of 2-imidazolyl-1-pyrazolylbenzenes reported by Ballesteros

Upon screening of the reaction conditions, triazapentalane **179** successfully underwent nucleophilic attack onto a gold-activated alkyne **185** forming vinyl gold carbenoid **186**, which then evolved into α -imino gold carbene **188** (Scheme 23). Subsequent trapping of the metallated species by nitrile **187** (used as a solvent) triggered intramolecular ring closing (**189**) forming tricyclic poly-aza heterocycle **190**.

As compound **190** was susceptible to interact with the gold catalyst due to the presence of donor sites, the addition of methanesulfonic acid was essential to release the catalyst and to obtain **191** as a salt. The neutral form of **191** could be achieved with a basic work-up.

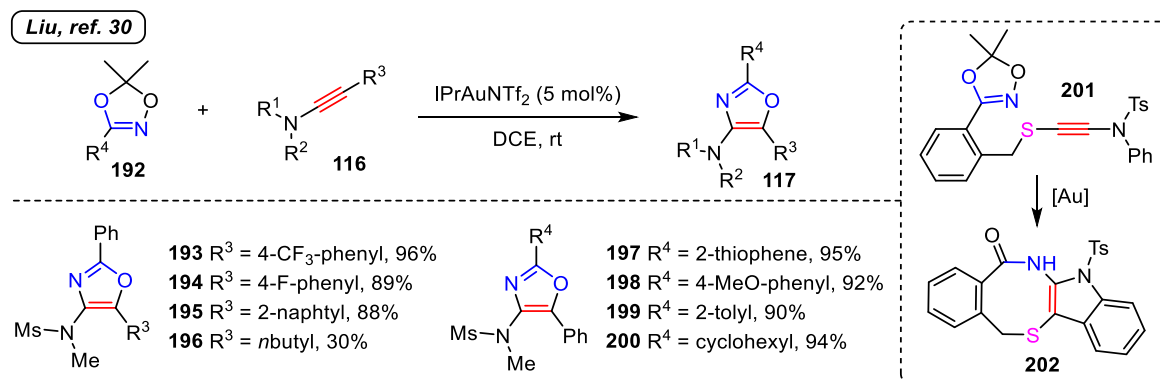
The combination of these insights into a one-pot procedure eventually provided a practical three component gold-catalysed synthesis of 2-imidazolyl-pyrazolylbenzenes *via* an α -imino-gold carbene intermediate formed *in situ* after the first catalytic cycle.



Scheme 23: Proposed mechanism for the synthesis of 2-imidazolyl-1-pyrazolylbenzenes via the formation of triazapentalanes as nucleophilic nitrene equivalents reported by Ballesteros

Similarly to *N*-pyridinium aminides previously discussed, more recently, dioxazoles **192** were also envisioned as source of nitrene to construct functionalised 4-amino oxazoles **117** (Scheme 24).³⁰ Heteroaryl, cyclic, and polycyclic ynamides bearing electron-deficient, electron-rich or neutral substituents reacted smoothly with dioxazoles furnishing substituted oxazoles in moderate to excellent yield. Alkyl ynamides also react similarly to their aryl counterparts delivering 5-alkyl oxazoles **196**, albeit in significantly lower yield.

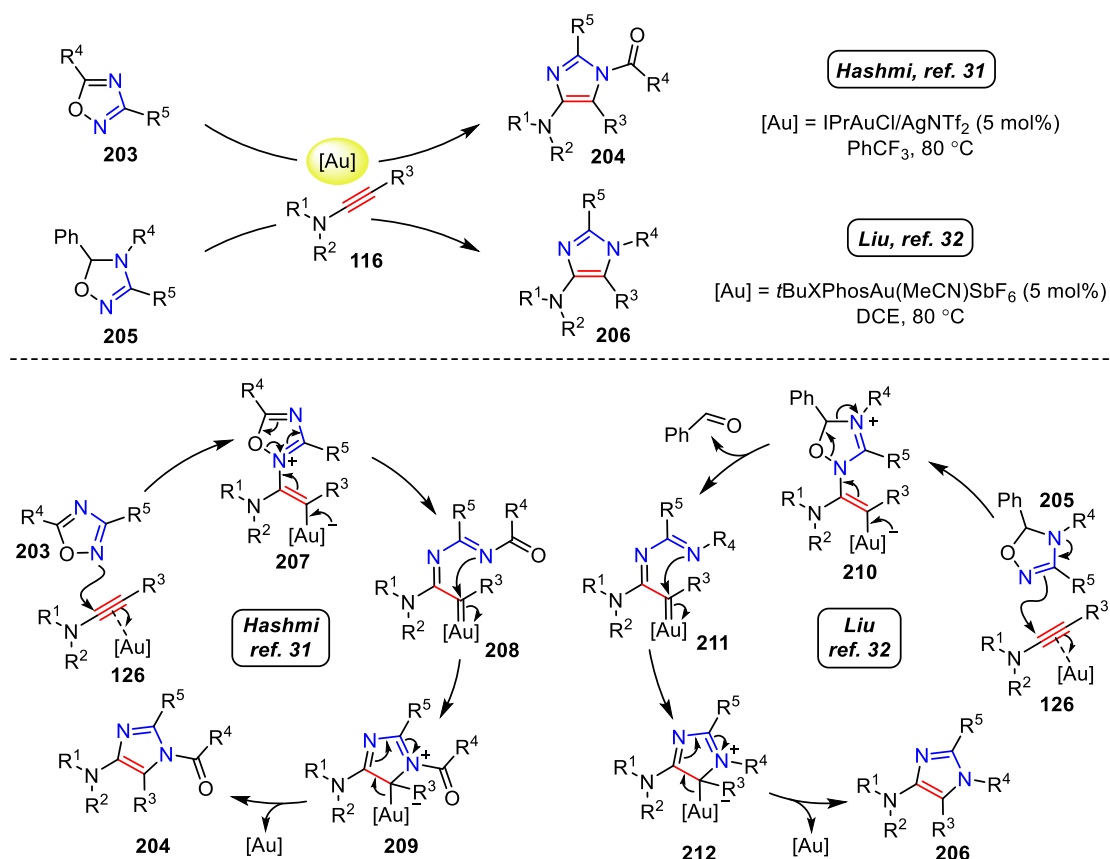
A control experiment on which dioxazole tethered ynamide **201** cyclised efficiently forming polycycle **202**, demonstrated the participation of a *N*-acyl α -imino gold carbene intermediate comparable to that of aminides. Yet in this case, the gold carbene is generated from the dioxazole ring opening and acetone elimination.



Scheme 24: Synthesis of oxazoles employing dioxazoles as nucleophilic nitrenoids

One of the latest nitrogen transfer reagents discovered are 1,2,4-oxadiazoles **203** and **205**, reported by Hashmi and co-workers³¹ and Liu and co-workers³² independently (Scheme 25). These nitrenoids participated in a gold catalysed [3+2] annulation with ynamides to form functionalised 4-aminoimidazoles **204** and **206**, respectively.

In Hashmi's methodology the substituent in position 4 of the oxadiazole remains as a pendant *N*-acyl group in the final oxazole (**204**). In contrast, Liu's transformation requires of a substituted 5-phenyl-4,5-dihydro-1,2,4-oxadiazole as starting material. In this way benzaldehyde is released from the reaction mixture upon ring opening of the oxadiazole core and the final oxazole **206** is eventually formed.



Scheme 25: Gold-catalysed synthesis of imidazoles reported by Hashmi and Liu respectively. Top: general reactions; Bottom: comparison of the proposed mechanisms

1.4. Conclusions

In the present chapter, nitrenes have been introduced as powerful electrophilic species to construct nitrogen containing compounds. Nonetheless, their practicality as nitrene transfer agents is limited due to poor functional group tolerance and poor selectivity. Some of these inconveniences have been partially solved with the utilisation of metallanitrenes, which are electrophilic nitrene equivalents relatively easy to generate *in situ*.

In particular, rhodium nitrenes became versatile intermediates to synthesise complex aza-heterocycles. Although rhodium nitrenes allow a superior control of the nitrene reactivity,

they still lack broad compatibility with many functionalities and frequently lead to undesired side-reactions and/or products.

During the last decade, a complementary route for the generation of nitrene character has been achieved using nucleophilic nitrenoids in combination with π -acid activated alkynes. Nucleophilic nitrenoids show superb ability especially to generate α -imino gold carbenes providing access to a wide array of transformations, such as cyclopropanation, 1,2-migration, C-H insertion or 4- π electrocyclicisation, from a common intermediate. In this way, powerful synthetic methodologies to construct nitrogen containing heterocycles, with excellent stereocontrol and in an atom economical manner can be accessed.

Numerous intra- and intermolecular methodologies have been developed employing nitrenoids as azides, aminides, azirines, oxazoles, dioxazoles, among others, with ynamides. This fact renders a prosperous future to the field with many attractive methodologies being developed on an ongoing basis.

The present thesis explores the potential of *N*-pyridinium *N*-heteroaryl aminides and other 1,3-*N,N*-dipoles as promising novel nucleophilic nitrenoids in gold-catalysed formal [3+2] cycloadditions with ynamides. The proposed building blocks are conceived as a means to rapidly produce complex functionally adorned heterocycles in a modular fashion.

CHAPTER 2:
***N*-PYRIDINIUM *N*-BENZO(HETEROARYL)
AMINIDES AS NUCLEOPHILIC NITRENOIDS**

In the previous chapter, nitrene transfer reactions onto π -acid activated alkynes have been presented as a potent strategy to construct complex aza-containing compounds. The use of nitrenoids to synthesise imidazole derivatives is one of the focus of this thesis.

Several compounds bearing an imidazole fragment show attractive physicochemical properties and biological activity. For instance, the imidazole motif is frequently found in natural products,³³ pharmaceuticals³⁴ and agrochemicals.³⁵ Ionic liquids³⁶ and fluorescent materials³⁷ commonly contain an imidazole core embedded in their structure. Apart from these, imidazoles also serve as precursors of *N*-heterocyclic carbenes (NHCs) to use in organometallics.³⁸ Therefore, the development of robust and general strategies to access these compounds is highly desirable.

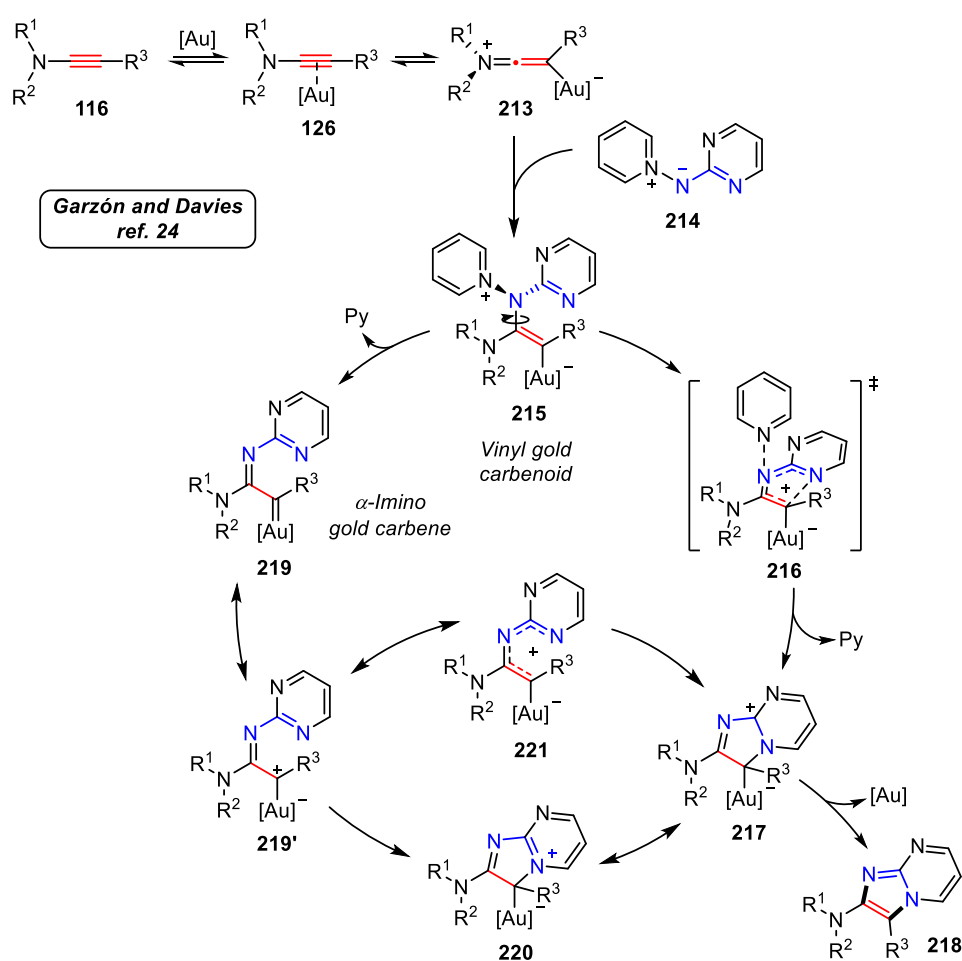
Chapter two commences with a brief presentation of the research previously accomplished by Miguel Garzón from the Davies group with *N*-pyridinium *N*-diazinyl aminides. That section sets the ground for the main topic discussed in chapter 2: reactivity and scope of *N*-pyridinium *N*-benzo(heteroaryl)aminides.

2.1. *N*-Pyridinium *N*-diazinyl aminides as 1,3-*N,N*-dipoles

Following the investigation of *N*-pyridinium *N*-acyl aminides as oxazole precursors, Garzón and Davies explored 1,3-*N,N*-dipole reactivity from *N*-pyridinium *N*-diazinyl aminides as means to construct imidazole derived heterocycles. These nucleophilic nitrenoids displayed analogous reactivity patterns to that of *N*-pyridinium *N*-acyl aminides in the gold-catalysed formal [3+2] cycloaddition with ynamides as previously discussed.²⁴

The desired nucleophilic nitrenoid reactivity was proposed to arise upon π -acid activation of the ynamide **116-126** forming gold keteniminium complex **213** (Scheme 26). Aminide **214**

approaches perpendicularly to the π -system, undergoing nucleophilic attack on the α -carbon of the ynamide. After reconfiguration of the aminide in vinyl gold carbenoid **215**, this could evolve in a concerted manner. Nucleofuge elimination occurs simultaneously to cyclisation *via* bis-hetero- 4π electrocyclicisation (**216-217**) by the development of a partial positive charge on the system. Final deauration and regeneration of the aromaticity of the fused ring would deliver imidazole **218** and recover the catalyst.

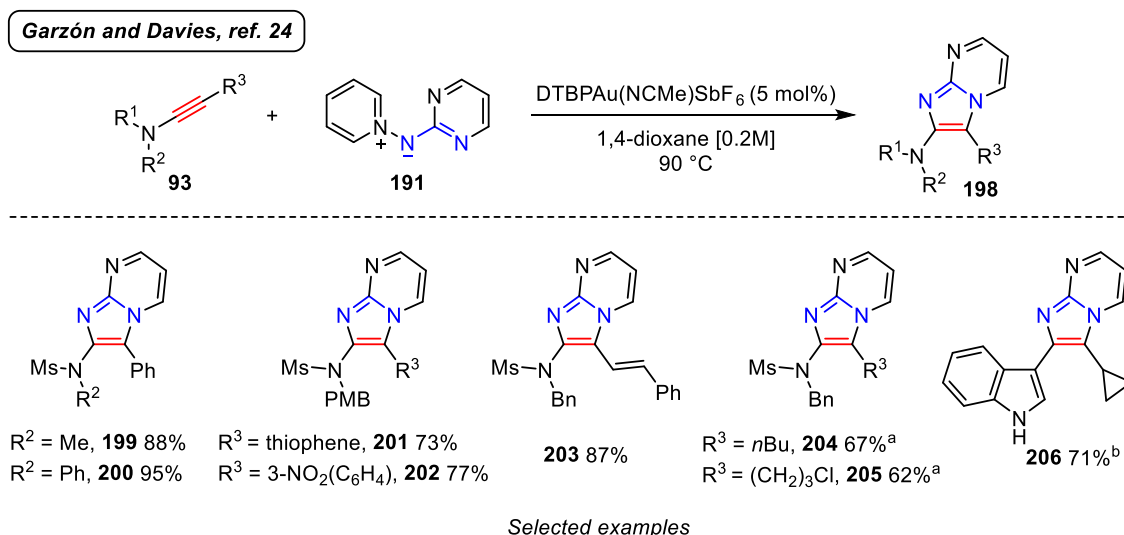


Scheme 26: Proposed mechanism for the formation of imidazolyl fused diazines reported by Garzón and Davies

Alternatively, vinyl gold carbenoid **215** could undergo a stepwise process. Nucleofuge elimination would lead to the formation of α -imino gold carbene/carbenoid **219-219'**, which

subsequently undergoes intramolecular attack from that nitrogen lone pair giving intermediate **220**. Otherwise, a 4- π electrocyclisation could also be possible from intermediate **221** due to the highly delocalised positive charge in **219'**. For cyclisation to occur, a *cis* configuration of **219'** is required, which would be disfavoured depending on the steric bulk of substituent R³, hampering the cyclisation process.

The reaction scope was evaluated across a range of ynamides utilising aminide **214** in the presence of a phosphite gold(I) complex (Scheme 27). *N*-Alkyl and *N*-aryl groups with different electron-rich and electron-deficient substituents in the *C*-terminus of the ynamide provided the desired fused heterocycle in good yields (**222-225**). Ene-ynamides and alkyl ynamides also proved to be suitable substrates in the cycloaddition affording the cyclisation pathway over (**226-228**) other possible side-reactions, such as Nazarov cyclisation or 1,2-C-H insertion.²⁰



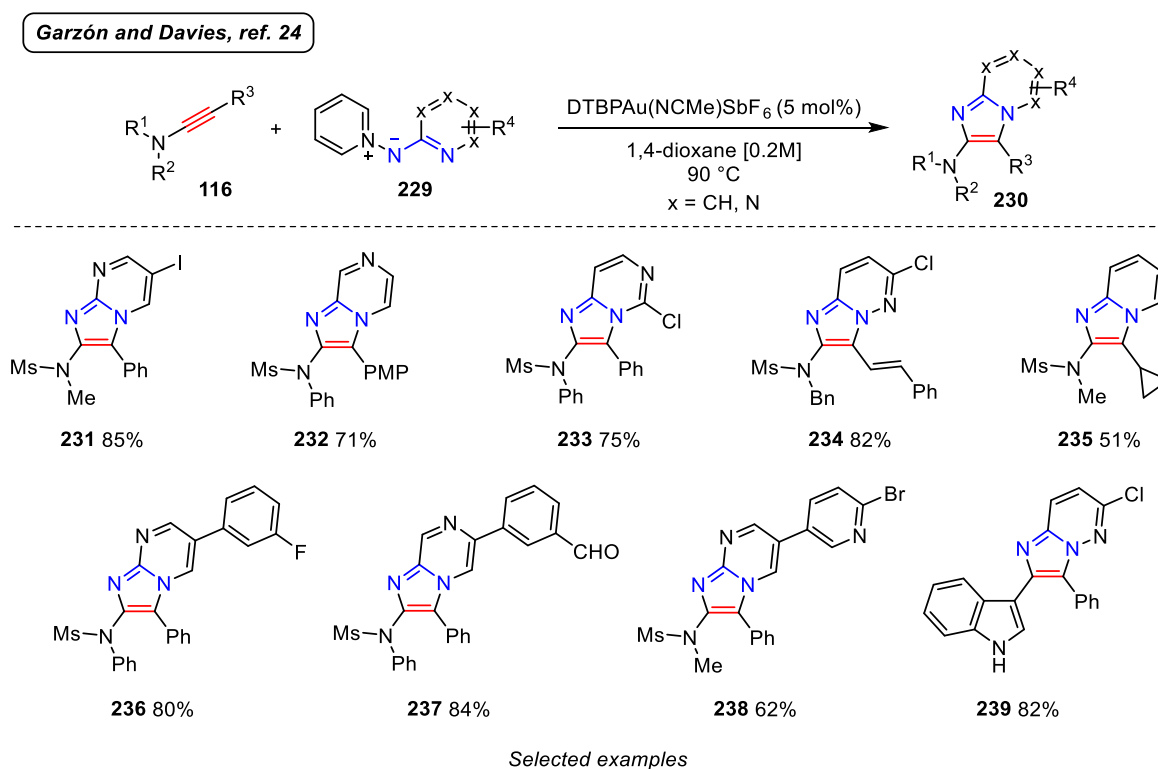
Scheme 27: Ynamide scope with *N*-pyridinium *N*-diazinyl aminide **191 in the gold catalysed cycloaddition reported by Garzón and Davies. ^a Using PicAuCl₂ (5 mol%); ^b Using 1,2-DCB at 120 °C**

The 3-(cyclopropylethynyl)-1*H*-indole also underwent the transformation in reasonable yield to give imidazole **229** but required higher temperature for good conversion. The distant

nitrogen is in conjugation with the alkyne and is able to activate the triple bond and to control the regioselectivity of the attack through an allene-like intermediate.

Structural variations on the aminide were introduced by employing diverse chlorinated diazine precursors, which could also be functionalised. In this way, eight different *N*-pyridinium *N*-diazinyl aminides and a *N*-pyridine derivatives were prepared to expand the scope of the transformation.

The combination of different ynamides with functionalised *N*-diazinyl aminides allowed to readily introducing a wide range of poly-aza substitution patterns in the imidazole structure (**231-239**) (Scheme 28).



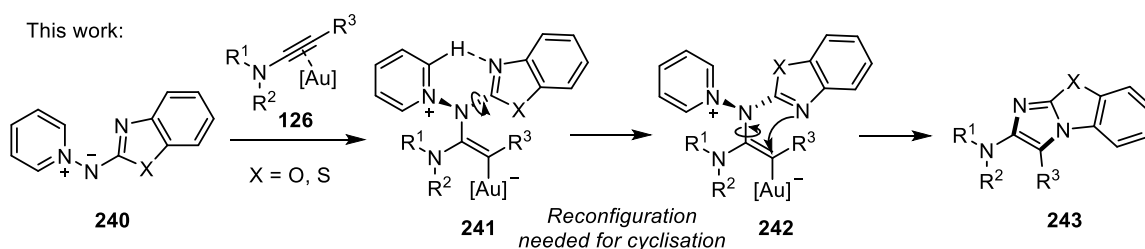
Scheme 28: Aminide scope in the gold catalysed cycloaddition reported by Garzón and Davies

Diazinyl aminides proved excellent substrates despite presenting electron-deficient heteroaryl rings, which could have made them less prone to undergo cyclisation. Limitations in the

reaction scope arose when employing an electron-rich *N*-pyridinium *N*-pyridine aminide, which did not afford complete conversion to imidazo[1,2-*a*]pyridine **235**. It was proposed that this was due to the higher aromaticity of the pyridine ring compared to that of the diazine ring. Consequently, disruption of the aromaticity of the pyridine to undergo cyclisation would have a higher activation barrier.

2.2. Synthesis of tri-fused imidazolyl heterocycles

Inspired by the potential of the 1,3-*N,O*- and 1,3-*N,N*-dipoles in the gold mediated cycloaddition, we sought to further explore the scope of this methodology to assemble more varied structural and functional complex imidazole based compounds. To this end, *N*-pyridinium *N*-benzo(thia/oxa)zole aminides **240** were conceived as new nucleophilic nitrenoids to open up access to valuable and rarely-explored poly-fused heteroaromatics **243** (Scheme 29).



Scheme 29: Proposed reactivity pathway to form tri-fused imidazoles

At the outset of the study, we considered that these aminides could be more challenging substrates for the annulation reaction. First, the (thia/oxa)zole ring is π -electron-rich as opposed to the π -deficient character of the diazinyI aminides investigated previously in the group. Therefore, either starting materials or products could function as ligands for the gold complex and could capture the catalyst.

Second, intramolecular H-bonding interactions in the aminide structure, which have previously been reported by Builla and co-workers,³⁹ could hamper the aminide from achieving the adequate reactive conformation and from accomplishing cyclisation.

Considering the lack of precedent for the preparation and reactivity of these species, problems in the synthesis of aminide derivatives could potentially arise during their preparation. In addition, aminides could also show issues of stability or handling.

Yet, the potential applications and uses of the resulting tri-fused compounds in biology, pharmaceutical or material science encouraged us to investigate deeply these new species.

2.2.1. Imidazole-fused benzo(heteroaryls) in medicinal and material science

The imidazo[2,1-*b*]benzo(heteroaryl) motif is present in many biologically active molecules and shows attractive pharmaceutical and medicinal properties, for instance as kinase inhibitors⁴⁰ (**244** and **246**) or antibacterial agents⁴¹ (**247**) (Figure 2).

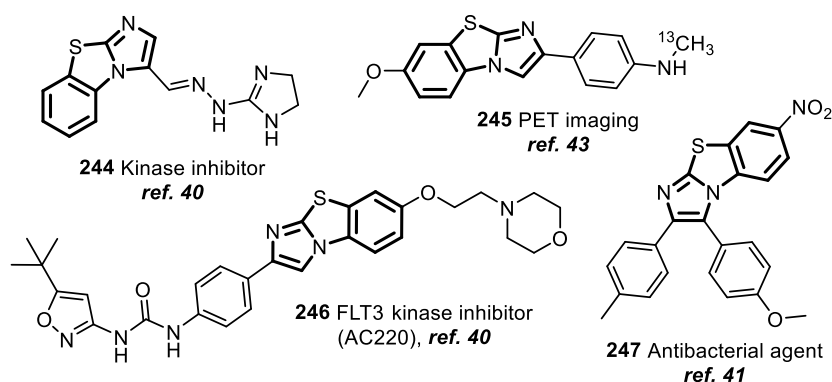
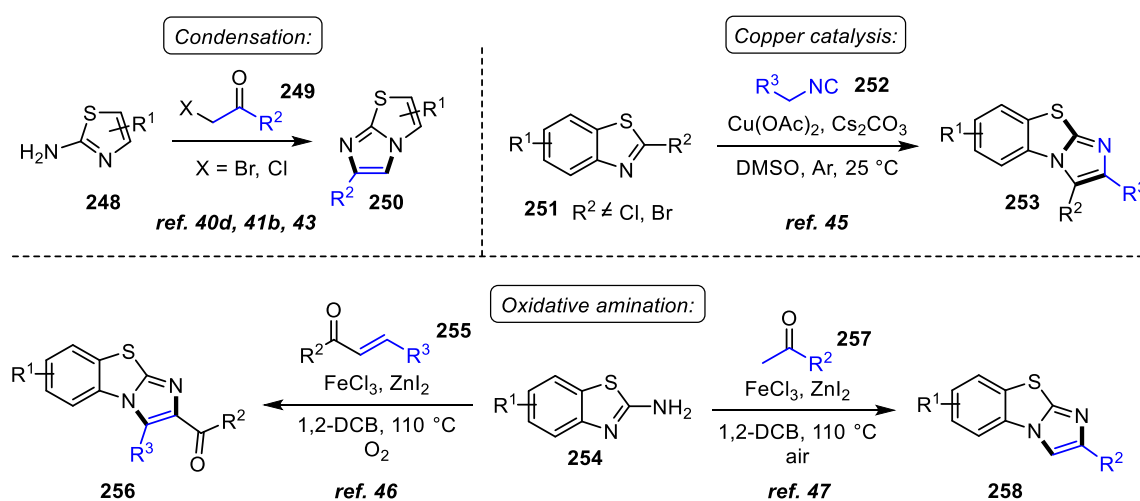


Figure 2: Biomedical active compounds containing an imidazo[2,1-*b*]benzothiazole framework

Other compounds possessing this core are known to exhibit antitumor activity against common cancers.^{40b, 42} Labelled molecules bearing this motif are used as pharmacophores for

PET-based imaging of A β plaques in Alzheimer's disease⁴³ (**245**). Additionally, imidazo[2,1-*b*]benzothiazoles are considered valuable building blocks in organic chemistry and have significant applications in material science.⁴⁴

Despite their numerous applications, routes to assemble the tricyclic imidazo[2,1-*b*]benzothiazole core are not straightforward, especially regarding the synthesis of some substitution patterns. Condensation of an aromatic amine **229** with an α -halo-carbonyl derivative **230** prevails as one of the most extended protocols to synthesize the fused imidazoles (Scheme 30).^{40d, 41b, 43} Wang and co-workers reported a copper catalysed transformation of isocyanides **252** with benzothiazoles **251**.⁴⁵ Oxidative amination of 2-aminobenzothiazoles **254** with α,β -unsaturated ketones **255** or ketones **257** also gives access to the tri-fused skeleton.



Scheme 30: Common routes to assemble the tri-fused imidazo[2,1-*b*]benzothiazole motif

Some disadvantages of the previous methodologies involve laborious preparation of the starting materials and limited functional group compatibility of the precursors. The nitrenoid approach presented in this thesis would allow to access more varied and functionalised imidazole derivatives in a modular fashion.

2.3. Aims and objectives

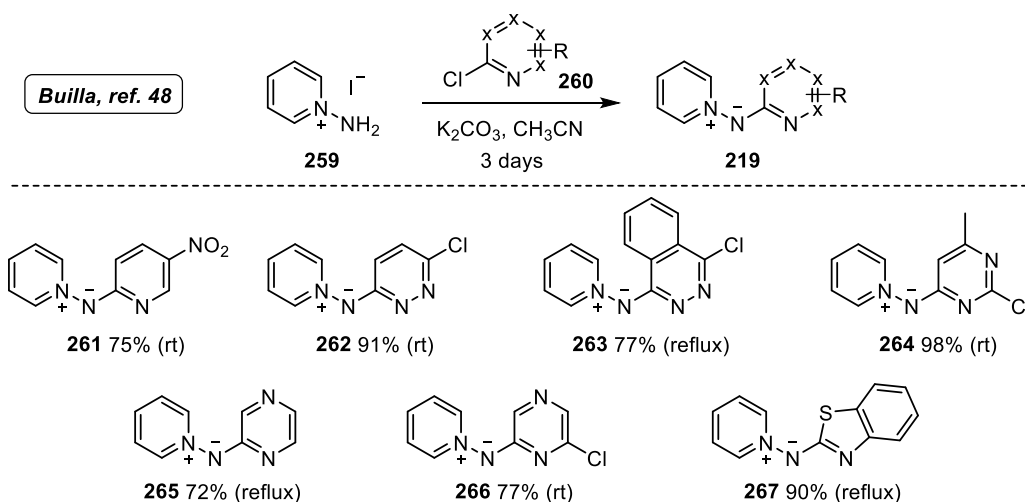
The main objective of this chapter is to explore the reactivity and scope of *N*-pyridinium *N*-benzo(heteroaryl) aminides as new nitrenoids. In particular, the main goal was the preparation of ynamides and aminides in a practical manner, as they are the primary species studied throughout the thesis. Investigation of the aminide scope is aimed by developing a main route to synthesise benzo(heteroaryl) aminide precursors, in addition to analyse the ynamide scope in the gold-catalysed [3+2] dipolar cycloaddition with benzo(thia/oxa)zole aminides.

We also sought to compare the reactivity of the new aminides in the gold-catalysed annulation with respect to other aminides series previously investigated in the Davies group to evaluate the versatility of the transformation.

2.4. Results and Discussion

2.4.1. Synthesis of *N*-pyridinium *N*-benzo(heteroaryl) aminides

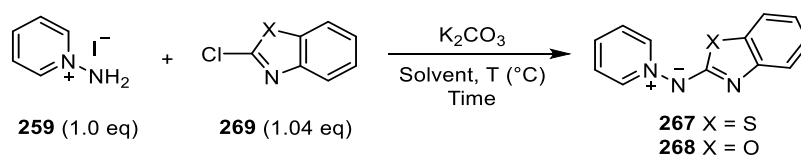
The applicability of *N*-pyridinium *N*-benzo(heteroaryl) aminides has been scarcely explored in the literature. Builla and co-workers⁴⁸ reported the first preparation in 2004, in which different 2-chloroheterocycles **260** reacted with *N*-aminopyridinium iodide (**259**) and potassium carbonate in acetonitrile at reflux for 3 days, affording the corresponding *N*-pyridinium aminides **261-267** (Scheme 31).



Scheme 31: Synthesis of aminides reported by Builla and co-workers

Our initial focus was to make the preparation of aminide **267** more practical, mainly to reduce the reaction time (Table 1). Acetonitrile and methanol were selected as solvent systems due to the high polarity of the aminides.

Table 1: Screening of the conditions for aminide formation



Entry	Aminide	Solvent	T (°C)	Time (h)	Purification method	Yield ^a (%)
1	X = S	CH ₃ CN	rt	72	Filtration + column	>100
2	X = S	MeOH	rt	24	Filtration + column	>100
3	X = S	CH ₃ CN	83	20	Filtration + column	>100
4	X = S	MeOH	65	22	Filtration + column	>100
5	X = S	CH ₃ CN	83	20	Filtration + extraction + column	93
6	X = S	MeOH	65	21	Filtration + extraction + column	90
7	X = S	MeOH	rt	22	Filtration + extraction + column	95
8	X = S	MeOH	rt	24	Extraction + column	98
9	X = O	MeOH	rt	16	Extraction + column	92

^a Isolated yield after purification by the stated method

The reaction was performed at reflux and at room temperature using both solvents (entries 1-4). The yields obtained after filtration through Celite and purification by flash column chromatography were over 100%, suggesting the presence of inorganic impurities or the product in the form of a potassium salt.

The work-up procedure was then changed and we then proceeded to treat the crude mixture with a solution of NaOH [2.5 M] followed by extraction with CH₂Cl₂ (entries 5-7). In this way high yields of **267** were achieved giving analytically pure aminide as a bright yellow powder. In order to achieve a more practical preparation, the same reaction was performed without carrying out the filtration (entry 8). Since the conversion was maintained (compared entry 7 and 8), it was decided to proceed with this procedure for the preparation of **267**. An analogous procedure was followed to synthesise aminide **268** (Entry 9).

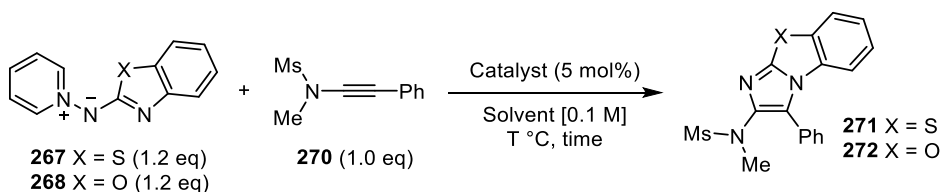
2.4.2. Investigating the reactivity of the new nitrenoids in the [3+2] gold catalysed cycloaddition

The reactivity of *N*-pyridinium *N*-benzo(thia/oxa)zole aminides **267** and **268** was tested in the gold catalysed cycloaddition using ynamide **270**. As starting point, the new aminides were tested under the optimised reaction conditions utilised for the diazynil series. Preliminary results showed lower reactivity of the *N*-benzo(thia/oxa)zole aminides, and thus an optimisation survey was performed by Garzón (Table 2).

Moderate conversion was achieved when employing phosphite gold(I) as a catalyst regardless of the solvent used (entries 1-3). Dichloro(2-pyridinecarboxylato)gold afforded higher conversion especially at high temperatures in shorter reaction times (entries 4-6). No reactivity was observed in the absence of catalyst (entry 7) or when using zinc triflate replacing a gold complex (entry 8). 1,2-Dichlorobenzene at 125 °C was established as the

ideal reaction conditions employing a more electrophilic gold(III) catalyst (entries 6 and 10), which provided imidazolyl benzo(thia/oxa)zole **271** and **272** in excellent yields, with relatively short reaction times and complete regioselectivity.

Table 2: Summary of the screening accomplished by Garzón



Entry	Aminide	Catalyst	Solvent	T (°C)	t (h)	Yield (%) ^a
1	X = O	DTBPAu(NCMe)SbF ₆	1,4-dioxane	90	24	(26)
2	X = O	DTBPAu(NCMe)SbF ₆	<i>m</i> -xylene	120	24	44
3	X = O	DTBPAu(NCMe)SbF ₆	1,2-DCB	125	24	44
4	X = O	PicAuCl ₂	1,4-dioxane	90	24	81
5	X = O	PicAuCl ₂	1,2-DCB	90	24	76
6	X = O	PicAuCl ₂	1,2-DCB	125	6	84
7	X = O	--	1,2-DCB	125	24	--
8	X = O	Zn(OTf) ₂	C ₆ H ₅ Cl	100	24	--
9	X = S	PicAuCl ₂	1,4-dioxane	90	24	50
10	X = S	PicAuCl ₂	1,2-DCB	125	8	87

^a Isolated yield after purification by flash column chromatography. Yield in parenthesis calculated by ¹H NMR spectroscopy against a known quantity of 1,2,4,5-tetramethylbenzene. Reaction optimization performed by Garzón

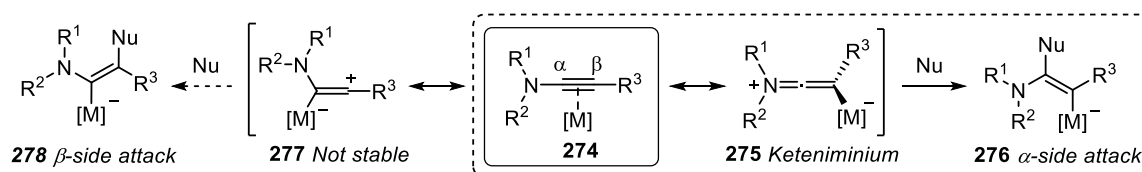
2.4.3. Ynamides as electron-rich alkynes

At this stage, we sought to further study the reactivity of aminides **267** and **268** by testing them with a range of ynamides in order to prove the generality of these compounds as nucleophilic nitrene equivalents.

2.4.3.1. Introduction to ynamides

Ynamides were considered excellent reaction partners for the gold-catalysed formal [3+2] dipolar cycloaddition due to their ability to coordinate to π -acid catalysts, but more importantly because they provide regioselective control.

Formally, ynamides are electronically biased triple bonds owing to the presence of an adjacent nitrogen atom. The nitrogen activates and polarises the alkyne allowing for more controllable reactivity. Coordination of the ynamide to a metal complex (**274**) forms a resonance keteniminium intermediate (**275**), which selectively directs the attack of the nucleophile towards the α -position of the ynamide (**276**) (Scheme 32).



Scheme 32: Ynamide controls the regioselectivity of the reaction

Depending on the nature of the R^1 substituent, several classes of ynamides are reported in the literature, such as yne-amides, yne-carbamates, yne-phosphoramides and yne-sulfonamides.^{23a} This work mainly focuses on the use of yne-sulfonamides **282** to study the gold-catalysed formal [3+2] cycloaddition with nucleophilic nitrenoids (Figure 3).

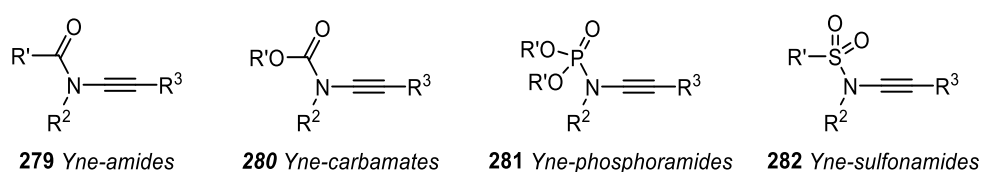
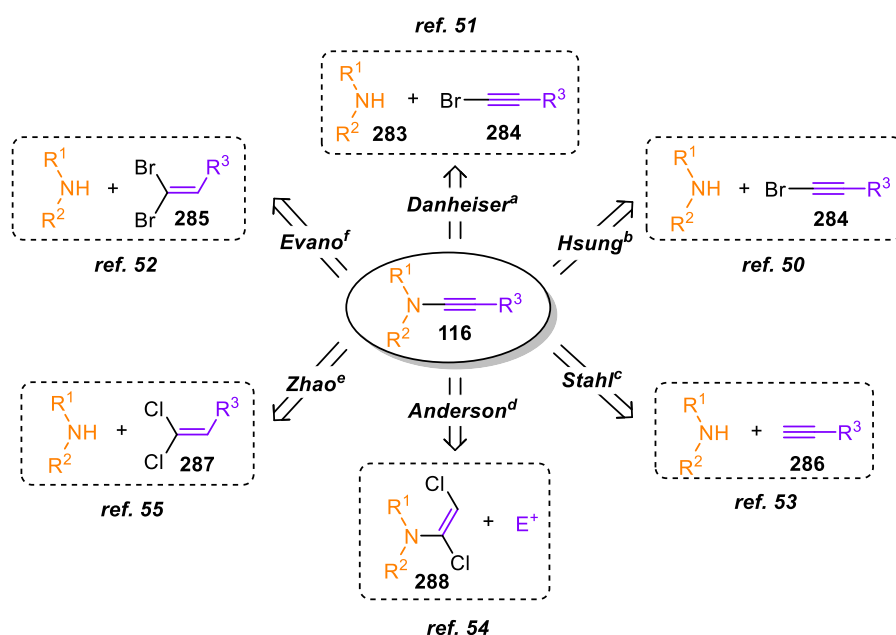


Figure 3: Most common types of ynamides

Due to their stability and easy handling, many transformations make use of these species as precursors to build up molecular complexity. In addition, they are regular building blocks in many synthetic routes and participate in the preparation of natural products.⁴⁹

Numerous protocols have been described in the literature for ynamide preparation (Scheme 33). The use of haloenamides under copper catalysis is the main route employed by many

groups. For instance, while Hsung⁵⁰ and Danheiser⁵¹ utilises bromoalkynes (**284**), Evano's⁵² methodology requires 1,1-dibromoalkenes (**285**). Stahl⁵³ developed a copper catalysed oxidative amination of terminal alkynes (**286**). In addition, initial transition metal free strategies have been improved by Anderson⁵⁴ and Zhao⁵⁵ using 1,2- and 1,1-dichloroenamides (**288** and **287**), respectively. The latter provides a straightforward route for terminal ynamide preparation.



Scheme 33: Reported methodologies to synthesise ynamides.^a Using KHMDS, CuI, pyridine at rt; ^b Using CuSO₄·5 H₂O (5-20 mol%), 1,10-phenanthroline, K₃PO₄, toluene at 60-95 °C; ^c CuCl₂ (20 mol%), Na₂CO₃, pyridine, O₂ (1 atm), toluene at 70 °C; ^d Using 1) PhLi, THF, -78 °C; 2) "E⁺", THF, -78 °C to rt; ^e Using Cs₂CO₃ or NaH, DMSO at 70 °C; ^f Using CuI (12 mol%), DMEDA (18 mol%), Cs₂CO₃, dioxane at 60 °C or DMF at 70 °C

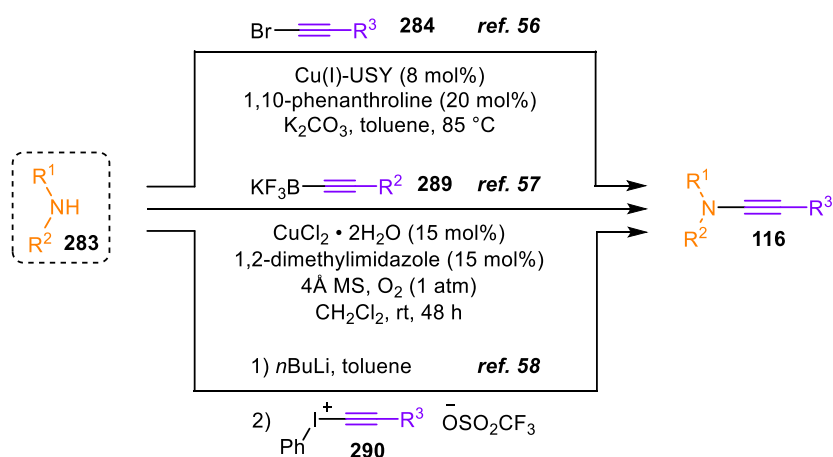
While Hsung's methodology is more effective using lactams, oxazolidinones or cyclic amides, Evano's allows the use of tosylamines. Ynamides bearing acyclic carbamates are successfully formed employing Danheiser's conditions. Complementary to these, Stahl's methodology permits to introduce alkyl substituents in the carbon end of the π -system. The advantage of this procedure over the rest is the direct use of commercially available terminal

alkynes, albeit requiring a significant loading of the amide starting material (5 eq.) and an oxygen atmosphere.

Carbamates, cyclic and bulky amides can be applied in the ynamide formation using Anderson's reaction conditions. Finally, Zhao's transition-metal free procedure can be used for the preparation of ynamides bearing substituents such as aniline sulfonamides, oxazolidinones, indoles, carbazoles, among others. Terminal or internal ynamides can be synthesised employing Zhao's methodology as well.

In general, the wide applicability and practicality of these routes rely on the use of inexpensive starting materials and the introduction of valuable functionality. Nevertheless, stepwise preparation of the haloenamides and the instability of di-bromoenamides or bromoalkynes are the main issues of some of the aforementioned methodologies.

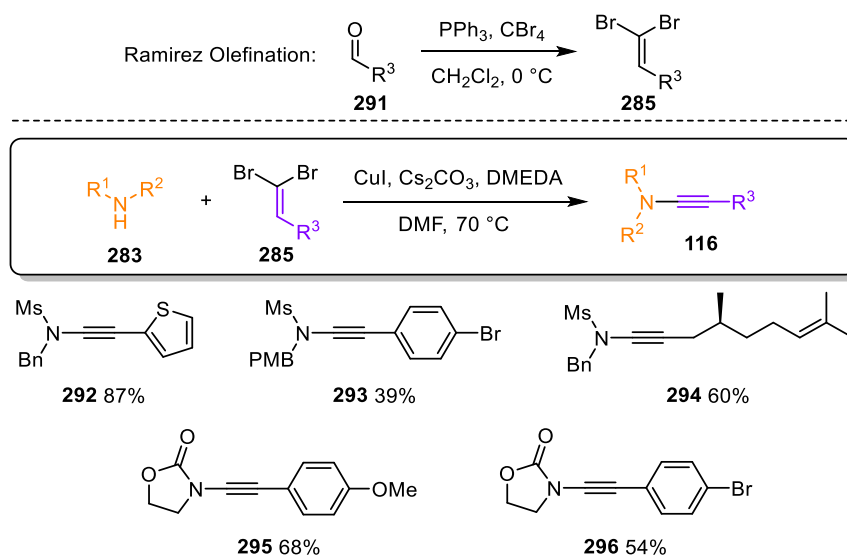
Other alternative methods for ynamide formation reported in the literature consist on using copper-zeolites,⁵⁶ potassium alkynyltrifluoroborates (**289**)⁵⁷ or alkynyliodonium salts (**290**)⁵⁸ (Scheme 34).



Scheme 34: Other methodologies reported for the preparation of ynamides

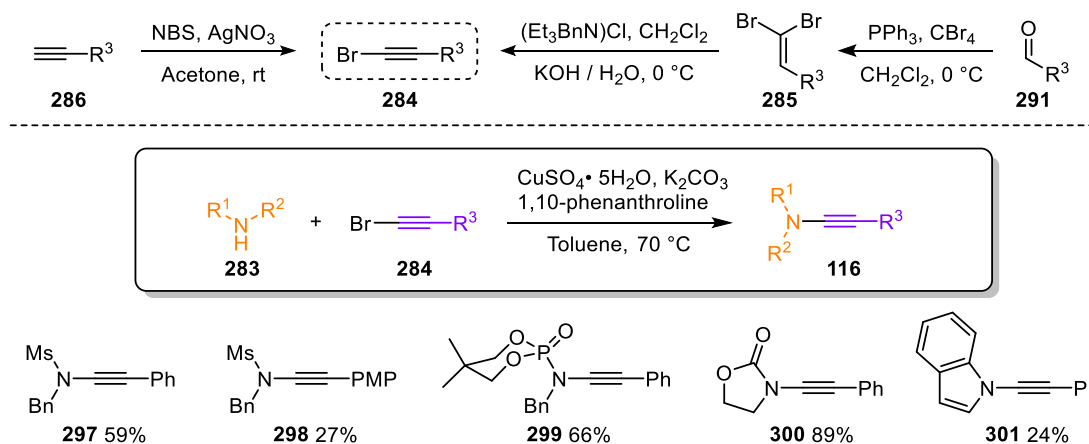
2.4.3.2. Ynamide preparation via 1,2-dibromoolefins or via bromo alkynes

Ynamides utilised in this work were prepared following Evano,⁵² Hsung⁵⁰ or Anderson⁵⁴ methodology. Ynemides prepared using Anderson's procedure are presented in Chapter 4. The procedure reported by Evano⁵² required aldehydes **291** to be converted to their corresponding 1,1-dibromoalkenes following the Ramirez Olefination⁵⁹ (Scheme 35). Dibromoalkenes **285** were then reacted with sulfonamides **283** or oxazolidinones under copper(I) catalysis.



Scheme 35: Ynamides prepared following Evano's method

Hsung's methodology required a bromoalkyne **284** to be coupled with the sulfonamide or amide of choice by copper(II) catalysis (Scheme 36). Bromoalkynes **284** were accessible from the reaction of the corresponding terminal alkyne **286** with NBS catalysed by a silver salt. They needed to be used within 24 hours in the ynamide formation step due to their instability. 1,1-Dibromoolefins **285** also served as suitable precursors, since they could be converted into bromo alkynes **284** using triethylbenzylammonium chloride.



Scheme 36: Ynamides prepared following Hsung's procedure

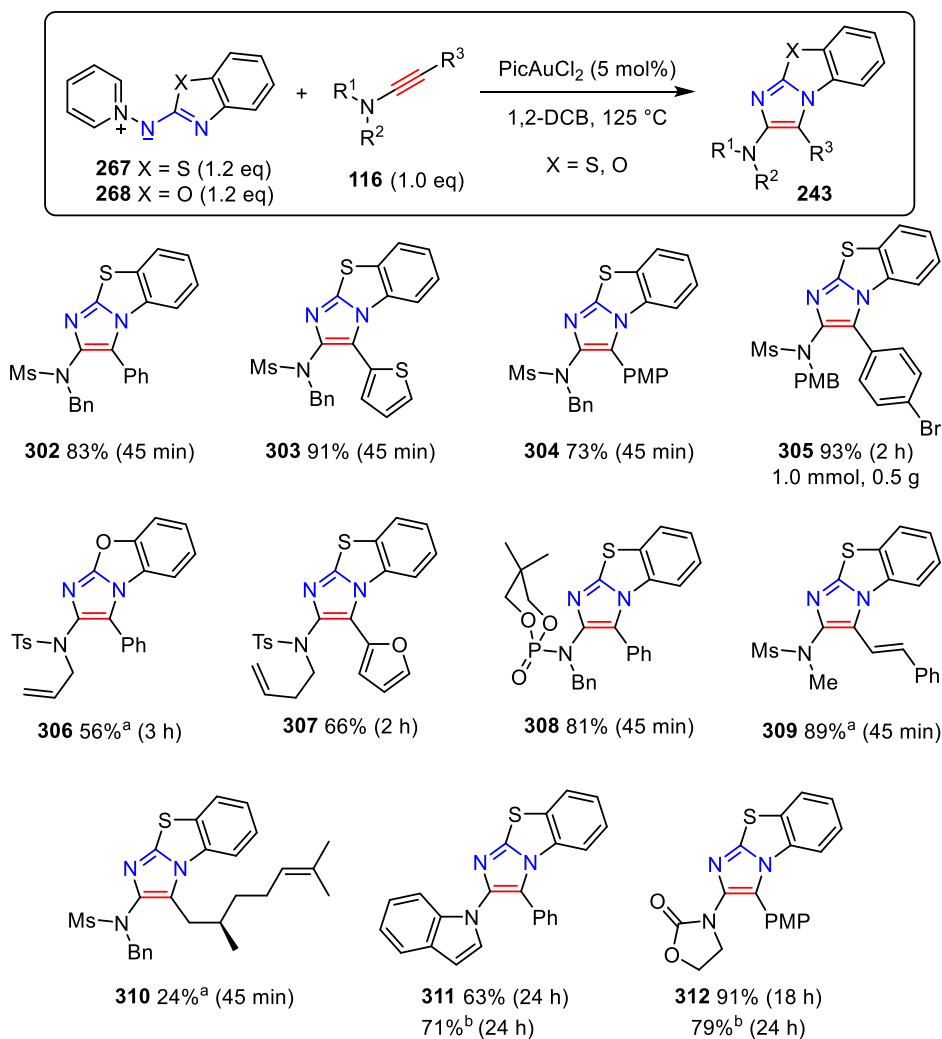
Apart from the ones presented in Scheme 35 and Scheme 36, several ynamides that were used in the gold catalysed cycloaddition reaction throughout this thesis were prepared by other members of the group, as mentioned in the collaboration statement (see Appendix).

2.4.4. Ynamide scope in the gold-catalysed formal [3+2] dipolar cycloaddition with *N*-pyridinium *N*-benzo(thia/oxa)zole aminides

The reactivity of aminides **267** and **268** was evaluated across a range of ynamides utilising the optimised reaction conditions obtained by Garzón (Scheme 37).

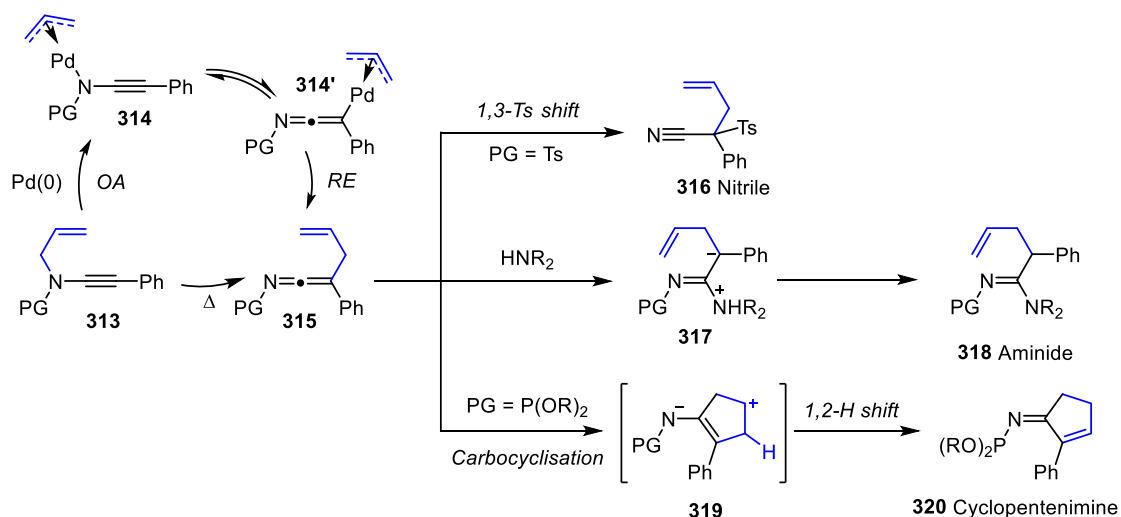
N-Benzyl, *N*-alkyl and *N*-*p*-methoxybenzyl substituents on the sulfonamide moiety were well tolerated. Variations on the ynamide at the carbon substituent with more electron-rich or electron-deficient heteroaryls proved successful (**302-305**). The robustness of the reaction was showcased with the preparation **305** on 1.0 mmol scale.

N-Phosphoryl-ynamide **299** functioned well as stabilising group on the ynamide structure, providing imidazole **308** in excellent yield and in similar reaction times.



Scheme 37: Study of the ynamide scope with *N*-pyridinium *N*-benzothiazole aminides in the gold-catalysed formal [3+2] cycloaddition. ^a Using 1,2-dioxane at 90 °C; ^b Using DTBPu(NCMe)₃SbF₆ as catalyst.

N-Allyl-ynsulfonamides are known to undergo intra aza-Claisen rearrangements in the presence of a palladium(0) source or when heated (Scheme 38).⁶⁰ Despite the temperature required for the gold mediated annulation, an *N*-allyl-ynsulfonamide underwent the cycloaddition preferentially over the aforementioned thermal intramolecular aza-Claisen rearrangement forming imidazole **306**.



Scheme 38: Aza-Claisen rearrangement known in the literature of *N*-allyl-ynsulfonamides

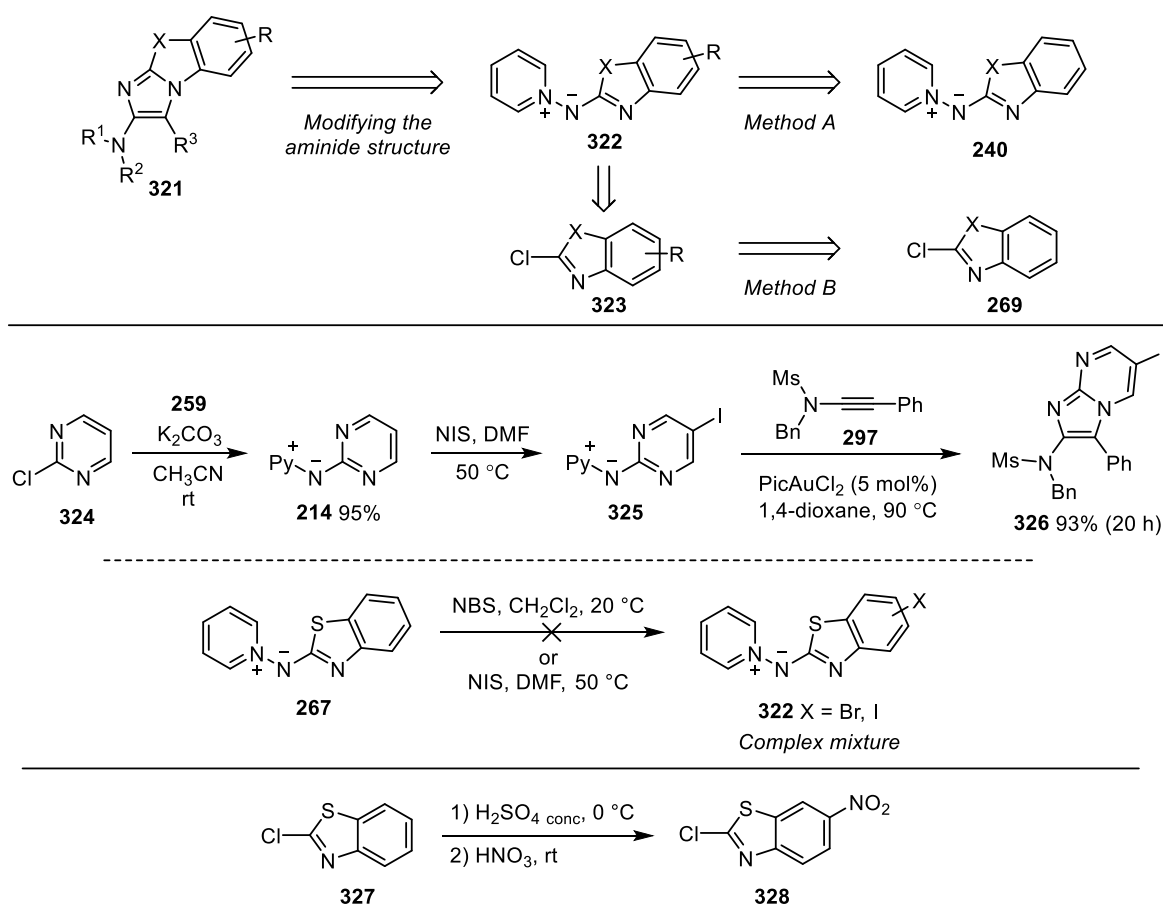
An ene-ynamide prepared from *trans*-cinnamaldehyde afforded imidazole **309** with excellent conversion despite the tendency of ene-ynamides to undergo cyclopropanation under gold catalysis.^{16, 61}

The introduction of alkyl substituents in position 3 of the imidazole proved troublesome. The use of milder reaction conditions did not improve the conversion (see example **286**). It is believed that a competing $1,2\text{-C-H}$ insertion onto the α -imino gold carbene intermediate (see Scheme 14) is faster than the desired intramolecular cyclisation resulting in poor conversion to **310**. Yet still, no product from a $1,2\text{-C-H}$ insertion could be isolated.

N-Indolyl and *N*-oxazolidinolyl ynamides were also compatible with this transformation giving imidazoles **311** and **312**, respectively, in good yield. Nonetheless, longer reaction times were required to achieve complete conversion. This fact could be due to the delocalisation of the nitrogen lone pair across the indole ring or the amide motif of the oxazolidinone.

2.4.5. Introducing variations on the nitrenoid structure

Having proved the potential of *N*-pyridinium *N*-benzo(thia/oxa)zoles as a new class of nucleophilic nitrenoids, our next aim was directed towards introducing more functionality on the imidazole heterocycle using functionalised aminides. Two main strategies were considered, the first approach consisted of direct halogenation of the aminide core (**240**) (Scheme 39-top).



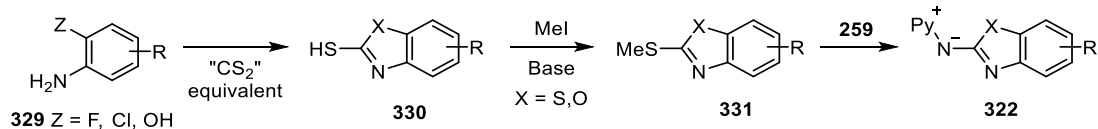
Scheme 39: Top: Planned strategies to functionalise the imidazole derivatives through the aminide. Middle: Attempted halogenation on the aminide core. Bottom: Nitration of 2-chlorobenzothiazole

As in the *N*-pyridinium *N*-diazinyl series, halogenation followed by cross-coupling reaction proved an effective route to further vary the aminide structure (see **324** to **326**).²⁴ Unfortunately, in the *N*-pyridinium *N*-benzo(thia/oxa)zole aminide series control of the

regioselectivity was a problem when either bromination or iodination were attempted for subsequent modifications (**267** to **322**).

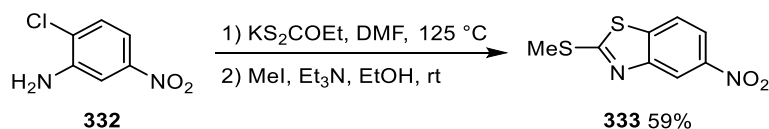
We then proceeded by modifying 2-chlorobenzo(thia/oxa)zole precursors **323**. 2-Chlorobenzothiazole **327** was nitrated forming 2-chloro-6-nitrobenzo[*d*]thiazole **328** as a single regioisomer in excellent yield. Further modifications were attempted on **327** and **328** such as halogenation of the benzene ring or reduction of the nitro group, respectively. However, issues in controlling the regioselectivity and polysubstitution in the electrophilic aromatic substitution reaction restricted the applicability of this approach.

To circumvent these problems, an alternative strategy employing commercially available *o*-halo or *o*-hydroxy aniline derivatives **329** was attempted (Scheme 40). In that case, functionality was installed prior to formation of the benzo(thia/oxa)zole ring. Anilines were to be reacted with a CS₂ equivalent, delivering thiol-benzoheterocycles **330** that were subsequently methylated. Thioamides **331** were used as electrophiles in the synthesis of aminides **322** and thus, problems regarding regioselectivity and poly-substitution were overcome.

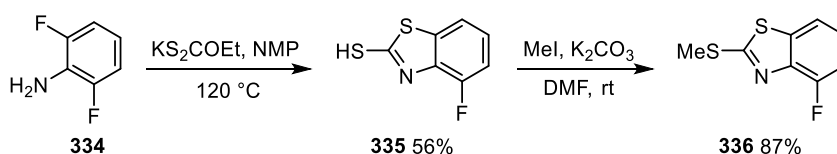


Scheme 40: Proposed strategy via thioamides to synthesise benzo(heteroaryl) precursors

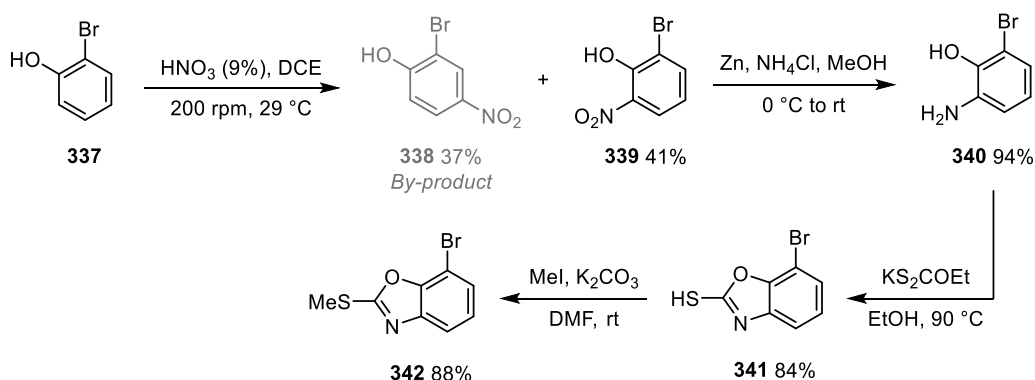
2-Chloro-5-nitroaniline was treated with potassium ethylxanthate in DMF to form the corresponding thiol. As purification of the thiol was troublesome, a practically more convenient two-step sequence utilising the same reagents was performed delivering 2-(methylthio)-5-nitrobenzo[*d*]thiazole **333** in good yield.



The introduction of a substituent in the 4-position of the aminide precursor was achieved starting from 2,6-difluoroaniline. Formation of **335** using potassium ethyl xanthate and NMP at 120°C , followed by methylation, delivered sulfide **336** in 87% yield.

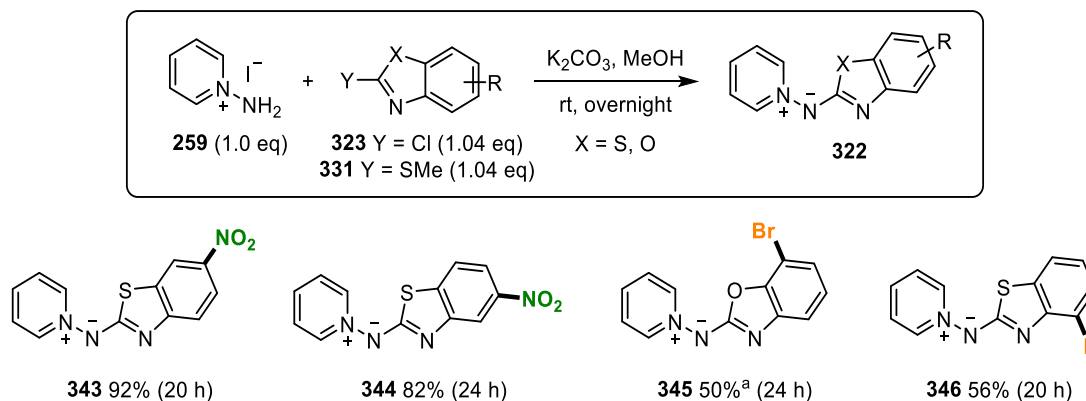


An effective but lengthier route was required to prepare benzoxazole **342** bearing a bromide substituent. Commercially available 2-bromo-6-nitrophenol was sonochemically nitrated following Bhanage's procedure.⁶² Precise control of the speed of the stirring was crucial to favour *ortho* nitration over *para* substitution. Subsequent reduction with zinc metal provided amine **340** in excellent yield. Thiol formation and methylation proceed smoothly giving access to 7-bromo methyl sulfide **342**.



With two complementary routes established for the preparation of functionalised aminide precursors, 2-chloro and 2-methylsulfide benzo(heteroaryls) (**323** and **331**) were tested with *N*-aminopyridinium iodide (Scheme 41). Gratifyingly, both chlorides and sulfide groups functioned well as leaving groups in the $\text{S}_\text{N}\text{Ar}$ reaction. All precursors reacted smoothly

giving access to a range of functionalised nitrenoids **343-346**. Nitrated benzoheteroaryls afforded better conversions than the halogenated ones. In case of aminides **345** and **346**, starting material was recovered even after prolonged reaction times.



Scheme 41: Novel functionalised aminides. ^a Utilising CH₃CN at 83 °C

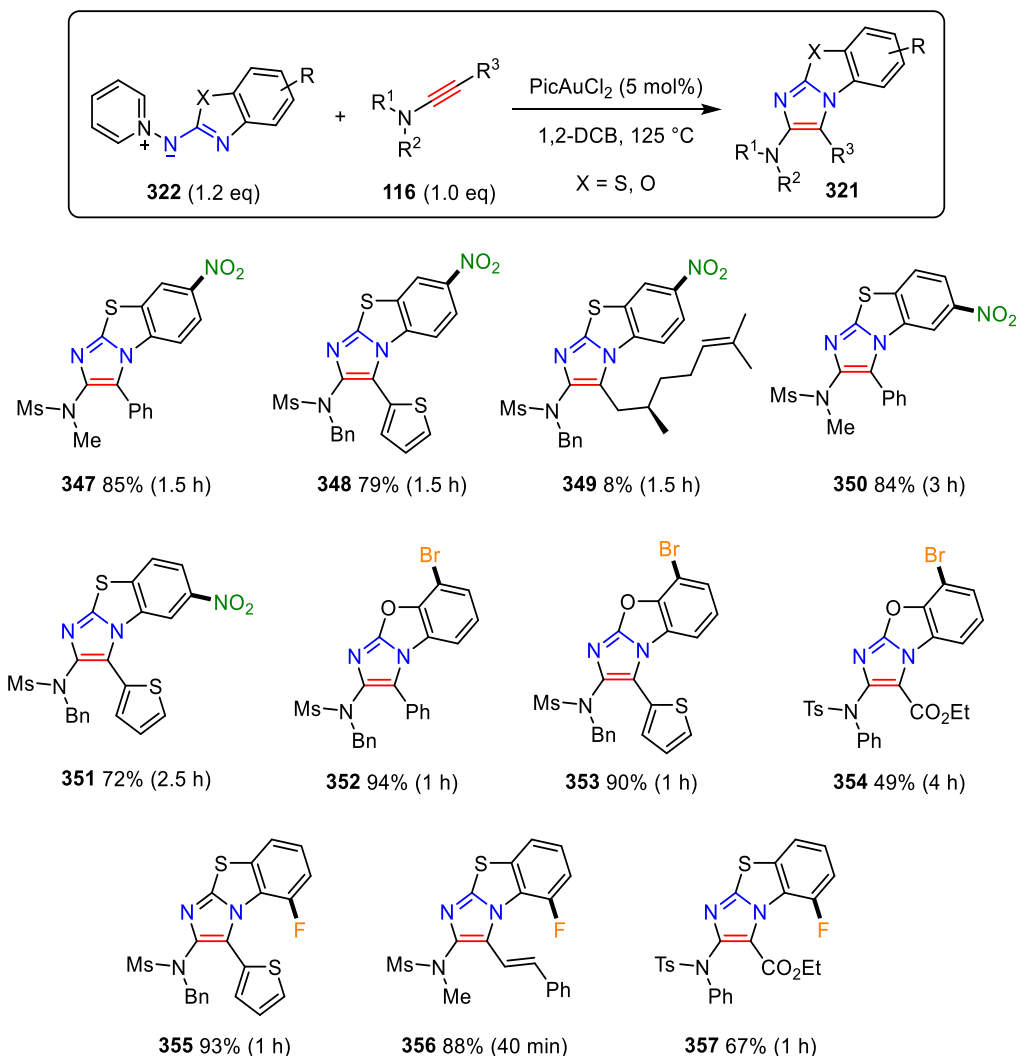
2.4.6. Surveying the reactivity of the functionalised aminides

With a collection of functionalised benzo(thia/oxa)zole aminides in hand, our next target was set on exploring their reactivity in the formal [3+2]-dipolar cycloaddition. Ynamides bearing interesting functionalities or that afforded good conversions in our previous study were chosen to analyse the behaviour of these aminides in the cycloaddition reaction.

The majority of nitrenoids performed the transformation at 125 °C in 1,2-DCB smoothly (Scheme 42). The reactions were fast, clean, proceeded with complete conversion and defined regioselectivity.

Regarding the aminide scope, the relative position of the nitro or halogen substituent in the aminide had no or little impact in the cyclisation. Slightly longer reaction times were required to reach completion when utilising more electron-deficient aminides bearing a nitro group (**347-351**). This could be attributed to the larger delocalization of the negative charge of the

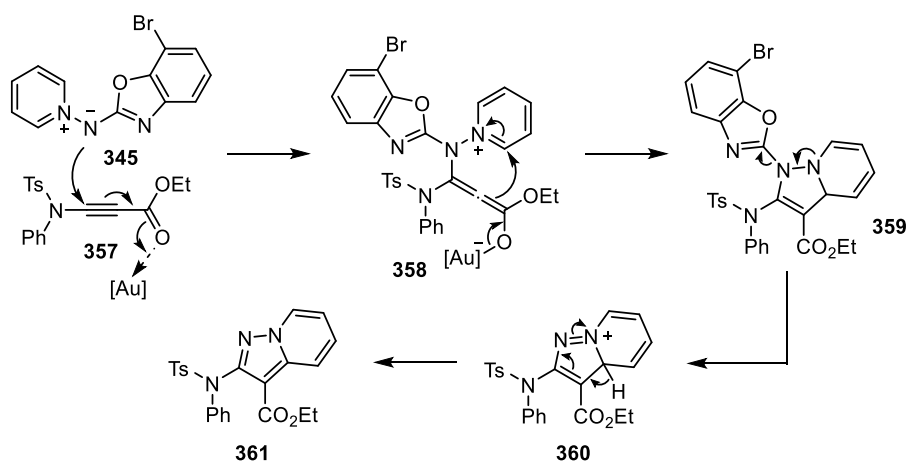
N,N-dipole across the benzothiazole ring when a nitro group is present. As a result, the cyclisation is slowed down.



Scheme 42: Synthesis of highly functionalised imidazo[2,1-*b*]benzo(heteroaryls)

As observed when investigating the ynamide scope, *N*-alkyl ynamides were unsuitable substrates, as exemplified by the low yield of imidazole **351**. In contrast, ene-ynamide (forming **355**) underwent the transformation smoothly without detecting the presence of any other by-products of a possible cyclopropanation side-reaction.^{16, 61}

An ester derived ynamide afforded moderate yield of **354** and **357** when reacted with aminides **345** and **346**, respectively. We hypothesise that this decrease in reactivity observed could be due to a side-reaction to form a pyrazole derivative. This undesired pathway has previously been observed in the *N*-pyridinium *N*-acyl aminide series by Gillie *et al.*²² who manage to isolate and fully characterise the pyrazole side-product. In this case, we proposed that π -activation of the carbonyl by the gold complex could lead to the formation of intermediate **358**, which can then cyclise to form **359** (Scheme 43). Elimination of the benzoxazole group and subsequent rearomatization of **360** would deliver pyrazole **361**.



Scheme 43: Proposed pyrazole formation side reaction using ynamide 332 based on the results reported by Gillie *et al.*

2.4.7. Mechanistic considerations

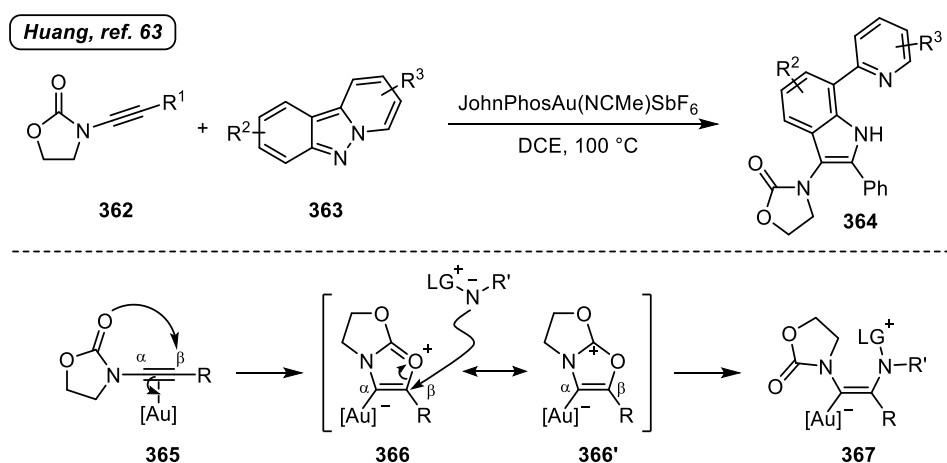
Having demonstrated the ability of these new nitrenoids to display the required 1,3-*N,N*-dipole in the synthesis of tri-fused heterocycles with ynamides, an analogous mechanistic rationale to that of the *N*-diazinyl aminides was proposed (see scheme 26).

In general, high conversions to the corresponding imidazoles were observed, the only exception being when using alkyl ynamides. This suggests that a competing 1,2-C-H insertion is faster than the desired intramolecular cyclisation.

In contrast, when alkyl ynamides were used with *N*-diazinyl aminides they proved good substrates (see scheme 27). This fact highlights that cyclisation of the pyrimidinyl ring has lower activation energy than that of the benzo(thia/oxa)xole ring. The difference in reactivity observed is in agreement with the lower reactivity of *N*-benzo(thia/oxa)zole aminides with respect to the *N*-diazinyl ones as 1,3-*N,N*-dipoles.

2.4.8. Oxazolidinone based ynamides in the gold catalysed cycloaddition

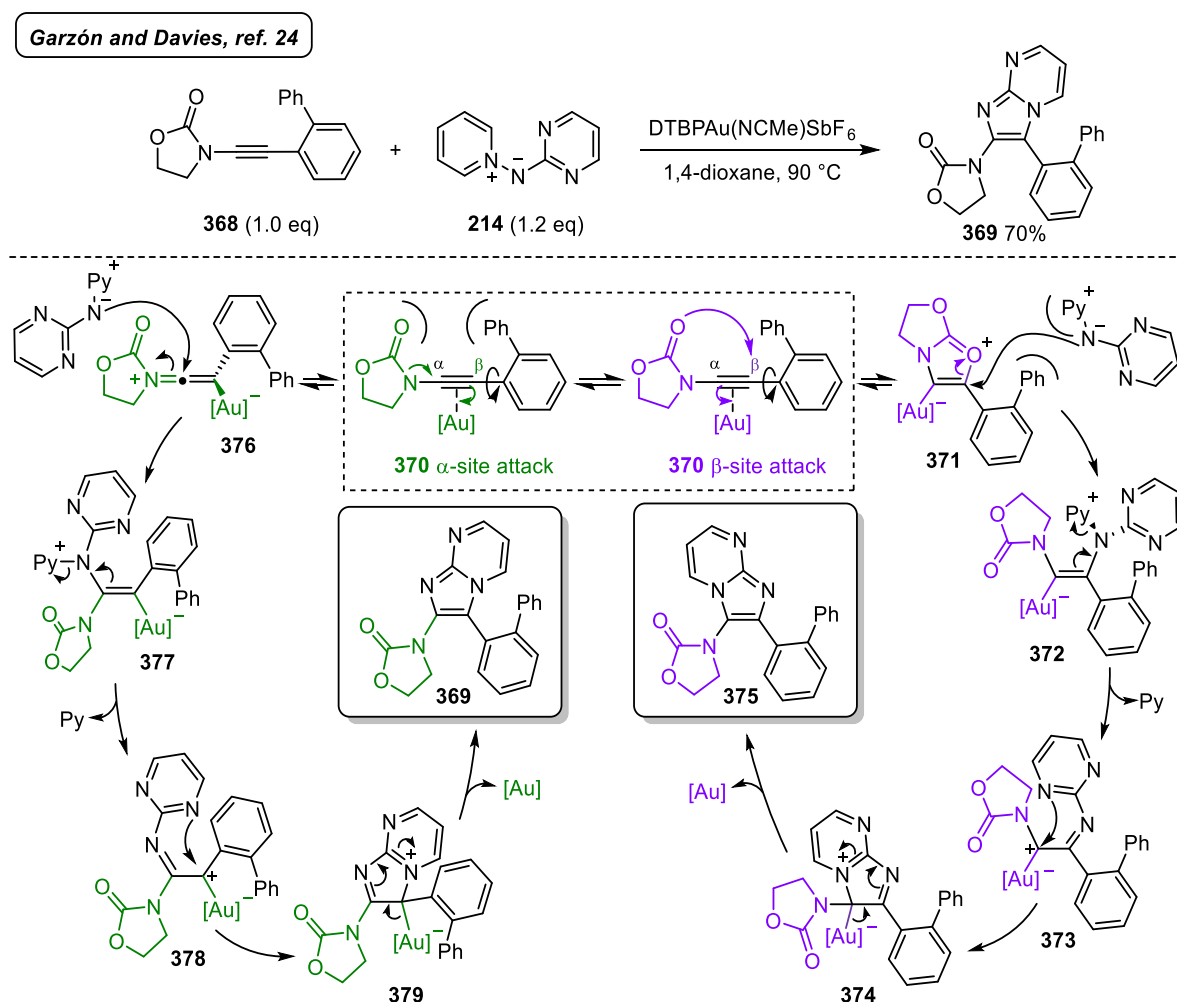
In 2016, Huang and co-workers⁶³ reported the synthesis of 3-amido-indoles **364** through a β -site selective formal [3+2] cycloaddition of oxazolidinonyl ynamides **362** with pyrido[1,2-*b*]indazoles **363** (Scheme 44-top).



Scheme 44: Top: Synthesis of 3-amido indoles through a gold-catalysed formal [3+2] cycloaddition reported by Huang. Bottom: Proposed mechanism for β -site selective activation of the ynamide

This unprecedented regioselectivity using ynamides, as opposed to the commonly observed α -attack onto the keteniminium intermediate, was explained by the oxazolidinone moiety generating a stable 5,5-fused carbocation (**366-366'**) from which β -addition of the nucleophile was favoured (Scheme 44-bottom).

With Huang's precedent, we wondered if in the example reported by Garzón and Davies²⁴ during their investigation of the ynamide scope in the *N*-diazinyl aminide series (Scheme 45-top), β -site selective attack had occurred when using oxazolidinonyl ynamide **368**.

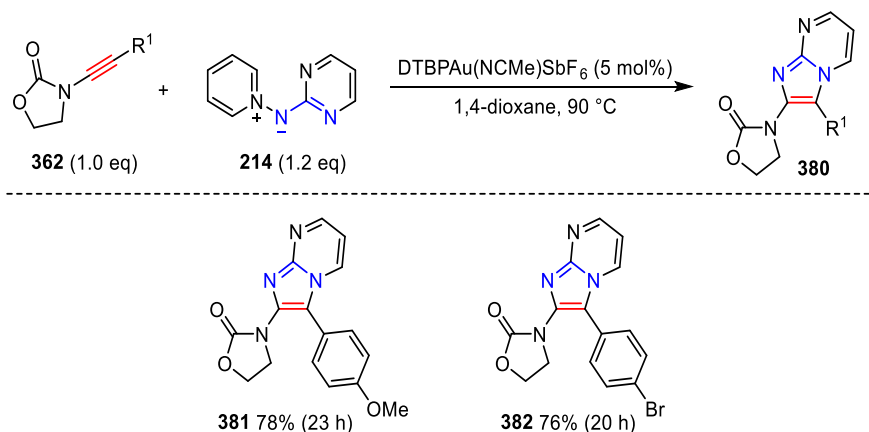


Scheme 45: Top: Result reported by Garzón assuming α -site selective attack onto the ynamide. Bottom: proposed reaction pathways for α - and β -site attack

Initially, it was assumed that the aminide would have undergone the common α -site attack on the gold-activated ynamide, yet the formation of the other regioisomer from β -attack could also be a viable reaction pathway (Scheme 45-bottom).

The steric impact of a bulky phenyl group in the *ortho* position of ynamide **370** could have been sufficient to block the attack of the carbonyl onto the β -site allowing only a α -site attack (**370** to **369**). To corroborate this result, a brief study of oxazolidinonyl ynamides without this steric issue was conducted (Scheme 46). Ynamides **295** and **296** bearing substituents in position 4 of the phenyl group were prepared following Evans's procedure⁵² (Scheme 35).

Oxazolidinonyl ynamides were reacted with *N*-pyridinium *N*-diazinyl aminide **214** employing the conditions optimised by Garzón²⁴ (DTBPAu(NCMe)SbF₆ (5 mol%), 1,4-dioxane at 90 °C) and the regioselective outcome of the catalysis products was then analysed by spectroscopic techniques.



Scheme 46: Oxazolidinonyl ynamides in the formal [3+2]-dipolar cycloaddition

A NOESY experiment of imidazodiazine **382** was run to verify the outcome from the gold catalysed cycloaddition (Figure 4). Imidazo[1,2-*a*]pyrimidinyl oxazolidinone **382** showed coupling between H3 and H4. Proton H4 showed interaction with H7 since it is relatively

close in space. A faint signal corresponding to the interaction H4-H6 was also observed. There is no coupling observed between H7 and H3, which it should have been observed if it was the β -site attack product. The crystal structure of **382** allowed the final regioselective outcome to be confirmed (Figure 5-see Appendix for crystallographic data). This agrees with the proposed structure from an α -site selective attack.

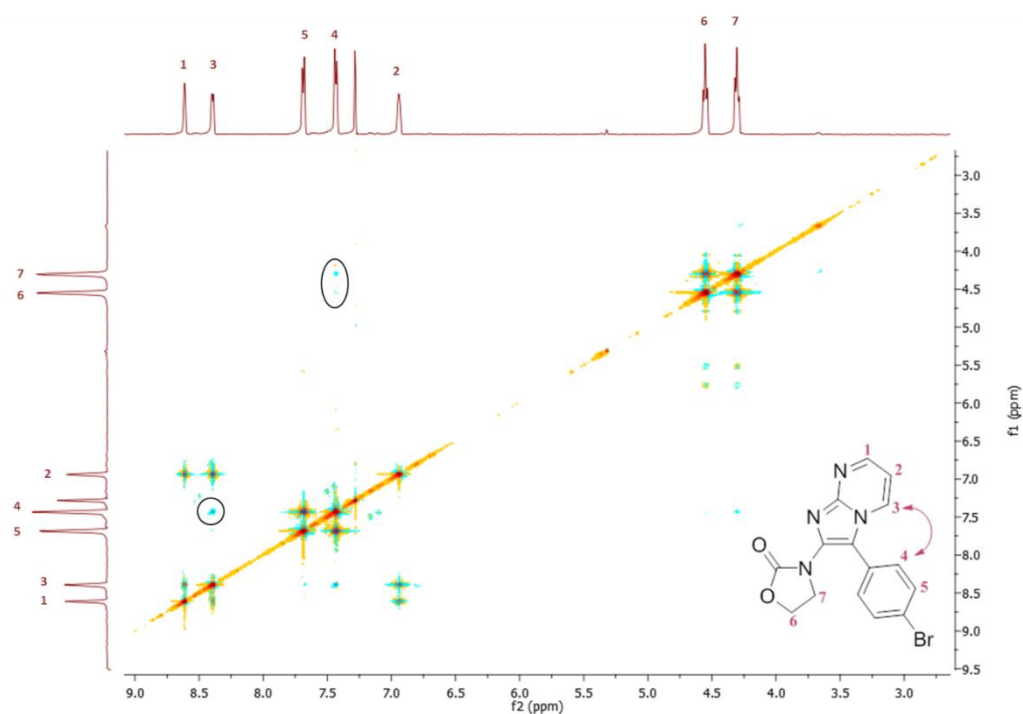


Figure 4: NOESY spectra of imidazole 382

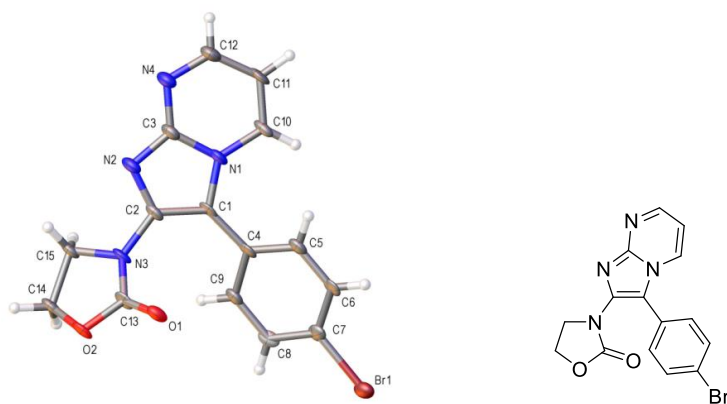


Figure 5: Crystal structure of imidazole 382 with ellipsoids drawn at the 50% probability level. X-Ray crystallography was obtained and solved by Dr Louise Male (University of Birmingham)

2.5. Conclusions

N-Pyridinium *N*-benzo(thia/oxa)zole aminides have been investigated as nucleophilic nitrenoids. These robust and bench stable species can be easily prepared from commercially available starting materials *via* a modular synthetic route through chloro or thioamide precursors containing different functionalities.

N-Pyridinium *N*-benzo(thia/oxa)zole aminides have proved excellent 1,3-*N,N*-dipole equivalents in the gold-catalysed formal [3+2]-dipolar cycloaddition with ynamides, despite their more π -electron rich character in comparison to *N*-pyridinium *N*-diazinyl aminides.

The new aminides allowed access to highly functionalised imidazo[2,1-*b*]benzo(thia/oxa)zoles in excellent yield, with complete regioselectivity and good functional group tolerance.

Further investigation needs to be performed to assemble a complete picture to prove formation of key reaction intermediates. Another area of significant interest would be to analyse the potential biological activity and properties of the imidazo[2,1-*b*]benzo(thia/oxa)heterocycles for pharmaceutical industry.

CHAPTER 3:
NEW SCAFFOLDS FOR THE GOLD-CATALYSED
FORMAL [3+2] DIPOLAR CYCLOADDITION:
URACIL, RHODANINE AND THIOHYDANTOIN
BASED AMINIDES

3.1. Introduction

3.1.1. New approach to construct molecular complexity

In the previous chapter, aminides were presented as powerful synthetic tools to access functionalised imidazole-based heterocycles *via* a gold catalysed cycloaddition with ynamides. Only two main families of fused imidazoles have been investigated thus far: imidazo[2,1-*b*]diazines and imidazo[2,1-*b*]benzo(thia/oxa)zoles^{24, 65} (Figure 6-left). We then sought to expand the scope of this transformation utilising different 1,3-*N,N*-dipoles. Eventually, to access a wider range of poly-aza imidazolyl heterocycles by means of a nucleophilic nitrenoid approach. Our interest towards accessing more diverse imidazolyl derivatives arises from the numerous applications of compounds containing a fused imidazolyl core in biomedicine and material science.

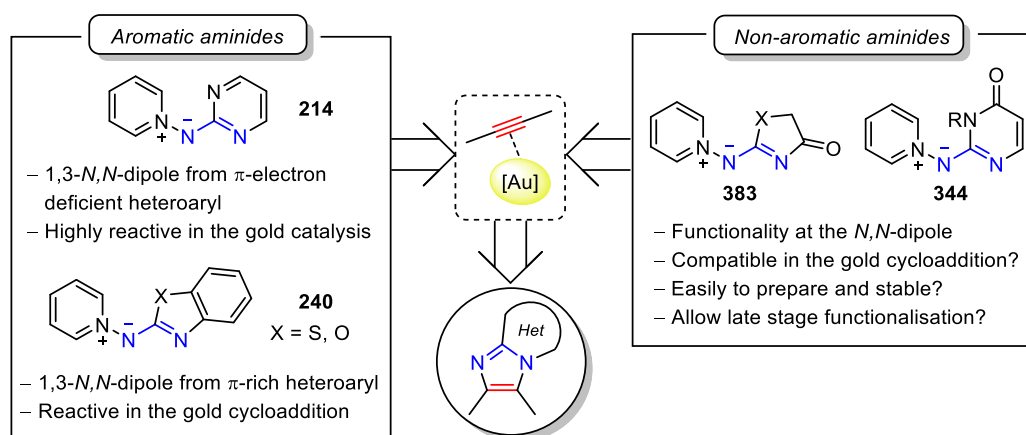


Figure 6: Previous investigated aminides (left) and proposed new nitrenoids (right)

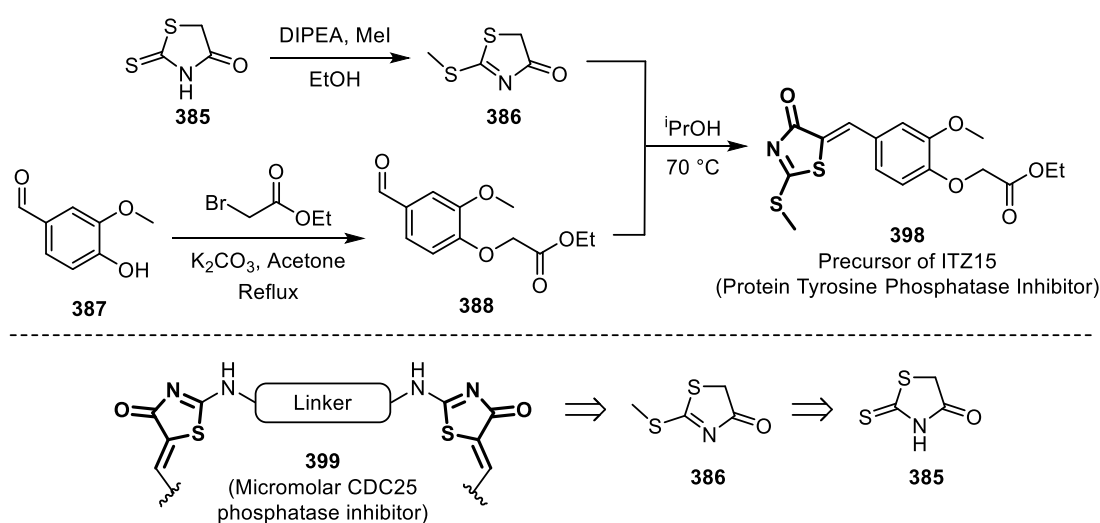
Therefore, we sought to explore new nitrenoid cores –rhodanine, thiohydantoin and uracil– as potential 1,3-*N,N*-dipoles bearing an amide-like functionality (Figure 6-right). These and similar heterocycles are present in the structure of many biological compounds and materials.

Additionally, they contain attractive reactive sites that could allow late stage functionalisation of the catalysis products.

Several points were taken into consideration at the outset of this investigation. A robust synthetic route is necessary to prepare the nitrenoids in a practical and easily scalable manner. Nucleophilic character is required from a non-aromatic *N*-heteroaryl motif (**383** and **384**), which differs significantly from the previous families investigated within the Davies group (**214** and **240**). The heteroatoms embedded in the aminide structure could act as a ligand and sequester the catalyst.

3.1.2. Biological activity and physical properties of molecules containing the new heterocycles

Rhodanine **385** and 2-(methylthio)thiazol-4(5*H*)-one **386** (Scheme 47) are common building blocks in organic chemistry to construct thiazolone based compounds.⁶⁶ These precursors are integrated in the early stage of many synthetic routes to readily assemble highly valuable 5-ylidene-4-thiazolone derivatives such as **398** and **399**.



Scheme 47: Applications of 2-rhodanine and (2-methylthio)rhodanine in the preparation of phosphatase inhibitors

The thiazolone unit is widely featured in molecules with interesting biological properties in medicinal chemistry displaying antitumor,⁶⁷ anti-inflammatory,⁶⁸ anti-tubercular,⁶⁹ or antimicrobial activity⁷⁰ (Figure 7). Many inhibitors such as **400**,⁷¹ **401** or **402** (Epalrestat)⁷² bear that core. The 5-ylidene-4-thiazolone is found in the structure of some photosensitizers such as **403** for dye-sensitized solar cell (DSSC) applications⁷³ or in **404**, which is applied in photodynamic therapy (PDT).⁷⁴

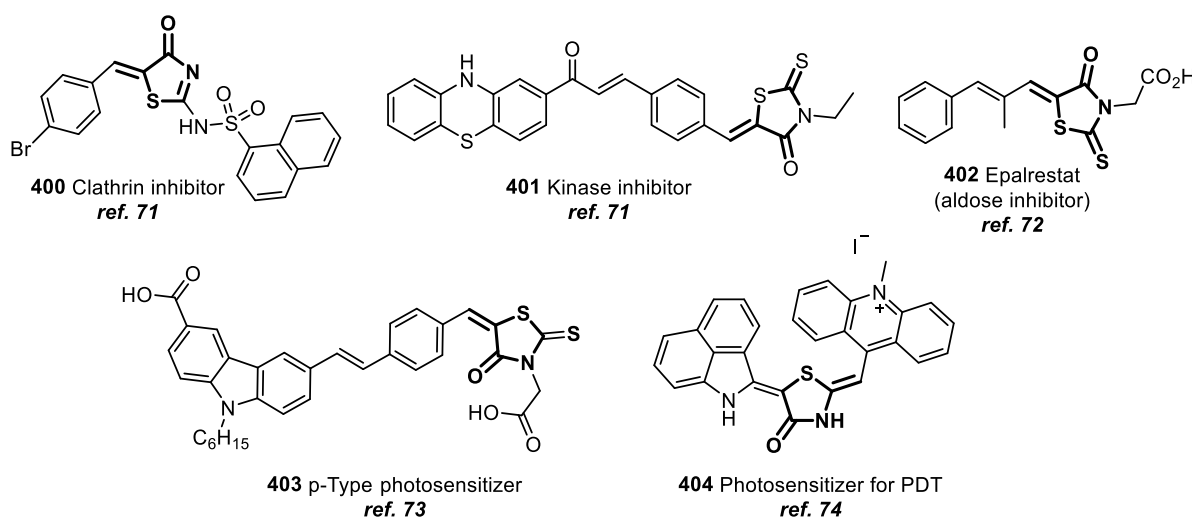


Figure 7: Examples of inhibitors and dyes bearing a 5-(ylidene)thiazolone motif in their structure

5-(Ylidene)-2-thioxo-4-imidazolidinone derivatives are installed in the structure of numerous compounds investigated as inhibitors⁷⁵ (**405**), anticancer⁷⁶ (**406**), anti-inflammatory (**408**) and anti-fungal⁷⁷ (**409**) agents (Figure 8). Certain corrosion inhibitors⁷⁸ (**410**), chromophores⁷⁹ (**411**) and fluorogenic dyes⁸⁰ (**407**) for fluorescence bioimaging also contain this core.

In the same manner to its sulfur analogue, Knoevenagel condensation is one of the conventional transformations utilised to integrate the 2-thioxo-4-imidazolidinone pattern in highly functionalised molecules as has been illustrated in some of the previous examples.⁸¹

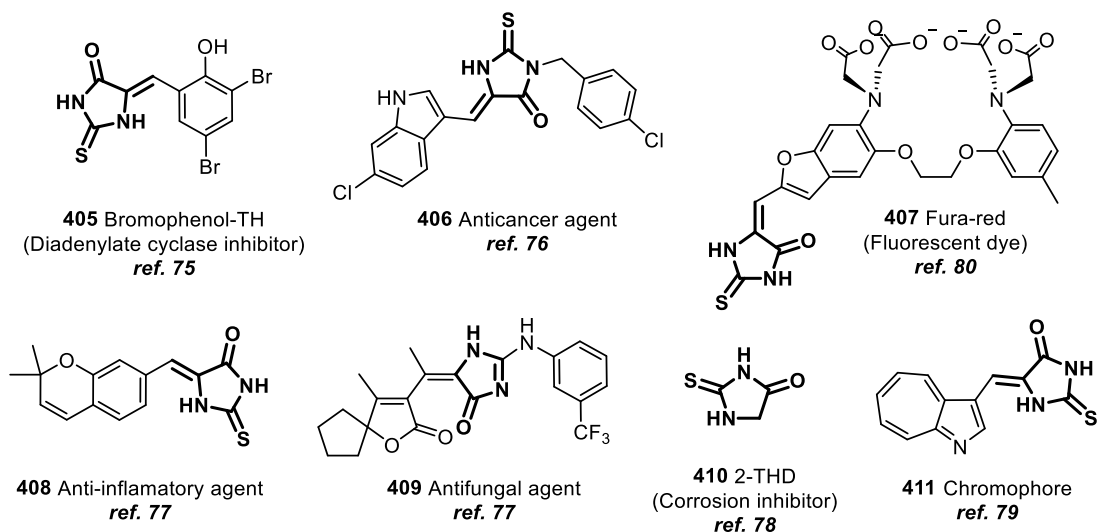


Figure 8: Examples of biological molecules and materials showing a thiohydantoin core

The introduction of the new targets in the gold catalysed cycloaddition proposed in this thesis would give access to imidazo[2,1-*a*]/[2,1-*b*]fused cores, which are present in compounds with interesting biomedical applications (Figure 9). For instance, the imidazo[2,1-*b*]thiazol-3(2*H*)-one core is found in a family of inhibitors displaying cGAS antagonist activity⁸² such as **412** and **413**. Certain protein kinase inhibitors⁸³ also present this bicyclic motif (**414**).

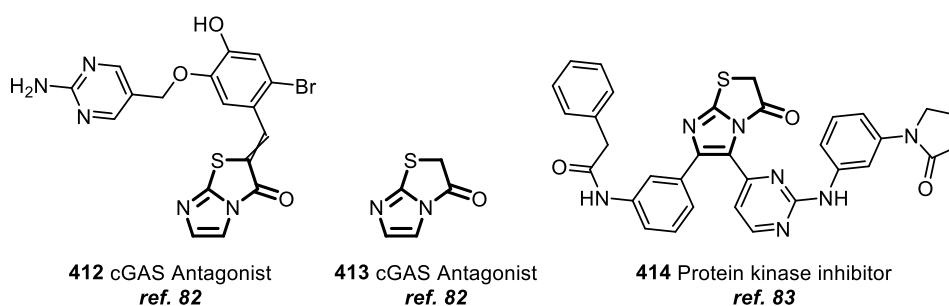


Figure 9: Compounds bearing an imidazo[2,1-*b*]thiazol-3(2*H*)-one core

Nitrogen 5,5-fused ring systems bearing an imidazo[1,2-*a*]imidazolone unit also display interesting biological properties (Figure 10) such as corticotropin-releasing factor receptor type 1 (CRF₁R) antagonists⁸⁴ (**415**) or lymphocyte function-associated antigen-1 (LFA-1) inhibitors⁸⁵ (**416**).

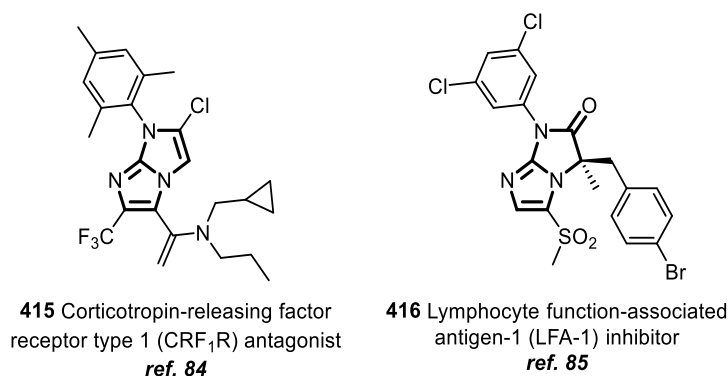


Figure 10: Compounds showing an imidazo[1,2-*a*]imidazolone unit

The last of the new aminides proposed was inspired by the nitrogenous base uracil. This six membered ring is present in crucial biological molecules such as DNA⁸⁶ and has a pivotal role in the regulation of the body's metabolism.⁸⁷ Of special interest is 5-fluorouracil (**417**) and its analogues⁸⁸ due to their ability to inhibit RNA replication enzymes, as well as their use as drugs to treat colon and breast cancer (Figure 11).

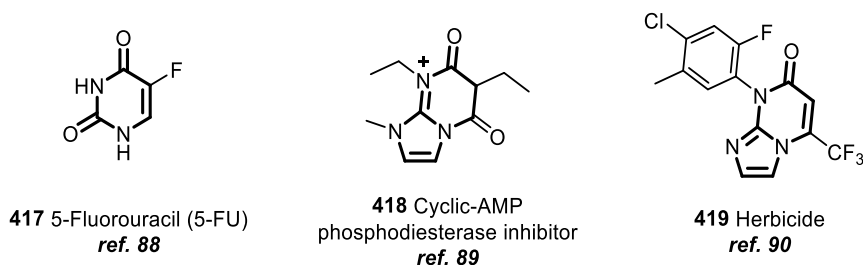


Figure 11: Uracil and imidazo[1,2-*a*]pyrimidinone derivatives

The fused imidazo[1,2-*a*]pyrimidinone unit is found in several purine deoxynucleoside analogues that have been utilised as anticancer agents⁸⁹ (**418**) or herbicides⁹⁰ (**419**).

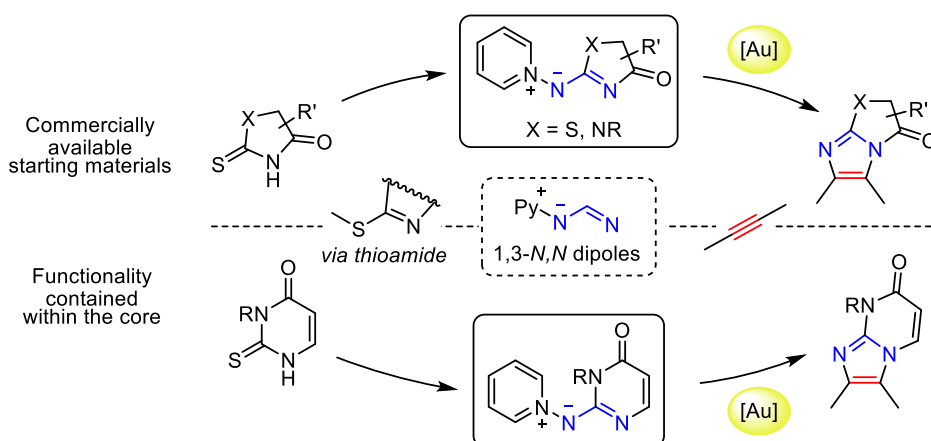
3.2. Aims and objectives

The main aim is to expand the scope of the aminides in gold-catalysed annulations to other non-aromatic 1,3-*N,N*-dipoles incorporating amide functionality. Moreover, the design of a

modular route for aminide preparation is also targeted to deeply investigate their ability to react as nitrenoids in the gold-catalysed formal [3+2] cycloaddition reaction with ynamides.

3.3. Results and Discussion

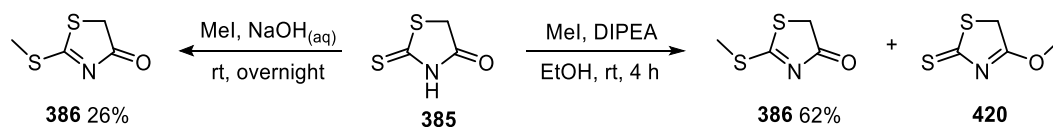
The displacement of sulfides as a strategy to create a wide variety of *N*-benzo(heteroaryl) aminide precursors, presented in chapter 2, has proved itself noticeably general. A similar approach was envisioned to synthesise the novel aminides utilising thioamide functionality (Scheme 48).



Scheme 48: Proposed synthetic route towards the new imidazole heterocycles

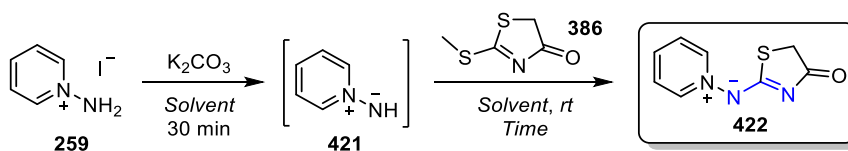
3.3.1. *N*-Pyridinium *N*-thiazolone aminides: new type of nitrenoids for the gold catalysed cycloaddition

The study commenced by exploring 2-rhodanine as an aminide precursor. The construction of the *N*-thiazolone nitrenoid began by methylating commercially available **385** with aqueous NaOH and methyl iodide.⁹¹ As this procedure provided low conversion of **386**, a different method using DIPEA in ethanol with methyl iodide was attempted. This caused a substantial improvement giving *S*-methylated **386** in moderate yield, albeit with the *O*-methylated regioisomer **420** as by-product.



Subsequently, aminide formation with **386** was attempted using the conditions show in Table 3. Preliminary results gave promising conversion when using methanol as a solvent (entry 1). The reaction did not proceed with isopropanol (entry 2) and no improvement was seen in acetonitrile (entry 3).

Table 3: Screening of work-up and purification method for aminide 422



Entry	Solvent	T (°C)	T (h)	Yield (%)	Purification method
1	MeOH	rt	2	53	NaOH [2.0 M] extraction
2	(CH ₃) ₂ CHOH	rt	4	--	NaOH [2.0 M] extraction
3	CH ₃ CN	rt	2	43	NaOH [2.0 M] extraction
4	MeOH	rt	2	3	NaOH [0.5 M] extraction
5	MeOH	rt	2	5	NaOH [1.0 M] extraction
6	MeOH	rt	2	19	NaOH [2.0 M] extraction
7	CH ₃ CN	rt	3	24	H ₂ O extraction
8	MeOH	rt	2	45	H ₂ O extraction
9	MeOH	rt	20	36	Filtration though celite
10	MeOH	rt	17	57	NaOH [2.0 M] extraction

^a Isolated yield after purification by the stated method

Methanol was kept as solvent and the work-up was then investigated as it was thought to be the main cause of the low yield due to the high solubility of the aminides in water. Work-ups using aqueous sodium hydroxide concentrations lower than 2.0 M were inefficient (entries 4-6). Similar results occurred when using water in the work-up (entries 7-8). Filtration through Celite to remove inorganic salts and avoid aqueous extraction proved inefficient (entry 9). Eventually, it was decided to perform the reactions over 24 hours for simplicity using

conditions shown in entry 1 (entry 10). The X-ray crystal structure of **422** is shown in Figure 12, for crystallographic data see Appendix.

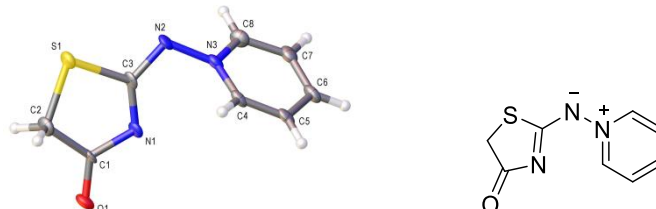
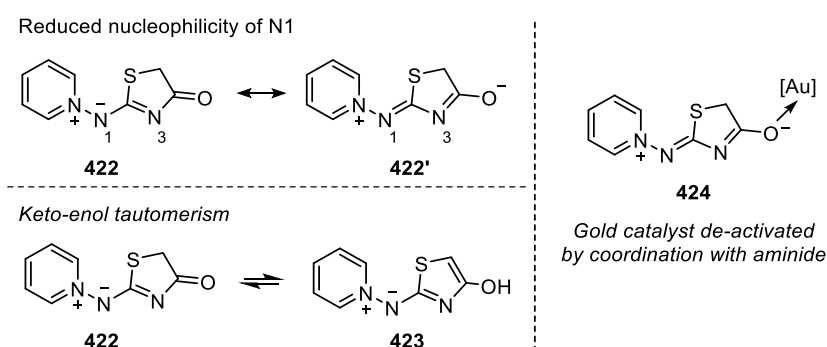


Figure 12: Crystal structure of aminide **378** with ellipsoids drawn at the 50% probability level. X-Ray crystallography was obtained and solved by Dr Louise Male (University of Birmingham)

3.3.1.1. Exploring the reactivity of the *N*-pyridinium *N*-thiazolone aminide

At the outset of the study, we considered that aminide **422** would be a challenging target as it shows some structural features that could potentially interfere in the desired cycloaddition pathway. The carbonyl group is in direct conjugation with the *N,N*-dipole and it could significantly reduce the nucleophilicity at *N1* (Scheme 49). A tautomeric keto-enol equilibrium may also interfere in the reaction. Finally, aminide-catalyst interaction **424** as a result of carbonyl activation by the gold complex could lead to sequestering the catalyst.

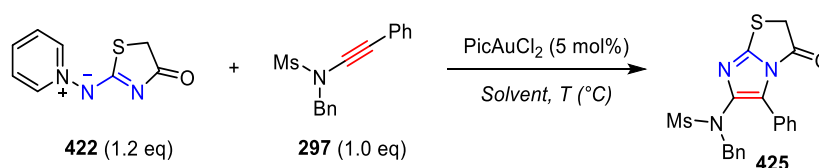


Scheme 49: Electronic features of the *N*-pyridinium *N*-thiazolone aminide preventing successful reactivity

Aminide **422** was tested in the gold catalysed cycloaddition with ynamide **297** (Table 4). Preliminary analysis of the ^1H NMR spectra of the crude reaction mixture showed significant

amounts of remaining starting material, in addition to some small resonances apparently from numerous species. Due to the abundance of species and starting material, no product could be isolated and characterised, despite many attempts. Variation of solvent or temperature did not enhance the reactivity to form **425** (entries 1-6).

Table 4: Surveying the reactivity of N-pyridinium N-2-thiazolone aminide 422

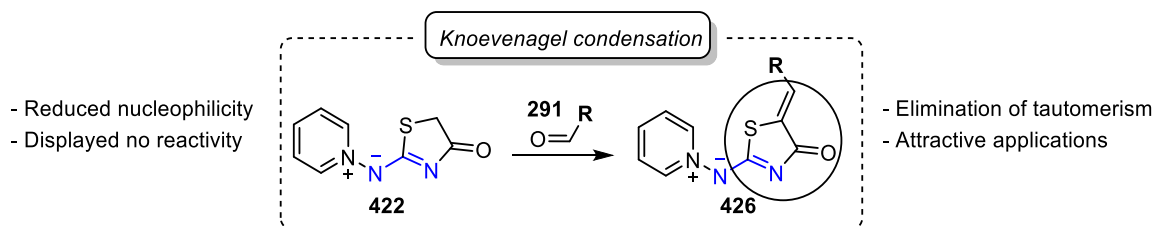


Entry	Solvent	T (°C)	T (h)	379 (%) ^a
1	1,4-dioxane	90	3	Complex mixture
2	Toluene	90	3	Complex mixture
3	<i>m</i> -xylene	120	2	Complex mixture
4	1,2-DCB	125	3	Complex mixture
5	1,4-Dioxane	90	20	Complex mixture
6	1,2-DCB	125	20	Complex mixture

^a Analysis by ¹H NMR spectroscopy using 1,2,4,5-tetramethylbenzene as internal standard

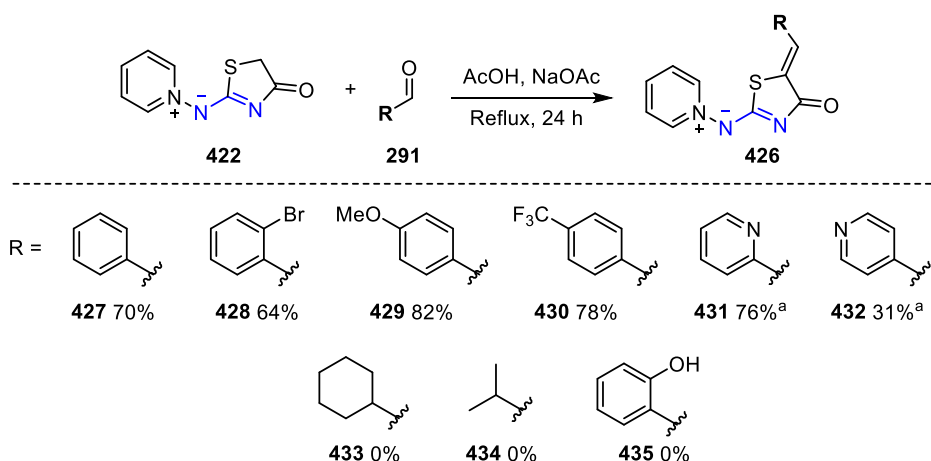
3.3.1.2. Modifications on the thiazolone aminide structure

We sought to amend the aminide structure to improve its electronic features towards a more reactive nitrenoid behaviour. Knoevenagel condensation was selected as a practical transformation to conveniently eliminate the enolisable protons in **422** Scheme 50 (Scheme 50). Thiazolone containing heterocycles bearing a 5-ylidene substituent are commonly found in biologically active compounds as shown in section 3.1.2.



Scheme 50: Structural modifications of aminide 422

Aminide **422** was decorated utilising several aldehydes **291** to construct a set of 5-(ylidene)thiazolone based aminides, by employing a mixture of acetic acid/sodium acetate (Scheme 51). In general, aryl aldehydes produced the corresponding condensation products in moderate to good yields (**427-432**).



Scheme 51: Formation of N-pyridinium N-thiazolone aminides through Knoevenagel condensation. ^a Aminide was not stable in air

Attempted formation of aminides **431**, **432** and **435** failed possibly due to a self-condensation reaction similar to that reported by Shaabani and co-workers⁹² when studying tetronic acids. Consistent with other studies, alkyl aldehydes did not afford the desired nitrenoids (**433**, **434**) due to the formation of two possible enolates.

Two different stereoisomers can be obtained from the condensation reaction. Previous examples reported in the literature employing similar substrates show preferential formation

of the *Z* isomer. As expected, the less sterically hindered *Z*-isomer was achieved and its structure was confirmed by the crystal structure of aminide **429** (Figure 13). From this result, the same stereoselective outcome was assumed for the rest of aminides formed by Knoevenagel condensation.

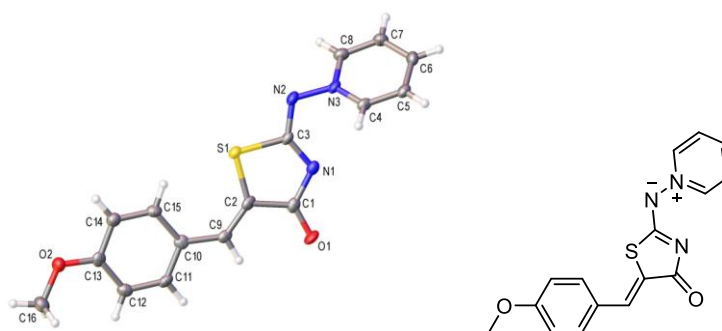


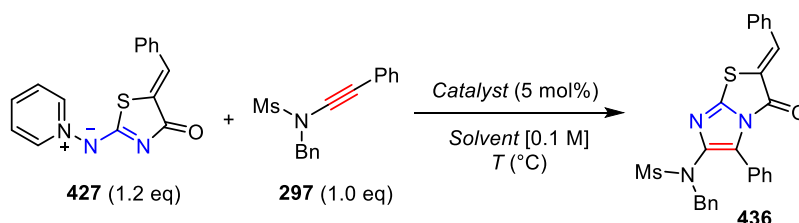
Figure 13: Crystal structure of aminide **429** with ellipsoids drawn at the 50% probability level. X-Ray crystallography was obtained and solved by Dr Louise Male (University of Birmingham)

Subsequently, the reactivity of this collection of nitrenoids was explored in the formal gold catalysed cycloaddition commencing with aminide **427** and ynamide **297** (Table 5). To our delight, dichloro(2-pyridinecarboxylato)gold afforded promising conversion to imidazole[2,1-*b*]thiazolone **437** (entry 1). This observation reflected the electronic switch of the thiazolone core now displaying moderate nitrenoid character. Gold(I) catalysts were also tested but appeared unreactive (entries 2-3). At reduced temperatures the reaction did not proceed to completion even after prolonged times (entries 4-7). However, with 1,2-DCB at 125 °C, complete conversion of the ynamide was observed in just 5 hours yielding imidazole **437** in 74% (entry 8).

Increasing concentration (entry 9) or number of equivalents of aminide **427** (entry 10) did not improve the outcome. The robustness of the reaction was tested using “wet” 1,2-DCB which delivered **437** in acceptable yield (entry 11). Finally, no reaction occurred in the absence of

the catalyst (entry 12) or in the presence of trifluoromethanesulfonic acid (entry 13), the latter having shown catalytic activity in certain cycloaddition processes also catalysed by gold.⁹³

Table 5: Screening of the reaction conditions for the gold-catalysed formal [3+2] cycloaddition with *N*-5-(ylidene)thiazolone aminide **427**

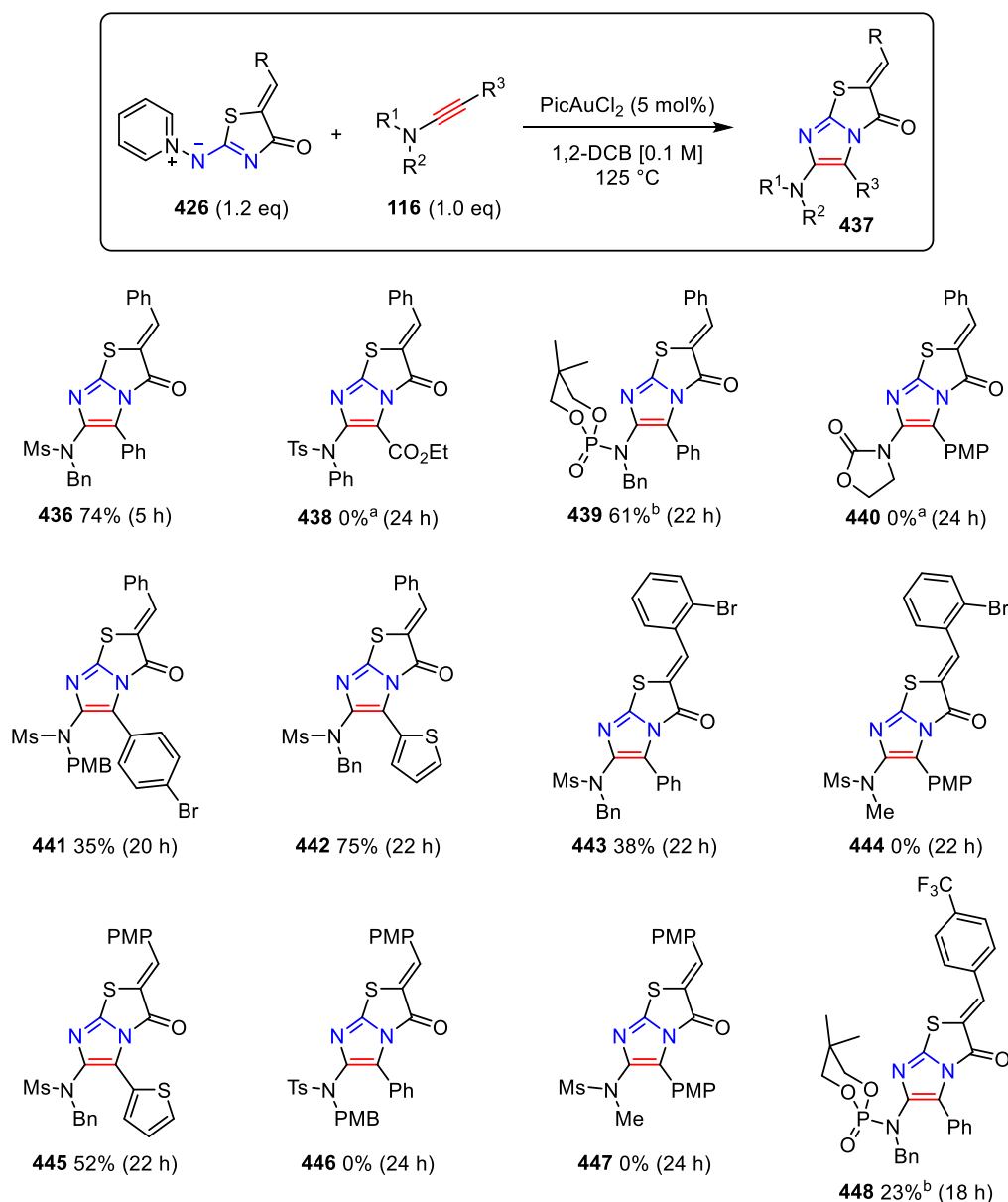


Entry	Catalyst	Solvent	T (°C)	T (h)	Yield (%) ^a
1	PicAuCl ₂	1,4-dioxane	90	24	(55)
2	DTBPAu(NCMe)SbF ₆	1,4-dioxane	90	19	0
3	IPrAuNTf ₂	1,4-dioxane	90	24	0
4	PicAuCl ₂	THF	60	26	0
5	PicAuCl ₂	Toluene	90	22	(8)
6	PicAuCl ₂	1,4-dioxane	100	24	(68)
7	PicAuCl ₂	<i>m</i> -xylene	110	22	(48)
8	PicAuCl ₂	1,2-DCB	125	5	74
9	PicAuCl ₂	1,2-DCB [0.2 M]	125	5	54
10	PicAuCl ₂	1,2-DCB ^b	125	5	58
11	PicAuCl ₂	1,2-DCB	125	5	64 ^c
12	--	1,2-DCB	125	5	0
13	PicAuCl ₂	1,2-DCB	125	5 min	0 ^d

^a Isolated yield after purification by flash column chromatography; Yield in parenthesis obtained by ¹H NMR spectroscopy with 1,2,4,5-tetramethylbenzene as an internal standard; ^b Using 1.5 eq of aminide; ^c Using non-dried 1,2-DCB; ^d Reaction performed adding 1.0 eq of TfOH as catalyst.

3.3.1.3. Exploring the reactivity of the new aminides

With optimised conditions in hand, the library of *N*-pyridinium *N*-thiazolone based aminides was taken into the gold catalysed cycloaddition with several ynamides. In this case the transformation was found to be not as general as with previous nitrenoids (Scheme 52).



Scheme 52: Screening of the reactivity of 5-(ylidene)thiazolone aminides. ^a Using 1,4-dioxane at 90 °C; ^b Not possible to purify completely

The reaction of aminide **427** with the most reactive and stable ynamides afforded moderate to good yields (**436**, **439**, **441**, **442**). In contrast, remaining starting material and decomposition impurities were recovered when using ynamides **357** and **295** after flash column chromatography, even at lower temperatures. 2-Bromophenylidene aminide **428** proved to be relatively sensitive, giving poor or no conversion to **443** and **444** respectively. *p*-Methoxybenzylidene aminide **429** did not prove very reactive. While it afforded moderate

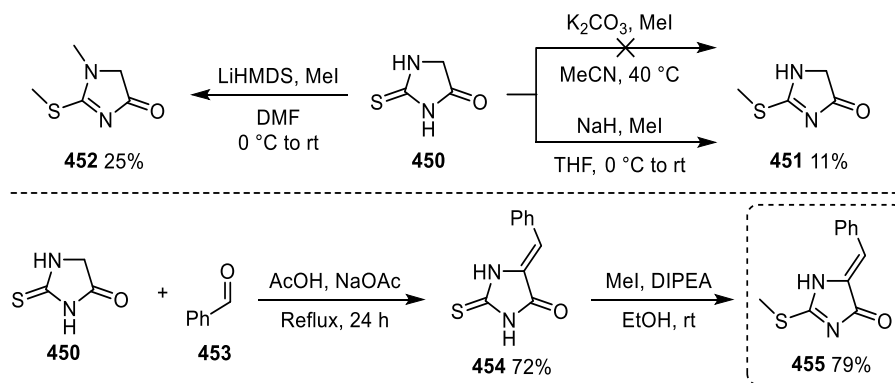
conversion to **445**, only starting material was recovered from several attempts to form imidazoles **446** and **447**. Imidazole **448** was observed in the crude reaction mixture but it was not possible to isolate.

While providing a proof of principle of the features required for effective 1,3-*N,N*-dipoles, this preliminary study showcased that these type of aminides were not generally applicable in the annulation chemistry with ynamides.

3.3.2. Introduction of the imidazolone core in the *N*-pyridinium aminide series

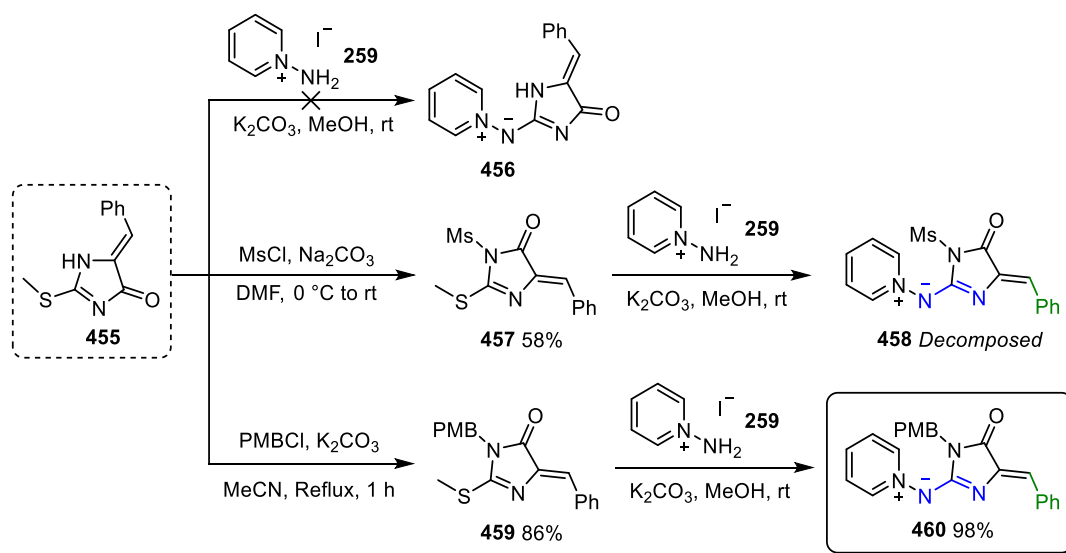
In view of the results observed with *N*-pyridinium *N*-(5-benzylidene)thiazolone aminides, we then sought to explore whether the sulfur atom of the thiazolone core was deleterious. To this end, the preparation of an *N*-pyridinium *N*-imidazolone aminide was attempted applying an analogous approach *via* a thioamide precursor.

Methylation using LiHMDS was attempted on 2-thioxoimidazolidin-4-one **450**, but did not afford product **452** (Scheme 53). Other bases such as potassium carbonate and sodium hydride were tested but proved unproductive. In contrast, condensation with benzaldehyde afforded **454**, which after methylation, allowed readily access to thiamide **455** in synthetically useful yield and with straightforward purification.



Scheme 53: Top: Attempted methylations on 2-thiohydantoin; Bottom: Knoevenagel condensation of 2-thiohydantoin and subsequent methylation

Formation of aminide **456** was directly attempted using **455** and *N*-aminopyridinium iodide, yet proved fruitless (Scheme 54). *N*-Protection of **455** with methanesulfonyl chloride and sodium carbonate gave mesylated hydantoin **457** in moderate yield. While aminide formation appeared to proceed on the basis of NMR spectroscopy, isolation of the corresponding mesyl protected aminide **458** proved unsuccessful due to instability issues.



Scheme 54: Synthetic route applied for *N*-pyridinium *N*-imidazolone aminide preparation

Protection of **455** with *p*-methoxybenzyl chloride delivered **459** in high yield. The reaction of the latter with **259** and potassium carbonate rendered *N*-pyridinium *N*-1-(4-methoxybenzyl)(5-

benzylidene)imidazolone aminide **460** as a bright orange solid in excellent yield. Once more, sulfide(heteroaryls) proved ideal substrates for aminide formation, yet requiring prior functional group protection. The crystal structure of **460** (Figure 14, see Appendix for crystallographic data) revealed that the carbonyl was adjacent to the PMB-protected nitrogen instead of to the *N,N*-dipole.

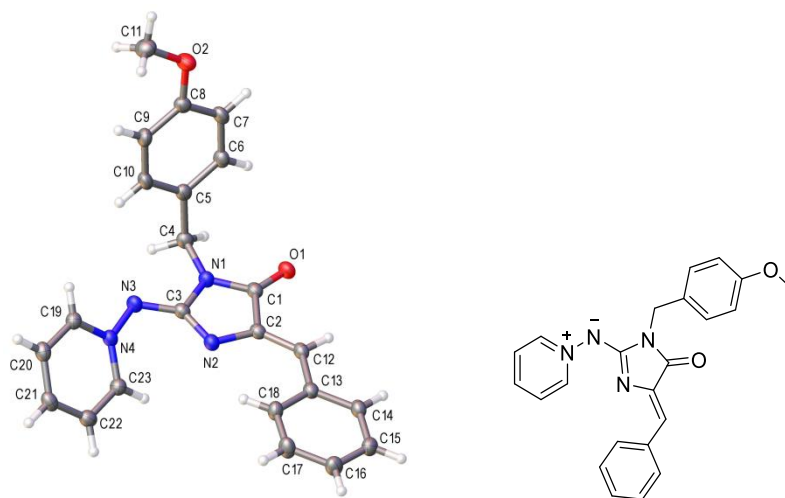
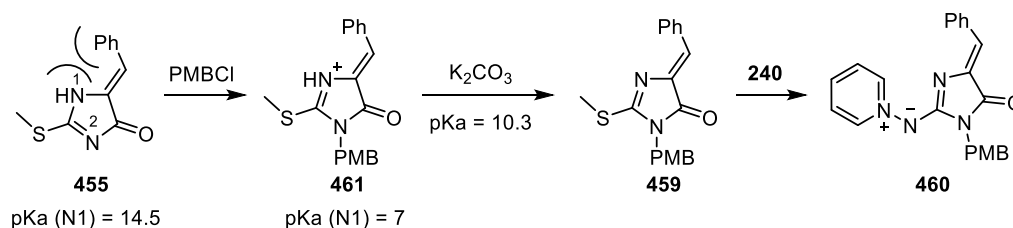


Figure 14: Crystal structure of aminide **460** with ellipsoids drawn at the 50% probability level. X-Ray crystallography was obtained and solved by Dr Louise Male (University of Birmingham)

This fact suggests that the *p*-methoxybenzyl protection was accomplished on the less sterically hindered nitrogen (Scheme 55). The bulkiness of the ylidene group could have favoured the protection of *N*2 in **455** resulting in the formation of **461-459**. Reaction of the latter with *N*-aminopyridinium iodide afforded aminide **460**.

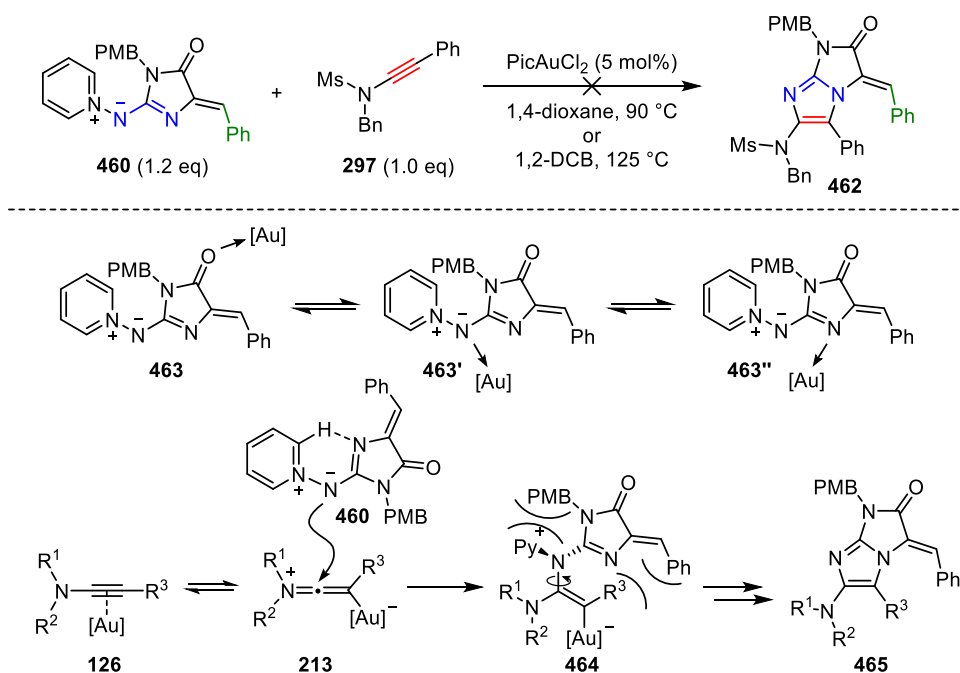


Scheme 55: Proposed pathway leading to the formation of aminide **460**

Aminide **460** was then examined in the gold-catalysed formal [3+2] cycloaddition with ynamide **297** (Scheme 56). Similar to the *N*-pyridinium *N*-(5-ylidene)thiazolone series, it did not display nitrenoid reactivity with either of the two general sets of reaction conditions.

It is believed that the lack of reactivity of **460** could be due to a decrease in the nucleophilicity of the *N,N*-dipole by the presence of an imidazolone ring. Another additional reason could be that the catalyst might be trapped by an aminide-gold interaction through the *N* or *O*, which would stop the cycloaddition pathway (**463** to **463''**).

Steric issues also play an important role. As mentioned in section 2.1, the aminide needs to acquire a perpendicular orientation to undergo effective attack onto the keteniminium intermediate. In the case of imidazolone **460**, its large substituents in addition to the intramolecular H-bonding interaction may cause issues to adopt the required perpendicular orientation and therefore the reaction is suppressed (**464** to **465**).



Scheme 56: Top: Attempted formation of fused imidazole **462; Bottom: Proposed side-interactions: Potential gold-aminide coordination and steric hindrance caused by the aminide substituents in the cyclisation event**

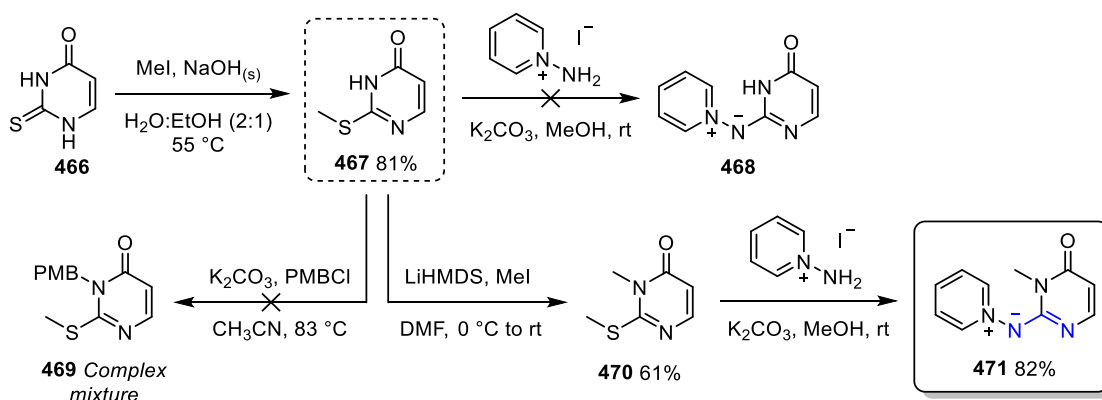
3.3.3. Preparation of an *N*-pyridinium *N*-pyrimidinone aminide to form new 5,6-fused imidazoles

Further investigation of the aminides containing an amide-like functionality was accomplished by the preparation of an *N*-pyridinium *N*-pyrimidinone aminide.

Thus far, the presence of a carbonyl in direct conjugation with the *N,N*-dipole has proved to be a major challenge while investigating the previous aminide series. The proposed new *N*-pyrimidinone aminide would contain a carbonyl in a more distant position, and thus, it is expected to exhibit distinct nitrenoid character.

3.3.3.1. Synthetic route to form an *N*-pyridinium *N*-pyrimidinone aminide

Having seen the effectivity of thioamides as aminide precursors in the previous series, it was decided to proceed in the same manner to form the new scaffold. Commercially available 2-thiouracil **466** was methylated following Tibiletti's *et al.* work⁹⁴ which delivered *S*-methylated **467** in excellent yield (Scheme 57).



Scheme 57: Synthetic route to form *N*-pyridinium *N*-pyrimidinone aminide

Analogously to the *N*-imidazolone series, direct aminide formation with *N*-aminopyridinium iodide and **467** did not afford aminide **468**; only starting material was recovered. Instead,

attempted *p*-methoxybenzyl protection gave a complex inseparable mixture (**469**). On the contrary, a second methylation of **467** using LiHMDS allowed us to form precursor **470** in moderate conversion, with partial recovery of the starting material.

Aminide formation was then attempted employing the standard conditions. Gratifyingly, the reaction proceeded smoothly. Purification was straightforward consisting of a base wash with NaOH_(aq) [2.0 M], extraction of the aqueous phase with CH₂Cl₂, followed by flash column chromatography. In this way, *N*-pyridinium *N*-(3-methyl)pyrimidinone **471** was prepared in 82% yield on gram scale (1.1 grams). The structure was confirmed by X-Ray analysis (Figure 15, see Appendix for crystallographic data).

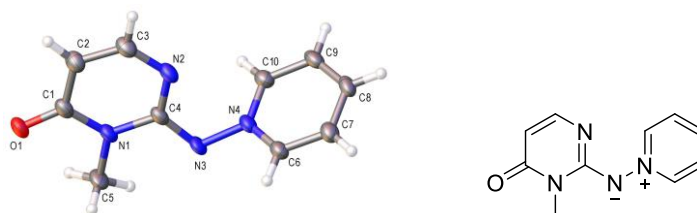
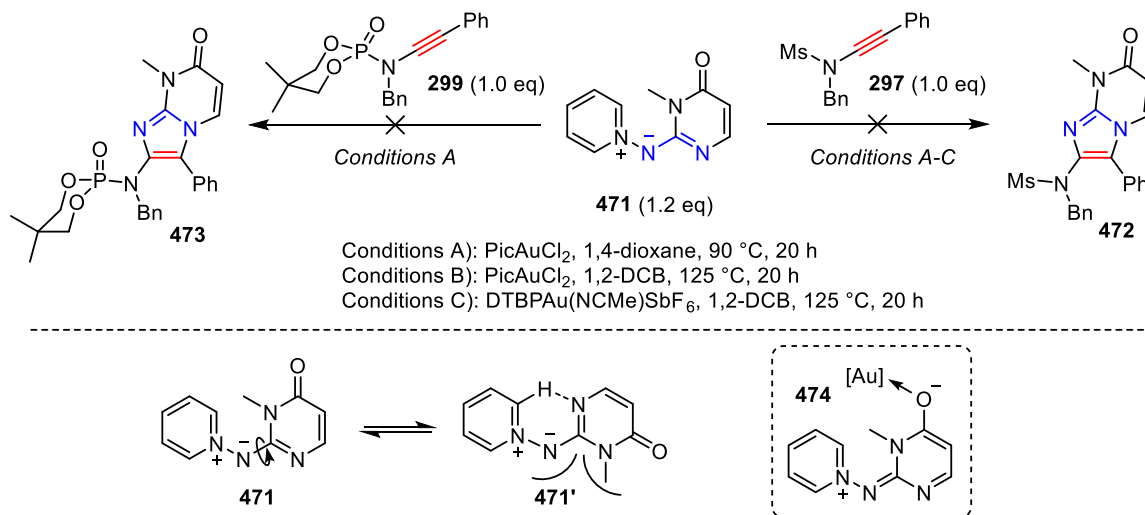


Figure 15: Crystal structure of aminide **471 with ellipsoids drawn at the 50% probability level. X-Ray crystallography was obtained and solved by Dr Louise Male (University of Birmingham)**

Having a robust and scalable route to form **471** we then explored its reactivity in the gold-catalysed formal [3+2] cycloaddition with ynamide **299** and **297** (Scheme 58). Aminide **471** did not reveal nucleophilic character with either a gold(I) or a gold(III) catalyst. An increase of the temperature did not see any improvement on the reactivity.

Scheme 58-bottom highlights the potential issues of this aminide in the gold cycloaddition similar to those discussed in schemes 60 and 67. The intramolecular hydrogen-bond interaction with the *ortho* hydrogen of the pyridine ring could impede the cyclisation to take place (**471'**). Delocalization of the negative charge of the *N,N*-dipole into the alkene in

conjugation with the carbonyl could notoriously reduce its nucleophilicity. Finally, the gold complex could potentially be poisoned by interaction with the aminide (**474**).



Scheme 58: Top: Testing the reactivity of nitrenoid **471** in the [3+2] gold catalysed cycloaddition. Bottom: Potential structural and electronic issues of aminide **471** towards cycloaddition

3.4. Conclusions

A modular synthetic route has been developed for the preparation of new aminides containing amide-like functionality on gram scale *via* thioamide precursors.

N-Pyridinium *N*-thiazolone aminide was synthesised in moderate yield after initial purification problems were resolved. As this aminide was unreactive in the gold-catalysed formal [3+2] cycloaddition, additional modifications were conducted introducing an appended 5-ylidene motif by Knoevenagel condensation. This proved advantageous as the new *N*-(5-ylidene)thiazolone aminides displayed moderate reactivity in the gold mediated transformation giving in some cases good yields but being limited in scope.

Structurally analogous *N*-(5-ylidene)imidazole aminides did not display 1,3-*N,N*-dipole character despite bearing the appended alkene motif. The steric bulk of the *p*-methoxyldiene and benzyldiene groups is thought to prevent the required reactive conformation.

N-Pyridinium *N*-pyrimidinone aminide, which contains the carbonyl in a more distant position with respect to the *N,N*-dipole, however in direct conjugation, also lacked nitrenoid reactivity.

It is believed the carbonyl unit plays a crucial role causing the absence of reactivity of the new nitrenoids. It is proposed it affects the catalytic process in two ways: by decreasing the nucleophilicity of the *N,N*-dipole and by potentially trapping the gold complex through the carbonyl *via* a gold-aminide interaction.

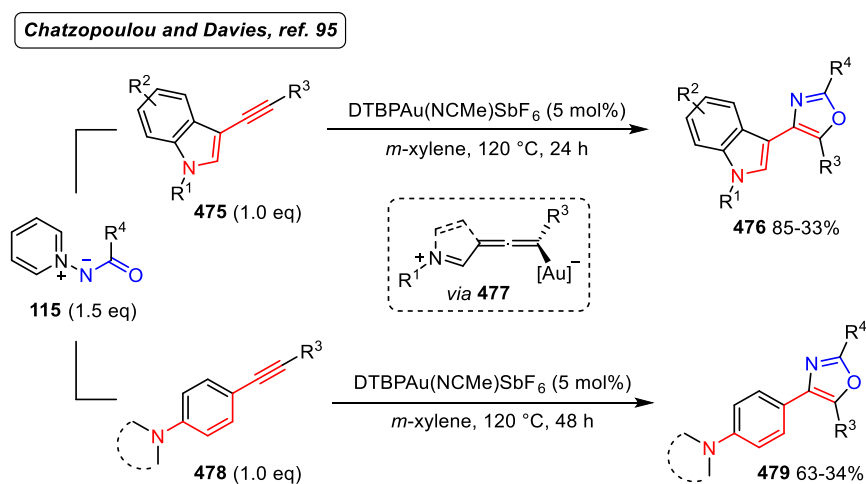
The other species taking part in the process is the ynamide. Further investigation of its role and the effect of other π -systems as ynamide surrogates in the gold cycloaddition with these new nitrenoids is discussed in chapter 4.

CHAPTER 4:
THIOYNAMIDES: NEW ELECTRON-RICH ALKYNES
FOR THE GOLD-CATALYSED FORMAL
[3+2] CYCLOADDITION

4.1. Heteroatom-donor activation of the alkyne

Throughout the investigation of gold-catalysed formal [3+2] cycloadditions in the Davies group, more emphasis has recently been placed on the nature of the alkyne. While ynamides have been most commonly used as electron-rich alkynes providing regiocontrol, π -acid activation of other heteroatom-donor alkynes has also been examined.

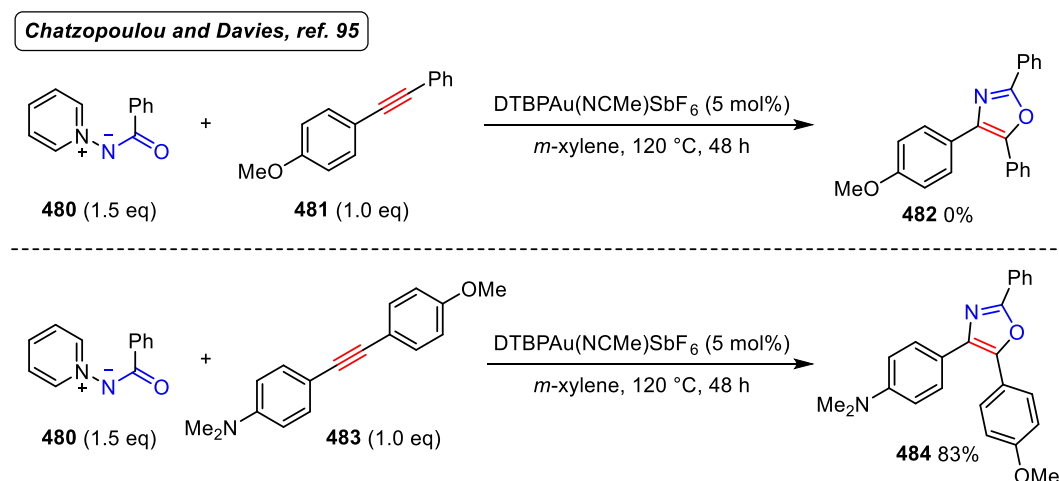
In the *N*-pyridinium *N*-acyl aminide series, Chatzopoulou and Davies⁹⁵ reported activation of the alkyne by a remote nitrogen in 3-indolyl ynamines **475** to access oxazole **476** through an allene-like intermediate **477** (Scheme 59). Several phenylethynyl aniline derivatives **478** also provided superb regiocontrol in the activation of the triple bond. Reactions proceeded smoothly tolerating a wide variety of functional groups in the terminal carbon end of the ynamines.



Scheme 59: Study of the reactivity displayed by a distant nitrogen in the oxazole formation reported by Chatzopoulou and Davies

The authors also investigated *p*-alkoxy benzene substituents as electron-donor groups (**481**), however these did not deliver the desired oxazoles **482** (Scheme 60-top). The difference between amino and alkoxy as activating groups was further demonstrated in a competition

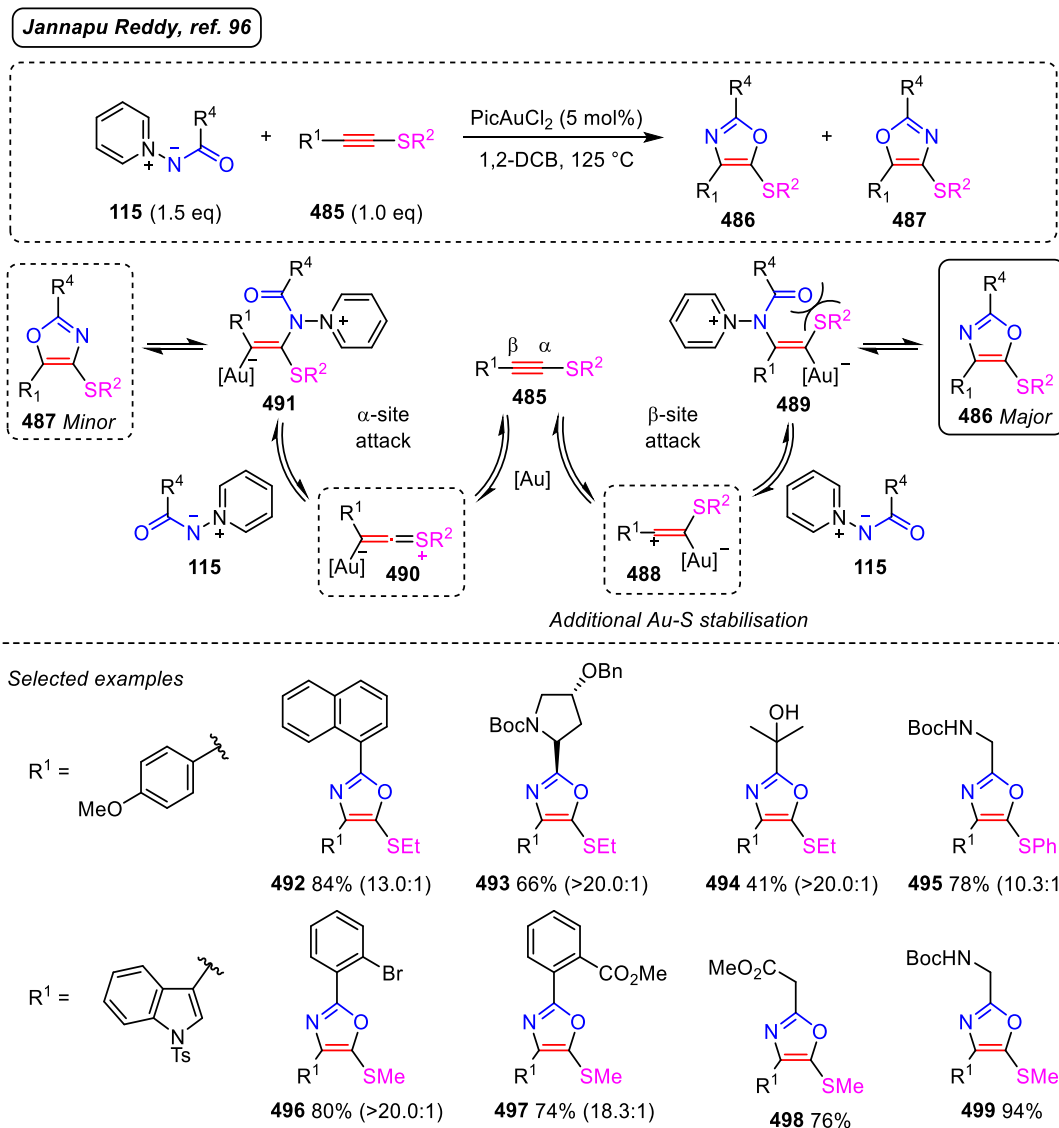
experiment (Scheme 60-bottom). The superiority of the nitrogen lone pair to donate electron density to the alkyne compared to the oxygen was illustrated by the formation of oxazole **484** as a single regioisomer.



Scheme 60: Top: Attempted activation of the alkyne by a remote alkoxy group. Bottom: Competition experiment between amino and alkoxy group for alkyne activation

A rather distinct mode of activation was recently reported by Jannapu Reddy *et al.*⁹⁶ utilising alkynyl thioethers **485** with *N*-acyl aminides **115** (Scheme 61). Activation of the alkyne is proposed to arise from π -coordination between the triple bond and the gold complex in cooperation with a stabilising Au-S interaction (**488**). In this way, β -selective attack of the aminide to the π -system provides 5-(thio)-2,4-substituted oxazoles (**486**), which show the opposite regioselectivity to that obtained with ynamides relative to the heteroatom.

An electron-donating group on the carbon substituted end of the alkyne enhanced the polarisation of the two *sp*-hybridised carbons and stabilises the cationic intermediate (**488**). When less electron-donating groups were introduced on R¹, traces of regioisomer **487** resulting from an α -attack to the alkynyl system were detected, albeit as a minor by-product.

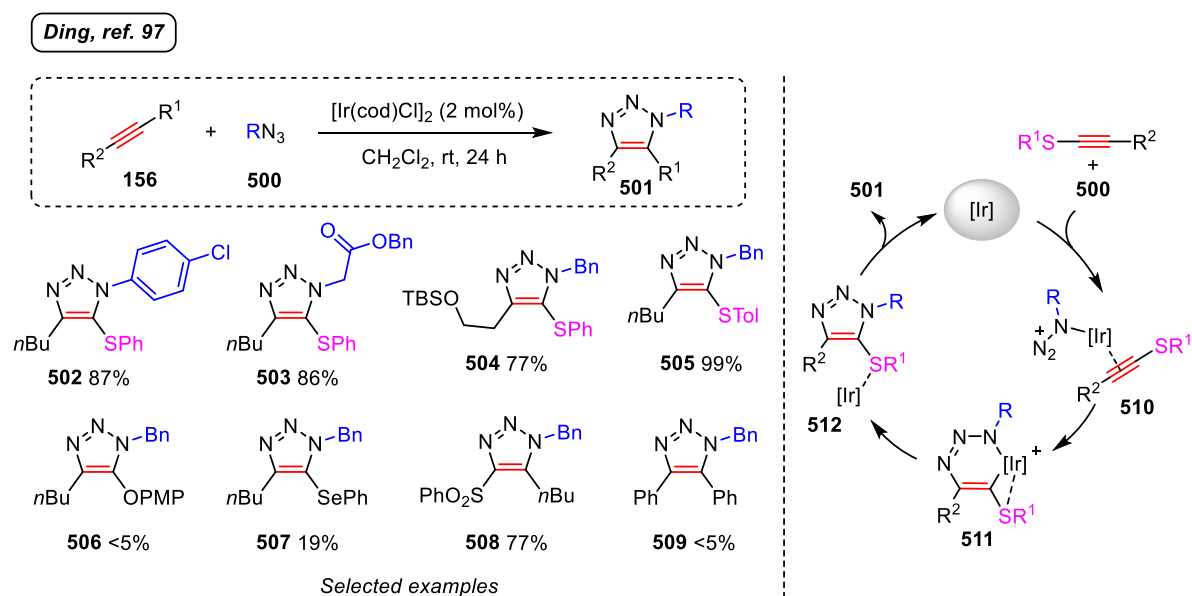


Scheme 61: Gold-catalysed formal [3+2] cycloaddition of alkynyl thioethers with *N*-acyl aminides reported by Jannapu Reddy et al.

The reaction proved general across a variety of highly functionalised *N*-acyl aminides giving high regioselectivities of the 5-thio substituted oxazoles in all cases (**492–499**). Varying the *S*-substituent affected the reactivity due to the steric interaction of the acyl group with the thioether group during the cyclisation event (**489**). As a result, larger groups at R² were detrimental for the transformation. Modifications on the other terminus of the alkyne ranged from aryl, alkyl, mono-, bis- and tri-substituted phenyl to *N,N*-dimethyl aniline and 3-indolyl derivatives.

In 2014, Ding *et al.*⁹⁷ reported the first iridium catalysed azide-alkynyl thioether annulation to synthesise 5-thio-1,2,3-substituted triazoles **501** (Scheme 62-left). The ability of alkynyl thioethers to act as electron-rich alkynes was demonstrated. Coordination of the iridium complex to the *sp*-carbon adjacent to the heteroatom is assisted by the sulfur substituent and provides regiocontrol in the oxidative cyclisation step (**511**).

Mild reaction conditions allow for excellent functional group tolerance, facilitating the introduction of otherwise troublesome functionalities such as silyl groups, amines, esters and alcohols in the triazole core (**502-505**). Several alkyl and aryl azides proved stable and undergo the transformation giving the corresponding triazoles in good to excellent yield.

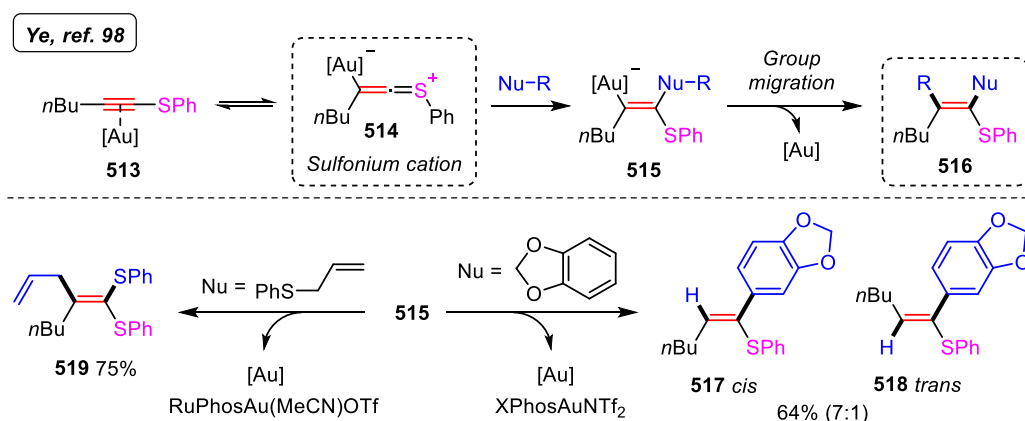


Scheme 62: Iridium catalysed 1,3-dipolar cycloaddition developed by Ding *et al.*

Other heteroatom-linked alkynes were also examined. While oxygen and selenium alkynyl derivatives provide low yield of triazoles **506** and **507**, an electron withdrawing group in the alkyne showed good reactivity but formed the opposite regioisomer (**508**). Internal alkynes proved unreactive (**509**).

The proposed mechanistic rationale involves dual coordination of the azide and the alkynyl thioether to the iridium complex **510** (Scheme 62-right). Oxidative cyclisation delivers intermediate **511**, which undergoes reductive elimination (**512**) and finally delivers provides **501**.

The ketenesulfonium intermediate has been invoked in the intermolecular gold catalysed α -addition to alkynyl thioethers reported by Ye *et al.*⁹⁸ (Scheme 63). It was proposed that upon gold-coordination to the alkyne (**513-514**), a variety of C-, S- and O- nucleophiles undergo nucleophilic attack at the *sp*-carbon adjacent to the sulfide group forming **515**. Depending on the nature of the carbon or sulfur nucleophile, protodeauration or group migration from the sulfur substituent, respectively, furnished the final tri-substituted alkenyl sulfides **516**.



Scheme 63: Gold catalysed synthesis of alkenyl sulfides with alkynyl thioethers reported by Ye *et al.*

Stereoselective *cis* addition across the triple bond was confirmed by X-ray data of the products. This fact contrasts with the commonly observed *trans* additions onto gold-activated alkynes, which proceeds by a gold activation of the triple bond and subsequent outer-sphere attack of the nucleophile.⁹⁹

Alkynyl thioethers have also been employed as dienophiles,¹⁰⁰ in cross-coupling reactions¹⁰¹ and other transformations.¹⁰²

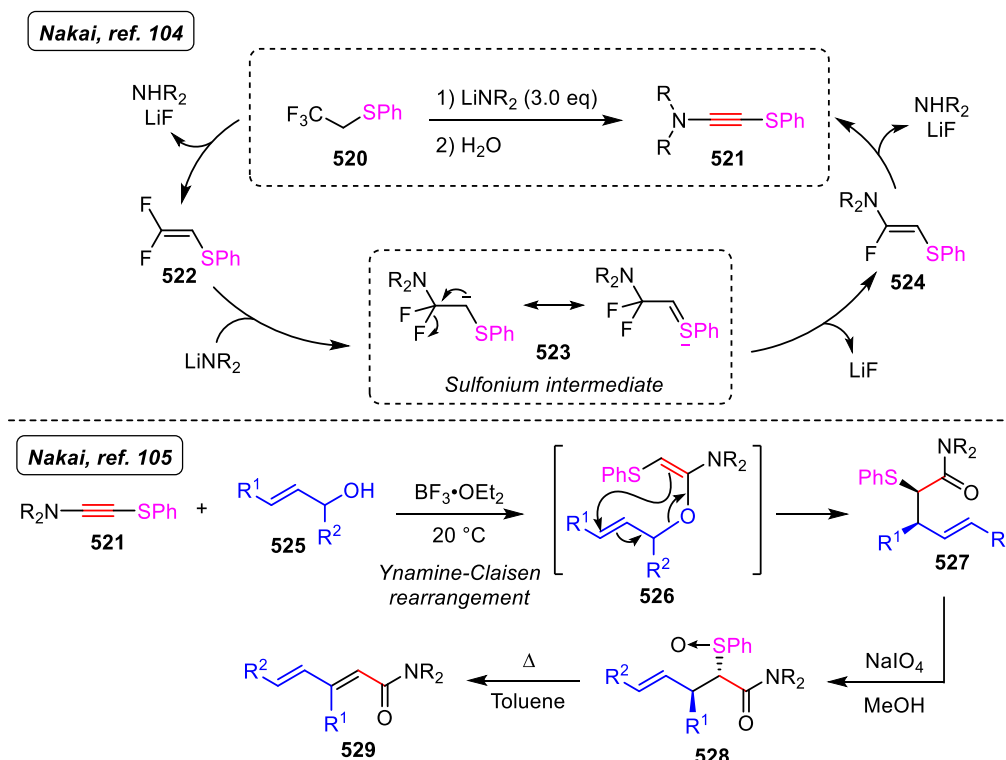
4.2. Introduction to thioynamides

Inspired by the aforementioned work using sulfur substituted alkynes, we attempted to modify the ynamide structure by introducing a sulfide substituent on the other end of the triple bond. Thioynamides could display distinctly enhanced coordination features towards the gold complex than ynamides in the gold mediated annulation investigated throughout this thesis.

The reactivity and applications of thioynamides as building blocks have scarcely been explored. Closely related thioynamines have been investigated by Viehe, who pioneered the first preparation of *N,N*-(ethynylthio)amines from dichlorothioethers in 1969.¹⁰³

Following Viehe's work, Nakai *et al.*¹⁰⁴ developed a general procedure to prepare *N,N*-(ethynylthio)amines **521** employing trifluoroethyl sulfides **520** as precursors (Scheme 64-top). The reaction of the latter with 3 equivalents of lithium diisopropylamide afforded the desired thioynamines **521** in high yields.

It was suggested that the formation of these species involved the participation of a stable carbanion (**523**), which underwent sequential addition-elimination to form the sulfur containing ynamine species. The reactivity of ynamines was then tested in the ynamine-Claisen rearrangement to stereoselectively form amides **527**. After oxidation and thermal decomposition, α,β -unsaturated amides **529** were obtained (Scheme 64-bottom).¹⁰⁵



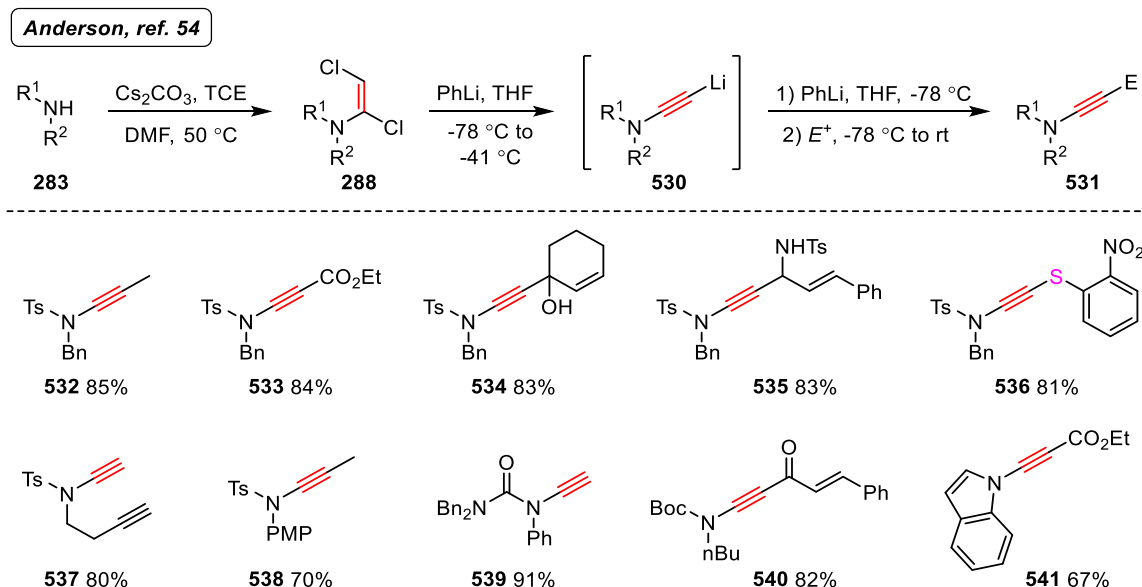
Scheme 64: Nakai's thioynamine formation and application in the formation of α,γ -unsaturated amides

Inspired by these methodologies, a few examples of the preparation of thioynamines were reported during the 1970s and 1980s,¹⁰⁶ yet they passed seemingly unnoticed due to requiring harsh conditions and lengthy synthetic routes to form these relatively unstable species.

In 2015, Anderson and co-workers⁵⁴ developed a robust protocol for the preparation of ynamides from secondary amines or sulfonamides (Scheme 65). The methodology consisted of a two-step sequence converting **283** to their corresponding 1,2-dichloroenamides **288** using trichloroethene.

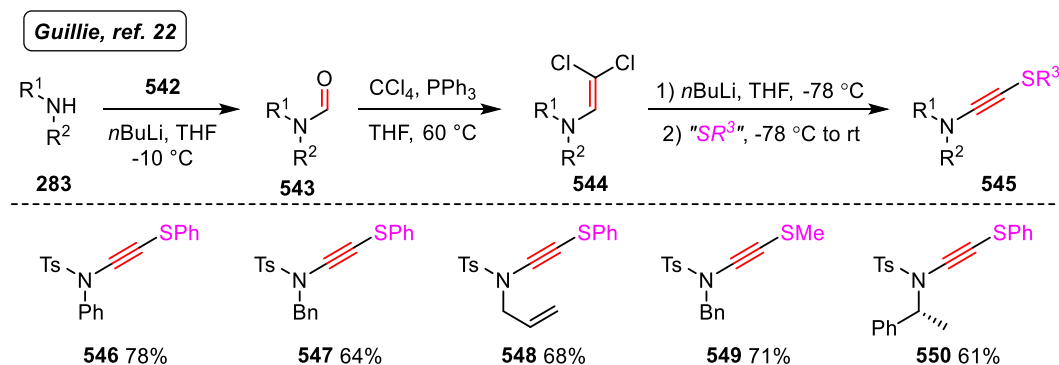
Elimination of HCl with phenyllithium followed by lithium halogen exchange resulted in the formation of lithium acetylide species **530**, which were then trapped with a range of electrophiles to afford functionalised ynamides **531**. In particular, the use of 1,2-bis(2-

nitrophenyl)disulfide as an electrophile gave thioynamide **541**, which was the single example reported of thioynamide formation in Anderson's work.



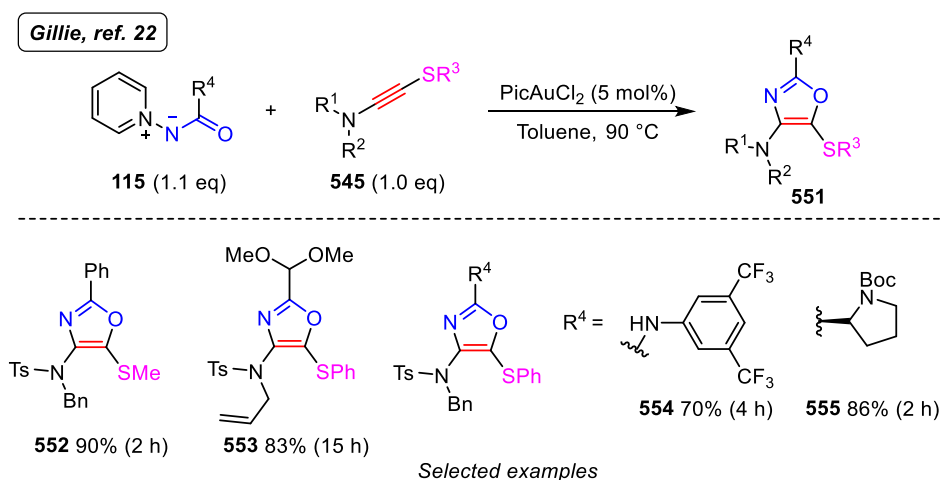
Scheme 65: Formation of ynamides reported by Anderson

While expanding the ynamide scope in the gold-mediated oxazole formation reaction, Gillie *et al.*²² developed a synthetic route to access thioynamides **545** (Scheme 66). Reaction of a range of *p*-toluenesulfonamides **283** with formylbenzotriazole (**542**) delivered tosyl-formamides **543** that were converted to 1,1-dichloroenamides **544** using tetrachloromethane and triphenylphosphine. Dichloroenamides were reacted with *n*-butyllithium and the corresponding lithium acetylides were trapped with either elemental sulfur, followed by iodomethane, or by *S*-phenylbenzenesulfonylthioate to give access to sulfur containing ynamides **546-550**.



Scheme 66: Synthetic route developed by Gillie et al. to synthesise thioynamides

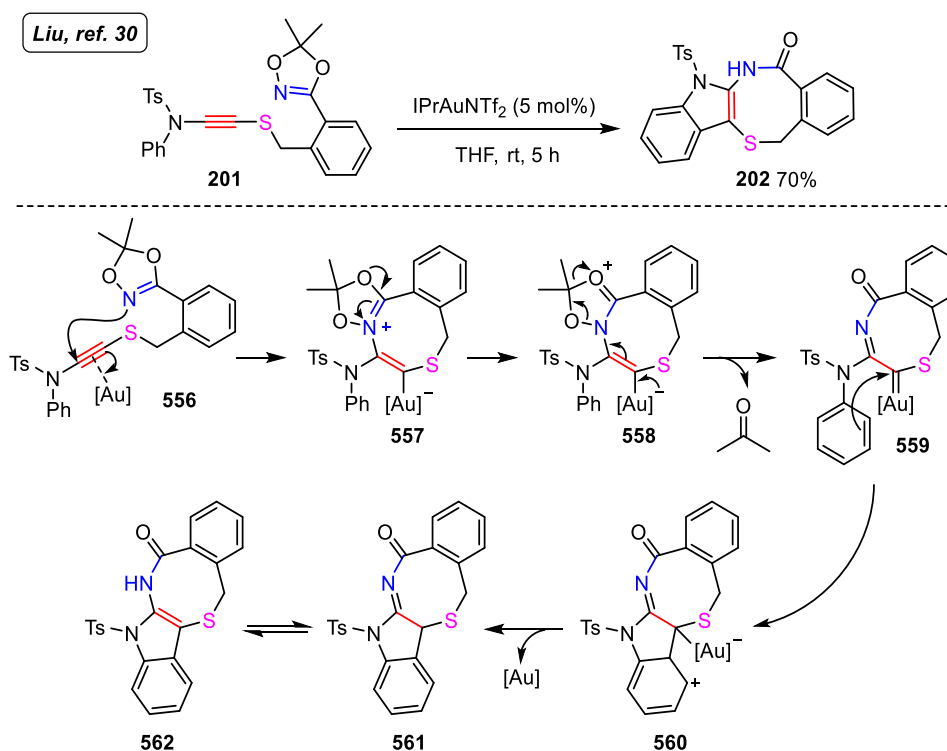
With a collection of thioynamides in hand, attractive functionality was readily introduced in the oxazole core **551** (Scheme 67). In all cases, a single product was achieved bearing the sulfide group in the 5-position (**552-555**). These were the first examples of thioynamides reported in an intermolecular gold mediated transformation.



Scheme 67: Intermolecular gold catalysed dipolar cycloaddition of thioynamides and N-acyl aminides reported by Gillie et al.

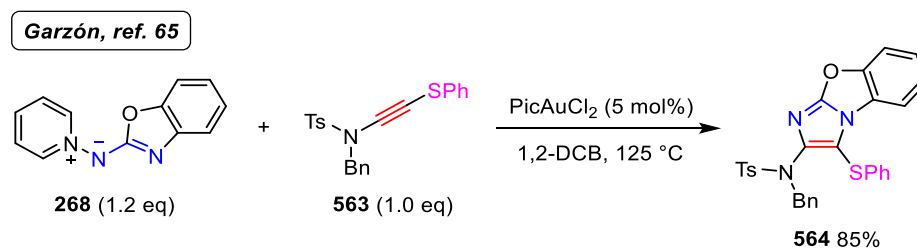
An intramolecular gold-catalysed annulation employing thioynamides was reported by Liu and co-workers (Scheme 68).³⁰ Thioynamide **201** bearing a pendant dioxazole underwent intramolecular nucleophilic attack onto the electronically biased alkyne forming vinyl gold carbenoid **557**. Subsequent rearrangement of the dioxazole core delivered oxonium

intermediate **558**, which underwent a ring opening reaction releasing acetone. α -Imino-gold carbene **559** is trapped by the *N*-phenyl group and forms polycycle **560**. Gold elimination furnished **561** that tautomerised to **562**.



Scheme 68: Gold catalyzed intramolecular cycloaddition of dioxazolyl thioynamide 180 reported by Liu

Inspired by the synthetic potential of thioynamides and alkynyl thioethers in the oxazole chemistry, the Davies group recently reported an example of 3-(thio)substituted benzo[*d*]imidazo[2,1-*b*]oxazole (**564**) using *N*-pyridinium *N*-benzoxazole aminide **268** with thioynamide **563** (Scheme 69).⁶⁵ Despite the difference between the reactivity of the 1,3-*N,O*- (**115**) and 1,3-*N,N*-dipoles (**268**), comparable conversion and reaction times to that of the 5-(thio)substituted oxazole formation (**551**) was achieved, albeit requiring more forcing reaction conditions.



Scheme 69: Gold-catalysed formal [3+2] cycloaddition of *N*-benzothiazole aminides and thioynamides reported by Garzón et al.

As demonstrated with the previous examples, sulfur containing alkynes are suitable π -systems in gold mediated processes. Moreover, they are valuable precursors to sulfones as well as pseudo-halide equivalents for late-stage modifications.

4.2. Results and Discussion

In view of the compatibility of the sulfur containing ynamides with 1,3-*N,N*-dipoles, we sought to further explore their suitability as electron rich π -systems with the aminides introduced in chapter 3.

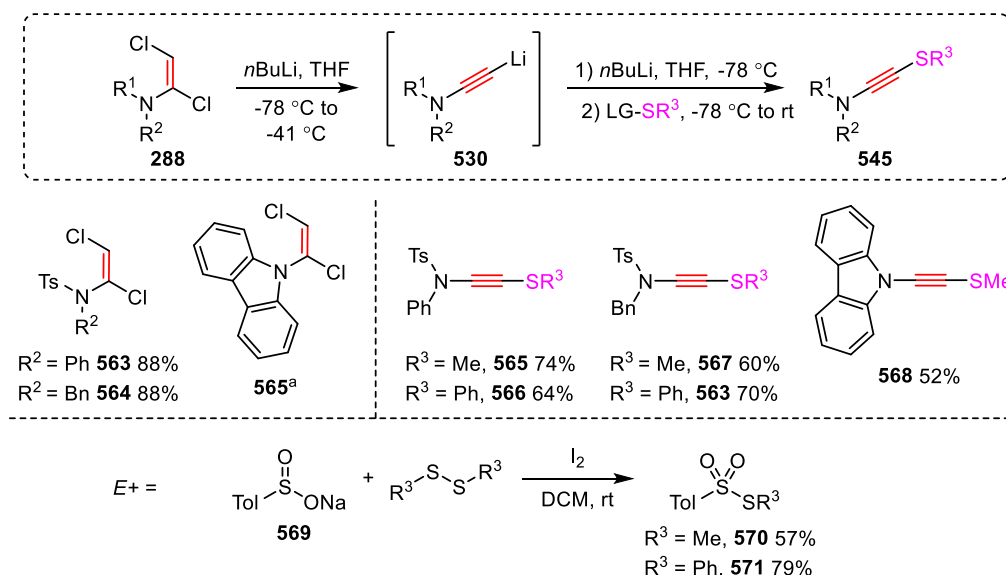
4.2.1. Preparation of thioynamides

From the example reported in Anderson's work in the preparation of an ynamide bearing a sulfur substituent (see Scheme 65),⁵⁴ a general synthetic route for thioynamide formation was envisioned. The use of a range of sulfur containing electrophiles allowed us to establish a general procedure for thioynamide preparation in a practical and scalable manner. A summary of 1,2-dichloroenamides (**500-502**) and thioynamides (**565-568**) synthesised for the purpose of this investigation is shown in scheme 70.

Slow addition of TCE into the reaction mixture is advisable to achieve better conversion to the corresponding dichloroenamides. Depending on the scale of the reaction (more than 1.5

millilitres of TCE), an automatic syringe pump is highly recommended to be used. As 1,2-dichloroethyne is formed, vigorous stirring is needed to avoid both the emergence of hot spots in the vessel and encapsulation/trapping of the evolving gas in the caesium carbonate salt stirring in the flask. The encapsulated 1,2-dichloroethyne is highly flammable and can cause an explosion in the presence of oxygen.

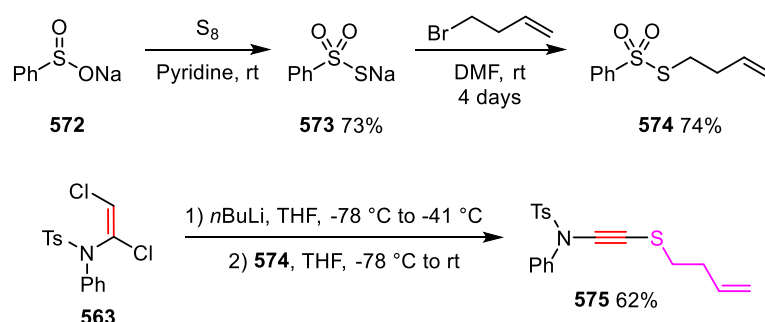
The electrophiles (**570** and **571**) were prepared following Girijavallabhan's work.¹⁰⁷ Although giving moderate yields, the procedure was easily scalable (up to 5.3 grams) using inexpensive sodium *p*-toluenesulfinate **569**.



Scheme 70: 1,2-Dichloroenamides, sulfonothioates and thioynamides synthesised in this work. ^a Example prepared by Pascal Delany

Purification of thioynamides by flash column chromatography proved troublesome due to the similar polarity of by-products, desired products and remaining unreacted starting material. Recrystallization was then attempted, and upon refinement of the optimal solvent conditions, the most effective solvent system to purify *S*-methylated **565** and **567** was CH₂Cl₂/hexane. The *S*-phenyl analogues **566** and **563** were crystallized from hot ethanol.

Formation of a *S*-homoallyl ynamide was achieved by a three-step route commencing with oxidation of sulfonate **572** to sulfonylthioate **573** using molecular sulfur (Scheme 71). The S_N2 reaction of **573** with 4-bromobutene formed *S*-homoallyl sulfonylthioate **574**.¹⁰⁸ Lithiation of dichloroenamide **563** using **574** as the electrophile delivered thioynamide **575**, which was stored at low temperatures and under argon due to its propensity to decompose.

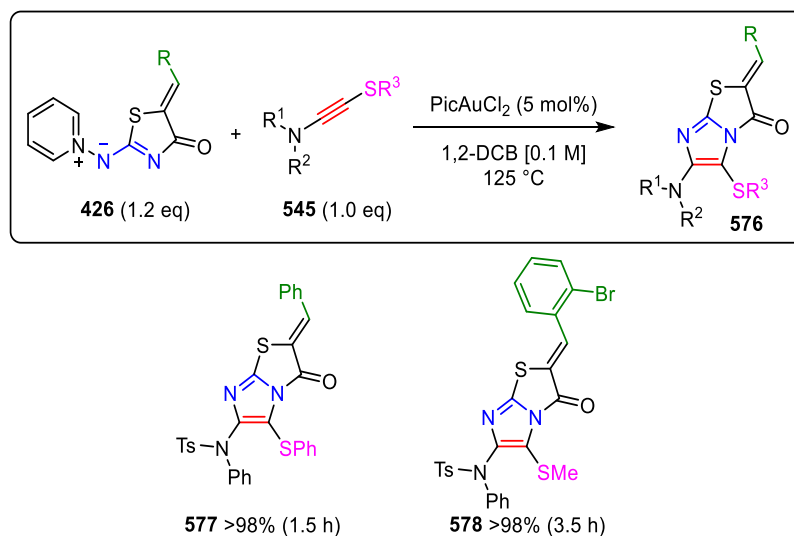


Scheme 71: Synthetic route to prepare *S*-homoallyl thioynamide **575**

4.2.2. Investigating the reactivity of thioynamides in the gold-catalysed formal [3+2] cycloaddition

The reactivity of thioynamides **545** was firstly investigated with *N*-pyridinium *N*-(5-ylidene)thiazolone aminides **426**, since they displayed moderate reactivity when tested with non-sulfur substituted ynamides (see Scheme 52). *N*-Thiazolone aminide **427** reacted smoothly with ynamide **566** affording imidazo[2,1-*b*]thiazolone **577** in quantitative yield, in just 1.5 hours and with the same regioselectivity to that observed with standard ynamides (Scheme 72).

In the same manner, aminide **428** bearing a pendant 2-bromophenyl substituent afforded complete conversion to **578**. These preliminary results suggest the sulfide group on the thioynamide has a significant impact in the gold transformation. Encouraged by these results, we further explored the intriguing reactivity of thioynamides with other nitrenoids.

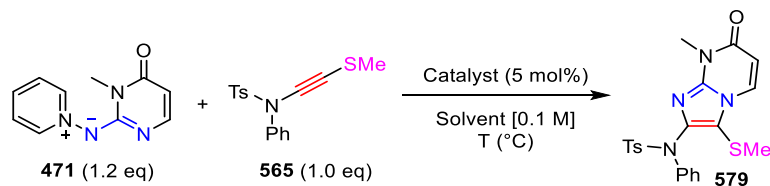


Scheme 72: Exploring the reactivity of thioynamides in the gold catalysed cycloaddition

The study began using thioynamide **565** with aminide **471** (Table 6), which was unreactive with ynamides. Surprisingly, in just 3 hours imidazo[1,2-*a*]pyrimidinone **579** was formed in synthetically useful yield (entry 1), and its structure was confirmed by X-ray crystallography (Figure 16, see Appendix for crystallographic data). A brief survey of the reaction conditions was accomplished in order to improve the conversion and reaction time.

Reaction conditions optimised for other *N*-pyridinium aminides did not represent a noticeable improvement in this scenario, as lengthy reaction times were required to achieve complete conversion (entries 2-3). When the number of equivalents of **471** was increased to 1.5, excellent conversion to the fused imidazole **579** was achieved in just 2 hours.

Variations of the temperature resulted in lower conversion and longer reaction times (entries 5-7). However, the reaction took place even at room temperature, indicating the crucial effect of the sulfide moiety in the transformation (entry 5). Gold(I) catalysts were screened but proved inefficient (entries 8-10).

Table 6: Screening of the reaction conditions of aminide 471 with thioynamide 565

Entry	Eq of 471	Catalyst	Solvent	T (°C)	T (h)	Yield (%) ^a
1	1.2	PicAuCl ₂	1,4-dioxane	90	3	78
2	1.2	PicAuCl ₂	Toluene	60	24	86
3	1.2	PicAuCl ₂	1,2-DCB	125	5	71
4	1.5	PicAuCl ₂	1,4-dioxane	90	2	92
5	1.5	PicAuCl ₂	1,4-dioxane	rt	3 days	50
6	1.5	PicAuCl ₂	1,4-dioxane	60	4.5	(72)
7	1.5	PicAuCl ₂	Toluene	60	24	85
8	1.5	DTBPAu(NCMe)SbF ₆	1,4-dioxane	60	24	47
9	1.5	DTBPAu(NCMe)SbF ₆	1,4-dioxane	90	24	41
10	1.5	IPrAuNTf ₂	1,4-dioxane	90	24	//

^a Isolated yields after purification by flash column chromatography. Yield in parenthesis determined by ¹H NMR using 1,2,4,5-tetramethylbenzene as internal standard.

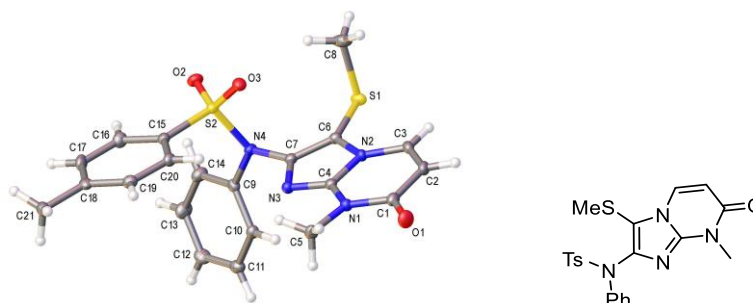
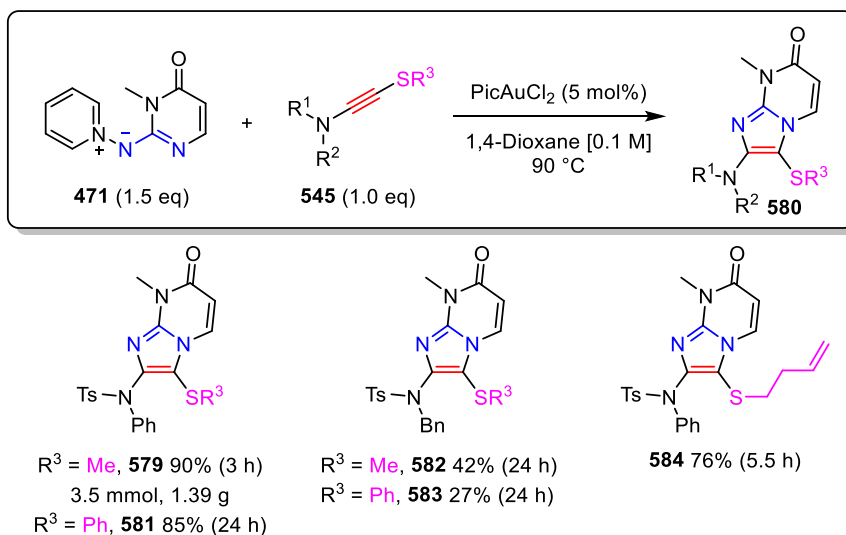


Figure 16: Crystal structure of imidazole 579 with ellipsoids drawn at the 50% probability level. X-Ray crystallography was obtained and solved by Dr Louise Male (University of Birmingham)

With the optimised conditions in hand, the thioynamide scope was investigated (Scheme 73). Both aryl and alkyl thioynamides proved excellent substrates. The reaction was robust and scalable as exemplified with the formation of 1.39 grams of imidazole **579**. Interestingly, the substituents on the *S*-group substantially affected the conversion, ranging from moderate to excellent: smaller groups (*S*-methyl) afforded higher conversion than *S*-phenyl or *S*-homoallyl

groups. This agrees with the results previously reported in the Davies group when investigating the reaction of *N*-acyl aminides with alkynyl thioethers (see Scheme 61).



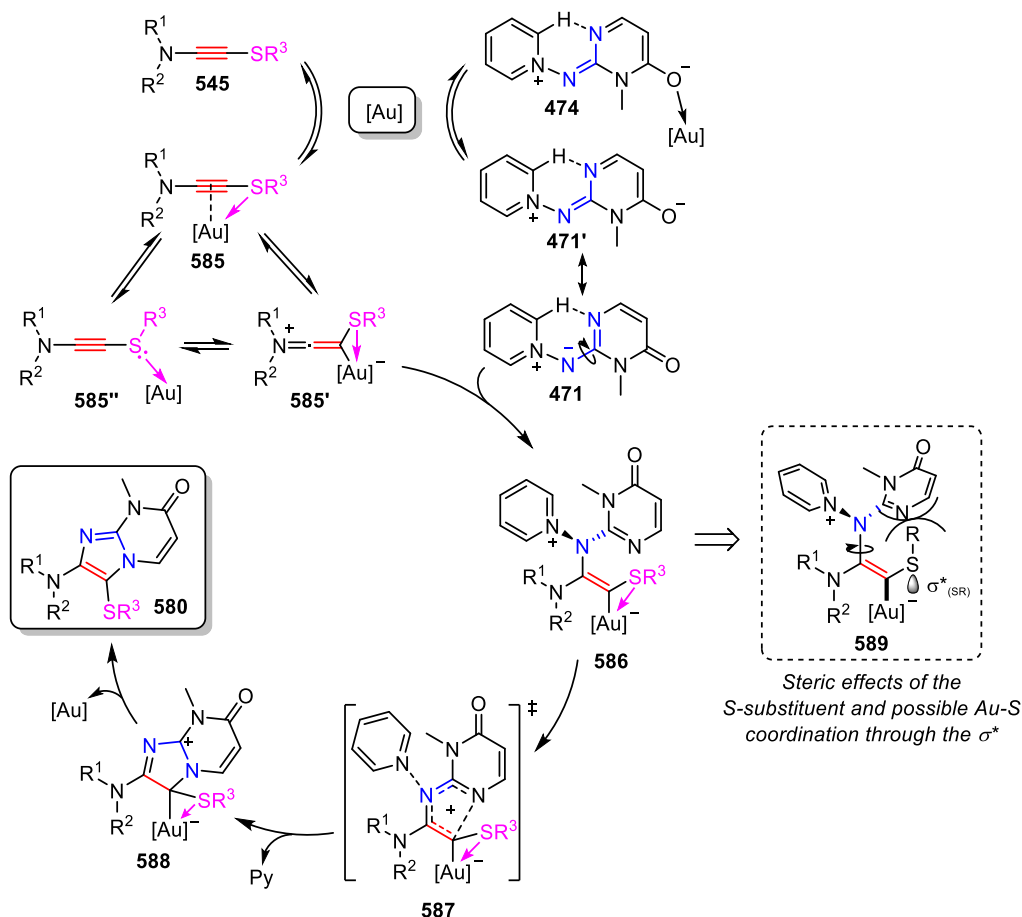
Scheme 73: Gold catalysed cycloaddition of thioynamides with *N*-pyrimidinone aminide

The substituents on the *N*-end of the ynamide also affected the reactivity. In general, *N*-phenyl ynamides provide significantly better conversion than the analogous ynamides bearing a *N*-benzyl group. When employing *N*-benzyl ynamides, complete conversion to **582** and **583** was not achieved and the unreacted ynamide was recovered.

4.2.3. Mechanistic proposal

From a mechanistic point of view, the results obtained thus far suggest an intriguing sulfur effect aiding some of the key steps of the transformation. From a wider perspective, there is several equilibria taking place in the reaction mixture on which the gold complex might be involved (Scheme 74, **545** to **585''** and **474** to **471**). Consequently, the actual concentration of active aminide, (thio)ynamide and catalyst might be altered.

As discussed in chapter 3, the new aminides are highly electron-rich species and could interact with the gold catalyst (**474**) leading to unproductive reaction pathways. This interaction would justify the lack of reactivity observed with *N*-thiazolone, *N*-imidazolone and *N*-pyrimidinone aminides due to catalyst poisoned.



Scheme 74: Proposed mechanism for the gold-catalysed formal [3+2] cycloaddition with thioynamides

The change in reactivity observed when aminide **471** was reacted with thioynamide **565** could be explained by a more effective gold-aminide coordination assisted by the sulfide group. Several factors could cause this: one of the lone pairs of the sulfur could form a dative bond with the gold complex (shown in scheme 74 as an arrow from the sulfur towards the gold complex), aiding formation of a π -complex, and then favouring the formation of

keteniminium **585'**. A complementary Au-S interaction could arise also from the overlap of the [Au]-C bond with the σ^* of the SR group (**589**), favouring as well the formation of **585'**.

Beyond the enhanced reactivity, no experimental or spectroscopic evidence has been achieved thus far to confirm any of these proposed interactions, and indeed the nature and importance of any interaction could change at different points of the mechanism. The overall impact will be referred to as the *sulfur-effect* throughout the present chapter, yet, it will be omitted in the schemes for clarity.

This Au-S interaction could prevent, or significantly decrease, the undesired gold-nitrenoid coordination and favour a higher concentration of the activated alkyne **585**. Nucleophilic attack of the aminide onto the active species **585'** is now feasible, thus triggering the cycloaddition process.

The range in reactivity observed when investigating the SR^3 substituent of the thioynamide could be caused by a blockage of the electrophilic metal centre during the intramolecular cyclisation event (**589**). The stabilising S-Au interaction results in a restricted conformation of the S-R group positioning it S-trans to the gold complex. Consequently, larger substituents ($\text{R} = \text{Ph}$) obstruct the approach of the pyrimidinone ring to the electrophilic center more than smaller groups ($\text{R} = \text{Me}$), causing a decrease in the conversion.

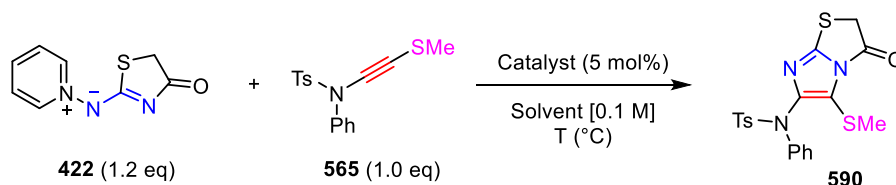
The groups on the sulfonamide also significantly affect in the process. It was observed that the presence of a *N*-benzyl group was notoriously detrimental for the yield and reaction time compared to *N*-phenyl. We proposed this drop in the reactivity is caused by a blockage between the benzyl group and the imposed S-R group conformation preventing the Au to be released.

4.2.4. Further insights on the reactivity of thioynamides

To widen the scope of the transformation provided by *S,N*-substituted alkynes, *N*-thiazolone and *N*-5-(ylidene)imidazolone aminides were next examined.

A brief screening of the reaction conditions was accomplished using aminide **522** (Table 7). Dichloro(2-pyridinecarboxylato)gold was chosen as a reference catalyst due to its suitability in the previous study (see Table 6). Problems of solubility were observed using toluene due to the high polarity of the aminide, which did not completely dissolve in toluene (entry 1).

Table 7: Survey for the gold catalysed cycloaddition of aminide 422 with thioynamide 565



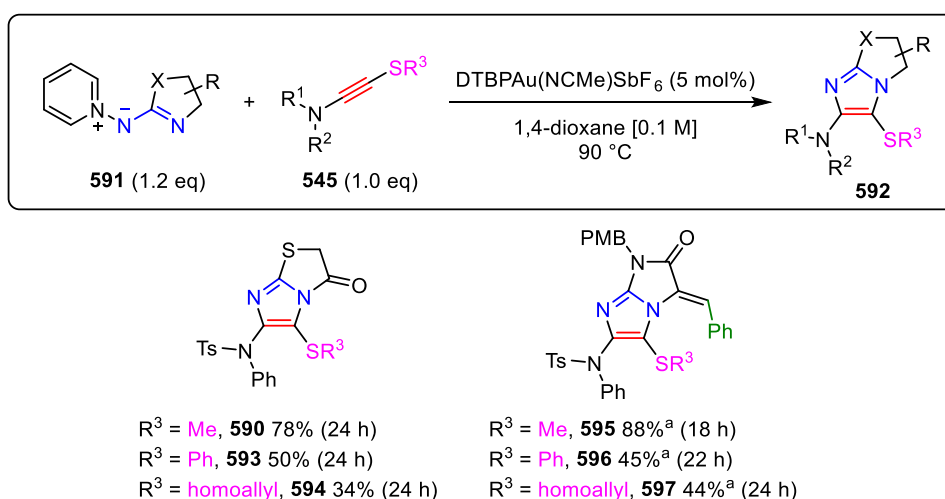
Entry	Eq of 422	Catalyst	Solvent	T (°C)	T (h)	Yield (%) ^a
1	1.2	PicAuCl ₂	Toluene	60	24	10
2	1.2	PicAuCl ₂	1,4-dioxane	60	24	(38)
3	1.2	PicAuCl ₂	1,4-dioxane	90	4.5	69
4	1.2	PicAuCl ₂	1,2-DCB	125	5	48
5	1.5	PicAuCl ₂	1,4-dioxane	90	24	20
6	1.2	DTBPAu(NCMe)SbF ₆	1,4-dioxane	90	24	(78)
7	1.5	DTBPAu(NCMe)SbF ₆	1,4-dioxane	90	24	(35)
8	1.2	IPrAuNTf ₂	1,4-dioxane	90	24	(8)

^a Isolated yields after purification by flash column chromatography; Yields in parenthesis determined by ¹H NMR using 1,2,4,5-tetramethylbenzene as internal standard.

The temperature was then varied: low temperatures resulted in slow reactions with poor conversions (entries 1 and 2); 1,4-dioxane at 90 °C gave good conversion in relatively short reaction time (entry 3). In contrast, an increase of the temperature to 125 °C led to decomposition of the aminide (entry 4). Increasing the equivalents of aminide to 1.5 was deleterious (entry 5). Interestingly, cationic phosphite gold(I) DTBPAu(NCMe)SbF₆ was a

better catalyst affording imidazole **590** in 78% yield, with only 1.2 equivalents of aminide (compare entry 6 and 7). Finally, a more electron-rich gold(I) catalyst (IPrAuNTf₂) was tested, resulting in very poor conversion (entry 8).

With the optimised conditions in hand, the thioynamide scope was then explored with **422** and **460** (Scheme 75). Previous electronic and steric issues were overcome and direct access to non-aromatic imidazo[2,1-*b*]thiazoles was achieved for the first time employing our synthetic strategy (**590-594**).



Scheme 75: Screening of the thioynamide scope with *N*-thiazolone and *N*-imidazolone aminides. ^a Utilising PicAuCl₂ as catalyst

N-Imidazolone aminide **460** also displayed exceptional reactivity giving access to poly-aza fused imidazoles **595-597**. In all cases a single imidazole regioisomer was achieved with analogous regioselectivity to that of the previous series, as was conformed by the crystal structure of **590** and **595** (Figure 17 and Figure 18, see Appendix for crystallographic data). In keeping with the results shown in Scheme 73, a marked decreased in reactivity was observed when bulkier substituents were introduced in the sulfide group.

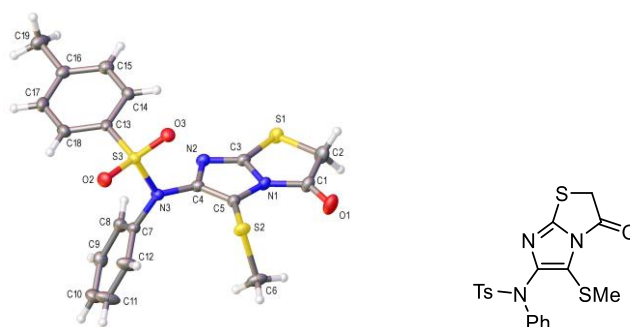


Figure 17: Crystal structure of imidazole 590 with ellipsoids drawn at the 50% probability level. X-Ray crystallography was obtained and solved by Dr Louise Male (University of Birmingham)

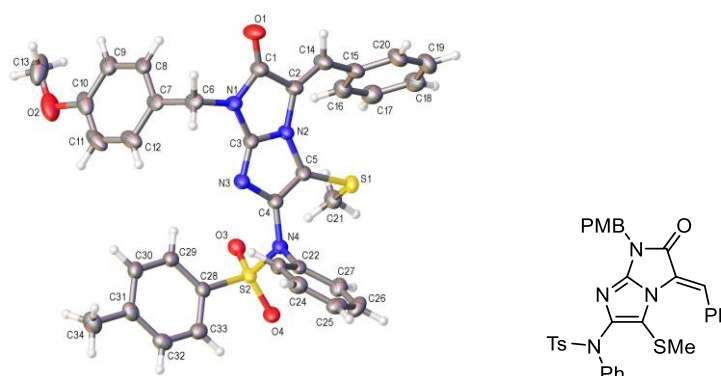
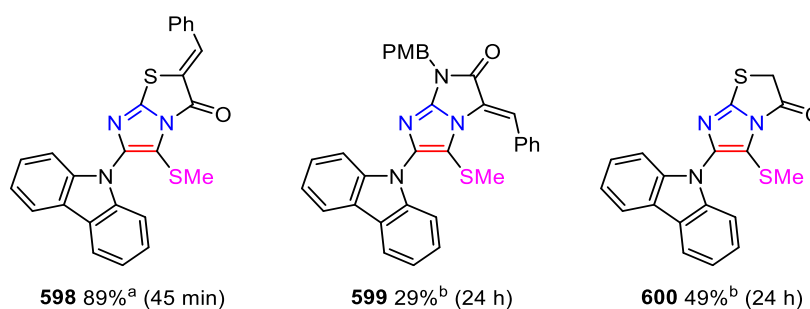


Figure 18: Crystal structure of imidazole 595 with ellipsoids drawn at the 50% probability level. X-Ray crystallography was obtained and solved by Dr Louise Male (University of Birmingham)

Finally, carbazole derived thioynamine **568** was tested to see the impact of a cyclic thioynamine in the transformation (Scheme 76). A consistent reactivity trend was observed across the aminides tested with 5-benzylidene **427** being noticeably more reactive than aminides **460** and **422**.

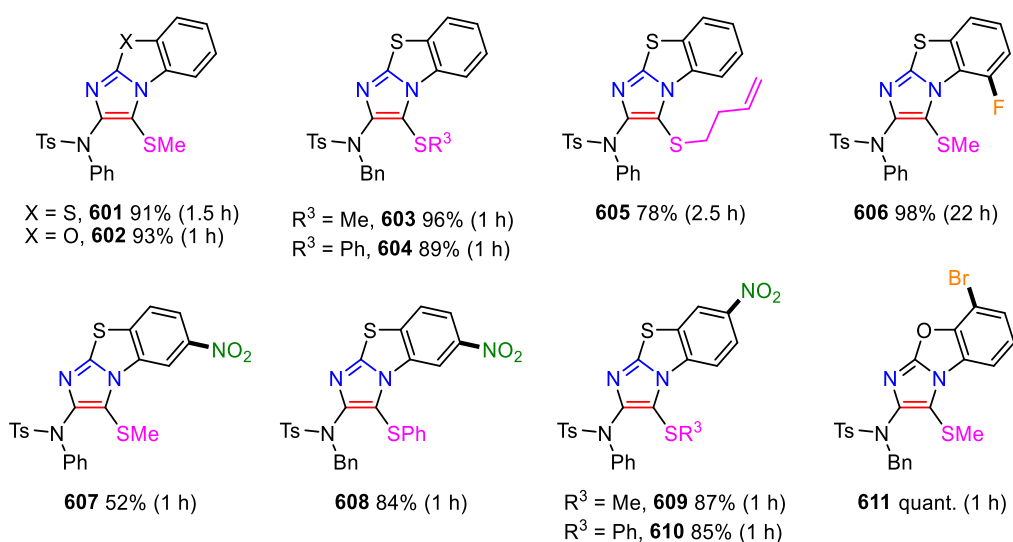


Scheme 76: Effect of a cyclic thioynamine in the gold catalysed cycloaddition; ^a Utilising PicAuCl₂, 1,2-DCB at 125 °C; ^b Utilising PicAuCl₂, 1,4-dioxane at 90 °C.

Compounds bearing both a carbazole and an (ylidene)thiazolone motif are frequently found in material science and utilised as photosensitizers^{73b} due to their donor-acceptor electronic properties. Therefore, this synthetic route could be applied to access these types of materials displaying interesting photoelectronic properties.

4.2.5. Study of the thioynamide scope with *N*-benzo(heteroaryl) and *N*-diazinyl aminides

The promising results accomplished utilising thioynamides encouraged us to further investigate their reactivity with *N*-pyridinium *N*-benzo(heteroaryl) aminides (Scheme 77).



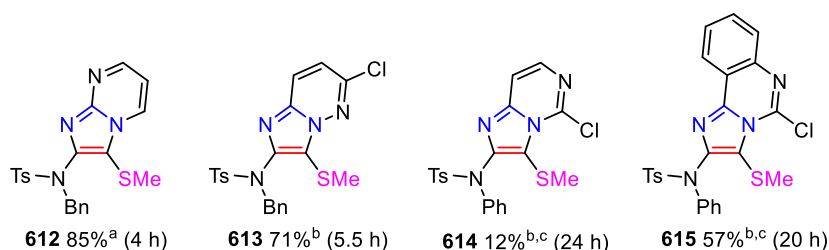
Scheme 77: Exploring the reactivity of thioynamides with *N*-benzo(heteroaryl)aminides. Reaction conditions: PicAuCl₂ (5 mol%), 1,2-DCB at 125 °C

In general, reactions were fast, regioselective, and both *S*-methyl and *S*-phenyl groups were readily introduced at the 4-position of the imidazole. Unlike the previously investigated nitrenoids, the steric bulk of sulfide substituents did not prove significantly deleterious to yields (compare **603** and **604** or **609** and **610**). With these aminides, the intramolecular cyclisation might be a fast process, which could potentially occur in a concerted manner with

pyridine elimination. As a result, the sulfide group would be displaced out of the imidazole-benzothiazole plane and therefore, it does not obstruct the cyclisation.

The reaction of *S*-homoallyl ynamide **575** provided relatively lower yield of imizado[2,1-*b*]benzothiazole **605** compared to its SMe analogue. Nitro and halogenated aminides underwent the cycloaddition smoothly. The only exception being **607** due to a troublesome purification.

Compatibility was also observed between thioynamides and *N*-pyridinium *N*-diazinyl aminides, yet in general lengthy reaction times were needed compared to previous examples to achieve complete conversion to the corresponding imidazoles **612-615** (Scheme 78). While good conversion **612** and **613** was achieved, formation of imidazole **614** was sluggish; 65% of ynamide was recovered even after 24 hours. In addition, moderate reactivity was observed for imidazole **615**.

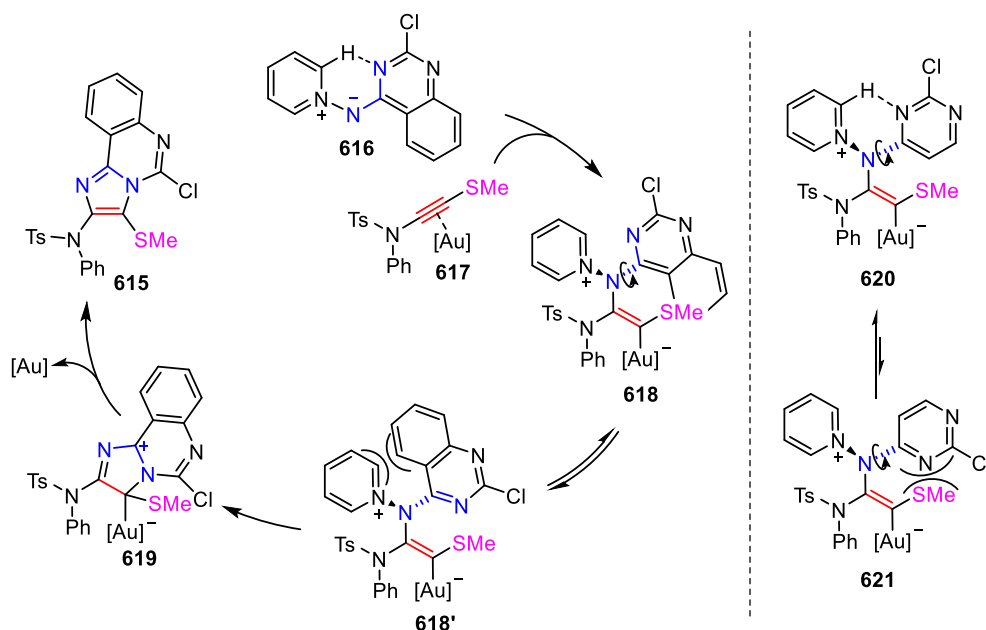


Scheme 78: *N*-Pyridinium *N*-diazinyl aminides in the gold catalysed cycloaddition with thio ynamides;
^a Utilising DTBPAu(NCMe)SbF₆, 1,4-dioxane at 90 °C; ^b Utilising PicAuCl₂, 1,4-dioxane at 90 °C; ^c Reactions repeated twice, equal conversion to the corresponding imidazole and recovery of the starting ynamide was obtained in both attempts

Despite the structural similarity between imidazoles **614** and **615**, there is a clear difference in conversion. The steric clash in **618** (Scheme 79) between the *S*-methyl group and the benzene moiety could favour reconfiguration of the aminide nitrogen to the more stable conformation (**618'**). In **618'**, elimination of the pyridine group would be a favourable and fast process to

form a more stable intermediate (**619**), which has the positive charge stabilised by the two fused rings. In the case of the formation of imidazole **614**, reconfiguration on **620** to intermediate **621** would not be straightforward because intermediate **620** is stabilised by an intramolecular H-bond interaction and has no steric hindrance. Therefore, the high energy barrier required to form **621** would disfavour the cyclisation process.

As the cyclisation is likely to be the rate limiting step, the formation of intermediate **619** would be the driving force to form **615** and the reason why **615** is obtained in higher conversion than **614**.

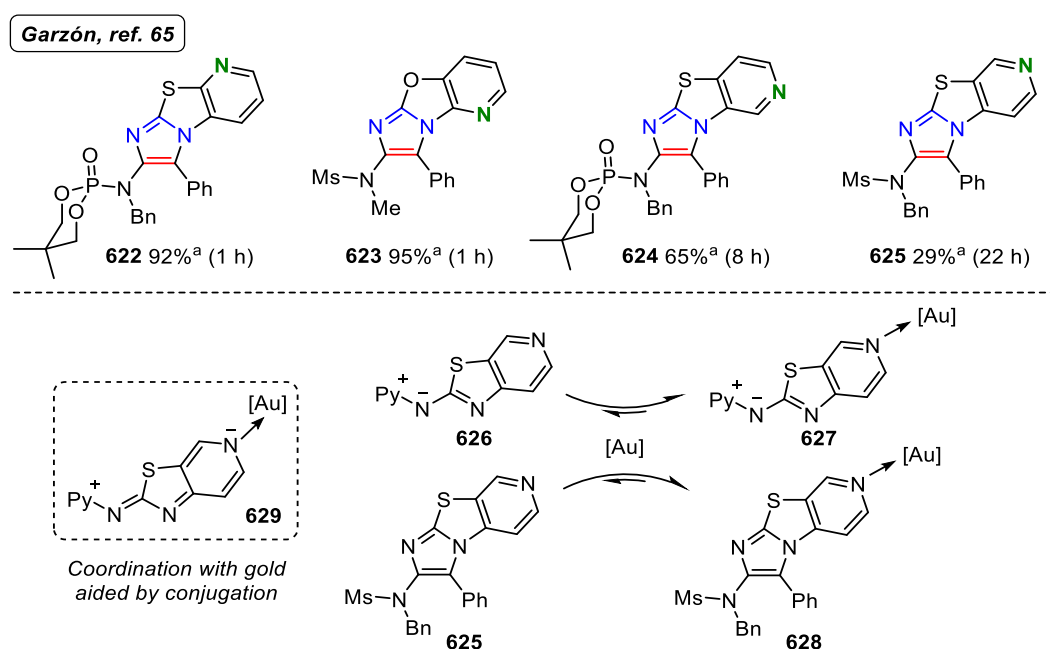


Scheme 79: Potential steric issues in the formation of imidazoles **614 and **615** during the gold-cycloaddition**

Compared to the other series of nitrenoids, *N*-benzo(heteroaryl) aminides did not show a significant enhancement in the reactivity when reacting with thioamides. In contrast, the gold catalysed cycloaddition of thioamides with *N*-diazinyl aminides seemed to be relatively disadvantageous.

4.2.6. Improving the reactivity of other aminides

Garzón previously synthesised a set of pyridine-fused benzothiazole aminides and tested them in the gold catalysed cycloaddition with ynamides (Scheme 80).⁶⁵ These proved to be effective 1,3-*N,N*-dipoles, however their conversion ranged significantly from poor to excellent. While the formation of imidazoles **622** and **623** bearing a nitrogen in 4-position and 7-position proceeded smoothly, imidazoles **624** and **625**, containing a nitrogen in 5-position and 6-position respectively, afforded lower conversion and required lengthy reaction times.



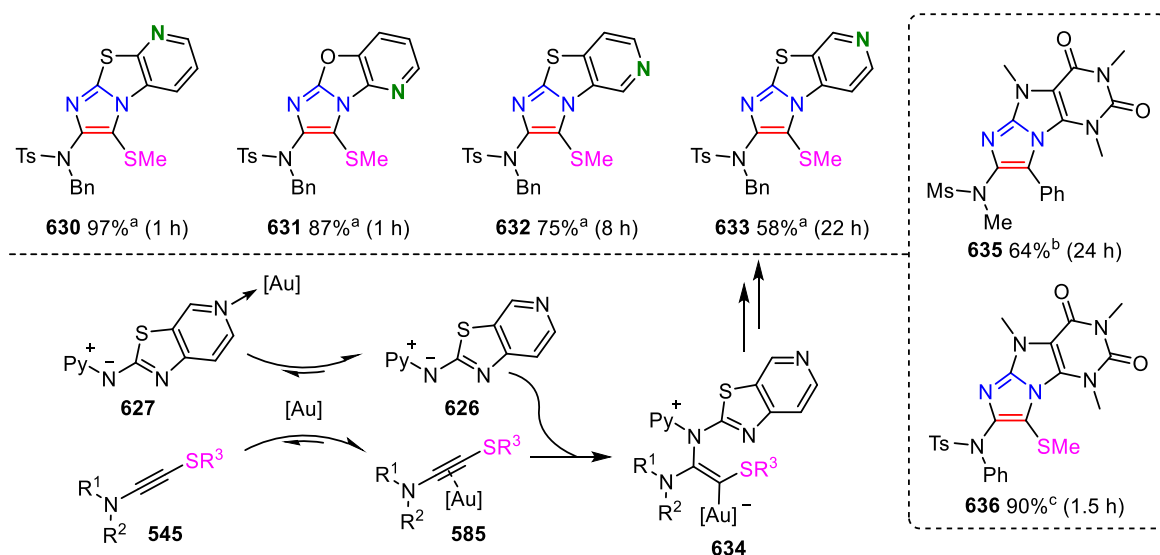
Scheme 80: Top: Study of pyridine fused *N*-benzo(heteroaryl) aminides in the gold catalysed cycloaddition with ynamides undertaken by Garzón; ^a Utilising $PicAuCl_2$, 1,2-DCB at 125 °C. Bottom: Proposed poisoning aminide-gold side reaction

Garzón and Davies proposed that the difference in reactivity was due to the variation on the position of the nitrogen in the pyridine ring. The pyridinyl nitrogen in position 5 or 6 (either in aminides or products) could have the ability to sequester the gold complex (**629** and **628**). In these positions the nitrogen was more sterically accessible or activated by conjugation with

the *N,N*-dipole (5- and 6-) and showed higher ability to interact with the catalyst resulting in a decrease of the conversion to **624** and **625**.

Taking advantage of the reactivity displayed by thioynamides, a new study of pyridine-fused benzoheteroaryl aminides with thioynamides was accomplished (Scheme 81-top). Gratifyingly, a marked improvement on the yield was found, whilst maintaining the same reactivity trend. The position of the nitrogen on the pyridine ring continues to play an important role on the reactivity of this series of nitrenoids. However, the presence of a sulfur moiety introduced *via* the thioynamide allows for a better conversion to imidazoles **632** and **633**, respectively.

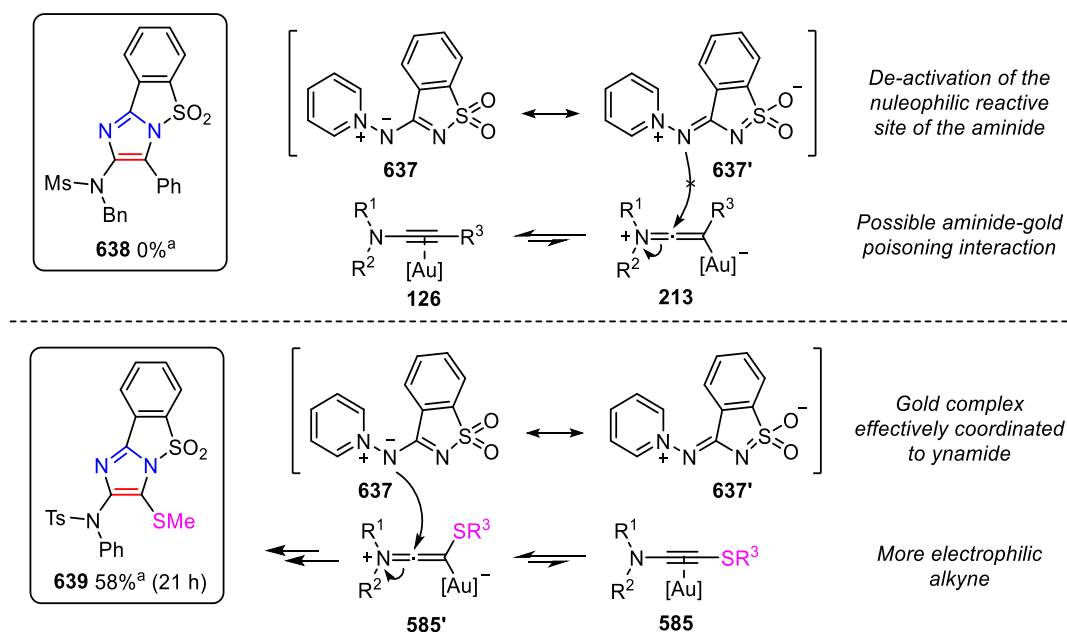
These results show the ability of thioynamides to prevent, to a certain extent, undesired poisoning *via* gold-aminide coordination due to the excellent S-Au interaction formed during the activation of the π -system (Scheme 81-bottom).



Scheme 81: Top: Thioynamides in the gold catalysed cycloaddition with pyridine fused *N*-benzo(heteroaryl) aminides. Bottom: Additional sulfur-effect in the activation of the π -system. Right: Caffeine based tri-fused imidazole. ^a Utilising PicAuCl₂, 1,2-DCB at 125 °C; ^b Example prepared by Garzón; ^c Utilising PicAuCl₂, 1,4-dioxane at 90 °C.

Capitalising on this sulfur-gold interaction, a caffeine based aminide prepared by Garzón, also exhibited better conversion when reacted with thioynamide **565**, yielding 8-(methylthio)imidazo[1,2-*e*]purine **636** in excellent yield (Scheme 81-right).

The advantageous effect of *N,S*-heteroalkynes in the gold catalysed strategy was further demonstrated utilising a saccharin derived aminide previously synthesised by Garzón. Aminide **637** was tested with ynamide **297** and did not give conversion to the desired tricyclic product **638** (Scheme 82-top). This could be attributed to deactivation of the *N,N*-dipole by the presence of an electron-withdrawing sulfonyl group, which could also be acting as a ligand for the gold complex.



Scheme 82: Comparison of ynamide versus thioynamide reactivity with *N*-saccharine aminide **568; ^a Utilising $PicAuCl_2$, 1,4-dioxane at 90 °C**

In contrast, when methyl sulfide ynamide **565** was reacted alongside **637** in the gold catalysed cycloaddition, moderate conversion, to imidazole **639** was achieved (see Figure 19). This significant result suggests that the alkyne is more electrophilic and the reaction can take place

using soft nucleophiles or more general 1,3-dipoles. For X-ray crystal data of imidazole **639** see Appendix.

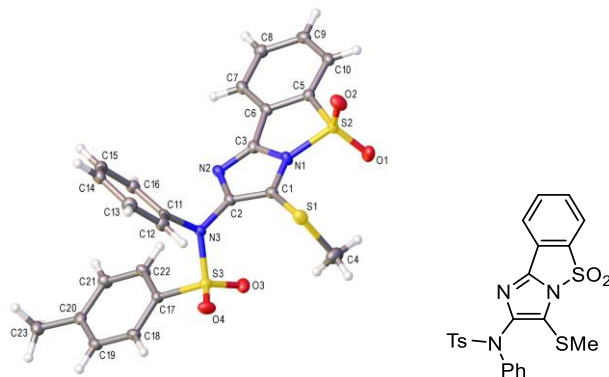
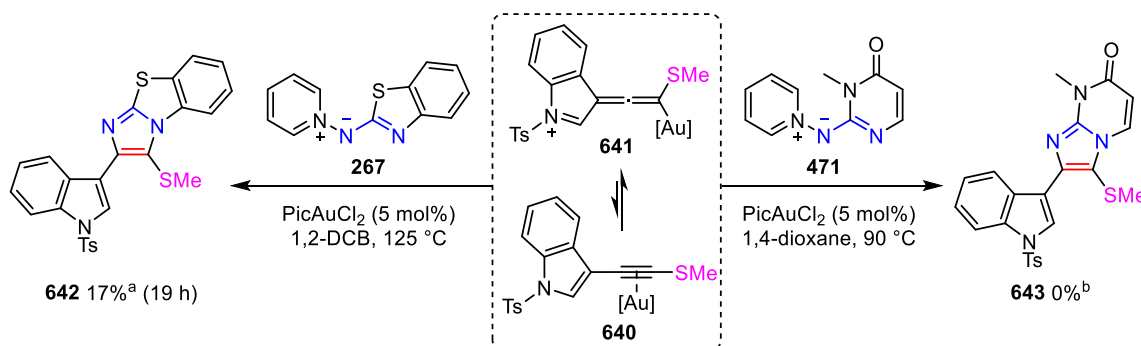


Figure 19: Crystal structure of imidazole **639** with ellipsoids drawn at the 50% probability level. X-Ray crystallography was obtained and solved by Dr Louise Male (University of Birmingham)

Finally, to test whether a distant nitrogen in conjunction with a sulfide moiety is sufficient to activate the π -system, 3-((methylthio)ethynyl)-1-tosyl-1*H*-indole ynamide **640** was tested with aminides **267** and **471**. As shown in scheme 83, a sharp loss and no reactivity was observed, respectively with these aminides. These results reiterate the decreased reactivity of *N*-benzothiazole and especially *N*-pyrimidinone aminides compared to the *N*-acyl series, which have previously been studied with indolyl ynamides and demonstrated to be suitable substrates (see Scheme 59).⁹⁵

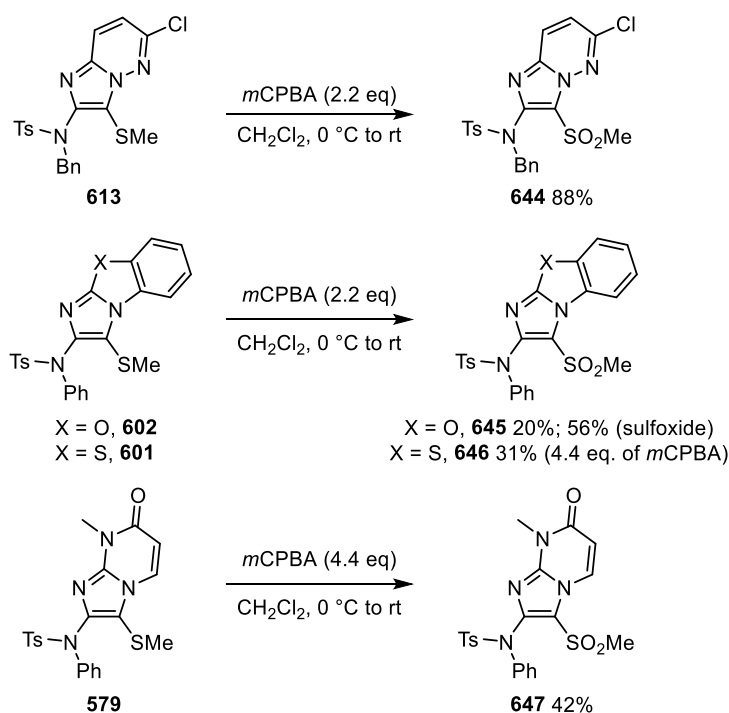


Scheme 83: Investigating the reactivity of indolyl-thioynamide **640** in the gold catalysed cycloaddition

While aiding in the gold-ynamide coordination, the sulfide alone group is not activating enough to promote the reaction. The presence of a nitrogen adjacent to the triple bond is crucial to successfully activate the electrophilic *sp* carbon centre, as demonstrated with the use of thioynamides throughout this chapter.

4.2.5. Post catalytic transformations

Capitalising on the sulfide moieties introduced *via* thioynamides, oxidation of the sulfide group to the corresponding sulfone **644** was successfully achieved with compound **613** (Scheme 84).

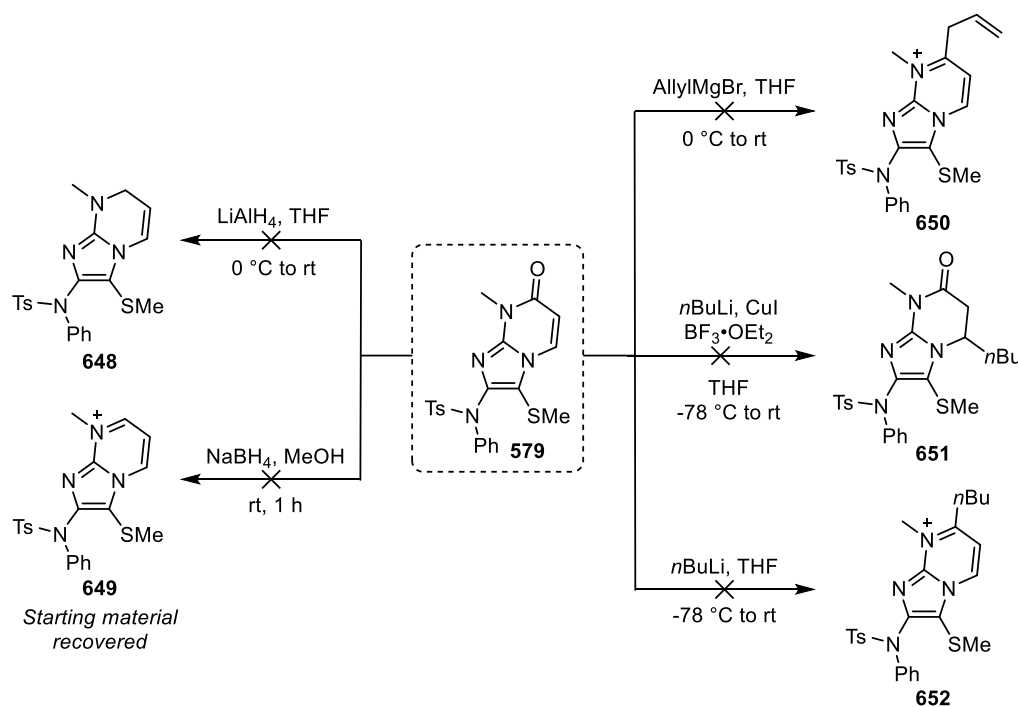


Scheme 84: Attempted oxidations of the sulfides

Imidazoles **602** and **601** provided the desired sulfone in poor yield. In the formation of imidazole **646**, an increase of the number of equivalents of *m*-chloroperbenzoic acid was required to achieve improved yield. Oxidation was also attempted utilising hydrogen peroxide

yet was unsuccessful. Oxidation of **579** to sulfone **647** was achieved in moderate yield due to a potential epoxidation side reaction from the alkene. Yet, no by-product was possible to isolate.

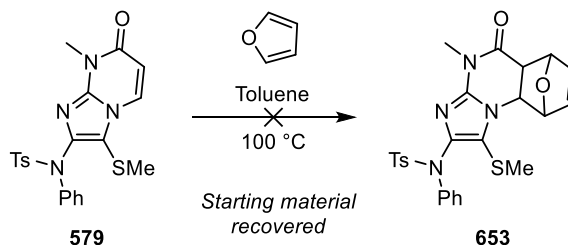
Reduction of the amide of fused imidazo-uracil **579** was not successful either when sodium borohydride or lithium aluminium hydride were used (Scheme 85). Several 1,2- and 1,4-additions were attempted using Grignards, organocuprates and organolithium reagents but also failed (**650-652**). The highly conjugated sp^2 system reduces the electrophilicity of the α,β -unsaturated ketone.



Scheme 85: Attempted reductions and 1,2-, 1,4- additions to uracil derivative 579

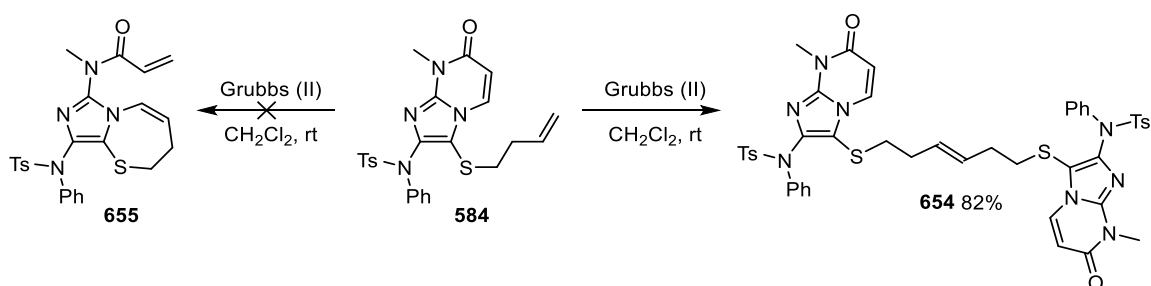
Another additional modification attempted on the tri-fused imidazole core was a Diels-Alder reaction, which have previously been reported on uracil derivatives,¹⁰⁹ yet no adduct was seen in the reaction of imidazole **579** and furan (Scheme 86). The reaction might require harsher

conditions as furan is known to undertake Diels-Alder reactions at significantly elevated temperatures.



Scheme 86: Attempted Diels-Alder reaction on uracil-imidazole 579

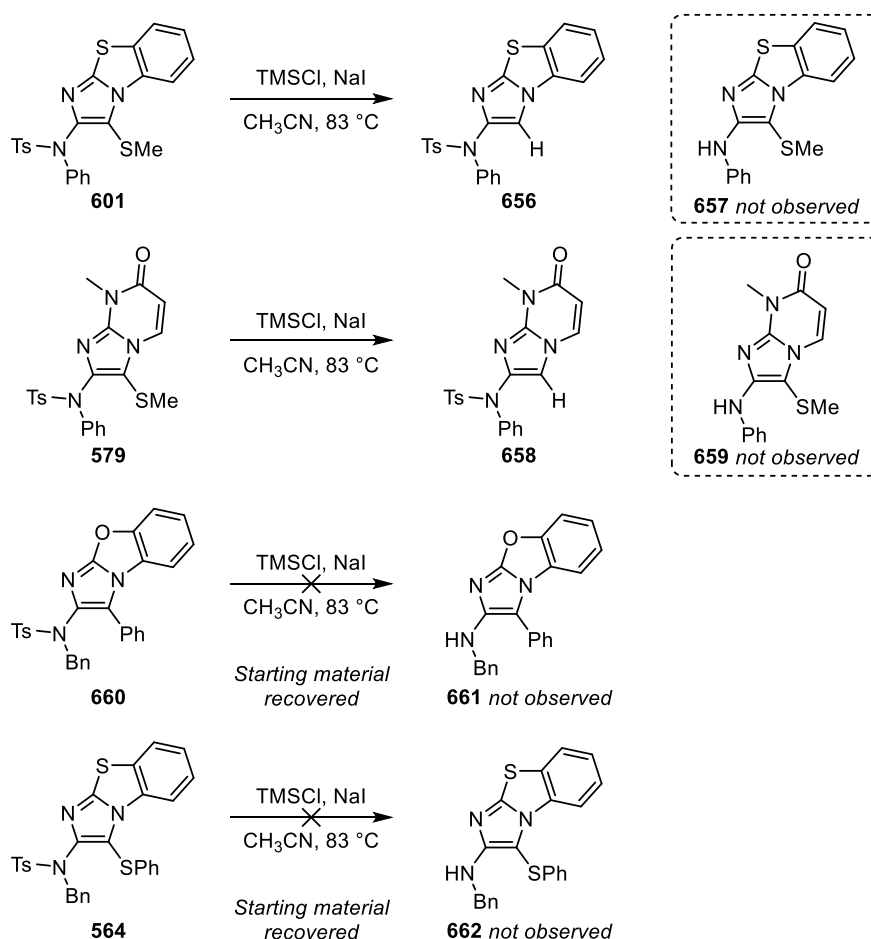
Reaction of **584** with Grubbs 2nd generation catalyst underwent an intermolecular metathesis reaction in place of the desired intramolecular reaction to give dimer **654**. The stereochemistry of **654** could not be assigned as the symmetry of the system prevents differentiation of the cis/trans splitting in the ¹H-NMR and a single crystal has not been successfully grown yet (Scheme 87).



Scheme 87: Intra- and intermolecular metathesis reactions on uracil derivative

Deprotections of the sulfonamide group of **305**, **579**, **308** and **602** were attempted (see Appendix) yet none of them proved fruitful. A range of conditions were tested on several substrates, but none of them delivered the secondary amine; just starting material was recovered.

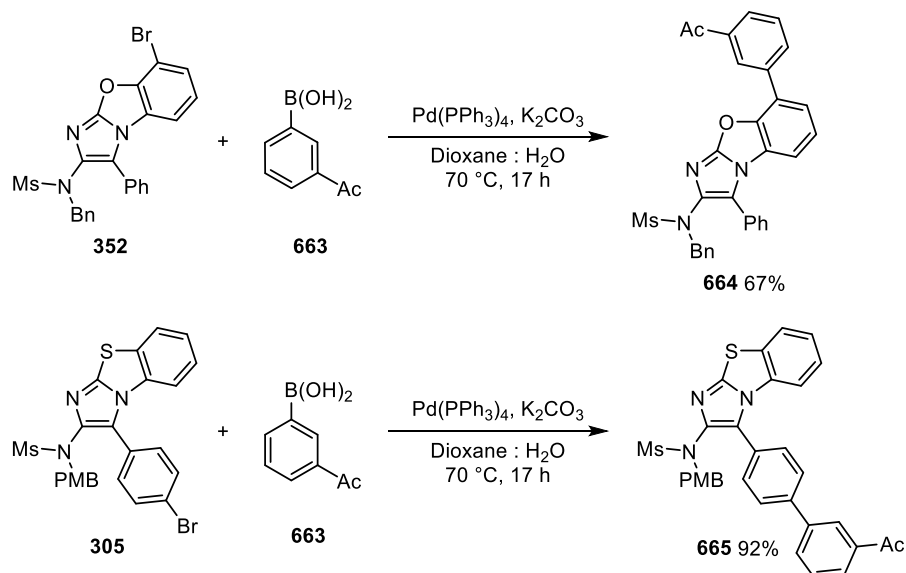
A rather unexpected result was achieved employing trimethylsilyl chloride and sodium iodide in an attempt to cleave the *p*-toluenesulfonyl group (Scheme 88). The reaction of trimethylsilyl chloride and sodium iodide forms trimethylsilyl iodide, which is known to be a suitable species to cleave sulfonyl groups.¹¹⁰ Interestingly, ¹H NMR analysis overlapping the starting material spectra with that obtained from the reactions suggested cleavage of the methylsulfide group instead of aminide deprotection. The proposed products **656** and **658** could not be purified by flash column chromatography despite multiple attempts. The deprotected amine was not observed in any case.



Scheme 88: Attempted tosyl deprotections using TMSCl and NaI

Tosyl cleavage was also attempted with compound **660**, which does not bear a labile sulfide group, but just starting material was recovered. Imidazole **564** with a less labile SPh group was tested using the same conditions but proved unreactive towards deprotection as well.

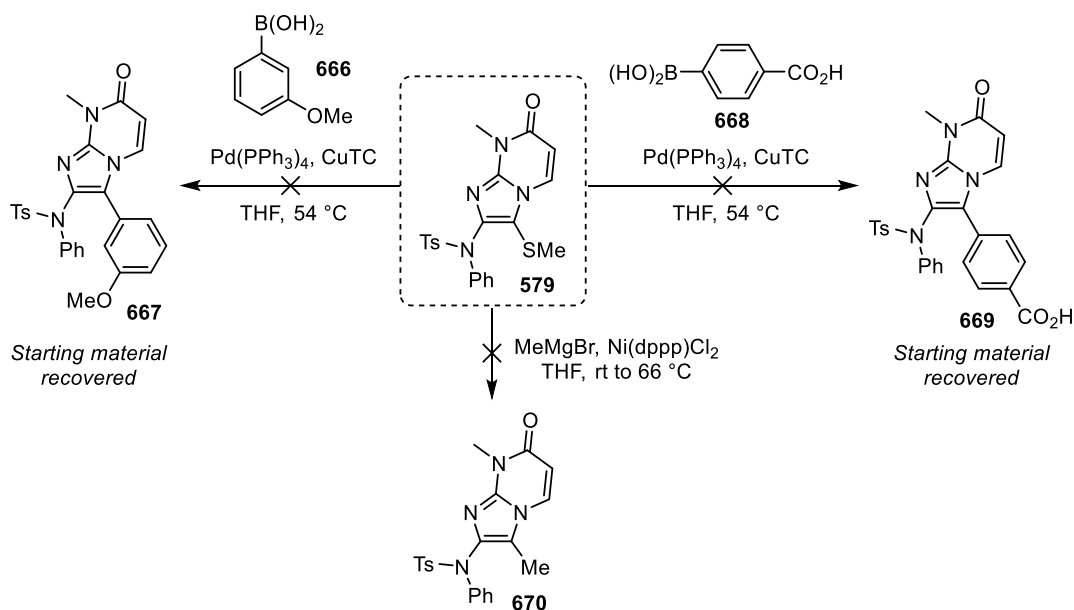
The cycloaddition strategy presented in this thesis allows the introduction of halide substituents for further modifications of the post-catalysis products. Capitalising on the bromide groups introduced in the benzo(thi/oxa)zolyli imidazoles through the ynamide or the aminide, Suzuki cross-coupling reactions provided with poly-aromatic compounds **664** and **665** (Scheme 89).



Scheme 89: Suzuki cross-coupling reactions on imidazole-fused systems

4.2.5.1. Exploiting the methylsulfide functionality

The S-methyl group is known to be suitable moiety for palladium and nickel cross-coupling reactions with boronic acids.¹¹¹ Nevertheless, Liebeskind-Srogl or Kumada cross-couplings were not productive when attempted on imidazo-uracil **579** (Scheme 90).

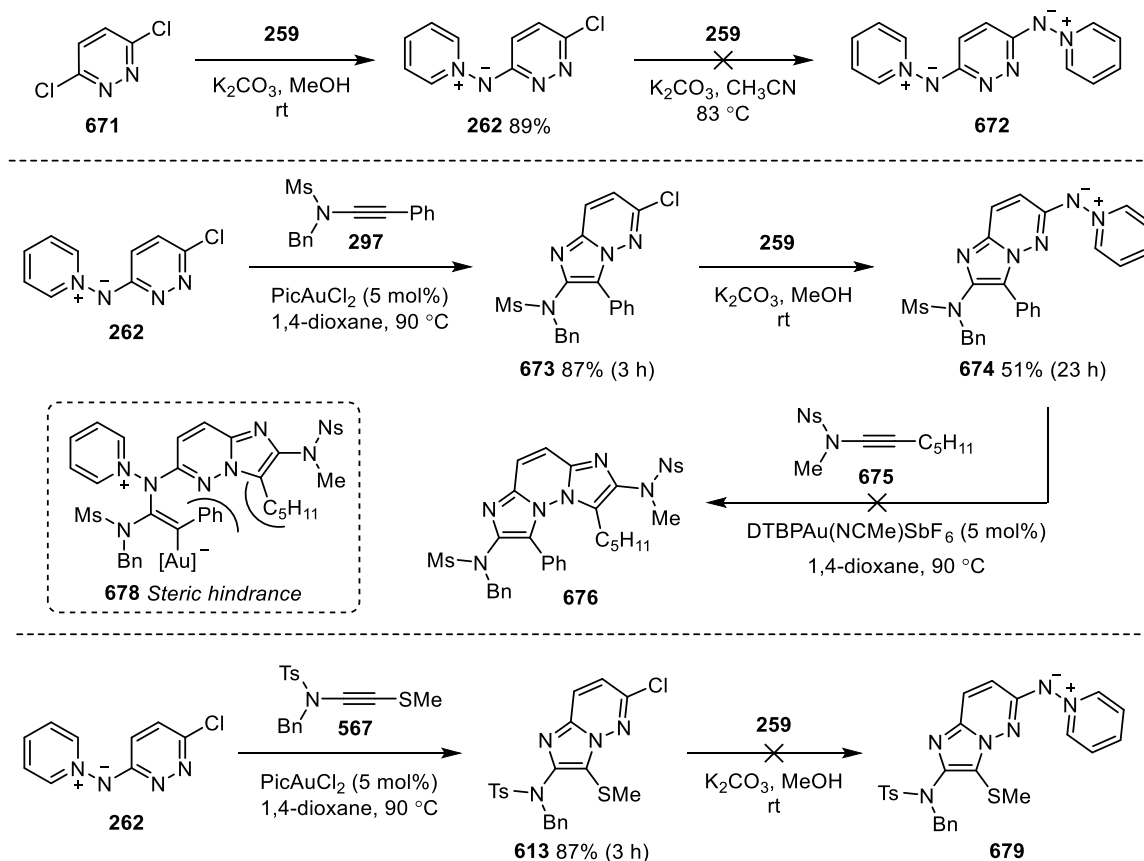


Scheme 90: Attempted Liebeskind-Srogl and Kumada cross-couplings

At the outset of the project, the preparation of double aminide **672** was attempted using (6-chloropyridazin-3-yl)(pyridin-1-ium-1-yl)amide **262**, but this route prove ineffective (Scheme 91-top). An alternative route was envisioned consisting on a sequence of aminide formation-gold catalysis reactions. Aminide **262** was reacted with ynamide **297** to give **673** in a good yield. Subsequent reaction of **673** with *N*-amino pyridinium iodide (**259**) formed bicyclic aminide **674** in 51% yield. A second cycloaddition reaction using ynamide **674** was expected to be smoothly due to the presence of a flexible alkyl chain on the carbon-end of the ynamide. Nevertheless, the reaction with **674** proved fruitless, potentially due to the steric hindrance of the system in the cyclisation step (**678**).

In order to achieve the diimidazo[1,2-*b*:2',1'-*f*]pyridazine core, we took advantage of the methodology presented in chapter 4 using thioynamides to introduce a smaller methylsulfide group in 4-position of imidazole **673** (Scheme 91-bottom). Following an analogous synthetic approach, formation of imidazole **613** using thioynamide **567** proceeded smoothly, however the aminide formation step with *N*-aminopyridinium iodide was troublesome (**679**). A

possible explanation is that chloride and sulfide might be competing as leaving groups in the S_NAr reaction, which would lead to various side-products, as was observed by TLC.



Scheme 91: Attempted double aminide formation with chlorodiazine aminide 262

4.4. Conclusions

Thioynamides have been introduced as powerful electron-rich alkynes in the gold-catalysed formal [3+2] cycloaddition strategy. The straightforward and scalable preparation of these building-blocks allowed us to explore their features with *N*-pyridinium aminides.

A remarkable improvement of the reactivity was seen when employing thioynamides with the previously unreactive nitrenoids. The lack of 1,3-*N,N*-dipole reactivity in the reaction with ynamides (chapter 3) was overcome, achieving moderate to excellent conversion to the

corresponding imidazole products. This fact has been attributed to a putative sulfur effect that aids the formation of the keteniminium intermediate, and therefore, unproductive aminide-gold catalyst interactions have been subdued.

N-Benzo(heteroaryl) and *N*-diazinyl aminides also proved compatible with these heteroalkynes. Within these series, an enhancement of reactivity was achieved with those nitrenoids that either by steric or electronic reasons were not effective 1,3-*N,N*-dipoles.

These sulfur containing alkynes allowed us to access novel fused imidazolyl derivatives and to expand the scope of our methodology to more complex and highly functionalised heterocycles.

Future work could be conducted by further exploring the role and mode of coordination of the thioynamide with the gold species, as it would allow for a better understanding of the reactivity discussed throughout this chapter. Additionally, spectroscopic evidence of the putative poisoning aminide-gold complex interaction discussed throughout chapter 3 is needed and highly desirable. Following investigations can also be directed at modifying the functionality of the imidazole heterocycles.

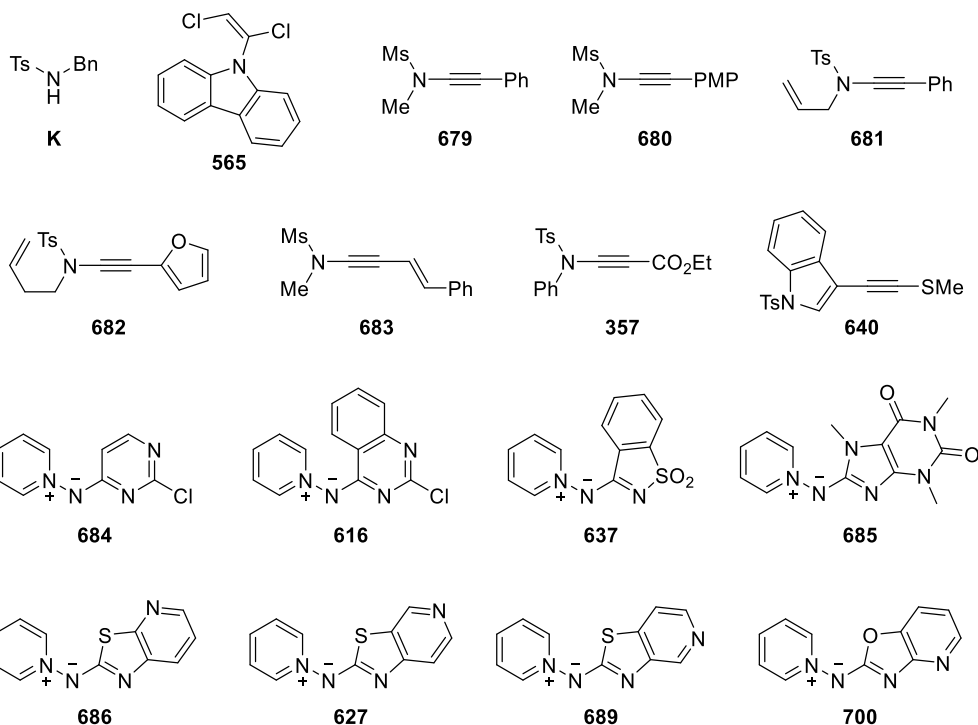
APPENDIX

1. General information

Commercially available chemicals/reagents were purchased from major suppliers (Aldrich, Fisher, Acros Organic, Alfa Aesar, Fluorochem or VWR) and used without further purification. All reactions were stirred using Teflon coated magnetic stirrer bars. Reactions performed under argon atmosphere were carried out in flame or heat-gun dried glassware at high vacuum and backfilled with argon utilising dry solvents. Solvents were dried utilising either a Pure Solv-MD solvent purification system (CH_2Cl_2 , THF, toluene and CH_3CN) or over 4 Å molecular sieves, which were previously activated by heating them to 300 °C with a heating matle and under high vacuum, during at least 24 hours, (DMF, 1,4-dioxane, *m*-xylene and 1,2-DCB). Reactions requiring heating were performed using preheated paraffin oil baths or metal heating blocks on stirrer hotplates and the temperature was controlled using an external prove. Low temperature reactions were performed with the following cooling baths: 0 °C (ice/water), -41 °C (dry ice/ CH_3CN), -78 °C (dry ice/acetone) controlled with an external thermometer. All reactions were monitored by thin layer chromatography on Merck silica gel 60 F₂₅₄ (aluminium support) TLC plates, which were developed utilising UV fluorescence (254 nm) or the following stains: potassium permanganate/ Δ , vanillin/ Δ , ninhydrin/ Δ or anisaldehyde/ Δ . Flash column chromatography was performed on Sigma Aldrich silica gel 60 (40-63 μm). ^1H NMR and ^{13}C NMR spectra were recorded using Bruker AVIII300 (^1H = 300 MHz, ^{19}F = 282 MHz, ^{31}P = 121 MHz), Bruker AVIII400 (^1H = 400 MHz, ^{13}C = 101 MHz) or Bruker AVNEO500 spectrometers in commercial TMS free deaured solvents at 300 K. ^{13}C NMR spectra were recorded utilising the UDEFT, JMOD or PENDANT pulse sequences from the Bruker standard pulse program library. NMR spectra were processed using MestReNova software. Chemical shifts (δ) are given in ppm relative to TMS and are calibrated using residual solvent peaks (CDCl_3 : $\delta_{\text{C}} \equiv 77.16$; residual CHCl_3 in CDCl_3 : $\delta_{\text{H}} \equiv$

7.26 ppm; DMSO- d_6 : $\delta_C \equiv 39.52$ ppm; residual DMSO in DMSO- d_6 : $\delta_H \equiv 2.50$ ppm).¹¹² Spectral data for 1H NMR spectroscopy is reported as follows: chemical shift (multiplicity, coupling constant, number of protons) and for ^{13}C NMR spectroscopy: chemical shift. The following abbreviations were used to assign multiplicity: s (singlet), d (doublet), t (triplet), q (quadruplet), dd (doublet of doublets), td (triplet of doublets), tt (triplet of triplets), ddd (doublet of doublet of doublets), ddt (doublet of doublet of triplets), br. (broad), m (multiplet), app. (apparent). Coupling constants (J) are given in Hz to one decimal place. 2D COSY, HSQC and HMBC spectra were recorded in order to assist with NMR assignment when necessary. Melting points were measured in open capillaries using a Stuart Scientific melting point apparatus and are uncorrected. Infra-red spectra were recorded neat using a Perkin-Elmer Spectrum 100 FTIR spectrometer using a ATR attachment; only the most intense or representative absorbances (ν_{max}) are reported in cm^{-1} . Mass spectra were obtained using Waters GCT Premier (EI), Waters LCT (ES) or Waters Synapt (ES) spectrometers. High resolution spectra used a lock-mass to adjust the calibrated mass scale.

The following compounds were prepared by other members of the Davies's group (Miguel Garzón, Matt Ball-Jones, Onyeka Abumsele, Pascal Delany). After verification of their purity by 1H NMR, and purification by flash column chromatography or recrystallization if needed, they were utilised in the ynamide formation or gold-catalysed cycloaddition.



2. Synthetic procedures and characterization data

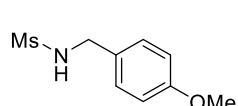
2.1. Synthesis of ynamide and thioynamide precursors

N-Benzylmethanesulfonamide (A)

Ms-N-Bn Following a reported procedure,¹¹³ a solution of benzylamine (10.0 mmol, 1.09 mL, 2.0 eq.) in dry THF (10 mL) was cooled down to 0 °C. Methanesulfonyl chloride (5.0 mmol, 0.39 mL, 1.0 eq.) was added dropwise and the mixture was allowed to warm up to room temperature and stirred for 4 h. After this time, the solvent was removed under reduced pressure and the product was re-dissolved in EtOAc (30 mL). HCl [2 M] (30 mL) was added and the biphasic mixture was extracted. The organic phase was dried with Na₂SO₄, filtered off and concentrated under reduced pressure giving sulfonamide **A** as a white solid (925 mg, 99%); mp: 59–61 °C (lit. 59–60 °C); ¹H NMR (300 MHz, CDCl₃): δ = 7.40–7.31 (m, 5H), 4.69 (br. s, NH, 1H), 4.33 (d, *J* = 6.0 Hz, 2H), 2.87 (s, 3H); ¹³C NMR (101 MHz, CDCl₃): δ =

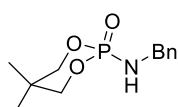
136.8 (C), 129.1 (2×CH), 128.3 (CH), 128.1 (2×CH), 47.37 (CH₂), 41.29 (CH₃); IR (neat): ν = 3224, 3021, 1456, 1294, 1132, 1060, 975, 737, 695; MS (EI): m/z 106.07 [M–Ms+H]⁺. Analytical data match those reported in the literature.¹¹³

***N*-(4-Methoxybenzyl)methanesulfonamide (B)**



Following a reported procedure,¹¹³ a solution of 4-methoxybenzylamine (40.0 mmol, 5.2 mL, 2.0 eq.) in dry THF (40 mL) was cooled down to 0 °C. Methanesulfonyl chloride (20.0 mmol, 1.6 mL, 1.0 eq.) was added dropwise precipitating a white cake-like solid. The mixture was allowed to warm up to room temperature and stirred for 2.5 h. After this time, the solvent was removed under reduced pressure and the product was re-dissolved in EtOAc (50 mL). HCl [2 M] (30 mL) was added and the biphasic mixture was extracted. The organic phase was dried with MgSO₄, filtered off and concentrated under reduced pressure. Purification by flash column chromatography [hexane:EtOAc (1:1)] gave sulfonamide **B** as a white fluffy solid (3.95 g, 92%); mp: 103–105 °C (lit. 96–97 °C); ¹H (300 MHz, CDCl₃): δ = 7.27 (d, J = 8.7 Hz, 2H), 6.89 (d, J = 8.7 Hz, 2H), 4.60 (br. s, 1H), 4.26 (d, J = 5.9 Hz, 2H), 3.81 (s, 3H), 2.86 (s, 3H); IR (neat): ν = 3263, 1614, 1513, 1302, 1134, 1030, 841, 814; MS (EI): m/z 135.08 [M–Ms+H]⁺. Analytical data match those reported in the literature.¹¹⁴

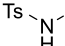
***2*-(Benzylamino)-5,5-dimethyl-1,3,2-dioxaphosphinane 2-oxide (C)**

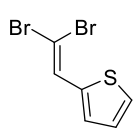


Following a reported procedure,¹¹⁵ to a solution of benzylamine (2.5 mmol, 0.27 mL, 1.0 eq.) in dry CH₂Cl₂ (1.5 mL), trimethylamine was added (3.75 mmol, 0.52 mL, 1.5 eq.). The mixture was cooled down to 0 °C and 2-chloro-5,5-dimethyl-1,3,2-dioxaphosphinane 2-oxide (3.0 mmol, 554 mg, 1.2 eq.) was added

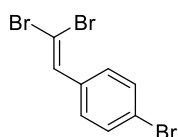
portionwise. The reaction mixture was allowed to warm up to room temperature and was stirred for 20 h. The reaction was diluted with water (10 mL) and the organic phase separated. The aqueous phase was extracted with CH₂Cl₂ (3×25 mL). The combined organic layers were washed with brine (25 mL), dried over MgSO₄, filtered off and concentrated under reduced pressure. Purification by flash column chromatography [hexane:EtOAc:CH₂Cl₂ (1:4:1)] gave sulfonamide **C** as a white-off solid (632 mg, 99%); mp: 122–124 °C (lit. 120–122 °C); IR (neat): ν = 3150, 2959, 1456, 1226, 1061, 1019, 824, 724, 693, 628; MS (ES): m/z 256.11 [M+H]⁺. Analytical data match those reported in the literature.¹¹⁵

4-Methyl-N-phenylbenzenesulfonamide (D)

 Following a reported procedure,¹¹⁶ to a solution of aniline (10.0 mmol, 0.91 mL, 1.0 eq.) in CH₂Cl₂ (33 mL), pyridine (60.0 mmol, 4.8 mL, 6.0 eq.) was added, followed by the dropwise addition of a solution of *p*-toluenesulfonyl chloride (12.0 mmol, 2.29 g, 12.0 eq.) in CH₂Cl₂ (10 mL) using a dropping funnel. The reaction mixture was stirred for 21 h at room temperature. The reaction mixture was concentrated under reduced pressure *ca.* 50 mL and HCl [1 M] (20 mL) was added. The organic phase was dried over Na₂SO₄, filtered off and concentrated under reduced pressure. Purification by flash column chromatography [hexane:EtOAc (1:1)] gave sulfonamide **D** as a pale pink solid (2.38 g, 96%); mp: 99–101 °C (lit. 101–103 °C); ¹H NMR (300 MHz, CDCl₃): δ = 7.75 (d, *J* = 8.3 Hz, 2H), 7.38–7.27 (m, 4H), 7.24–7.11 (m, 3H), 6.79 (br. d, *J* = 9.4 Hz, 1H), 2.46 (s, 3H); ¹³C NMR (101 MHz, CDCl₃): δ = 144.0 (C), 136.7 (C), 136.2 (C), 129.8 (2×CH), 129.4 (2×CH), 127.4 (2×CH), 125.3 (CH), 121.6 (2×CH), 21.6 (CH₃); IR (neat): ν = 3234, 1598, 1481, 1415, 1335, 1154, 1090, 908, 753, 693, 560. Analytical data match those reported in the literature.¹¹⁶

2-(2,2-Dibromovinyl)thiophene (E)

Following a reported procedure,¹¹⁷ to a solution of CBr₄ (11.0 mmol, 3.65 g, 2.2 eq.) in dry CH₂Cl₂ (15 mL) cooled to 0 °C was added PPh₃ (22.0 mmol, 5.77 g, 4.4 eq.) in *ca.* 1 g portions over 10 min. The mixture was stirred for 30 min at 0 °C and thiophene-2-carbaldehyde (5.0 mmol, 0.46 mL, 1.0 eq.) was added dropwise over 10 min. The reaction mixture was stirred for 3 h at 0 °C evolving from yellow to dark brown. After completion, pentane was added precipitating a beige cake solid. The supernatant was filtered through a pad of celite and the precipitated cake was redissolved in the minimum amount of CH₂Cl₂. Pentane was added again precipitating a beige solid (the process was repeated 4 times more). The combined supernatants were concentrated under reduced pressure. Purification of the residue by flash column chromatography [hexane:EtOAc (95:5)] afforded dibromolefin **E** as a pale yellow solid (911 mg, 68%) which was used within 24 h in the ynamide formation; ¹H NMR (300 MHz, CDCl₃): δ = 7.03 (dd, *J* = 5.1, 3.7 Hz, 1H), 7.25 (d, *J* = 3.7 Hz, 1H), 7.39 (dd, *J* = 5.1, 0.5 Hz, 1H), 7.66 (s, 1H); ¹³C NMR (101 MHz, CDCl₃): δ = 138.2 (C), 131.0 (CH), 130.2 (CH), 127.3 (CH), 126.7 (CH), 87.1 (C); IR (neat): ν = 3307, 2924, 2852, 2360, 2252, 2163, 2067, 2047, 2036, 1990, 1950, 1639, 1211, 1054, 698; MS (EI): *m/z* 267.9 [M]⁺. Analytical data match those reported in the literature.¹¹⁸

1-Bromo-4-(2,2-dibromovinyl)benzene (F)

Following a reported procedure,¹¹⁷ to a solution of CBr₄ (11.0 mmol, 3.65 g, 2.2 eq.) in dry CH₂Cl₂ (25 mL) cooled to 0 °C was added PPh₃ (22.0 mmol, 5.77 g, 4.4 eq.) in *ca.* 1 g portions over 10 min. The mixture was stirred for 30 min at 0 °C and 4-bromobenzaldehyde (5.0 mmol, 925 mg, 1.0 eq.) was added portionwise over 10 min. The reaction mixture was stirred for 1.5 h at 0 °C. After completion, pentane was added

precipitating a beige cake solid. The supernatant was filtered through a pad of celite and the precipitated cake was redissolved in the minimum amount of CH_2Cl_2 . Pentane was added again precipitating a beige solid (the process was repeated 4 times more). The combined supernatants were concentrated under reduced pressure. Purification of the residue by flash column chromatography [hexane:EtOAc (4:1)] afforded dibromolefin **F** as a pale yellow solid (1.66 g, 97%) which was used within 24 h in the ynamide formation; mp: 33–35 °C (lit. 36–37 °C); ^1H NMR (300 MHz, CDCl_3): δ = 7.53–7.47 (m, 2H), 7.44–7.37 (m, 3H); ^{13}C NMR (101 MHz, CDCl_3): δ = 135.9 (CH), 134.3 (C), 131.8 (2×CH), 130.1 (2×CH), 122.8 (C), 90.7 (C); MS (EI): m/z 340.0 $[\text{M}]^+$. Analytical data match those reported in the literature.¹¹⁹

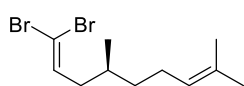
1-(2,2-Dibromovinyl)-4-methoxybenzene (G)



Following a reported procedure,¹¹⁷ to a solution of CBr_4 (11.0 mmol, 3.65 g, 2.2 eq.) in dry CH_2Cl_2 (25 mL) cooled to 0 °C was added PPh_3 (22.0 mmol, 5.77 g, 4.4 eq.) in *ca.* 1 g portions over 10 min. The mixture was stirred for 1 h at 0 °C and 4-methoxybenzaldehyde (5.0 mmol, 0.12 mL, 1.0 eq.) was added dropwise over 10 min. The reaction mixture was stirred for 2 h at 0 °C. After completion, pentane was added precipitating a beige cake solid. The supernatant was filtered through a pad of celite and the precipitated cake was redissolved in the minimum amount of CH_2Cl_2 . Pentane was added again precipitating a beige solid (the process was repeated 4 times more). The combined supernatants were concentrated under reduced pressure. Purification of the residue by flash column chromatography [hexane:EtOAc (95:5)] afforded dibromolefin **G** as a pale yellow solid (958 mg, 66%) which was used within 24 h in the ynamide formation; mp: 35–37 °C (lit. 37–38 °C); ^1H NMR (300 MHz, CDCl_3): δ = 7.52 (d, J = 8.9 Hz, 2H), 7.41 (s, 1H), 6.90 (d, J = 8.9 Hz, 2H), 3.83 (s, 3H); ^{13}C NMR (101 MHz, CDCl_3): δ = 159.8 (C), 136.4 (CH), 130.0

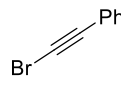
(2×CH), 127.9 (C), 113.9 (2×CH), 87.4 (C), 55.4 (CH₃); IR (neat): ν = 3321, 2931, 2838, 2183, 2154, 2055, 1987, 1605, 1509, 1460, 1307, 1249, 1178, 1031, 867, 803. Analytical data match those reported in the literature.¹²⁰

(S)-1,1-Dibromo-4,8-dimethylnona-1,7-diene (H)

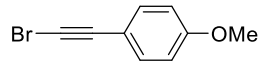


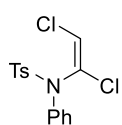
Following a reported procedure,¹¹⁷ to a solution of CBr₄ (11.0 mmol, 3.65 g, 2.2 eq.) in dry CH₂Cl₂ (15 mL) cooled to 0 °C was added PPh₃ (22.0 mmol, 5.77 g, 4.4 eq.) in *ca.* 1 g portions over 10 min. The mixture was stirred for 5 min at 0 °C and a solution of 2,6-lutidine (11.0 mmol, 1.27 mL, 2.2 eq.) in dry CH₂Cl₂ (10 mL) was added following by the dropwise addition of citronellal (5.0 mmol, 0.90 mL, 1.0 eq.) over 10 min. The reaction mixture was stirred for 2 h at 0 °C. After completion, pentane was added precipitating a beige cake solid. The supernatant was filtered through a pad of celite and the precipitated cake was redissolved in the minimum amount of CH₂Cl₂. Pentane was added again precipitating a beige solid (the process was repeated 4 times more). The combined supernatants were concentrated under reduced pressure. Purification of the residue by flash column chromatography [hexane:EtOAc (95:5)] afforded dibromolefin **H** as a colourless oil (1.28 g, 86%) which was used within 24 h in the ynamide formation; ¹H NMR (300 MHz, CDCl₃): δ = 6.40 (t, *J* = 7.3 Hz, 1H), 5.09 (tsept, *J* = 7.1, 1.2 Hz, 1H), 2.20–1.86 (m, 5H), 1.69 (d, *J* = 1.2 Hz, 3H), 1.64 (s, 3H), 1.45–1.15 (m, 2H), 0.92 (d, *J* = 6.7 Hz, 3H); ¹³C NMR (101 MHz, CDCl₃): δ = 137.8 (CH), 131.6 (C), 124.5 (CH), 89.0 (C), 40.2 (CH₂), 36.7 (CH₂), 32.2 (CH), 25.9 (CH₃), 25.7 (CH₂), 19.6 (CH₃), 17.8 (CH₃); IR (neat): ν = 2959, 2916, 2851, 2184, 2144, 2038, 2015, 1994, 1618, 1454, 1378, 1232, 1115, 934, 893, 778; HRMS (EI): *m/z* calculated for C₁₁H₁₈⁷⁹Br₂: 307.9775, found 307.9783 [M]⁺. Analytical data match those reported in the literature.¹²¹

(Bromoethynyl)benzene (I)

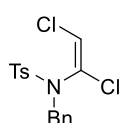

 Following a reported procedure,²² to a solution of phenylacetylene (10.0 mmol, 1.1 mL, 1.0 eq.) in acetone (100 mL) NBS (11.0 mmol, 1.96 g, 1.1 eq.) and AgNO₃ (0.5 mmol, 85.0 mg, 0.005 eq.) were added. The reaction mixture was stirred at room temperature for 2.5 h. The crude mixture was concentrated under reduced pressure *ca.* 50 mL and then hexane (50 mL) was added precipitating a white solid. The precipitate was filtered off and the filtrate was concentrated under reduced pressure affording **I** as a yellow oil (1.68 g, 93%) which was used directly in the ynamide formation; ¹H NMR (300 MHz, CDCl₃): δ = 7.47–7.44 (m, 2H), 7.35–7.29 (m, 3H); ¹³C NMR (101 MHz, CDCl₃): δ = 132.2 (2×CH), 128.8 (CH), 128.5 (2×CH), 122.9 (C), 80.2 (C), 49.9 (C). Analytical data match those reported in the literature.¹²²

1-(Bromoethynyl)-4-methoxybenzene (J)


 Following a reported procedure,¹²³ to a solution of **G** (1.0 mmol, 292 mg, 1.1 eq.) and benzyltriethylammonium chloride (0.9 mmol, 200 mg, 1.0 eq.) in CH₂Cl₂ (18 mL) under vigorous stirring at 0 °C was added dropwise a solution of KOH (0.2 mol, 11.3 mg, 230 eq.) in water (9 mL). The reaction mixture was stirred for 1.5 h and then CH₂Cl₂ (10 mL) was added. The biphasic mixture was separated. The organic phase was washed with brine (10 mL), dried over Na₂SO₄, filtered off and concentrated under reduced pressure. Purification by flash column chromatography [hexane:EtOAc (95:5)] afforded bromoalkyne **J** as yellow oil (90 mg, 48%) which was used directly in the ynamide formation; ¹H NMR (300 MHz, CDCl₃): δ = 7.39 (d, *J* = 8.9 Hz, 2H), 6.84 (d, *J* = 8.9 Hz, 2H), 3.81 (s, 3H). Analytical data match those reported in the literature.¹²³

(E)-N-(1,2-Dichlorovinyl)-4-methyl-N-phenylbenzenesulfonamide (563)

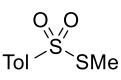
Following a reported procedure,⁵⁴ a two neck heat-gun dried flask under argon was charged with a mixture of sulfonamide **D** (10.0 mmol, 2.47 g, 1.0 eq.) and Cs₂CO₃ (15.0 mmol, 4.89 g, 1.5 eq.) in DMF (13 mL). The suspension was vigorously stirred at 50 °C for 5 min and trichloroethylene (11.0 mmol, 0.99 mL, 1.1 eq.) was added very slowly dropwise over 10 min (the use of a syringe pump in the addition is highly recommended). The reaction mixture was vigorously stirred until completion. The crude mixture was allowed to cool down to room temperature and it was diluted with a mixture of EtOAc:H₂O (2:1, 80 mL:40 mL). The aqueous phase was extracted with EtOAc (3×40 mL) and the combined organic phases were dried over MgSO₄, filtered off and concentrated under reduced pressure. Recrystallization from CH₂Cl₂:hexane afforded dichloroenamide **563** as a needled white solid (2.89 g, 84%); mp: 119–121 °C (lit. 115 °C); ¹H NMR (400 MHz, CDCl₃): δ = 7.65 (d, *J* = 8.4 Hz, 2H), 7.40–7.29 (m, 5H), 7.28–7.21 (m, 2H), 6.45 (s, 1H), 2.42 (s, 3H); ¹³C NMR (101 MHz, CDCl₃): δ = 144.7 (C), 137.8 (C), 135.7 (C), 130.8 (C), 129.54 (2×CH), 129.45 (2×CH), 129.2 (CH), 128.84 (2×CH), 128.76 (2×CH), 120.6 (CH), 21.8 (CH₃); IR (neat): ν = 3077, 1593, 1488, 1362, 1164, 1087, 801, 698, 592, 559; MS (ES): *m/z* 364.0 [M+Na]⁺. Analytical data match those reported in the literature.⁵⁴ **Note: vigorous stirring is needed to avoid the encapsulation of the emerging 1,2-dichloroethyne, which could cause an explosion in the presence of oxygen.**

(E)-N-Benzyl-N-(1,2-dichlorovinyl)-4-methylbenzenesulfonamide (564)

Following a reported procedure,⁵⁴ a two neck heat-gun dried flask under argon was charged with a mixture of sulfonamide **A** (4.0 mmol, 1.05 g, 1.0 eq.) and Cs₂CO₃ (6.0 mmol, 1.95 g, 1.5 eq.) in DMF (5 mL). The suspension was vigorously stirred at 50 °C

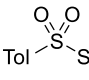
for 5 min and trichloroethylene (4.4 mmol, 0.40 mL, 1.1 eq.) was added very slowly dropwise over 10 min (the use of a syringe pump in the addition is highly recommended). The reaction mixture was vigorously stirred until completion. The crude mixture was allowed to cool down to room temperature and it was diluted with a mixture of EtOAc:H₂O (2:1, 20 mL:10 mL). The aqueous phase was extracted with EtOAc (3×20 mL) and the combined organic phases were dried over MgSO₄, filtered off and concentrated under reduced pressure. Recrystallization from CH₂Cl₂:hexane afforded dichloroenamide **564** as a white solid (1.25 g, 88%); mp: 140–142 °C (lit. 136–137 °C); ¹H NMR (300 MHz, CDCl₃): δ = 7.86 (d, *J* = 8.4 Hz, 2H), 7.37 (d, *J* = 8.4 Hz, 2H), 7.34–7.27 (m, 5H), 6.27 (s, 1H), 5.35–3.44 (br. s, 2H), 2.47 (s, 3H) *Broad resonance due to rotamers in this molecule*; ¹³C NMR (101 MHz, CDCl₃): δ = 144.9 (C), 137.2 (C), 133.5 (C), 129.9 (2×CH), 129.5 (2×CH), 128.6 (3×CH), 128.5 (2×CH), 121.8 (C), 51.9 (CH₂), 21.8 (CH₃) *one resonance was not observed due to overlap*; IR (neat): ν = 3038, 1594, 1457, 1357, 1169, 816, 705, 960, 607. Analytical data match those reported in the literature.⁵⁴ **Note: vigorous stirring is needed to avoid the encapsulation of the emerging 1,2-dichloroethyne, which could cause an explosion in the presence of oxygen.**

S-Methyl 4-methylbenzenesulfonothioate (**570**)

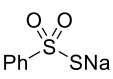

 Following a reported procedure,¹⁰⁷ to a solution of sodium 4-methylbenzenesulfinate (9.6 mmol, 1.86 g, 3.2 eq.) in CH₂Cl₂ (33 mL) was added dimethyl disulfide (2×5 mmol, 0.27 mL, 1.0 eq.) and iodine (6.0 mmol, 1.52 g, 2.0 eq.) turning the solution dark red. The reaction mixture was stirred at room temperature until completion. The crude reaction mixture was quenched with Na₂S₂O₃ (20 mL) and it was extracted with CH₂Cl₂ (3×20 mL). The combined organic phases were dried over MgSO₄, filtered off and concentrated under reduced pressure affording sulfonothioate **570** as a yellow

solid (1.16 g, 95%); ^1H NMR (300 MHz, CDCl_3): δ = 7.81 (d, J = 8.2 Hz, 2H), 7.35 (d, J = 8.2 Hz, 2H), 2.50 (s, 3H), 2.45 (s, 3H); ^{13}C NMR (101 MHz, CDCl_3): δ = 144.9 (C), 141.1 (C), 130.0 (2 \times CH), 127.3 (2 \times CH), 21.8 (CH_3), 18.1 (CH_3); IR (neat): ν = 2925, 1591, 1327, 1293, 1138, 1074, 809, 699, 654; MS (EI): m/z 202.1 $[\text{M}]^+$. Analytical data match those reported in the literature.¹⁰⁷

***S*-Phenyl 4-methylbenzenesulfonothioate (571)**

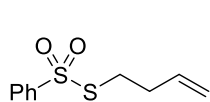
Following a reported procedure,¹⁰⁷ to a solution of diphenyl disulfide (10.0 mmol,  2.18 g, 1.0 eq.) in CH_2Cl_2 (111 mL), sodium 4-methylbenzenesulfinate (32.0 mmol, 6.28 g, 3.2 eq.) and iodine (20.0 mmol, 5.08 g, 2.0 eq.) were added. The resulting dark red solution was stirred at room temperature until completion. The crude reaction mixture was quenched with $\text{Na}_2\text{S}_2\text{O}_3$ (35 mL) and it was extracted with CH_2Cl_2 (3 \times 25 mL). The combined organic phases were dried over MgSO_4 , filtered off and concentrated under reduced pressure. Purification by flash column chromatography [hexane:toluene (3:2)] afforded sulfonothioate **571** as a beige solid (2.08 g, 79%); mp: 62–64 °C (lit. 73–74 °C); ^1H NMR (300 MHz, CDCl_3): δ = 7.51–7.44 (m, 3H), 7.40–7.30 (m, 4H), 7.20 (d, J = 8.0 Hz, 2H), 2.42 (s, 3H); ^{13}C NMR (101 MHz, CDCl_3): δ = 144.8 (C), 140.5 (C), 136.7 (2 \times CH), 131.4 (CH), 129.5 (4 \times CH), 128.2 (C), 127.7 (2 \times CH), 21.8 (CH_3); MS (ES): m/z 287.2 $[\text{M}+\text{Na}]^+$. Analytical data match those reported in the literature.¹⁰⁷

Sodium benzenesulfonothioate (573)

Following a reported procedure,¹²⁴ to a heat-gun dried flask under argon containing  a suspension of sodium benzenesulfinate (30.0 mmol, 4.92 g, 1.0 eq.) in pyridine (31 mL), sulfur (30.0 mmol, 962 mg, 1.0 eq.) was added. The reaction mixture was stirred for

3 h. The crude mixture was filtered off and washed with Et₂O. Purification of the solid collected by recrystallization with isopropanol afforded sulfonothioate **573** as a white-off solid (4.31 g, 73%); ¹H NMR (300 MHz, DMSO-d₆): δ = 7.80–7.67 (m, 2H), 7.42–7.28 (m, 3H); ¹³C NMR (101 MHz, DMSO-d₆): δ = 154.9 (C), 129.0 (CH), 127.8 (2×CH), 124.0 (2×CH); IR (neat): ν = 3057, 1443, 1188, 1114, 1060, 721, 685, 626; MS (ES): *m/z* 218.95 [M+Na]⁺. Analytical data match those reported in the literature.¹²⁴

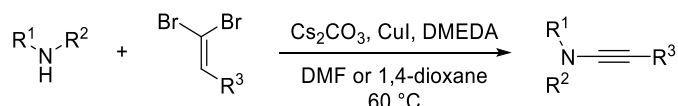
***S*-(But-3-en-1-yl) benzenesulfonothioate (574)**



Following a reported procedure,¹²⁵ a flask containing **573** (10.0 mmol, 1.96 g, 1.0 eq.) was evacuated and back-filled with argon (purged 3 times). Dry DMF (17 mL) was then added, and the solution was stirred at room temperature for 5 min. 4-Bromobut-1-ene (10.3 mmol, 1.04 mL, 1.03 eq.) was added dropwise over 5 min and the resulting reaction mixture was stirred at room temperature for 4 days. The crude mixture was poured into ice/water (50 mL) and extracted with Et₂O (6×15 mL). The combined organic phases were washed with saturated NaHCO₃ (aq) (50 mL), washed with brine (50 mL), dried over MgSO₄, filtered off and concentrated under reduced pressure. Purification by flash column chromatography afforded sulfonothioate **574** as an orange oil (1.69 g, 74%); ¹H NMR (300 MHz, CDCl₃): δ = 7.99–7.89 (m, 2H), 7.64 (tt, *J* = 7.3, 1.7 Hz, 1H), 7.60–7.56 (m, 2H), 5.67 (ddt, *J* = 17.1, 10.5, 6.8 Hz, 1H), 5.09–4.93 (m, 2H), 3.07 (t, *J* = 7.3 Hz, 2H), 2.42–2.28 (m, 2H); ¹³C NMR (101 MHz, CDCl₃): δ = 145.1 (C), 134.8 (CH), 133.8 (CH), 129.4 (2×CH), 127.1 (2×CH), 117.6 (CH₂), 35.3 (CH₂), 32.9 (CH₂); IR (neat): ν = 3069, 1447, 1322, 1138, 1076, 714, 684, 591; HRMS (ES): *m/z* calculated for C₁₀H₁₂O₂NaS₂: 251.0176, found 251.0176 [M]⁺. Analytical data match those reported in the literature.¹²⁵

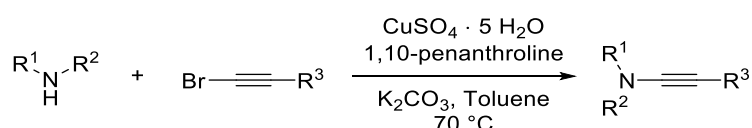
2.2. Synthesis of ynamides

General procedure 1 (GP1)



Following Evano's procedure,⁵² a heat-gun dried Radley tube containing sulfonamide (1.0 eq.), dibromolefin (1.5 eq.), Cs₂CO₃ (4.0 eq.) and CuI (12 mol%) was evacuated and back-filled with argon (purged 3 times). Dry and degassed DMF or 1,4-dioxane [0.5 M relative to the sulfonamide] and *N,N'*-dimethylethylenediamine (18 mol%) were carefully added. The resulting light blue suspension was stirred at 60 °C during 24-48 h. After completion, the crude mixture was allow to cool down to room temperature, filtered through a plug of silica, washed with EtOAc and concentrated under reduced pressure. Purification by flash column chromatography provide with the corresponding ynamide.

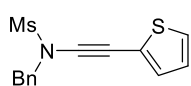
General procedure 2 (GP2)



Following Hsung's procedure,⁵⁰ a heat-gun dried Radley tube containing sulfonamide (1.0 eq.), bromoalkyne (1.0 eq.), CuSO₄ · 5 H₂O (12 mol%), 1,10-phenanthroline (24 mol%) and K₂CO₃ (64 mol%) was evacuated and back-filled with argon (purged 3 times). Dry toluene [1.0 M relative to the sulfonamide] was added and the resulting mixture was stirred at 70 °C during 24 h. After completion, the crude mixture was allowed to cool down to room temperature, filtered through a plug of silica, washed with EtOAc and concentrated under

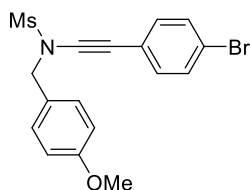
reduced pressure. Purification by flash column chromatography provide with the corresponding ynamide.

N-Benzyl-N-(thiophen-2-ylethynyl)methanesulfonamide (292)



Following **GP1** using sulfonamide **A** (248 mg, 1.3 mmol) and dibromolefin **E** (540 mg, 2.0 mmol) in 1,4-dioxane (2.6 mL). Purification by flash column chromatography [hexane:EtOAc (9:1)] delivered ynamide **292** as a beige solid (342 mg, 87%); mp: 72–74 °C (lit. 72–74 °C); ¹H NMR (300 MHz, CDCl₃): δ = 7.49–7.46 (m, 2H), 7.43–7.37 (m, 3H), 7.28 (dd, *J* = 5.2, 1.1 Hz, 1H), 7.19 (dd, *J* = 3.6, 1.1 Hz, 1H), 6.97 (dd, *J* = 5.2, 3.6 Hz, 1H), 4.72 (s, 2H), 2.93 (s, 3H); ¹³C NMR (101 MHz, CDCl₃): δ = 134.6 (C), 133.4 (CH), 129.1 (2×CH), 129.0 (2×CH), 128.9 (CH), 128.2 (CH), 127.2 (CH), 122.6 (C), 85.7 (C), 65.0 (C), 56.2 (CH₂), 39.4 (CH₃); IR (neat): ν = 3016, 1363, 1215, 1163, 1007, 962, 748, 704, 667; HRMS (ES): *m/z* calculated for C₁₄H₁₃NO₂S₂: 291.0388, found 291.0386 [M]⁺. Analytical data match those reported in the literature.⁶⁵

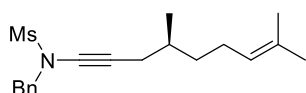
N-((4-Bromophenyl)ethynyl)-N-(4-methoxybenzyl)methanesulfonamide (293)



Following **GP1** using sulfonamide **B** (1.29 g, 6.0 mmol) and dibromolefin **F** (3.07 g, 9.0 mmol) in DMF (12.0 mL). Purification by flash column chromatography [hexane:EtOAc (9:1)] delivered ynamide **293** as a beige oil (1.28 g, 54%); mp: 74–76 °C; ¹H NMR (300 MHz, CDCl₃): δ = 7.42 (d, *J* = 8.5 Hz, 2H), 7.40 (d, *J* = 8.6 Hz, 2H), 7.21 (d, *J* = 8.5 Hz, 2H), 6.92 (d, *J* = 8.6 Hz, 2H), 4.65 (s, 2H), 3.82 (s, 3H), 2.91 (s, 3H); ¹³C NMR (101 MHz, CDCl₃): δ = 160.2 (C), 132.9 (2×CH), 131.7 (2×CH), 130.6 (2×CH), 126.5 (C), 122.2 (C), 121.7 (C), 114.3 (2×CH), 83.3 (C), 70.9 (C), 55.7 (CH₂), 55.4 (CH₃), 39.3 (CH₃); IR (neat): ν = 2242, 1611, 1514, 1352,

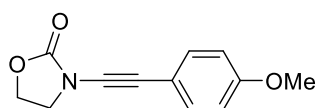
1248, 1160, 922, 816, 797, 759, 570; HRMS (ES): m/z calculated for $C_{12}H_{17}N_3O_5S^{79}Br$: 394.0072, found 394.0073 $[M+H]^+$.

(*R*)-*N*-Benzyl-*N*-(4,8-dimethylnon-7-en-1-yn-1-yl)methanesulfonamide (294**)**



Following **GP1** using sulfonamide **A** (371.35 mg, 2.01 mmol) and dibromolefin **H** (900 mg, 3.0 mmol) in DMF (4.1 mL). Purification by flash column chromatography [hexane:EtOAc (95:5)] delivered ynamide **294** as a colourless oil (402 mg, 60%); 1H NMR (300 MHz, $CDCl_3$): δ = 7.45–7.34 (m, 5H), 5.06 (tt, J = 7.1, 1.3 Hz, 1H), 4.57 (s, 2H), 2.86 (s, 3H), 2.18 (q, J = 5.6 Hz, 2H), 1.94 (d, J = 7.8 Hz, 2H), 1.68 (d, J = 0.8 Hz, 3H), 1.59 (s, 3H), 1.43–1.11 (m, 3H), 0.90 (d, J = 6.7 Hz, 3H); ^{13}C NMR (101 MHz, $CDCl_3$): δ = 135.0 (C), 131.6 (C), 129.1 (2 \times CH), 128.8 (2 \times CH), 128.7 (CH), 124.6 (CH), 74.0 (C), 70.3 (C), 55.8 (CH₂), 38.4 (CH₃), 36.2 (CH₂), 32.4 (CH), 25.9 (CH₃), 25.8 (CH₂), 25.7 (CH₂), 19.5 (CH₃), 17.8 (CH₃); IR (neat): ν = 2959, 2918, 2852, 2253, 1456, 1256, 1162, 1027, 957, 833, 770, 701; MS (ES): m/z 356.2 $[M+Na]^+$. Analytical data match those reported in the literature.²⁴

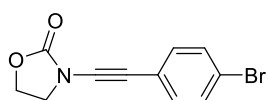
3-((4-Methoxyphenyl)ethynyl)oxazolidin-2-one (295**)**



Following **GP1** using oxazolidin-2-one (174 mg, 2.0 mmol) and dibromolefin **G** (876 mg, 3.0 mmol) in DMF (4.0 mL). Purification by flash column chromatography [hexane:EtOAc (3:2-1:1)] delivered ynamide **295** as a pale yellow solid (294 mg, 68%); 1H NMR (400 MHz, $CDCl_3$): δ = 7.38 (d, J = 8.9 Hz, 2H), 6.83 (d, J = 8.9 Hz, 2H), 4.50–4.44 (m, 2H), 4.01–3.95 (m, 2H), 3.81 (s, 3H); ^{13}C NMR (101 MHz, $CDCl_3$): δ = 159.8 (C), 156.2 (C), 133.61 (2 \times CH), 114.2 (C), 114.1 (2 \times CH), 77.7 (C), 71.0 (C), 63.1 (CH₂), 55.4 (CH₂), 47.2 (CH₃); IR (neat): ν = 2920, 2266, 1742, 1606,

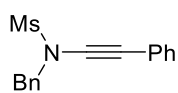
1419, 1176, 1087, 1024, 823, 750; HRMS (ES): m/z calculated for $C_{12}H_{11}NO_3Na$: 240.0637, found 240.0635 $[M]^+$. Analytical data match those reported in the literature.⁵³

3-((4-Bromophenyl)ethynyl)oxazolidin-2-one (**296**)

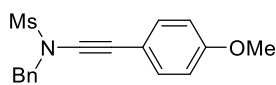


Following **GP1** using oxazolidin-2-one (131 mg, 1.5 mmol) and dibromolefin **F** (767 mg, 2.3 mmol) in DMF (3.0 mL). Purification by flash column chromatography [hexane:EtOAc (4:1)] delivered ynamide **296** as a pale beige solid (215 mg, 54%); 1H NMR (300 MHz, $CDCl_3$): δ = 7.44 (d, J = 8.5 Hz, 2H), 7.29 (d, J = 8.5 Hz, 2H), 4.55–4.46 (m, 2H), 4.05–3.96 (m, 2H); ^{13}C NMR (101 MHz, $CDCl_3$): δ = 155.8 (C), 133.1 (2 \times CH), 131.7 (2 \times CH), 122.5 (C), 121.3 (C), 80.1 (C), 70.5 (C), 63.2 (CH_2), 47.1 (CH_2); IR (neat): ν = 2927, 2264, 1752, 1422, 1213, 1163, 1007, 823, 745; HRMS (EI): m/z calculated for $C_{12}H_8NO_2^{79}BrNa$: 287.9636, found 287.9637 $[M+Na]^+$. Analytical data match those reported in the literature.¹²⁶

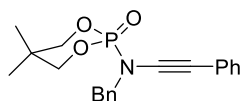
N-Benzyl-*N*-(phenylethynyl)methanesulfonamide (**297**)



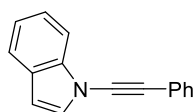
Following **GP2**, using sulfonamide **A** (987 mg, 5.3 mmol) and bromoalkyne **I** (965 mg, 5.3 mmol). Purification by flash column chromatography [hexane:EtOAc (4:1)] delivered ynamide **297** as a pale beige solid (1.24 g, 81%); 1H NMR (300 MHz, $CDCl_3$): δ = 7.53–7.47 (m, 2H), 7.45–7.27 (m, 8H), 4.72 (s, 2H), 2.94 (s, 3H); ^{13}C NMR (101 MHz, $CDCl_3$): δ = 134.6 (C), 131.5 (2 \times CH), 129.1 (2 \times CH), 128.94 (2 \times CH), 128.88 (CH), 128.4 (2 \times CH), 128.1 (CH), 122.6 (C), 82.1 (C), 71.7 (C), 56.0 (CH_2), 39.1 (CH_3); IR (neat): ν = 2927, 2264, 2244, 1750, 1421, 1350, 1158, 945, 792, 747, 691; MS (ES): m/z 308.22 $[M+Na]^+$. Analytical data match those reported in the literature.¹²⁷

N-Benzyl-N-((4-methoxyphenyl)ethynyl)methanesulfonamide (298)

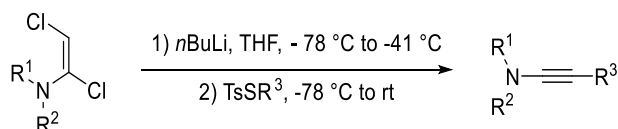
Following **GP2**, using sulfonamide **A** (200 mg, 1.1 mmol) and bromoalkyne **J** (228 mg, 1.1 mmol). Purification by flash column chromatography [hexane:EtOAc (4:1)] delivered ynamide **298** as a pale yellow oil (92 mg, 27%); mp: 63–64 °C (lit. 63–64 °C); ¹H NMR (300 MHz, CDCl₃): δ = 7.51–7.47 (m, 2H), 7.41–7.36 (m, 3H), 7.31 (d, *J* = 8.9 Hz, 2H), 6.82 (d, *J* = 8.9 Hz, 2H), 4.70 (s, 2H), 3.80 (s, 3H), 2.92 (s, 3H); ¹³C NMR (101 MHz, CDCl₃): δ = 159.8 (C), 134.8 (C), 133.6 (2×CH), 129.2 (2×CH), 128.9 (2×CH), 128.9 (CH), 114.5 (C), 114.1 (2×CH), 80.7 (C), 71.4 (C), 56.1 (CH₂), 55.5 (CH₃), 39.0 (CH₃); IR (neat): ν = 2922, 2852, 1513, 1353, 1249, 1160, 963, 774. Analytical data matches those reported in the literature.¹²⁸

2-(Benzyl(phenylethynyl)amino)-5,5-dimethyl-1,3,2-dioxaphosphinane 2-oxide (299)

Following **GP2** using sulfonamide **C** (511 mg, 2.0 mmol) and bromoalkyne **I** (471 mg, 2.6 mmol). Purification by flash column chromatography [hexane:EtOAc (7:3-3:2)] delivered ynamide **299** as a beige solid (470 mg, 66%); ¹H NMR (300 MHz, CDCl₃): δ = 7.49–7.43 (m, 2H), 7.42–7.29 (m, 3H), 7.25–7.19 (m, 5H), 4.58 (d, *J* = 9.0 Hz, 2H), 4.25 (app. t, *J* = 10.0 Hz, 2H), 4.19–4.10 (m, 2H), 1.17 (s, 3H), 1.08 (s, 3H); ¹³C NMR (101 MHz, CDCl₃): δ = 136.4 (C), 130.9 (2×CH), 128.8 (2×CH), 128.6 (2×CH), 128.3 (2×CH), 128.2 (CH), 127.3 (CH), 123.6 (C), 85.3 (d, *J* = 4.6 Hz, C), 78.3 (d, *J* = 6.6 Hz, 2×CH₂), 66.9 (d, *J* = 5.6 Hz, C), 55.0 (d, *J* = 6.1 Hz, CH₂), 32.3 (d, *J* = 6.5 Hz, C), 21.4 (d, *J* = 4.6 Hz, 2×CH₃) carbon resonances show doublets due to a conformation equilibrium; IR (neat): ν = 2968, 2899, 2245, 1358, 1266, 1050, 1007, 827, 748, 626; MS (ES): *m/z* 378.18 [M+Na]⁺. Analytical data match those reported in the literature.¹²⁹

1-(Phenylethynyl)-1H-indole (301)

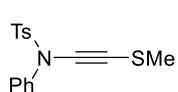
Following **GP2**, using 1H-indole (867 mg, 7.4 mmol) and bromoalkyne **I** (1.82 g, 10.0 mmol). Purification by flash column chromatography [hexane (100%)] delivered ynamide **301** as a pale yellow solid (382 mg, 24%); ^1H NMR (300 MHz, CDCl_3): δ = 7.67–7.58 (m, 2 H), 7.56–7.53 (m, 2H), 7.39–7.31 (m, 4H), 7.27 (d, J = 3.4 Hz, 1H), 7.25–7.18 (m, 1H), 6.59 (dd, J = 3.4, 0.7 Hz, 1H); ^{13}C NMR (101 MHz, CDCl_3): δ = 138.3 (C), 131.5 (2 \times CH), 129.0 (CH), 128.6 (2 \times CH), 128.2 (CH), 128.0 (C), 123.7 (CH), 122.8 (C), 122.1 (CH), 121.3 (CH), 111.5 (CH), 105.7 (CH), 80.9 (C), 70.7 (C); IR (neat): ν = 2922, 2249, 1521, 1457, 1347, 1203, 1163, 739, 688; HRMS (ES): m/z calculated for $\text{C}_{16}\text{H}_{11}\text{N}$: 217.0891, found 217.0885 $[\text{M}]^+$. Analytical data match those reported in the literature.⁹⁵

2.3. Synthesis of thioynamides**General Procedure 3 (GP3)**

Following Anderson's procedure,⁵⁴ a two neck heat-gun dried flask under argon containing a solution of dichloroenamide (1.0 eq.) in dry THF [0.25 M relative to the dichloroenamide] was cooled down to -78 °C. *n*-Butyllithium (1.6 M solution in hexane, 1.2 eq.) was added dropwise over 10 min. The mixture was stirred at -78 °C for 5 min and then warmed up to -41 °C for 30 min. After that time, the mixture was cooled down to -78 °C and a second portion of *n*-butyllithium (1.6 M solution in hexane, 1.0 eq.) was added dropwise over 10 min. The

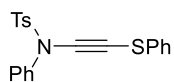
mixture was stirred at -78 °C for 10 min and sulfonothioate (1.2 eq.) was added. The reaction mixture was allowed to warm up to room temperature and stirred for 24 h. The crude reaction mixture was quenched with water and extracted with Et₂O. The combined organic phases were dried over Na₂SO₄, filtered off and concentrated under reduced pressure. Purification by flash column chromatography or recrystallization provide with the corresponding thioynamide.

4-Methyl-N-((methylthio)ethynyl)-N-phenylbenzenesulfonamide (565)



Following **GP3** using dichloroenamide **563** (1.54 g, 4.5 mmol) and sulfonothioate **570** (1.09 g, 5.4 mmol). Purification by recrystallization from CH₂Cl₂:hexane delivered thioynamide **565** as a beige pale solid (1.03 g, 72%); mp: 124–126 °C (lit. °C); ¹H NMR (300 MHz, CDCl₃): δ = 7.60 (d, *J* = 8.3 Hz, 2H), 7.37–7.25 (m, 5H), 7.25–7.18 (m, 2H), 2.44 (s, 3H), 2.33 (s, 3H); ¹³C NMR (101 MHz, CDCl₃): δ = 145.1 (C), 139.2 (C), 133.43 (C), 129.6 (2×CH), 129.2 (2×CH), 128.4 (3×CH), 126.4 (2×CH), 86.7 (C), 66.7 (C), 21.8 (CH₃), 20.6 (CH₃); IR (neat): ν = 2934, 2167, 1594, 1487, 1367, 1172, 1088, 782, 691, 661, 572; HRMS (ES): *m/z* calculated for C₁₆H₁₆NO₂S₂: 318.0622, found 318.0625 [M+H]⁺.

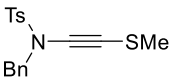
4-Methyl-N-phenyl-N-((phenylthio)ethynyl)benzenesulfonamide (566)



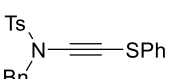
Following **GP3** using dichloroenamide **563** (685 mg, 2.0 mmol) and sulfonothioate **571** (635 mg, 2.4 mmol). Purification by recrystallization from EtOH delivered thioynamide **566** as a beige solid (485 mg, 64%); ¹H NMR (300 MHz, CDCl₃): δ = 7.64 (d, *J* = 8.4 Hz, 2H), 7.42–7.16 (m, 12H), 2.46 (s, 3H); ¹³C NMR (101 MHz, CDCl₃): δ = 145.3 (C), 138.9 (C), 134.1 (C), 133.4 (C), 129.8 (2×CH), 129.3 (2×CH), 129.2

(2×CH), 128.53 (CH), 128.47 (2×CH), 126.6 (CH), 126.4 (2×CH), 125.9 (2×CH), 92.9 (C), 61.6 (C), 21.9 (CH₃); IR (neat): ν = 2985, 2165, 1583, 1480, 1370, 1171, 1097, 781, 738, 662; HRMS (ES): m/z calculated for C₂₁H₁₇NO₂NaS₂: 402.0598, found 402.0596 [M+Na]⁺. Analytical data match those reported in the literature.²²

***N*-Benzyl-4-methyl-*N*-((methylthio)ethynyl)benzenesulfonamide (567)**

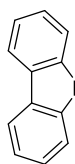

 Following **GP3** using dichloroenamide **564** (1.42 g, 4.0 mmol) and sulfonothioate **570** (971 mg, 4.8 mmol). Purification by flash column chromatography [hexane:toluene (5:95)] delivered thioynamide **567** as a pale yellow solid crystals (789 mg, 60%); ¹H NMR (400 MHz, CDCl₃): δ = 7.71 (d, J = 2H), 7.32–7.24 (m, 7H), 4.55 (s, 2H), 2.43 (s, 3H), 2.22 (s, 3H); ¹³C NMR (101 MHz, CDCl₃): δ = 144.7 (C), 135.0 (C), 134.8 (C), 129.7 (2×CH), 128.8 (2×CH), 128.6 (2×CH), 128.3 (CH), 127.8 (2×CH), 86.9 (C), 67.7 (C), 56.0 (CH₂), 21.8 (CH₃), 20.8 (CH₃); IR (neat): ν = 2924, 2152, 1596, 1427, 1356, 1166, 1089, 955, 660, 582; MS (ES): m/z 354.1 [M+Na]⁺. Analytical data match those reported in the literature.²²

***N*-Benzyl-4-methyl-*N*-((phenylthio)ethynyl)benzenesulfonamide (563)**


 Following **GP3** using dichloroenamide **564** (1027 mg, 2.9 mmol) and sulfonothioate **571** (952 mg, 3.6 mmol). Purification by flash column chromatography [hexane:toluene (7:3)] delivered thioynamide **563** as a pale yellow solid (800 mg, 70%); ¹H NMR (400 MHz, CDCl₃): δ = 7.73 (d, J = 8.4 Hz, 2H), 7.32–7.29 (m, 5H), 7.29–7.26 (m, 2H), 7.25–7.10 (m, 5H), 4.65 (s, 2H), 2.44 (s, 3H); ¹³C NMR (101 MHz, CDCl₃): δ = 144.9 (C), 134.9 (C), 134.7 (C), 134.4 (C), 129.8 (2×CH), 129.1 (2×CH), 129.0 (2×CH), 128.7 (2×CH), 128.5 (CH), 128.0 (2×CH), 126.4 (CH), 125.7 (2×CH), 93.2 (C), 62.5

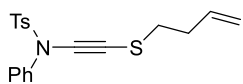
(C), 56.11 (CH₂), 21.8 (CH₃); IR (neat): ν = 2944, 2161, 1580, 1477, 1348, 1165, 1010, 727, 587; MS (ES): m/z 416.07 [M+Na]⁺. Analytical data match those reported in the literature.²²

9-((Methylthio)ethynyl)-9H-carbazole (568)



Following **GP3** using dichloroenamide **565** (524 mg, 2.0 mmol) and sulfonylthioate **570** (486 mg, 2.4 mmol). Purification by recrystallization from EtOH delivered thioynamide **568** as a pale yellow solid (248 mg, 52%); mp: 99–101 °C; ¹H NMR (400 MHz, CDCl₃): δ = 8.00 (d, J = 7.8 Hz, 2H), 7.70 (d, J = 8.1 Hz, 2H), 7.51 (app. td, J = 8.1, 1.1 Hz, 2H), 7.34 (app. td, J = 7.8, 0.8 Hz, 2H), 2.51 (s, 3H); ¹³C NMR (101 MHz, CDCl₃): δ = 141.3 (2×C), 126.9 (2×CH), 123.8 (2×C), 122.5 (2×CH), 120.4 (2×CH), 111.8 (2×CH), 81.8 (C), 69.8 (C), 21.2 (CH₃); IR (neat): ν = 2927, 2244, 2160, 1442, 1373, 1215, 1007, 971, 746; HRMS (EI): m/z calculated for C₁₅H₁₁NS: 237.0612, found 237.0613 [M]⁺.

N-((But-3-en-1-ylthio)ethynyl)-4-methyl-N-phenylbenzenesulfonamide (575)



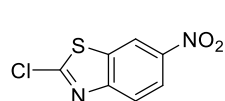
Following **GP3** using dichloroenamide **563** (342 mg, 1.0 mmol) and sulfonylthioate **574** (274 mg, 1.2 mmol). Purification by flash column chromatography [hexane:EtOAc (95:5)] delivered thioynamide **575** as an orange oil (221 mg, 62%); ¹H NMR (300 MHz, CDCl₃): δ = 7.60 (d, J = 8.3 Hz, 2H), 7.40–7.18 (m, 7H), 5.81 (ddt, J = 16.9, 10.2, 6.6 Hz, 1H), 5.16–5.02 (m, 2H), 2.67 (t, J = 7.4 Hz, 2H), 2.49–2.37 (m, 5H); ¹³C NMR (101 MHz, CDCl₃): δ = 145.1 (C), 139.2 (C), 135.8 (CH), 133.3 (C), 129.7 (2×CH), 129.2 (2×CH), 128.3 (3×CH), 126.3 (2×CH), 116.8 (CH₂), 88.1 (C), 64.7 (C), 35.6 (CH₂), 33.4 (CH₂), 21.8 (CH₃); IR (neat): ν = 3065, 2160, 1593, 1488, 1370, 1171, 919, 690,

663, 570; HRMS (ES): m/z calculated for $C_{19}H_{19}NO_2NaS_2$: 380.0755, found 380.0757 $[M+Na]^+$.

2.4. Synthesis of aminides from chapter 2

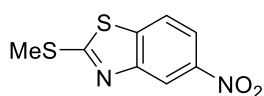
Preparation of precursors to aminides

2-Chloro-6-nitrobenzo[d]thiazole (328)



Following a reported procedure,¹³⁰ 2-chlorobenzothiazole (1.00 mL, 8.1 mmol) was added dropwise to concentrated sulfuric acid (4.6 mL, [1.77 M]) previously chilled with an ice bath with $NaCl_{(sol)}$. To that mixture, concentrated nitric acid was added dropwise (2.3 mL, 50.9 mmol) maintaining the temperature below 0 °C. The reaction mixture was allowed to warm up to room temperature and was stirred for 24 h. The crude reaction mixture was poured in a water/crushed ice mixture precipitating a yellow cake solid that was filtered under vacuum and washed with cold water. Recrystallization from EtOH of the resulting solid afforded benzothiazole **328** as a pale yellow solid (1.67 g, 97%); mp: 140–142 °C (lit. 140–142 °C); 1H NMR (300 MHz, $CDCl_3$): δ = 8.75 (d, J = 2.3 Hz, 1H), 8.38 (dd, J = 9.0, 2.3 Hz, 1H), 8.07 (d, J = 9.0 Hz, 1H); ^{13}C NMR (101 MHz, $CDCl_3$): δ = 159.0, 154.9, 136.6, 123.5, 122.4, 117.8 *one resonance for a quaternary carbon was not visible*; MS (ES): m/z 237.1 $[M+Na]^+$. Analytical data match those reported in the literature.¹³⁰

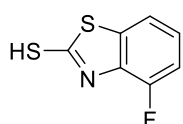
2-(Methylthio)-5-nitrobenzo[d]thiazole (333)



Following a reported procedure,^{66c} a heat-gun dried flask containing 2-chloro-5-nitroaniline (863 mg, 5.0 mmol) and potassium ethyl xanthate (1.76 g, 11.0 mmol) was evacuated and back filled with argon (purged 3 times). Dry DMF

(5 mL) was added and the mixture was stirred at 125 °C for 2.5 h. The mixture was allowed to cool down to room temperature and methyl iodide (0.78 mL, 12.5 mmol) was added dropwise followed by Et₃N (1.7 mL, 12.5 mL). The reaction mixture was diluted with EtOH (7.5 mL) and stirred at room temperature for 24 h. The crude mixture was diluted with EtOAc (20 mL) and washed with brine (20 mL). The organic layer was dried over Na₂SO₄, filtered off and concentrated under reduced pressure. Purification by flash column chromatography [hexane:EtOAc (96:4)] of the resulting solid afforded sulfide **333** as a yellow solid (663 mg, 59%); ¹H NMR (300 MHz, CDCl₃): δ = 8.69 (d, *J* = 2.1 Hz, 1H), 8.18 (dd, *J* = 8.8, 2.2 Hz, 1H), 7.87 (d, *J* = 8.8 Hz, 1H), 2.84 (s, 3H); ¹³C NMR (101 MHz, CDCl₃): δ = 142.2 (C), 121.3 (CH), 118.9 (CH), 116.7 (CH), 16.12 (CH₃) *two resonances for quaternary carbons not observed*; IR (neat): ν = 3105, 3090, 3011, 2926, 2834, 2659, 2284, 1919, 1594, 1572, 1508, 1447, 1429, 1416, 1343, 1321, 1242, 1142, 1086, 1075, 1021, 966, 883, 821, 739, 726, 680; MS (EI): *m/z* 226.0 [M]⁺. Analytical data match those reported in the literature.^{66e}

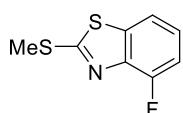
4-Fluorobenzof[d]thiazole-2-thiol (**335**)



Following a reported procedure,¹³¹ to a solution of 2,6-difluoroaniline (0.41 mL, 4.0 mmol) in NMP (4 mL) was added a solution of potassium ethyl xanthate (673 mg, 4.2 mmol) in NMP (4 mL). The mixture was stirred at 120 °C for 4 h. The crude suspension was allowed to cool down to room temperature and it was diluted with EtOAc (30 mL) and brine (30 mL). The organic phase was dried over Na₂SO₄, filtered off and concentrated under reduced pressure. Purification by flash column chromatography [hexane:EtOAc (4:1)] afforded thiol **335** as a pink fluffy solid (413 mg, 56%); ¹H NMR (300 MHz, CDCl₃): δ = 10.29 (s, 1H), 7.16 (m, 2H), 7.11 (m, 1H); IR (neat): ν = 3024, 2848, 1437,

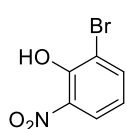
1239, 1064, 903, 761, 711; MS (ES): m/z 186.0 $[M+H]^+$. Analytical data match those reported in the literature.¹³¹

4-Fluoro-2-(methylthio)benzo[d]thiazole (336)



Following a reported procedure,¹³¹ to a solution of thiol **335** (463 mg, 2.5 mmol) in DMF (9.3 mL), K_2CO_3 (415 mg, 3.0 mmol) and methyl iodide (0.19 mL, 3.0 mmol) were added. The reaction mixture was stirred at room temperature for 20 h. The crude mixture was quenched with water (30 mL) and it was extracted with EtOAc (3×20 mL). The combined organic phases were dried over Na_2SO_4 filtered off and concentrated under reduced pressure. Purification by flash column chromatography [hexane:EtOAc (95:5)] afforded sulfide **336** as a yellow solid (435 mg, 87%); 1H NMR (300 MHz, $CDCl_3$): δ = 7.42 (dd, J = 8.0, 0.8 Hz, 1H), 7.15 (app. td, J = 8.0, 4.7 Hz, 1H), 7.05 (ddd, J = 10.5, 8.0, 0.8 Hz, 1H), 2.74 (s, 3H); ^{13}C NMR (101 MHz, $CDCl_3$): δ = 168.9, 154.2 (d, J = 255.1 Hz), 141.9 (d, J = 13.6 Hz), 137.7 (d, J = 3.5 Hz), 124.7 (d, J = 7.0 Hz), 116.5 (d, J = 4.0 Hz), 111.8 (d, J = 18.1 Hz), 15.9; IR (neat): ν = 3015, 1448, 1415, 1313, 1236, 1023, 905, 766, 725; MS (EI): m/z 199.0 $[M]^+$. Analytical data match those reported in the literature.¹³¹

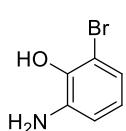
2-Bromo-6-nitrophenol (339)



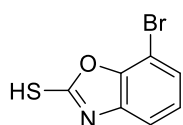
Following a reported procedure,⁶² to a solution of 2-bromophenol (2.12 mL, 20.0 mmol) in 1,2-DCE (40 mL) HNO_3 (9 wt%, 40 mmol) was added via an automatic syringe pump, maintaining an agitation speed of 200 rpm at 29 °C. The reaction was stirred under these conditions for 4 days. The organic layer was separated and the solvent was removed under reduced pressure. Purification of the crude by flash column

chromatography [hexane:EtOAc (99:1-98:2)] afforded phenol **339** as a bright yellow solid (1.77 g, 41%); ^1H NMR (300 MHz, CDCl_3): δ = 11.16 (s, OH, 1H), 8.11 (dd, J = 8.6, 1.6 Hz, 1H), 7.87 (dd, J = 7.8, 1.6 Hz, 1H), 6.92 (dd, J = 8.5, 7.9 Hz, 1H); ^{13}C NMR (101 MHz, CDCl_3): δ = 152.4 (C), 141.0 (CH), 124.6 (CH), 120.6 (CH), 114.4 (C), 113.5 (C); IR (neat): ν = 3192, 3090, 2898, 1611, 1578, 1538, 1443, 1370, 1309, 1250, 1142, 1098, 1070, 880, 832, 798, 742, 724; MS (EI): m/z 217.0 $[\text{M}+\text{H}]^+$. Analytical data match those reported in the literature.⁶²

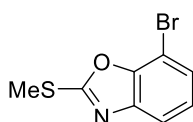
2-Amino-6-bromophenol (**340**)



Following a reported procedure,¹³² to a solution of phenol **339** (929 mg, 4.3 mmol) in MeOH (22 mL), zinc dust (2.81 g, 43.0 mmol) was added and the resulting suspension was cooled down to 0 °C. $\text{NH}_4\text{Cl}_{(\text{s})}$ (2.30 g, 43.0 mmol) was added portionwise over 5 min and the resulting green mixture was allowed to warm up to room temperature and stirred for 30 min. The crude mixture was filtered through a plug of celite and the filtrate was concentrated under reduced pressure. The residue was diluted with water (30 mL) and EtOAc (30 mL). The aqueous phase was extracted with EtOAc (5×20 mL). The combined organic phases were washed with water (30 mL), brine (30 mL), dried over Na_2SO_4 , filtered off and concentrated under reduced pressure affording aniline **340** as a black solid (708 mg, 88%); mp: 84–86 °C (lit. 84–86 °C); ^1H NMR (300 MHz, CDCl_3): δ = 6.86 (dd, J = 6.0, 3.6 Hz, 1H), 6.66 (s, 1H), 6.64 (d, J = 2.5 Hz, 1H), 4.14 (bs, 3H); ^{13}C NMR (101 MHz, CDCl_3): δ = 140.2 (C), 135.7 (C), 122.0 (CH), 121.2 (CH), 115.1 (CH), 110.2 (C); MS (ASAP): m/z 188.0 $[\text{M}]^+$. Analytical data match those reported in the literature.¹³²

7-Bromobenzo[d]oxazole-2-thiol (341)

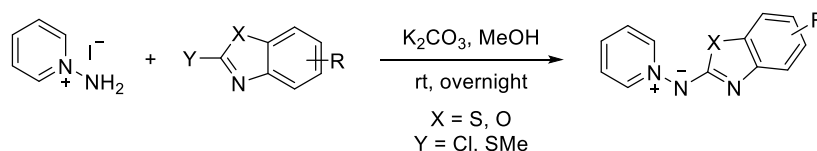
Following a reported procedure,¹³² a mixture of aniline **340** (638 mg, 3.4 mmol) and potassium ethyl xanthate (818 mg 5.1 mmol) in EtOH (3.4 mL) was stirred at 90 °C for 2 h. The crude reaction mixture was diluted with water (2 mL), the pH adjusted to 4.0 with AcOH, and the resulting dark green solid was collected, washed with water and dried under vacuum affording thiol **341** as a grey powder (657 mg, 84%); ¹H NMR (300 MHz, DMSO-d₆): δ = 14.15 (s, 1H), 7.45 (app. t, *J* = 4.5 Hz, 1H), 7.24–7.22 (m, 2H); ¹³C NMR (101 MHz, DMSO-d₆): δ = 179.8, 146.0, 132.5, 126.7, 126.4, 110.0, 100.8; IR (neat): ν = 3060, 2984, 1613, 1429, 1196, 1112, 915, 847, 768, 723, 656; MS (AP): *m/z* 231.9 [M+H]⁺. Analytical data match those reported in the literature.¹³²

7-Bromo-2-(methylthio)benzo[d]oxazole (342)

Following a reported procedure,¹³² to a solution of thiol **341** (690 mg, 3.0 mmol) in DMF (1.5 mL), K₂CO₃ (456 mg, 3.3 mmol) and methyl iodide (0.21 mL, 3.3 mmol) were added. The reaction mixture was stirred at room temperature for 3 min. The reaction mixture was quenched with NH₄Cl (sal. sol) (15 mL) and extracted with EtOAc (3×15 mL). The combined organic phases were washed with brine (15 mL), dried over Na₂SO₄, filtered and concentrated under reduced pressure. Purification by flash column chromatography afforded sulfide **342** as a red powder (564 mg, 77%); ¹H NMR (300 MHz, CDCl₃): δ = 7.52 (dd, *J* = 8.0, 0.9 Hz, 1H), 7.37 (dd, *J* = 8.0, 0.9 Hz, 1H), 7.16 (app. t, *J* = 8.0 Hz, 1H), 2.77 (s, 3H); ¹³C NMR (101 MHz, CDCl₃): δ = 166.5, 150.3, 142.8, 127.1, 125.6, 117.5, 101.9, 14.8; IR (neat): ν = 3060, 1501, 1419, 1259, 1196, 1113, 917, 773, 724; MS (ES): *m/z* 245.9 [M+H]⁺. Analytical data match those reported in the literature.¹³²

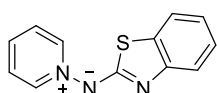
Synthesis of benzo(heteroaryl) aminides

General procedure 4 (GP4)



Following a modification of a literature method,⁴⁸ *N*-aminopyridinium iodide (1.0 eq.) and K_2CO_3 (3.0 eq.) were dissolved in methanol [0.1 M relative to the amount of *N*-aminopyridinium iodide]. The mixture was stirred at room temperature for 30 min until a permanent purple suspension appeared. The corresponding 2-halo or 2-methylsulfide benzoheterocycle (1.04 eq.) was added and the reaction mixture was stirred at room temperature for the indicated period of time. The solvent was removed under reduced pressure and the crude residue was dissolved in CH_2Cl_2 and washed with a solution of NaOH [2.5 M]. The aqueous phase was extracted with CH_2Cl_2 and the combined organic phases were dried over MgSO_4 , filtered off and concentrated under reduced pressure. Purification by flash column chromatography afforded the corresponding aminide.

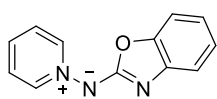
Benzo[d]thiazol-2-yl(pyridin-1-ium-1-yl)amide (267)



Following **GP4** using *N*-aminopyridinium iodide (1.11 g, 5.0 mmol), 2-chlorobenzothiazole (0.64 mL, 5.2 mmol) and K_2CO_3 (2.07 g, 15.0 mmol) for 24 h. Purification by flash column chromatography [EtOAc:MeOH (95:5-2:1)] afforded aminide **267** as a bright yellow powder (1.11 g, 98%); mp: 174–176 °C (lit. 174–176 °C); ^1H NMR (300 MHz, CDCl_3): δ = 9.64–9.55 (m, 2H), 7.57 (dd, J = 7.8, 0.8 Hz, 1H), 7.55–7.48 (m, 3H), 7.46 (dd, J = 8.0, 0.8 Hz, 1H), 7.24 (app. td, J = 7.8, 1.2 Hz, 1H), 7.03 (app. td, J =

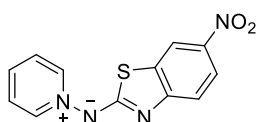
7.6, 1.2 Hz, 1H); ^{13}C NMR (101 MHz, CDCl_3): δ = 172.3 (C), 153.3 (C), 138.3 (CH), 131.13 (C), 130.96 (2 \times CH), 125.9 (2 \times CH), 125.3 (CH), 121.2 (CH), 120.5 (CH), 118.0 (CH); IR (neat): ν = 3070, 3050, 1590, 1551, 1467, 1351, 1290, 1193, 1012, 754; HRMS (ES): m/z calculated for $\text{C}_{12}\text{H}_{10}\text{N}_3\text{OS}$: 228.0595, found 228.0598 $[\text{M}+\text{H}]^+$. Analytical data match those reported in the literature.⁶⁵

Benzo[d]oxazol-2-yl(pyridin-1-ium-1-yl)amide (268)



Following **GP4** using *N*-aminopyridinium iodide (1.11 g, 5.0 mmol), 2-chlorobenzoxazole (0.59 mL, 5.2 mmol) and K_2CO_3 (2.07 g, 15.0 mmol) for 16 h. Purification by flash column chromatography [EtOAc:MeOH (4:1)] afforded aminide **268** as a bright yellow solid (970 mg, 92%); mp: 200–202 °C (lit. 200–202 °C); ^1H NMR (300 MHz, CDCl_3): δ = 9.60–9.54 (m, 2H), 7.63–7.53 (m, 3H), 7.35 (dd, J = 7.7, 0.9 Hz, 1H), 7.29 (dd, J = 7.5, 1.1 Hz, 1H), 7.15 (app. td, J = 7.5, 0.9 Hz, 1H), 7.04 (app. td, J = 7.7, 1.1 Hz, 1H); ^{13}C NMR (101 MHz, CDCl_3): δ = 166.3 (C), 147.5 (C), 143.7 (C), 138.6 (CH), 131.3 (2 \times CH), 126.1 (2 \times CH), 123.2 (CH), 120.9 (CH), 115.4 (CH), 108.5 (CH); IR (neat): ν = 3069, 3046, 1626, 1604, 1526, 1469, 1300, 1236, 1192, 1002; HRMS (ES): m/z calculated for $\text{C}_{12}\text{H}_9\text{N}_3\text{ONa}$: 234.0643, found 234.0641 $[\text{M}+\text{Na}]^+$. Analytical data match those reported in the literature.⁶⁵

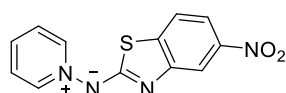
(6-Nitrobenzo[d]thiazol-2-yl)(pyridin-1-ium-1-yl)amide (343)



Following **GP4** using *N*-aminopyridinium iodide (111 mg, 0.5 mmol), chloride **328** (112 mg, 0.5 mmol) and K_2CO_3 (207 mg, 1.5 mmol) for 20 h. Purification by flash column chromatography [EtOAc:MeOH (95:5 to 4:1)] afforded aminide **343** as an orange powder (125 mg, 92%); mp: 258–260 °C (lit. 258–260 °C); ^1H

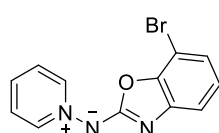
NMR (300 MHz, DMSO- d_6): δ = 9.17 (dd, J = 7.0, 1.2 Hz, 2H), 8.52 (d, J = 2.5 Hz, 1H), 8.22 (tt, J = 7.7, 1.2 Hz, 1H), 8.00–7.95 (m, 3H), 7.13 (d, J = 8.9 Hz, 1H); ^{13}C NMR (101 MHz, DMSO- d_6): δ = 142.3 (2 \times CH), 138.8 (CH), 127.5 (2 \times CH), 122.2 (CH), 116.8 (CH), 115.0 (CH) *the resonances for the quaternary carbons were not visible*; IR (neat): ν = 3011, 1451, 1317, 1142, 748, 666; HRMS (ES): m/z calculated for $\text{C}_{12}\text{H}_9\text{N}_4\text{O}_2\text{S}$: 273.0446, found 273.0445 $[\text{M}+\text{H}]^+$. Analytical data match those reported in the literature.⁶⁵

(5-Nitrobenzo[d]thiazol-2-yl)(pyridin-1-ium-1-yl)amide (344)



Following **GP4** using *N*-aminopyridinium iodide (178 mg, 0.8 mmol), sulfide **333** (188 mg, 0.8 mmol) and K_2CO_3 (332 mg, 2.4 mmol) for 20 h. Purification by flash column chromatography [EtOAc:MeOH (9:1)] afforded aminide **344** as a red powder (178 mg, 82%); mp: 242–244 °C (lit. 242–244 °C); ^1H NMR (400 MHz, CDCl_3): δ = 9.53–9.49 (m, 2H), 8.19 (d, J = 2.2 Hz, 1H), 7.89 (dd, J = 8.5, 2.2 Hz, 1H), 7.73 (tt, J = 7.7, 1.2 Hz, 1H), 7.67–7.59 (m, 3H); ^{13}C NMR (101 MHz, CDCl_3): δ = 139.0 (2 \times CH), 139.3 (C), 133.3 (CH), 126.3 (2 \times CH), 120.2 (CH), 116.0 (CH), 112.2 (CH) *three resonances for quaternary carbons were not visible*; IR (neat): ν = 3062, 1463, 1453, 1316, 1242, 768, 734, 665; HRMS (ES): m/z calculated for $\text{C}_{12}\text{H}_9\text{N}_4\text{O}_2\text{S}$: 273.0446, found: 273.0444 $[\text{M}+\text{H}]^+$. Analytical data match those reported in the literature.⁶⁵

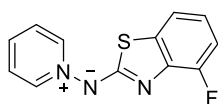
(7-Bromobenzo[d]oxazol-2-yl)(pyridin-1-ium-1-yl)amide (345)



Following **GP4** using *N*-aminopyridinium iodide (399 mg, 1.8 mmol), sulfide **342** (456 mg, 1.87 mmol) and K_2CO_3 (746 mg, 5.4 mmol) for 24 h. Purification by flash column chromatography [EtOAc:MeOH (9:1)] afforded aminide **345** as a yellow powder (263 mg, 50%); mp: 193–196 °C (lit. 193–196 °C); ^1H NMR (400 MHz,

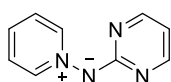
CDCl₃): δ = 9.54 (dd, J = 7.1, 1.3 Hz, 2H), 7.66–7.58 (m, 3H), 7.22 (dd, J = 7.9, 1.0 Hz, 1H), 7.13 (dd, J = 7.9, 1.0 Hz, 1H), 7.00 (app. t, J = 7.9 Hz, 1H); ¹³C NMR (101 MHz, CDCl₃): δ = 166.0 (C), 145.7 (C), 144.6 (C), 139.0 (2×CH), 132.2 (CH), 126.3 (2×CH), 124.4 (CH), 124.0 (CH), 114.2 (CH), 100.9 (C); IR (neat): ν = 3067, 1598, 1540, 1470, 1430, 1267, 1213, 971, 762; HRMS (ES): m/z calculated for C₁₂H₉N₃O⁷⁹Br: 289.9929, found: 289.9930 [M+H]⁺. Analytical data match those reported in the literature.⁶⁵

(4-Fluorobenzo[d]thiazol-2-yl)(pyridin-1-ium-1-yl)amide (346)



Following **GP4** using *N*-aminopyridinium iodide (361 mg, 1.6 mmol), sulfide **336** (337 mg, 1.7 mmol) and K₂CO₃ (675 mg, 4.9 mmol) for 24 h. Purification by flash column chromatography [hexane:EtOAc (1:4)] afforded aminide **346** as a yellow powder (191 mg, 48%); mp: 169–171 °C (lit. 169–171 °C); ¹H NMR (300 MHz, CDCl₃): δ = 9.63–9.58 (m, 2H), 7.64–7.52 (m, 3H), 7.37–7.29 (m, 1H), 7.02–6.92 (m, 2H); ¹³C NMR (101 MHz, CDCl₃): δ = 172.5 (C), 152.8 (d, J = 248.5 Hz, C), 141.6 (d, J = 12.4 Hz, C), 138.7 (2×CH), 133.7 (d, J = 4.5 Hz, C), 131.7 (CH), 126.1 (2×CH), 121.3 (d, J = 6.9 Hz, CH), 116.2 (d, J = 3.3 Hz, CH), 111.6 (d, J = 18.6 Hz, CH); IR (neat): ν = 3068, 1568, 1453, 1411, 1240, 750, 720, 704, 664; HRMS (ES): m/z calculated for C₁₂H₉N₃FS: 246.0501, found: 246.0505 [M+H]⁺. Analytical data match those reported in the literature.⁶⁵

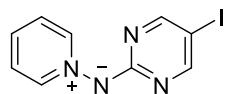
Pyridin-1-ium-1-yl(pyrimidin-2-yl)amide (214)



Following **GP4** using *N*-aminopyridinium iodide (1.11 g, 5.0 mmol), 2-chloropyrimidine (584 mg, 5.1 mmol) and K₂CO₃ (2.07 g, 15.0 mmol) for 24 h. Purification by flash column chromatography [EtOAc:MeOH (9:1)] afforded aminide **214** as a yellow powder (816 mg, 95%); ¹H NMR (300 MHz, CDCl₃): δ = 8.91–8.85 (m, 2H),

8.20 (d, $J = 4.7$ Hz, 2H), 7.77 (tt, $J = 7.7$, 1.4 Hz, 1H), 7.64–7.56 (m, 2H), 6.35 (t, $J = 4.7$ Hz, 1H); ^{13}C NMR (101 MHz, CDCl_3): $\delta = 166.8$ (C), 158.0 (2 \times CH), 142.7 (CH), 134.8 (2 \times CH), 126.3 (2 \times CH), 109.3 (CH); IR (neat): $\nu = 3111$, 1583, 1530, 1472, 1415, 1270, 982, 769, 691; MS (ES): m/z 173.08 $[\text{M}+\text{H}]^+$. Analytical data match those reported in the literature.²⁴

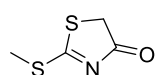
(5-Iodopyrimidin-2-yl)(pyridin-1-ium-1-yl)amide (325)



Following a reported procedure,¹³³ to a solution of aminide **214** (0.6 mmol, 100 mg, 1.0 eq.) in DMF (3 mL) was added *N*-iodosuccinimide (0.6 mmol, 144 mg, 1.1 eq.). The mixture was stirred at 55 °C for 3 h. The mixture was washed with H_2O (20 mL), extracted with CH_2Cl_2 (3 \times 15 mL). The combined organic phases were dried over Na_2SO_4 , filtered off and concentrated under reduced pressure. Purification by flash column chromatography [$\text{EtOAc}:\text{MeOH}$ (7:3)] afforded aminide **325** as a yellow solid (156 mg, 90%); ^1H NMR (300 MHz, CDCl_3): $\delta = 8.83$ – 8.75 (m, 2H), 8.24 (s, 2H), 7.77 (tt, $J = 7.6$, 1.5 Hz, 1H), 7.64–7.55 (m, 2H); ^{13}C NMR (101 MHz, CDCl_3): $\delta = 165.5$ (C), 162.4 (2 \times CH), 142.4 (2 \times CH), 134.6 (CH), 126.1 (2 \times CH), 72.6 (C); IR (neat): $\nu = 3108$, 1563, 1499, 1417, 1423, 1271, 1170, 781, 670; MS (ES): m/z 321.09 $[\text{M}+\text{Na}]^+$.

2.5. Synthesis of aminides from chapter 3 and 4

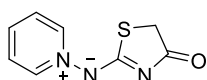
2-(Methylthio)thiazol-4(5H)-one (386)



Adapted from a reported procedure,^{66f} to a solution of **385** (2.00 g, 15.0 mmol) in EtOH (50 mL), *N,N*-diisopropylethylamine (2.87 mL, 16.5 mmol) and methyl iodide (1.03 mL, 16.5 mmol) were added. The reaction mixture was stirred at room temperature for 26 h. The crude mixture was diluted with cold NaHCO_3 (sat. sol) (20 mL) and CH_2Cl_2 (20 mL) and it was extracted with CH_2Cl_2 (4 \times 20 mL). The combined organic phases

were dried over Na_2SO_4 , filtered off and concentrated under reduced pressure. Purification by flash column chromatography [EtOAc (100%)] gave sulfide **386** as a beige solid (1.37 g, 62%); mp: 72–74 °C (lit. 72–74 °C); ^1H NMR (300 MHz, CDCl_3): δ = 4.00 (s, 2H), 2.74 (s, 3H); ^{13}C NMR (101 MHz, CDCl_3): δ = 202.8 (C), 187.6 (C), 39.9 (CH_2), 16.5 (CH_3); MS (EI): m/z 147.3 $[\text{M}]^+$. Analytical data match those reported in the literature.^{66f}

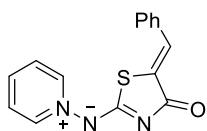
(4-Oxo-4,5-dihydrothiazol-2-yl)(pyridin-1-ium-1-yl)amide (422)



Following **GP4** using *N*-aminopyridinium iodide (1.11 g, 5.0 mmol), sulfide **386** (765 mg, 5.2 mmol) and K_2CO_3 (2.07 g, 15.0 mmol) for 17 h.

Extraction with $\text{NaOH}_{(\text{aq})}$ [2.0 M]. Purification by flash column chromatography [EtOAc:MeOH (9:1-7:3)] afforded aminide **422** as a beige fluffy solid (550 mg, 57%); mp: 225–228 °C; ^1H NMR (300 MHz, CDCl_3): δ = 8.82–8.79 (m, 2H), 8.05 (t, J = 7.8 Hz, 1H), 7.76 (app. t, J = 6.9 Hz, 2H), 3.90 (s, 2H); ^{13}C NMR (101 MHz, CDCl_3): δ = 188.2 (C), 185.0 (C), 142.7 (2 \times CH), 138.9 (CH), 126.7 (2 \times CH), 39.1 (CH_2); IR (neat): ν = 3030, 2924, 2151, 1652, 1453, 1356, 1167, 1088, 953, 756, 658; HRMS (ES): m/z calculated for $\text{C}_8\text{H}_8\text{N}_3\text{O}_2$: 194.0388 found, 194.0389 $[\text{M}+\text{H}]^+$.

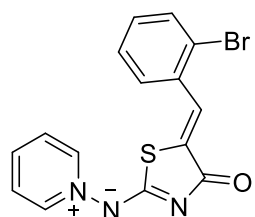
(Z)-(5-Benzylidene-4-oxo-4,5-dihydrothiazol-2-yl)(pyridin-1-ium-1-yl)amide (427)



Adapted from a reported procedure,^{76c} to a solution of aminide **422** (58.0 mg, 0.3 mmol) in glacial acetic acid (1.5 mL) sodium acetate (197 mg, 2.4 mmol) and benzaldehyde (0.06 mL, 0.6 mmol) were added. The mixture was stirred at 120 °C for 48 h. The crude mixture was allowed to cool down to room temperature precipitating an orange solid and acetic acid was removed under reduced pressure. The crude residue was diluted with HCl [1 M] (15 mL) and EtOAc (15 mL). The aqueous phase was

neutralised until pH 7 with NaHCO_3 (sat. sol) precipitating a yellow solid which was dried under vacuum affording aminide **427** as a pale yellow powder (59 mg, 70%); mp: 222–224 °C; ^1H NMR (300 MHz, CDCl_3): δ = 8.94 (d, J = 6.1 Hz, 2H), 8.07 (t, J = 6.8 Hz, 1H), 7.79 (app. t, J = 6.8 Hz, 2H), 7.73 (s, 1H), 7.60–7.53 (m, 2H), 7.48–7.40 (m, 2H), 7.34 (tt, J = 7.3, 1.3 Hz, 1H); ^{13}C NMR (101 MHz, CDCl_3): δ = 182.1 (C), 179.1 (C), 142.8 (2×CH), 139.2 (CH), 135.3 (C), 130.1 (C), 129.7 (2×CH), 129.0 (CH), 128.9 (2×CH), 128.5 (CH), 126.9 (2×CH); IR (neat): ν = 3108, 3013, 1656, 1599, 1496, 1465, 1233, 1002, 761, 668; HRMS (AP): m/z calculated for $\text{C}_{15}\text{H}_{12}\text{N}_3\text{OS}$: 282.0701, found: 282.0699 $[\text{M}+\text{H}]^+$.

(Z)-(5-(2-Bromobenzylidene)-4-oxo-4,5-dihydrothiazol-2-yl)(pyridin-1-ium-1-yl)amide
(**428**)



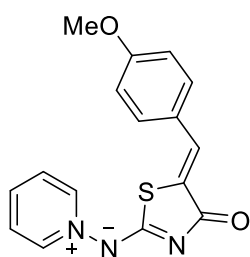
Adapted from a reported procedure,^{76c} to a solution of aminide **422** (135 mg, 0.7 mmol) in glacial acetic acid (3.5 mL) sodium acetate (459 mg, 5.6 mmol) and 2-bromobenzaldehyde (0.16 mL, 1.4 mmol) were added. The mixture was stirred at 120 °C for 22 h. The crude mixture was allowed to cool down to room temperature and the solvent was removed under reduced pressure. The crude residue was diluted with HCl [1 M] (15 mL) and EtOAc (15 mL). The aqueous phase was neutralised until pH 4 with NaHCO_3 (sat. sol) precipitating a yellow solid, which was collected with a Buchner funnel. Purification by flash column chromatography [CHCl_3 :EtOH (9:1)] afforded aminide **428** as a pale beige powder (163 mg, 64%); mp: 237–239 °C; ^1H NMR (300 MHz, CDCl_3): δ = 8.95–8.88 (m, 2H), 8.09 (tt, J = 7.8, 1.3 Hz, 1H), 7.98 (s, 1H), 7.84–7.76 (m, 2H), 7.65 (app. td, J = 8.1, 1.6 Hz, 2H), 7.39 (td, J = 7.4, 0.8 Hz, 1H), 7.17 (td, J = 7.7, 1.6 Hz, 1H); ^{13}C NMR (101 MHz, CDCl_3): δ = 181.2 (C), 178.8 (C), 142.8 (CH), 139.4 (CH), 135.7 (C), 133.7 (C), 133.5 (CH), 129.9 (CH), 128.9 (CH), 127.7 (CH), 127.0

(4×CH), 126.0 (C); IR (neat): ν = 3031, 1666, 1505, 1473, 1257, 1200, 1027, 756, 676;

HRMS (ES): m/z calculated for $C_{15}H_{11}N_3OS^{79}Br$: 359.9806, found: 359.9805 $[M+H]^+$.

(Z)-(5-(4-Methoxybenzylidene)-4-oxo-4,5-dihydrothiazol-2-yl)(pyridin-1-ium-1-yl)amide

(429)



Adapted from a reported procedure,^{76c} to a solution of aminide **422**

(193 mg, 1.0 mmol) in glacial acetic acid (5.0 mL) sodium acetate (328

mg, 4.0 mmol) and 4-methoxybenzaldehyde (60.8 μ L, 0.5 mmol) were

added. The mixture was stirred at 120 °C for 22 h. The crude mixture

was allowed to cool down to room temperature and the acetic acid was removed under

reduced pressure. The crude residue was diluted with HCl [1 M] (20 mL) and EtOAc (20

mL). The aqueous phase was neutralised until pH 8 with $NaHCO_3$ (sat. sol) precipitating a

yellow solid which was collected with a Buchner funnel. Purification by flash column

chromatography [EtOAc:MeOH (4:1-7:3)] afforded aminide **429** as a bright yellow powder

(129 mg, 83%); mp: 253–255 °C; 1H NMR (300 MHz, $CDCl_3$): δ = 8.97 (dd, J = 7.0, 1.2 Hz,

2H), 8.05 (tt, J = 7.7, 1.2 Hz, 1H), 7.78 (app. t, J = 7.0 Hz, 2H), 7.69 (s, 1H), 7.55–7.48 (m,

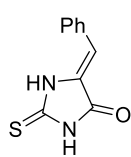
2H), 7.01–6.93 (m, 2H), 3.85 (s, 3H); ^{13}C NMR (101 MHz, $CDCl_3$): δ = 182.4 (C), 179.2 (C),

160.3 (C), 142.8 (2×CH), 138.94 (CH), 131.4 (2×CH), 128.9 (CH), 127.9 (CH), 127.5 (C),

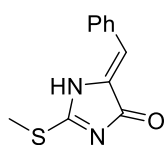
126.9 (2×C), 114.5 (2×CH), 55.5 (CH_3); IR (neat): ν = 2931, 1734, 1603, 1514, 1346, 1158,

1026, 754, 667; HRMS (ES): m/z calculated for $C_{16}H_{14}N_3O_2S$: 312.0807, found: 312.0806

$[M+H]^+$.

(Z)-5-Benzylidene-2-thioxoimidazolidin-4-one (454)

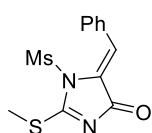
Adapted from a reported procedure,^{76c} to a solution of **450** (1.86 g, 16.0 mmol) in glacial acetic acid (80.0 mL) sodium acetate (5.25 g, 64.0 mmol) and benzaldehyde (0.81 mL, 8.0 mmol) were added. The mixture was stirred at 120 °C for 22 h. The crude mixture was allowed to cool down to room temperature and was poured into cold water (80 mL) precipitating a dark green solid. The residue was filtered off under vacuum and recrystallised from hot EtOH to afford thiohydantoin **454** as a dark green powder (1.18 g, 72%); ¹H NMR (300 MHz, DMSO-d₆): δ = 12.40 (br. s, 1H), 12.17 (br. s, 1H), 7.80–7.69 (m, 2H), 7.49–7.34 (m, 3H), 6.49 (s, 1H); ¹³C NMR (101 MHz, DMSO-d₆): δ = 179.3 (C), 165.8 (C), 132.2 (C), 130.2 (2×CH), 129.2 (CH), 128.8 (2×CH), 127.7 (C), 111.5 (CH); IR (neat): ν = 3191, 1721, 1641, 1478, 1091, 923, 765, 680. Analytical data match those reported in the literature.¹³⁴

(Z)-5-Benzylidene-2-(methylthio)-1,5-dihydro-4H-imidazol-4-one (455)

Adapted from a reported procedure,^{66f} to a solution of thiohydantoin **454** (511 mg, 2.5 mmol) in EtOH (8.3 mL), *N,N*-diisopropylethylamine (0.50 mL, 2.8 mmol) and methyl iodide (0.17 mL, 2.8 mmol) were added. The reaction mixture was stirred at room temperature for 20 h. The mixture was diluted with cold saturated NaHCO₃ (aq) (20 mL) and CH₂Cl₂ (20 mL) and it was extracted with CH₂Cl₂ (6×20 mL). The combined organic phases were dried over MgSO₄, filtered off and concentrated under reduced pressure. Purification by flash column chromatography [hexane:EtOAc (7:3)] gave sulfide **455** as a yellow fluffy solid (433 mg, 79%); ¹H NMR (300 MHz, CDCl₃): δ = 9.07 (br. s, 1H), 8.19–8.12 (m, 2H), 7.47–7.34 (m, 3H), 6.95 (s, 1H), 2.75 (s, 3H); ¹³C NMR (101 MHz, CDCl₃): δ = 171.8 (C), 162.5 (C), 138.8 (C), 134.4 (C), 132.1 (2×CH), 130.1 (CH), 128.8

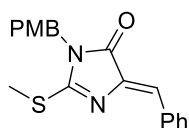
(2×CH), 124.4 (CH), 13.1 (CH₃); IR (neat): ν = 3019, 1705, 1634, 1399, 1186, 935, 888, 769, 691, 657; MS (ES): m/z 219.06 [M+H]⁺. Analytical data match those of the literature.¹³⁵

(Z)-5-Benzylidene-1-(methanesulfonyl)-2-(methylthio)-1,5-dihydro-4H-imidazol-4-one (457)



Sulfide **455** (109 mg, 0.5 mmol) and Na₂CO₃ (79.5 mg, 0.75 mmol) were dissolved in dry DMF (1.0 mL) in a heat-gun dried flask. The mixture was cooled to 0 °C and stirred for 5 min. Methanesulfonyl chloride (42.6 μ L, 0.6 mmol) was added dropwise and the reaction mixture was allowed to warm up to room temperature and stirred for 6 h. The mixture was quenched with water (6 mL) precipitating a yellow solid that was filtered off, washed with water (20 mL) and dried under vacuum to afford sulfide **457** as a white solid (85 mg, 58%); mp: 182–184 °C; ¹H NMR (300 MHz, CDCl₃): δ = 8.18–8.10 (m, 2H), 7.49–7.40 (m, 3H), 7.03 (s, 1H), 3.44 (s, 3H), 2.69 (s, 3H); ¹³C NMR (101 MHz, CDCl₃): δ = 166.9 (C), 159.9 (C), 135.4 (C), 133.8 (C), 132.5 (2×CH), 131.0 (CH), 129.0 (2×CH), 127.2 (CH), 42.0 (CH₃), 14.5 (CH₃); IR (neat): ν = 3025, 2925, 1751, 1496, 1358, 1157, 951, 759, 683; HRMS (ES): m/z calculated for C₁₂H₁₄N₂O₃S₂Na: 319.0187, found: 319.0186 [M+Na]⁺.

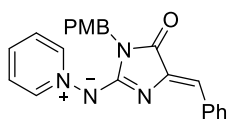
(Z)-5-Benzylidene-1-(4-methoxybenzyl)-2-(methylthio)-1,5-dihydro-4H-imidazol-4-one (459)



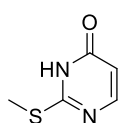
To a mixture of sulfide **455** (437 mg, 2.0 mmol) and K₂CO₃ (1.88 g, 7.0 mmol) in CH₃CN (100 mL) 4-methoxybenzyl chloride (0.27 mL, 4.2 mmol) was added. The reaction mixture was stirred at reflux for 7 h. The crude mixture was allowed to cool down to room temperature, diluted with water (30 mL) and the aqueous phase was extracted with EtOAc (3×20 mL). The combined organic phases were dried over

MgSO₄, filtered off and concentrated under reduced pressure. Purification by flash column chromatography [hexane:EtOAc (7:3)] afforded sulfide **459** as a bright yellow powder (583 mg, 86%); mp: 135–138 °C; ¹H NMR (300 MHz, CDCl₃): δ = 8.20–8.10 (m, 2H), 7.46–7.34 (m, 3H), 7.28 (d, *J* = 8.7 Hz, 2H), 6.99 (s, 1H), 6.85 (d, *J* = 8.7 Hz, 2H), 4.73 (s, 2H), 3.79 (s, 3H), 2.70 (s, 3H); ¹³C NMR (101 MHz, CDCl₃): δ = 170.1 (C), 165.2 (C), 150.5 (C), 138.5 (C), 134.6 (C), 132.1 (2×CH), 129.9 (CH), 129.5 (2×CH), 128.8 (2×CH), 128.0 (C), 124.2 (CH), 114.2 (2×CH), 55.4 (CH₃), 43.9 (CH₂), 13.4 (CH₃); IR (neat): ν = 2933, 1711, 1635, 1494, 1248, 1175, 1022, 771, 686; HRMS (ES): *m/z* calculated for C₁₉H₁₉N₂O₂S: 339.1167, found 339.1168 [M+H]⁺.

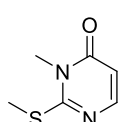
(Z)-(5-Benzylidene-1-(4-methoxybenzyl)-4-oxo-4,5-dihydro-1H-imidazol-2-yl)(pyridin-1-ium-1-yl)amide (460)



Following **GP4** using *N*-aminopyridinium iodide (333 mg, 1.5 mmol), sulfide **459** (528 mg, 1.6 mmol) and K₂CO₃ (622 mg, 4.5 mmol) for 18 h. Purification by flash column chromatography [EtOAc:MeOH (9:1)] afforded aminide **460** as a bright orange powder (512 mg, 98%); mp: 184–186 °C; ¹H NMR (300 MHz, CDCl₃): δ = 9.49–9.42 (m, 2H), 8.02–7.94 (m, 2H), 7.76 (tt, *J* = 7.6, 1.5 Hz, 1H), 7.67–7.57 (m, 2H), 7.39 (d, *J* = 8.7 Hz, 2H), 7.35–7.27 (m, 2H), 7.18 (tt, *J* = 7.4, 1.5 Hz, 1H), 6.82 (d, *J* = 8.7 Hz, 2H), 6.59 (s, 1H), 4.82 (s, 2H), 3.76 (s, 3H); ¹³C NMR (101 MHz, CDCl₃): δ = 170.3 (C), 161.5 (C), 158.9 (C), 141.6 (2×CH), 141.2 (C), 136.9 (C), 134.2 (CH), 130.3 (C), 130.0 (2×CH), 129.6 (2×CH), 128.4 (2×CH), 127.0 (CH), 126.0 (2×CH), 113.8 (2×CH), 112.2 (CH), 55.4 (CH₃), 42.5 (CH₂); IR (neat): ν = 2940, 1684, 1511, 1405, 1373, 1138, 1029, 763, 666; HRMS (ES): *m/z* calculated for C₂₃H₂₁N₄O₂: 385.1665, found 385.1669 [M+H]⁺.

2-(Methylthio)pyrimidin-4(3H)-one (467)

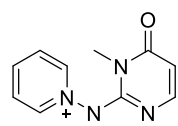
Following a reported procedure,⁹⁴ a mixture of **466** (3.84 g, 30.0 mmol) and finely powdered NaOH (1.28 g, 32.1 mmol) were dissolved in water (10.5 mL). The suspension was stirred to 68 °C until the solids were dissolved. EtOH (21 mL) was added and the mixture was cooled to 33 °C. Methyl iodide (1.9 mL, 30.3 mmol) was added dropwise and the reaction mixture was stirred at 55 °C for 20 min. The crude mixture was allowed to cool down to room temperature precipitating a white solid that was collected and dried under vacuum affording sulfide **467** as a white powder (3.46 g, 81%); ¹H NMR (300 MHz, CDCl₃): δ = 7.88 (d, *J* = 6.6 Hz, 1H), 6.24 (d, *J* = 6.6 Hz, 1H), 2.58 (s, 3H); IR (neat): ν = 3441, 2926, 1564, 1525, 1217, 1177, 976, 913, 822; MS (EI): *m/z* 142.02 [M]⁺. Analytical data match those reported in the literature.⁹⁴

3-Methyl-2-(methylthio)pyrimidin-4(3H)-one (470)

Following a reported procedure,¹³⁶ a heat-gun dried two neck flask under argon was charged with sulfide **467** (427 mg, 3.0 mmol) and dry DMF (11.5 mL). The solution was cooled to 0 °C and lithium bis(trimethylsilyl)amide ([1 M] solution in THF, 3.9 mL, 3.9 mmol) was added *via* syringe dropwise. The reaction mixture was stirred at 0 °C for 5 min and methyl iodide (0.24 mL, 3.9 mmol) was added dropwise at 0 °C. The reaction mixture was allowed to warm up to room temperature and was stirred for 17 h. The crude mixture was quenched with water (20 mL) and was extracted with EtOAc (6×20 mL). The combined organic phases were dried over MgSO₄, filtered off and concentrated under reduced pressure. Purification by flash column chromatography [hexane:EtOAc (3:2)] afforded sulfide **470** as a bright white solid (274 mg, 58%); mp: 123–125 °C (126–127 °C); ¹H NMR (300 MHz, CDCl₃): δ = 7.74 (d, *J* = 6.4 Hz, 1H), 6.19 (d, *J* = 6.4 Hz, 1H), 3.51 (s, 3H), 2.56 (s,

3H); ^{13}C NMR (101 MHz, CDCl_3): δ = 163.9 (C), 162.1 (C), 151.9 (CH), 109.9 (CH), 30.3 (CH₃), 15.1 (CH₃); MS (EI): m/z 109.0 $[\text{M-SMe}]^+$, 156.0 $[\text{M}]^+$. Analytical data match those reported in the literature.¹³⁶

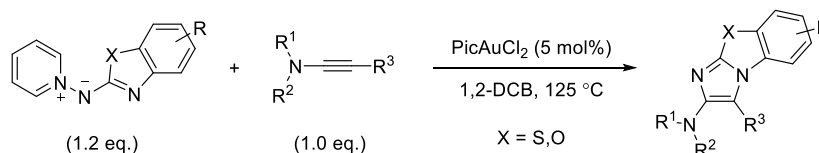
(1-Methyl-6-oxo-1,6-dihydropyrimidin-2-yl)(pyridin-1-ium-1-yl)amide (471)



Following **GP4** using *N*-aminopyridinium iodide (333 mg, 1.5 mmol), sulfide **470** (244 mg, 1.6 mmol) and K_2CO_3 (622 mg, 4.5 mmol) for 18 h. Extraction with $\text{NaOH}_{(\text{aq})}$ [2.0 M]. Purification by flash column chromatography [CH_2Cl_2 :MeOH (9:1)] afforded aminide **471** as a bright yellow powder (249 mg, 82%); mp: 231–233 °C; ^1H NMR (400 MHz, CDCl_3): δ = 8.62–8.57 (m, 2H), 7.94 (tt, J = 7.7, 1.3 Hz, 1H), 7.71–7.64 (m, 2H), 7.34 (d, J = 6.2 Hz, 1H), 5.61 (d, J = 6.2 Hz, 1H), 3.42 (s, 3H); ^{13}C NMR (101 MHz, CDCl_3): δ = 164.5 (C), 161.4 (C), 153.3 (CH), 144.4 (2 \times CH), 137.1 (CH), 126.5 (2 \times CH), 100.5 (CH), 27.7 (CH₃); IR (neat): ν = 3025, 1337, 1565, 1472, 1400, 1321, 1246, 1169, 800, 690; HRMS (ES): m/z calculated for $\text{C}_{10}\text{H}_{11}\text{N}_4\text{O}$: 203.0933, found 203.0938 $[\text{M}+\text{H}]^+$.

2.6. Cycloaddition products for chapter 2

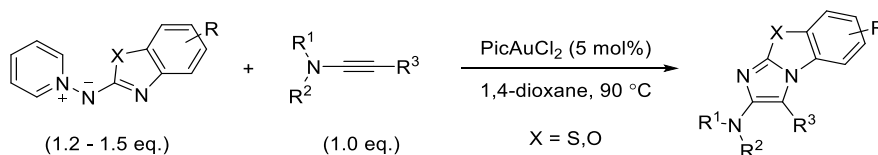
General procedure 5 (GP5)



A heat-gun dried Schlenk tube under argon was charged with (thio)ynamide (1.0 eq.), aminide (1.2 eq.) and dichloro(2-pyridinecarboxylate)gold (5 mol%) in dry 1,2-DCB (0.1 M relative to the (thio)ynamide) and the mixture was stirred at 125 °C for the specified time. The reaction

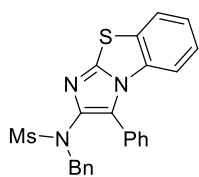
mixture was allowed to cool down to room temperature and was directly purified by flash column chromatography.

General procedure 6 (GP6)



A heat-gun dried Schlenk tube under argon was charged with (thio)ynamide (1.0 eq.), aminide (1.2 eq. or 1.5 eq) and dichloro(2-pyridinecarboxylate)gold (5 mol%) in dry 1,4-dioxane (0.1 M relative to the (thio)ynamide) and the mixture was stirred at 90 °C for the specified time. The reaction mixture was allowed to cool down to room temperature and the solvent was removed under reduced pressure. The residue obtained was purified by flash column chromatography.

N-Benzyl-*N*-(3-phenylbenzo[d]imidazo[2,1-*b*]thiazol-2-yl)methanesulfonamide (**302**)

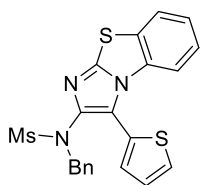


Following **GP5** using ynamide **297** (60.3 mg, 0.20 mmol) and aminide **267** (71.5 mg, 0.24 mmol) for 45 min. Purification by flash column chromatography [hexane:EtOAc (3:2)] afforded imidazole **302** as a white powder (72.5 mg, 83%); mp: 56–58 °C; ^1H NMR (300 MHz, CDCl_3): δ = 7.67 (dd, J = 8.0, 1.1 Hz, 1H), 7.42 (tt, J = 7.3, 2.5 Hz, 1H), 7.37–7.30 (m, 2H), 7.26 (app. td, J = 7.1, 1.1 Hz, 1H), 7.19–7.09 (m, 4H), 7.06–6.96 (m, 5H), 4.69 (s, 2H), 3.25 (s, 3H); ^{13}C NMR (101 MHz, CDCl_3): δ = 144.7 (C), 138.3 (C), 135.2 (C), 133.2 (C), 130.6 (2×CH), 129.7 (C), 129.3 (2×CH), 129.1 (CH), 128.4 (2×CH), 128.2 (2×CH), 127.8 (C), 127.7 (CH), 127.1 (C), 126.0 (CH), 125.0 (CH), 124.2 (CH), 114.1 (CH), 55.3 (CH_2), 38.3 (CH_3); IR (neat): ν = 2925,

1581, 1564, 1487, 1457, 1345, 1255, 1221, 1149, 1065, 1025, 958, 868, 790, 748, 701, 665;

HRMS (ES): m/z calculated for $C_{23}H_{19}N_3O_2NaS_2$: 456.0816, found 456.0815 $[M+Na]^+$.

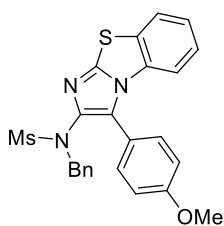
N-Benzyl-N-(3-(thiophen-2-yl)benzo[d]imidazo[2,1-b]thiazol-2-yl)methanesulfonamide
(303)



Following **GP5** using ynamide **292** (29.1 mg, 0.10 mmol) and aminide **267** (35.8 mg, 0.12 mmol) for 45 min. Purification by flash column chromatography [hexane:EtOAc (7:3)] afforded imidazole **303** as a yellow

solid (40.1 mg, 91%); mp: 177–179 °C; 1H NMR (300 MHz, $CDCl_3$): δ = 7.68 (d, J = 7.8 Hz, 1H), 7.49 (dd, J = 5.1, 1.2 Hz, 1H), 7.29 (app. td, J = 7.8, 1.1 Hz, 1H), 7.23–7.07 (m, 8H), 6.96 (dd, J = 3.4, 1.1 Hz, 1H), 4.75 (s, 2H), 3.20 (s, 3H); ^{13}C NMR (101 MHz, $CDCl_3$): δ = 145.4 (C), 140.2 (C), 135.4 (C), 133.0 (C), 131.6 (CH), 129.6 (C), 129.1 (2×CH), 128.9 (CH), 128.4 (2×CH), 127.8 (CH), 127.2 (CH), 126.5 (C), 126.2 (CH), 125.2 (CH), 124.2 (CH), 120.5 (C), 114.2 (CH), 55.1 (CH_2), 38.3 (CH_3); IR (neat): ν = 2927, 1587, 1486, 1460, 1379, 1337, 1258, 1226, 1155, 1053, 964, 938, 872, 785, 757, 740, 698, 677; HRMS (ES): m/z calculated for $C_{21}H_{18}N_3O_2S_3$: 440.0561, found 440.0567 $[M+H]^+$.

N-Benzyl-N-(3-(4-methoxyphenyl)benzo[d]imidazo[2,1-b]thiazol-2-yl)methanesulfonamide
(304)

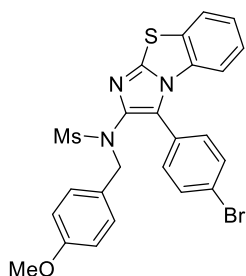


Following **GP5** using ynamide **298** (54.1 mg, 0.17 mmol) and aminide **267** (60.8 mg, 0.20 mmol) for 45 min. Purification by flash column chromatography [hexane:EtOAc (1:1)] afforded imidazole **304** as an orange powder (57.4 mg, 73%); mp: 164–166 °C; 1H NMR (300 MHz,

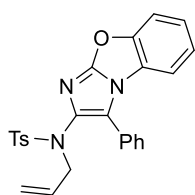
$CDCl_3$): δ = 7.66 (d, J = 7.9 Hz, 1H), 7.25 (app. t, J = 7.7 Hz, 1H), 7.19–6.95 (m, 9H), 6.91–

6.83 (m, 2H), 4.70 (s, 2H), 3.89 (s, 3H), 3.24 (s, 3H); ^{13}C NMR (101 MHz, CDCl_3): δ = 160.3 (C), 144.3 (C), 138.0 (C), 135.4 (C), 133.2 (C), 132.1 (2 \times CH), 129.7 (C), 129.3 (2 \times CH), 128.2 (2 \times CH), 127.7 (CH), 127.6 (C), 125.9 (CH), 125.0 (CH), 124.1 (CH), 119.2 (C), 114.0 (CH), 113.8 (2 \times CH), 55.5 (CH_3), 55.2 (CH_2), 38.3 (CH_3); IR (neat): ν = 2931, 2840, 1507, 1489, 1346, 1249, 1156, 1027, 962, 837, 752; HRMS (ES): m/z calculated for $\text{C}_{24}\text{H}_{21}\text{N}_3\text{O}_3\text{NaS}_2$: 486.0922, found 486.0918 $[\text{M}+\text{Na}]^+$.

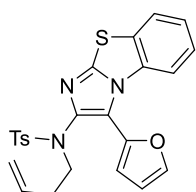
***N*-(3-(4-Bromophenyl)benzo[d]imidazo[2,1-*b*]thiazol-2-yl)-*N*-(4-methoxybenzyl) methanesulfonamide (305)**



Following **GP5** using ynamide **293** (394 mg, 1.00 mmol) and aminide **267** (272 mg, 1.20 mmol) for 2 h. Purification by flash column chromatography [hexane:EtOAc (3:2)] afforded imidazole **305** as a beige fluffy solid (502 mg, 93%); mp: 200–202 °C; ^1H NMR (400 MHz, CDCl_3): δ = 7.69 (dd, J = 8.0, 0.7 Hz, 1H), 7.45 (d, J = 8.7 Hz, 2H), 7.29 (app. td, J = 7.5, 1.2 Hz, 1H), 7.18 (app. td, J = 7.5, 1.2 Hz, 1H), 7.08–7.01 (m, 3H), 6.85 (d, J = 8.7 Hz, 2H), 6.54 (d, J = 8.7 Hz, 2H), 4.60 (s, 2H), 3.75 (s, 3H), 3.26 (s, 3H); ^{13}C NMR (101 MHz, CDCl_3): δ = 159.3 (C), 145.1 (C), 138.5 (C), 133.0 (C), 131.9 (2 \times CH), 131.5 (2 \times CH), 130.6 (2 \times CH), 129.7 (C), 127.1 (C), 126.8 (C), 126.1 (CH), 125.2 (CH), 124.3 (CH), 123.4 (C), 114.0 (CH), 113.5 (2 \times CH), 55.3 (CH_3), 54.8 (CH_2), 38.4 (CH_3) *one resonance for a quaternary carbon was not observed*; IR (neat): ν = 2926, 1515, 1494, 1336, 1248, 1161, 969, 823, 745, 663, 562; HRMS (ES): m/z calculated for $\text{C}_{24}\text{H}_{20}\text{N}_3\text{O}_3\text{NaS}_2^{79}\text{Br}$: 564.0027, found 564.0028 $[\text{M}+\text{Na}]^+$.

***N*-Allyl-4-methyl-*N*-(3-phenylbenzo[d]imidazo[2,1-*b*]oxazol-2-yl)benzenesulfonamide (306)**

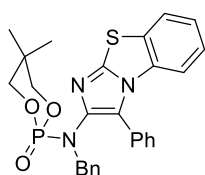
Following **GP6** using ynamide **681** (62.3 mg, 0.20 mmol) and aminide **268** (50.7 mg, 0.24 mmol) for 3 h. Purification by flash column chromatography [hexane:EtOAc (24:1)] afforded imidazole **306** as a white solid (50.1 mg, 56%); mp: 209–210 °C; ^1H NMR (400 MHz, CDCl_3): δ = 7.86–7.82 (m, 4H), 7.58–7.50 (m, 3H), 7.46 (tt, J = 7.3, 1.4 Hz, 1H), 7.40 (dd, J = 7.8, 0.9 Hz, 1H), 7.36–7.28 (m, 3H), 7.23 (app. td, J = 7.8, 0.9 Hz, 1H), 5.52 (ddt, J = 17.0, 10.5, 6.7 Hz, 1H), 4.93 (dd, J = 17.0, 1.2 Hz, 1H), 4.87 (dd, J = 10.5, 1.2 Hz, 1H), 4.00 (d, J = 6.7 Hz, 2H), 2.45 (s, 3H); ^{13}C NMR (101 MHz, CDCl_3): δ = 151.9 (C), 150.3 (C), 143.8 (C), 135.8 (C), 133.9 (C), 132.4 (CH), 129.6 (2 \times CH), 128.9 (2 \times CH), 128.81 (2 \times CH), 128.77 (2 \times CH), 128.7 (CH), 127.8 (C), 127.0 (C), 124.8 (CH), 124.0 (CH), 123.5 (C), 119.2 (CH_2), 112.5 (CH), 112.4 (CH), 53.7 (CH_2), 21.8 (CH_3); IR (neat): ν = 2921, 1629, 1576, 1477, 1340, 1162, 812, 743, 705, 661, 584; HRMS (ES): m/z calculated for $\text{C}_{25}\text{H}_{21}\text{N}_3\text{O}_3\text{SNa}$: 466.1201, found 466.1197 $[\text{M}+\text{Na}]^+$.

***N*-(But-3-en-1-yl)-*N*-(3-(furan-2-yl)benzo[d]imidazo[2,1-*b*]thiazol-2-yl)-4-methylbenzenesulfonamide (307)**

Following **GP5** using ynamide **682** (75.7 mg, 0.20 mmol) and aminide **267** (45.5 mg, 0.24 mmol) for 2 h. Purification by flash column chromatography [hexane:EtOAc (9:1-85:15)] afforded imidazole **307** as light brown solid (61.5 mg, 66%); mp: 174–176 °C; ^1H NMR (300 MHz, CDCl_3): δ = 7.78 (d, J = 8.3 Hz, 2H), 7.73–7.69 (m, 2H), 7.43–7.31 (m, 5H), 7.18 (dd, J = 3.4, 0.7 Hz, 1H), 6.65 (dd, J = 3.4, 1.9 Hz, 1H), 5.55 (ddt, J = 16.5, 9.8, 6.6 Hz, 1H), 4.89–4.83 (m, 2H), 3.46 (t, J = 7.2 Hz, 2H), 2.44 (s, 3H), 2.08 (app. q, J = 7.7 Hz, 2H); ^{13}C NMR (101 MHz, CDCl_3): δ = 145.8 (C), 143.8 (C), 143.4 (CH), 140.8 (C), 140.0 (C), 135.7 (C), 134.5 (CH), 133.0 (C), 129.7 (2 \times CH), 129.6

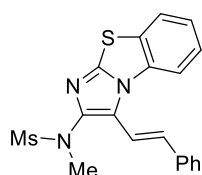
(C), 128.5 (2×CH), 126.5 (CH), 125.3 (CH), 124.0 (CH), 118.8 (C), 116.8 (CH₂), 114.8 (CH), 114.2 (CH), 112.2 (CH), 49.9 (CH₂), 32.5 (CH₂), 21.8 (CH₃); IR (neat): ν = 2924, 2324, 1480, 1338, 1158, 1087, 744, 666; HRMS (ES): m/z calculated for C₂₄H₂₂N₃O₃S₂: 464.1103, found 464.1099 [M+H]⁺.

2-(Benzyl(3-phenylbenzo[d]imidazo[2,1-b]thiazol-2-yl)amino)-5,5-dimethyl-1,3,2-dioxaphosphinane 2-oxide (308)



Following **GP5** using ynamide **299** (35.5 mg, 0.10 mmol) and aminide **267** (35.8 mg, 0.12 mmol) for 45 min. Purification by flash column chromatography [hexane:EtOAc (1:9)] afforded imidazole **308** as a yellow solid (41.0 mg, 81%); mp: 183–185 °C; ¹H NMR (300 MHz, CDCl₃): δ = 7.64 (dd, J = 8.1, 1.2 Hz, 1H), 7.45–7.30 (m, 3H), 7.25–7.05 (m, 9H), 6.98 (dd, J = 8.1, 1.2 Hz, 1H), 4.56 (d, J = 7.2 Hz, 2H), 4.30 (dd, J = 11.0, 5.0 Hz, 2H), 3.90 (dd, J = 19.0, 11.0 Hz, 2H), 1.09 (s, 3H), 0.91 (s, 3H); ¹³C NMR (101 MHz, CDCl₃): δ = 144.1 (C), 139.7 (d, J = 3.2 Hz, C), 137.0 (d, J = 4.8 Hz, C), 133.4 (C), 130.6 (2×CH), 129.9 (C), 129.0 (2×CH), 128.8 (CH), 128.4 (2×CH), 128.1 (2×CH), 127.9 (C), 127.3 (CH), 125.7 (CH), 125.0 (d, J = 6.2 Hz, C), 124.6 (CH), 124.1 (CH), 113.8 (CH), 76.7 (d, J = 5.9 Hz, 2×CH₂), 53.8 (d, J = 6.1 Hz, CH₂), 32.2 (d, J = 5.3 Hz, C), 29.8 (C), 22.1 (CH₃), 21.1 (CH₃); IR (neat): ν = 2971, 1486, 1379, 1252, 1212, 1054, 1004, 744, 697, 662; HRMS (ES): m/z calculated for C₂₇H₂₆N₃O₃NaSP: 526.1330, found 526.1326 [M+Na]⁺.

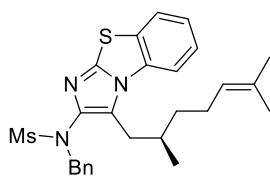
(E)-N-Methyl-N-(3-styrylbenzo[d]imidazo[2,1-b]thiazol-2-yl)methanesulfonamide (309)



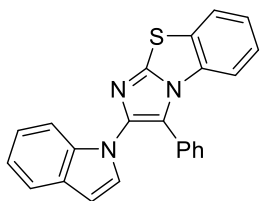
Following **GP6** using ynamide **683** (23.5 mg, 0.10 mmol) and aminide **267** (35.8 mg, 0.12 mmol) for 45 min. Recrystallization from hexane/CH₂Cl₂

afforded imidazole **309** as brown solid (34.1 mg, 89%); using 1,2-DCB at 125 °C (28.2 mg, 74%); mp: 222–224 °C; ^1H NMR (300 MHz, CDCl_3): δ = 7.92 (dd, J = 8.3, 0.9 Hz, 1H), 7.74 (dd, J = 7.8, 1.0 Hz, 1H), 7.62–7.53 (m, 2H), 7.51–7.28 (m, 7H), 3.33 (s, 3H), 3.20 (s, 3H); ^{13}C NMR (101 MHz, CDCl_3): δ = 144.8 (C), 140.5 (C), 136.9 (C), 134.1 (CH), 133.7 (C), 129.8 (C), 128.9 (2 \times CH), 128.5 (CH), 127.0 (2 \times CH), 126.6 (CH), 125.2 (CH), 124.4 (CH), 120.9 (C), 114.1 (CH), 112.4 (CH), 38.8 (CH_3), 36.8 (CH_3); IR (neat): ν = 3062, 1543, 1489, 1465, 1409, 1341, 1294, 1257, 1191, 1151, 1107, 1001, 965, 954, 877, 815, 769, 750, 740, 692, 675; HRMS (ES): m/z calculated for $\text{C}_{19}\text{H}_{18}\text{N}_3\text{O}_2\text{S}_2$: 384.0840, found 384.0835 $[\text{M}+\text{H}]^+$.

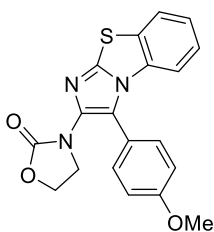
(*R*)-*N*-Benzyl-*N*-(3-(2,6-dimethylhept-5-en-1-yl)benzo[d]imidazo[2,1-*b*]thiazol-2-yl)methanesulfonamide (310)



Following **GP6** using ynamide **294** (33.4 mg, 0.10 mmol) and aminide **267** (35.7 mg, 0.12 mmol) for 45 min. Purification by flash column chromatography [hexane:EtOAc (3:2)] afforded imidazole **310** as a yellow oil (11.6 mg, 24%); ^1H NMR (300 MHz, CDCl_3): δ = 7.70 (dd, J = 7.6, 1.2 Hz, 1H), 7.58 (d, J = 8.3 Hz, 1H), 7.41–7.24 (m, 7H), 4.94 (t, J = 7.1 Hz, 1H), 4.84 (d, J = 4.6 Hz, 2H), 3.06 (s, 3H), 2.79 (dd, J = 15.3, 6.0 Hz, 1H), 2.62 (dd, J = 15.3, 9.3 Hz, 1H), 1.95–1.77 (m, 3H), 1.61 (s, 3H), 1.54 (s, 3H), 1.19–0.80 (m, 2H), 0.43 (d, J = 6.5 Hz, 3H); ^{13}C NMR (101 MHz, CDCl_3): δ = 143.8 (C), 138.8 (C), 136.1 (C), 133.6 (C), 131.6 (C), 130.1 (2 \times CH), 129.8 (C), 128.5 (2 \times CH), 128.2 (CH), 127.7 (C), 126.1 (CH), 124.8 (CH), 124.6 (CH), 124.3 (CH), 113.9 (CH), 55.0 (CH_2), 37.5 (CH), 36.9 (CH_2), 31.9 (CH_3), 30.9 (CH_2), 25.8 (CH_3), 25.5 (CH_2), 18.7 (CH_3), 17.8 (CH_3); IR (neat): ν = 2963, 2925, 2852, 1585, 1550, 1495, 1458, 1347, 1156, 961, 749, 699; HRMS (ES): m/z calculated for $\text{C}_{26}\text{H}_{31}\text{N}_3\text{O}_2\text{S}_2\text{Na}$: 504.1755, found 504.1759 $[\text{M}+\text{Na}]^+$.

2-(1*H*-Indol-1-yl)-3-phenylbenzo[*d*]imidazo[2,1-*b*]thiazole (311)

Following **GP5** using ynamide **301** (43.5 mg, 0.20 mmol) and aminide **267** (71.5 mg, 0.24 mmol) for 24 h. Purification by flash column chromatography [hexane:EtOAc (9:1)] afforded imidazole **311** as a pale pink crystalline solid (46.4 mg, 63%). Using ynamide **301** (10.9 mg, 0.05 mmol), aminide **267** (17.9 mg, 0.06 mmol) and DTBPAu(NCMe)SbF₆ (5 mol%) for 24 h afforded imidazole **311** as a pale pink solid (13.0 mg, 71%); mp: 172–174 °C; ¹H NMR (300 MHz, CDCl₃): δ = 7.76 (d, *J* = 7.8 Hz, 1H), 7.66–7.56 (m, 2H), 7.43 (s, 5H), 7.38–7.23 (m, 3H), 7.18 (app. td, *J* = 7.5, 1.2 Hz, 1H), 7.12 (app. td, *J* = 7.5, 1.2 Hz, 1H), 7.02 (d, *J* = 3.3 Hz, 1H), 6.50 (d, *J* = 3.3 Hz, 1H); ¹³C NMR (101 MHz, CDCl₃): δ = 145.3 (C), 140.0 (C), 133.9 (C), 133.4 (C), 130.5 (2×CH), 130.0 (C), 129.4 (CH), 129.2 (2×CH), 128.7 (C), 128.2 (CH), 127.9 (C), 126.0 (CH), 124.9 (CH), 124.4 (CH), 122.5 (CH), 120.7 (CH), 120.5 (CH), 113.9 (CH), 111.8 (CH), 103.7 (CH) *one resonance for a quaternary carbon was not observed*; IR (neat): ν = 3059, 2251, 1526, 1458, 1204, 1163, 742, 714, 690; HRMS (ES): *m/z* calculated for C₂₃H₁₆N₃S: 366.1065, found 366.1064 [M+H]⁺.

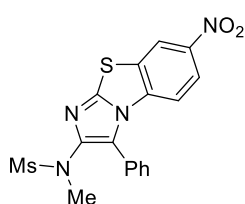
3-(3-(4-Methoxyphenyl)benzo[*d*]imidazo[2,1-*b*]thiazol-2-yl)oxazolidin-2-one (312)

Following **GP5** using ynamide **295** (43.4 mg, 0.20 mmol) and aminide **267** (71.5 mg, 0.24 mmol) for 18 h. Purification by flash column chromatography [hexane:EtOAc (3:7)] afforded imidazole **312** as a yellow solid (66.7 mg, 91%); mp: 88–90 °C; ¹H NMR (300 MHz, CDCl₃): δ = 7.68 (dd, *J* = 8.1, 0.9 Hz, 1H), 7.54 (d, *J* = 8.8 Hz, 2H), 7.28 (app. td, *J* = 7.5, 1.2 Hz, 1H), 7.19 (app. td, *J* = 7.5, 1.2 Hz, 1H), 7.12 (dd, *J* = 8.1, 0.8 Hz, 1H), 7.05 (d, *J* = 8.8 Hz, 2H), 4.44–4.35 (m, 2H), 3.97–3.87 (m, 5H); ¹³C NMR (101 MHz, CDCl₃): δ = 160.6 (C), 157.6

(C), 144.9 (C), 136.9 (C), 133.2 (C), 131.8 (2×CH), 129.8 (C), 125.9 (CH), 124.9 (CH), 124.3 (CH), 123.7 (C), 119.6 (C), 114.5 (2×CH), 113.8 (CH), 62.6 (CH₂), 55.5 (CH₃), 47.3 (CH₂); IR (neat): ν = 2923, 1751, 1488, 1407, 1244, 1024, 838, 726; HRMS (ES): m/z calculated for C₁₉H₁₆N₃O₃S: 366.0912, found 366.0915 [M+H]⁺.

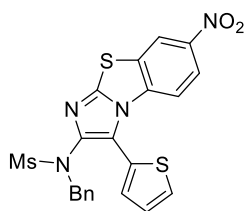
N-Methyl-N-(7-nitro-3-phenylbenzo[d]imidazo[2,1-b]thiazol-2-yl)methanesulfonamide

(347)



Following **GP6** using ynamide **679** (25.1 mg, 0.10 mmol) and aminide **343** (27.2 mg, 0.12 mmol) for 1.25 h. Purification by flash column chromatography [hexane:EtOAc (7:3-4:1)] afforded imidazole **347** as a bright yellow solid (39.1 mg, 97%); mp: 256–258 °C; ¹H NMR (300 MHz, CDCl₃): δ = 8.66 (d, J = 2.3 Hz, 1H), 8.14 (dd, J = 9.2, 2.3 Hz, 1H), 7.71–7.62 (m, 2H), 7.61–7.54 (m, 3H), 7.28 (d, J = 9.2 Hz, 1H), 3.21 (s, 3H), 3.17 (s, 3H); ¹³C NMR (101 MHz, CDCl₃): δ = 145.7 (C), 144.7 (C), 141.9 (C), 137.0 (C), 131.0 (C), 130.5 (2×CH), 130.2 (CH), 129.3 (2×CH), 126.5 (C), 122.1 (CH), 120.3 (CH), 113.8 (CH), 39.1 (CH₃), 37.2 (CH₃) *one resonance for a quaternary carbon was not observed*; IR (neat): ν = 3047, 2921, 2855, 1581, 1521, 1487, 1366, 1335, 1320, 1288, 1239, 1141, 950, 877, 787, 759, 746; HRMS (ES): m/z calculated for C₁₇H₁₄N₄O₄NaS₂: 425.0354, found 425.0357 [M+Na]⁺.

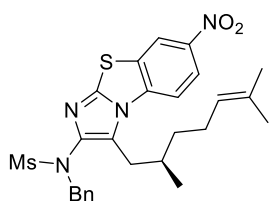
N-Benzyl-N-(7-nitro-3-(thiophen-2-yl)benzo[d]imidazo[2,1-b]thiazol-2-yl)methanesulfonamide (348)



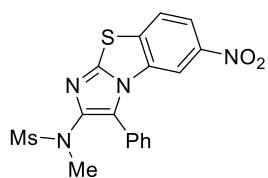
Following **GP5** using ynamide **292** (58.3 mg, 0.20 mmol) and aminide **343** (65.3 mg, 0.24 mmol) for 1.5 h. Purification by flash column chromatography [hexane:EtOAc (4:1)] afforded imidazole **348** as a pale

yellow solid (76.4 mg, 79%); mp: 152–155 °C (decomp.); ^1H NMR (400 MHz, CDCl_3): δ = 8.63 (d, J = 2.2 Hz, 1H), 8.12 (dd, J = 9.1, 2.2 Hz, 1H), 7.54 (dd, J = 5.2, 1.2 Hz, 1H), 7.23–7.08 (m, 7H), 6.99 (dd, J = 3.4, 1.2 Hz, 1H), 4.76 (s, 2H), 3.19 (s, 3H); ^{13}C NMR (101 MHz, CDCl_3): δ = 146.4 (C), 144.7 (C), 141.5 (C), 136.8 (C), 135.2 (C), 132.1 (CH), 130.8 (C), 129.7 (CH), 129.0 (2 \times CH), 128.5 (2 \times CH), 128.0 (CH), 127.6 (CH), 125.3 (C), 122.2 (CH), 121.2 (C), 120.2 (CH), 113.9 (CH), 55.0 (CH_2), 38.4 (CH_3); IR (neat): ν = 3311, 2490, 2263, 2167, 2077, 2048, 2031, 2008, 1637, 1342, 1156, 667; HRMS (ES): m/z calculated for $\text{C}_{21}\text{H}_{16}\text{N}_4\text{O}_4\text{NaS}_3$: 507.0231, found 507.0226 $[\text{M}+\text{Na}]^+$.

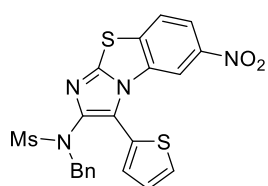
(*R*)-*N*-Benzyl-*N*-(3-(2,6-dimethylhept-5-en-1-yl)-7-nitrobenzo[*d*]imidazo[2,1-*b*]thiazol-2-yl)methanesulfonamide (349)



Following **GP5** using ynamide **294** (66.7 mg, 0.20 mmol) and aminide **343** (65.4 mg, 0.24 mmol) for 1.5 h. Purification by flash column chromatography [hexane:EtOAc (7:3)] afforded imidazole **349** as an orange oil (8.9 mg, 8%); ^1H NMR (300 MHz, CDCl_3): δ = 8.65 (d, J = 2.3 Hz, 1H), 8.30 (dd, J = 9.1, 2.3 Hz, 1H), 7.68 (d, J = 9.1 Hz, 1H), 7.39–7.34 (m, 3H), 7.27–7.25 (m, 2H), 4.92 (app. t, J = 7.1 Hz, 1H), 4.83 (d, J = 3.7 Hz, 2H), 3.05 (s, 3H), 2.81 (dd, J = 15.5, 6.0 Hz, 1H), 2.65 (dd, J = 15.5, 9.3 Hz, 1H), 1.96–1.74 (m, 3H), 1.62 (s, 3H), 1.55 (s, 3H), 1.18–1.02 (m, 2H), 0.43 (d, J = 6.6 Hz, 3H); ^{13}C NMR (101 MHz, CDCl_3): δ = 144.8 (C), 144.4 (C), 140.1 (C), 137.3 (C), 135.7 (C), 131.9 (C), 131.0 (C), 130.1 (2 \times CH), 128.6 (2 \times CH), 128.34 (CH), 128.3 (C), 124.3 (CH), 122.1 (CH), 120.4 (CH), 113.6 (CH), 54.9 (CH_2), 37.6 (CH_3), 36.8 (CH_2), 31.9 (CH), 30.8 (CH_2), 25.9 (CH_3), 25.5 (CH_2), 18.7 (CH_3), 17.9 (CH_3); IR (neat): ν = 3326, 2974, 2247, 2203, 2155, 1992, 1976, 1645, 1380, 1087, 1046, 880; HRMS (ES): m/z calculated for $\text{C}_{26}\text{H}_{30}\text{N}_4\text{O}_4\text{NaS}_2$: 549.1606, found 549.1601 $[\text{M}+\text{Na}]^+$.

N-Methyl-N-(6-nitro-3-phenylbenzo[d]imidazo[2,1-b]thiazol-2-yl)methanesulfonamide**(350)**

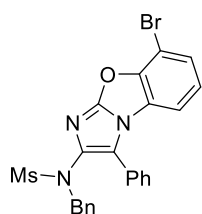
Following **GP5** using ynamide **679** (41.9 mg, 0.24 mmol) and aminide **344** (65.4 mg, 0.24 mmol) for 3.5 h. Purification by flash column chromatography [hexane:EtOAc (3:7)] afforded imidazole **350** as pale yellow powder (67.6 mg, 84%); mp: 266–268 °C; ¹H NMR (300 MHz, CDCl₃): δ = 8.22 (dd, *J* = 8.8, 2.1 Hz, 1H), 8.08 (d, *J* = 2.1 Hz, 1H), 7.87 (d, *J* = 8.8 Hz, 1H), 7.73–7.65 (m, 2H), 7.64–7.56 (m, 3H), 3.22 (s, 3H), 3.17 (s, 3H); ¹³C NMR (101 MHz, CDCl₃): δ = 146.1 (C), 144.8 (C), 141.4 (C), 137.2 (C), 133.2 (C), 130.4 (CH), 130.2 (2×CH), 129.5 (2×CH), 127.0 (C), 126.3 (C), 124.5 (CH), 119.9 (CH), 109.3 (CH), 39.1 (CH₃), 37.2 (CH₃); IR (neat): ν = 3094, 3035, 2935, 2852, 1613, 1580, 1579, 1531, 1488, 1468, 1445, 1334, 1242, 1187, 1147, 1086, 972, 957, 887, 787, 769, 737, 704, 667; HRMS (ES): *m/z* calculated for C₁₇H₁₄N₄O₄Na: 425.0354, found 425.0351 [M+Na]⁺.

N-Benzyl-N-(6-nitro-3-(thiophen-2-yl)benzo[d]imidazo[2,1-b]thiazol-2-yl)methanesulfonamide (351)

Following **GP5** using ynamide **292** (58.3 mg, 0.20 mmol) and aminide **344** (65.4 mg, 0.24 mmol) for 2.5 h. Purification by flash column chromatography [hexane:EtOAc (1:1)] afforded imidazole **351** as a yellow powder (69.9 mg, 72%); mp: 220–222 °C; ¹H NMR (300 MHz, CDCl₃): δ = 8.19 (dd, *J* = 8.8, 2.1 Hz, 1H), 7.99 (d, *J* = 2.1 Hz, 1H), 7.85 (d, *J* = 8.8 Hz, 1H), 7.56 (dd, *J* = 5.2, 1.2 Hz, 1H), 7.20–7.04 (m, 6H), 7.03 (dd, *J* = 3.6, 1.2 Hz, 1H), 4.76 (s, 2H), 3.19 (s, 3H); ¹³C NMR (101 MHz, CDCl₃): δ = 146.1 (C), 145.5 (C), 141.0 (C), 137.0 (C), 135.2 (C), 133.0

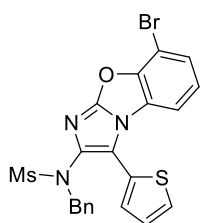
(C), 131.9 (CH), 129.8 (CH), 129.1 (2×CH), 128.5 (2×CH), 128.0 (CH), 127.8 (CH), 125.1 (C), 124.4 (CH), 121.5 (C), 120.0 (CH), 109.4 (CH), 55.0 (CH₂), 38.4 (CH₃); IR (neat): ν = 3106, 2921, 1732, 1581, 1526, 1487, 1453, 1381, 1331, 1247, 1227, 1209, 1157, 1026, 960, 882, 847, 830, 786, 761; HRMS (ES): m/z calculated for C₂₁H₁₆N₄O₄NaS₃: 507.0231, found 507.0232 [M+Na]⁺.

N-Benzyl-N-(8-bromo-3-phenylbenzo[d]imidazo[2,1-b]oxazol-2-yl)methanesulfonamide (352)



Following **GP5** using ynamide **297** (57.1 mg, 0.20 mmol) and aminide **345** (69.6 mg, 0.24 mmol) for 1 h. Purification by flash column chromatography [hexane:Et₂O (7:3)] afforded imidazole **352** as a white solid (92.9 mg, 94%); mp: 174–176 °C; ¹H NMR (400 MHz, CDCl₃): δ = 7.45 (dd, J = 8.1, 1.1 Hz, 1H), 7.38–7.33 (m, 5H), 7.20 (dd, J = 8.1, 1.1 Hz, 1H), 7.09 (t, J = 8.1 Hz, 1H), 7.06–7.03 (m, 1H), 6.99–6.96 (m, 4H), 4.68 (s, 2H), 3.27 (s, 3H); ¹³C NMR (101 MHz, CDCl₃): δ = 151.3 (C), 148.1 (C), 134.7 (C), 133.7 (C), 129.3 (2×CH), 128.8 (CH), 128.7 (2×CH), 128.6 (2×CH), 128.2 (CH), 128.1 (2×CH), 127.8 (CH), 127.5 (C), 126.7 (C), 125.1 (CH), 124.0 (C), 111.2 (CH), 104.8 (C), 55.4 (CH₂), 38.4 (CH₃); IR (neat): ν = 3032, 1727, 1625, 1576, 1459, 1337, 1152, 764, 701; HRMS (ES): m/z calculated for C₂₃H₁₉N₃O₃S⁷⁹Br: 496.0331, found 496.0335 [M+H]⁺.

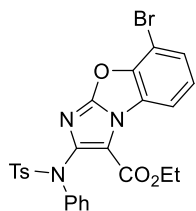
N-Benzyl-N-(8-bromo-3-(thiophen-2-yl)benzo[d]imidazo[2,1-b]oxazol-2-yl)methanesulfonamide (353)



Following **GP5** using ynamide **292** (58.3 mg, 0.20 mmol) and aminide **345** (69.6 mg, 0.24 mmol) for 1 h. Purification by flash column chromatography

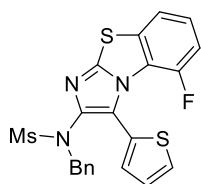
[hexane:Et₂O (4:1)] afforded imidazole **353** as a white powder (90.6 mg, 90%); mp: 214–216 °C; ¹H NMR (300 MHz, CDCl₃): δ = 7.47 (dd, *J* = 3.2, 1.0 Hz, 1H), 7.45 (dd, *J* = 3.2, 1.0 Hz, 1H), 7.40 (dd, *J* = 5.1, 1.1 Hz, 1H), 7.24 (dd, *J* = 3.6, 1.1 Hz, 1H), 7.18–7.02 (m, 7H), 4.74 (s, 2H), 3.22 (s, 3H); ¹³C NMR (101 MHz, CDCl₃): δ = 151.4 (C), 148.0 (C), 134.9 (C), 134.8 (C), 129.4 (CH), 129.1 (2×CH), 128.3 (CH), 128.2 (2×CH), 127.9 (CH), 127.49 (CH), 127.46 (CH), 126.7 (C), 125.3 (CH), 117.9 (C), 111.4 (CH), 104.9 (C), 55.2 (CH₂), 38.2 (CH₃) *one resonance for a quaternary carbon was not observed*; IR (neat): ν = 2931, 1624, 1578, 1336, 1151, 968, 772, 715, 634; HRMS (ES): *m/z* calculated for C₂₁H₁₆N₃O₃NaS₂⁷⁹Br: 523.9714, found 523.9711 [M+Na]⁺.

Ethyl 8-bromo-2-((4-methyl-N-phenylphenyl)sulfonamido)benzo[d]imidazo[2,1-b]oxazole-3-carboxylate (354)



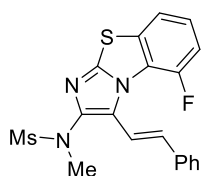
Following **GP5** using ynamide **357** (68.7 mg, 0.20 mmol) and aminide **345** (68.6 mg, 0.24 mmol) for 4 h. Purification by flash column chromatography [hexane:EtOAc (4:1)] afforded imidazole **354** as a pale yellow solid (54.4 mg, 49%); mp: 239–242 °C; ¹H NMR (300 MHz, CDCl₃): δ = 8.37 (dd, *J* = 8.2, 1.1 Hz, 1H), 7.70 (d, *J* = 8.3 Hz, 2H), 7.55 (dd, *J* = 8.2, 1.1 Hz, 1H), 7.52–7.45 (m, 2H), 7.34–7.21 (m, 6H), 4.53 (q, *J* = 7.2 Hz, 2H), 2.44 (s, 3H), 1.56 (t, *J* = 7.2 Hz, 3H); ¹³C NMR (101 MHz, CDCl₃): δ = 159.3 (C), 152.2 (C), 148.1 (C), 143.9 (C), 143.8 (C), 139.8 (C), 138.2 (C), 129.4 (2×CH), 129.0 (2×CH), 128.9 (CH), 128.7 (2×CH), 128.6 (2×CH), 128.0 (CH), 127.9 (C), 126.0 (CH), 115.4 (C), 115.1 (CH), 104.3 (C), 61.8 (CH₂), 21.8 (CH₃), 14.6 (CH₃); IR (neat): ν = 2922, 1698, 1572, 1359, 1168, 1059, 773, 666, 570; HRMS (ES): *m/z* calculated for C₂₅H₂₁N₃O₅SBr: 554.0385, found 554.0389 [M+H]⁺.

***N*-Benzyl-*N*-(5-fluoro-3-(thiophen-2-yl)benzo[d]imidazo[2,1-*b*]thiazol-2-yl)methanesulfonamide (355)**



Following **GP5** using ynamide **292** (58.3 mg, 0.20 mmol) and aminide **346** (58.9 mg, 0.24 mmol) for 1 h. Purification by flash column chromatography [hexane:EtOAc (3:2)] afforded imidazole **355** as a pale beige powder (85.3 mg, 93%); mp: 243–245 °C; ¹H NMR (400 MHz, CDCl₃): δ = 7.47 (dd, *J* = 8.1, 0.9 Hz, 1H), 7.44 (dd, *J* = 5.2, 1.1 Hz, 1H), 7.29–7.15 (m, 4H), 7.14–7.09 (m, 2H), 7.02 (dd, *J* = 5.2, 3.5 Hz, 1H), 6.97 (ddd, *J* = 11.1, 8.1, 0.9 Hz, 1H), 6.85 (dd, *J* = 3.5, 1.1 Hz, 1H), 4.73 (s, 2H), 3.14 (s, 3H); ¹³C NMR (101 MHz, CDCl₃): δ = 149.8 (d, *J* = 256.2 Hz, C), 145.2 (C), 141.1 (C), 135.5 (C), 132.17 (C), 132.14 (CH), 129.2 (2×CH), 128.5 (CH), 128.5 (2×CH), 127.9 (CH), 127.4 (d, *J* = 5.6 Hz, C), 126.4 (CH), 126.1 (d, *J* = 6.8 Hz, CH), 121.6 (C), 119.6 (d, *J* = 3.9 Hz, CH), 114.0 (d, *J* = 19.6 Hz, CH), 55.3 (CH₂), 38.5 (CH₃) *one resonance for a quaternary carbon was not visible*; IR (neat): ν = 3009, 2929, 1581, 1496, 1347, 1155, 766, 698, 586; HRMS (ES): *m/z* calculated for C₂₁H₁₇N₃O₂FS₃: 458.0467, found 458.0471 [M+H]⁺.

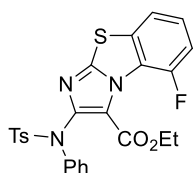
***(E)*-*N*-(5-Fluoro-3-styrylbenzo[d]imidazo[2,1-*b*]thiazol-2-yl)-*N*-methylmethanesulfonamide (356)**



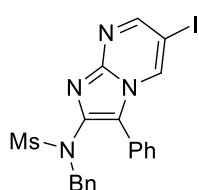
Following **GP5** using ynamide **683** (20.9 mg, 0.09 mmol) and aminide **346** (21.8 mg, 0.09 mmol) for 40 min. Purification by flash column chromatography [hexane:EtOAc (7:3-3:2)] afforded imidazole **356** as a beige solid (31.8 mg, 88%); mp: 237–239 °C; ¹H NMR (300 MHz, CDCl₃): δ = 7.60–7.57 (m, 2H), 7.53 (dd, *J* = 8.0, 1.1 Hz, 1H), 7.50 (d, *J* = 3.3, 2H), 7.42–7.33 (m, 3H), 7.33–7.20 (m, 2H) 3.31 (s, 3H), 3.22 (s, 3H); ¹³C NMR (101 MHz, CDCl₃): δ = 149.6 (d, *J* = 250.7 Hz, C),

144.3 (C), 140.5 (C), 137.4 (C), 133.3 (CH), 132.5 (C), 128.8 (2×CH), 128.2 (CH), 127.0 (2×CH), 126.3 (d, $J = 7.4$ Hz, CH), 125.6 (C), 121.9 (C), 120.1 (d, $J = 2.5$ Hz, CH), 114.1 (d, $J = 21.3$ Hz, CH), 113.7 (d, $J = 19.7$ Hz, CH), 38.6 (CH₃), 37.2 (CH₃); IR (neat): $\nu = 3091$, 3027, 2934, 2852, 1584, 1553, 1531, 1493, 1448, 1337, 1247, 1188, 1146, 1077, 971, 959, 917, 894, 766, 752, 707, 693; HRMS (ES): m/z calculated for C₁₉H₁₆N₃O₂NaFS₂: 424.0566, found 424.0568 [M+Na]⁺.

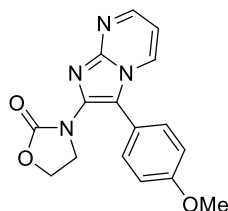
Ethyl 5-fluoro-2-((4-methyl-N-phenylphenyl)sulfonamido)benzo[d]imidazo[2,1-b]thiazole-3-carboxylate (357)



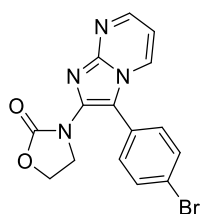
Following **GP5** using ynamide **357** (68.7 mg, 0.20 mmol) and aminide **346** (58.9 mg, 0.24 mmol) for 1 h. Purification by flash column chromatography [hexane:EtOAc (7:3)] afforded imidazole **357** as a white solid (68.1 mg, 67%); mp: 188–190 °C; ¹H NMR (300 MHz, CDCl₃): $\delta = 7.68$ (d, $J = 8.3$ Hz, 2H), 7.52–7.44 (m, 3H), 7.35 (app. td, $J = 8.2, 4.5$ Hz, 1H), 7.29–7.25 (m, 5H), 7.20 (ddd, $J = 11.1, 8.3, 1.1$ Hz, 1H), 4.51 (q, $J = 7.2$ Hz, 2H), 2.4 (s, 3H), 1.5 (t, $J = 7.2$ Hz, 3H); ¹³C NMR (101 MHz, CDCl₃): $\delta = 159.3$ (C), 150.4 (d, $J = 254.7$ Hz, C), 147.3 (C), 145.4 (C), 143.9 (C), 140.0 (C), 136.4 (C), 132.2 (C), 129.5 (2×CH), 129.1 (2×CH), 128.8 (2×CH), 128.7 (2×CH), 128.1 (CH), 126.6 (d, $J = 7.0$ Hz, CH), 122.0 (d, $J = 14.7$ Hz, C), 120.3 (C), 119.6 (d, $J = 3.2$ Hz, CH), 114.2 (d, $J = 19.7$ Hz, CH), 62.3 (CH₂), 21.8 (CH₃), 14.3 (CH₃); IR (neat): $\nu = 2989$, 2924, 1724, 1490, 1358, 1304, 1163, 1087, 778, 658, 563; HRMS (ES): m/z calculated for C₂₅H₂₀N₃O₄FS₂Na: 532.0777, found 532.0773 [M+Na]⁺.

N-Benzyl-N-(6-iodo-3-phenylimidazo[1,2-a]pyrimidin-2-yl)methanesulfonamide (326)

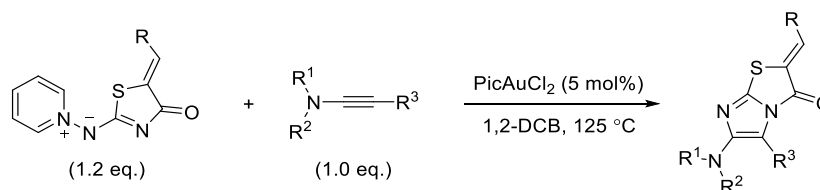
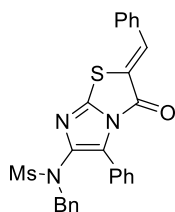
Following **GP6** using ynamide **297** (113 mg, 0.4 mmol), aminide **325** (134 mg, 0.5 mmol) for 20 h. Purification by flash column chromatography [hexane:EtOAc (3:2)] afforded imidazole **326** as a yellow solid (173 mg, 93%); mp: 178–180 °C; ¹H NMR (400 MHz, CDCl₃): δ = 8.63 (d, *J* = 2.3 Hz, 1H), 8.44 (d, *J* = 2.3 Hz, 1H), 7.46–7.36 (m, 3H), 7.20–7.13 (m, 2H), 7.10 (tt, *J* = 7.0 Hz, 1.8 Hz, 1H), 7.02–6.93 (m, 4H), 4.77 (s, 2H), 3.31 (s, 3H); ¹³C NMR (101 MHz, CDCl₃): δ = 155.2 (CH), 143.5 (C), 140.4 (C), 135.7 (CH), 134.8 (C), 129.6 (2×CH), 129.5 (CH), 129.2 (4×CH), 128.2 (2×CH), 127.9 (CH), 125.4 (C), 122.0 (C), 74.7 (C), 55.4 (CH₂), 38.5 (CH₃); IR (neat): ν = 2925, 1687, 1474, 1350, 1325, 1157, 960, 816, 757, 691, 663, 565; HRMS (ES): *m/z* calculated for C₂₀H₁₈N₄O₂S¹²⁷I: 505.0195, found 505.0194 [M+H]⁺.

3-(3-(4-Methoxyphenyl)imidazo[1,2-a]pyrimidin-2-yl)oxazolidin-2-one (381)

Following **GP6** using ynamide **295** (43.4 mg, 0.20 mmol) and aminide **214** (41.3 mg, 0.24 mmol) and DTBPAu(NCMe)SbF₆ for 23 h. Purification by flash column chromatography [EtOAc:MeOH (9:1)] afforded imidazole **381** as a yellow powder (48.5 mg, 78%); mp: 176–178 °C; ¹H NMR (400 MHz, CDCl₃): δ = 8.55 (dd, *J* = 4.1, 2.0 Hz, 1H), 8.36 (dd, *J* = 6.9, 2.0 Hz, 1H), 7.46 (d, *J* = 8.8 Hz, 2H), 7.04 (d, *J* = 8.8 Hz, 2H), 6.87 (dd, *J* = 6.9, 4.1 Hz, 1H), 4.50 (dd, *J* = 8.8, 7.1 Hz, 2H), 4.22 (d, *J* = 8.8, 7.1 Hz, 2H), 3.86 (s, 3H); ¹³C NMR (101 MHz, CDCl₃): δ = 160.3 (C), 156.2 (C), 150.0 (CH), 145.6 (C), 138.9 (C), 131.03 (CH), 130.97 (2×CH), 119.3 (C), 116.1 (C), 115.0 (2×CH), 109.3 (CH), 62.9 (CH₂), 55.5 (CH₃), 46.6 (CH₂); IR (neat): ν = 2916, 1749, 1508, 1420, 1251, 1155, 1021, 793, 758, 583; HRMS (ES): *m/z* calculated for C₁₆H₁₅N₄O₃: 311.1144, found 311.1147 [M+H]⁺.

3-(3-(4-Bromophenyl)imidazo[1,2-a]pyrimidin-2-yl)oxazolidin-2-one (382)

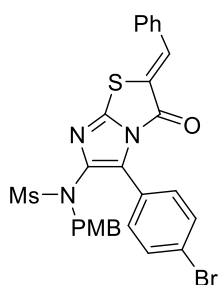
Following **GP6** using ynamide **296** (53.2 mg, 0.20 mmol) and aminide **214** (41.3 mg, 0.24 mmol) and DTBPAu(NCMe)SbF₆ for 20 h. Purification by flash column chromatography [EtOAc (100%)] afforded imidazole **382** as a pale yellow solid (54.5 mg, 76%); mp: 201–204 °C; ¹H NMR (400 MHz, CDCl₃): δ = 8.59 (dd, *J* = 4.1, 2.0 Hz, 1H), 8.38 (dd, *J* = 6.9, 2.0 Hz, 1H), 7.66 (d, *J* = 8.6 Hz, 2H), 7.41 (d, *J* = 8.6 Hz, 2H), 6.92 (dd, *J* = 6.9, 4.1 Hz, 1H), 4.53 (dd, *J* = 8.7, 7.1 Hz, 2H), 4.28 (dd, *J* = 8.7, 7.1 Hz, 2H); ¹³C NMR (101 MHz, CDCl₃): δ = 155.8 (C), 150.3 (CH), 145.8 (C), 139.6 (C), 132.8 (2×CH), 131.0 (2×CH), 130.8 (CH), 126.6 (C), 123.6 (C), 114.4 (C), 109.6 (CH), 63.1 (CH₂), 46.4 (CH₂); IR (neat): ν = 3101, 2921, 2852, 1753, 1421, 1194, 1065, 957, 828, 765; HRMS (ES): *m/z* calculated for C₁₅H₁₂N₄O₂⁷⁹Br: 359.0144, found 359.0146 [M+H]⁺.

2.7. Cycloaddition products for chapter 3**(Z)-N-Benzyl-N-(2-benzylidene-3-oxo-5-phenyl-2,3-dihydroimidazo[2,1-b]thiazol-6-yl)methanesulfonamide (436)**

Following **GP5** using ynamide **297** (28.4 mg, 0.10 mmol) and aminide **427** (33.7 mg, 0.12 mmol) for 5 h. Purification by flash column chromatography [hexane:EtOAc (4:1)] afforded imidazole **436** as a yellow powder (36.3 mg, 74%); mp: 203–206 °C; ¹H NMR (300 MHz, CDCl₃): δ = 7.98 (s, 1H), 7.61–7.48 (m, 5H), 7.38–7.27 (m, 5H), 7.14 (tt, *J* = 7.2, 1.5 Hz, 1H), 7.09–6.95 (m, 4H), 4.62 (s, 2H), 3.20 (s,

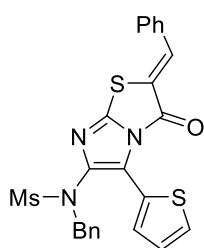
3H); ^{13}C NMR (101 MHz, CDCl_3): δ = 159.9 (C), 145.6 (C), 140.2 (C), 138.3 (CH), 134.5 (C), 133.0 (C), 131.4 (CH), 130.7 (2 \times CH), 130.3 (C), 129.9 (2 \times CH), 129.6 (2 \times CH), 129.2 (2 \times CH), 129.1 (CH), 128.3 (2 \times CH), 128.0 (CH), 127.9 (2 \times CH), 124.9 (C), 124.2 (C), 54.9 (CH_2), 39.1 (CH_3); IR (neat): ν = 2924, 2853, 1733, 1495, 1340, 1154, 961, 761, 686; HRMS (EI): m/z calculated for $\text{C}_{26}\text{H}_{22}\text{N}_3\text{O}_3\text{S}_2$: 488.1103, found 488.1100 $[\text{M}+\text{H}]^+$.

(Z)-N-(2-benzylidene-5-(4-bromophenyl)-3-oxo-2,3-dihydroimidazo[2,1-b]thiazol-6-yl)-N-(4-methoxybenzyl)methanesulfonamide (441)



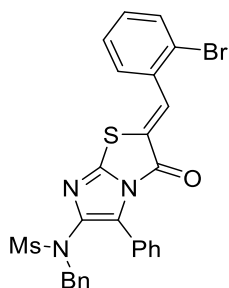
Following **GP5** using ynamide **293** (78.6 mg, 0.20 mmol) and aminide **427** (67.5 mg, 0.24 mmol) for 20 h. Purification by flash column chromatography [hexane:EtOAc (4:1)] afforded imidazole **441** as a yellow solid (42.3 mg, 35%); mp: 162–164 °C; ^1H NMR (400 MHz, CDCl_3): δ = 8.00 (s, 1H), 7.63–7.46 (m, 5H), 7.39 (d, J = 8.6 Hz, 2H), 7.14 (d, J = 8.6 Hz, 2H), 6.85 (d, J = 8.5 Hz, 2H), 6.54 (d, J = 8.5 Hz, 2H), 4.54 (s, 2H), 3.75 (s, 3H), 3.23 (s, 3H); ^{13}C NMR (101 MHz, CDCl_3): δ = 159.9 (C), 159.5 (C), 146.0 (C), 140.2 (C), 138.7 (CH), 132.9 (C), 131.5 (CH), 131.3 (2 \times CH), 131.0 (2 \times CH), 130.8 (2 \times CH), 130.6 (2 \times CH), 129.6 (2 \times CH), 129.5 (C), 126.2 (C), 123.9 (C), 123.4 (C), 113.6 (CH), 55.3 (CH_3), 54.5 (CH_2), 39.0 (CH_3) one resonance for a quaternary carbon was not observed; IR (neat): ν = 1732, 1595, 1508, 1348, 1249, 1152, 1064, 818, 761, 663; HRMS (ES): m/z calculated for $\text{C}_{28}\text{H}_{27}\text{N}_3\text{O}_5\text{S}_2^{79}\text{Br}$: 628.0576, found 628.0577 $[\text{M}+\text{CH}_3\text{OH}+\text{H}]^+$.

(Z)-N-benzyl-N-(2-benzylidene-3-oxo-5-(thiophen-2-yl)-2,3-dihydroimidazo[2,1-b]thiazol-6-yl)methanesulfonamide (442)



Following **GP5** using ynamide **292** (58.3 mg, 0.20 mmol) and aminide **427** (67.5 mg, 0.24 mmol) for 22 h. Purification by flash column chromatography [hexane:EtOAc (4:1)] afforded imidazole **442** as a red oil (74.5 mg, 75%); ^1H NMR (400 MHz, CDCl_3): δ = 8.03 (s, 1H), 7.61–7.48 (m, 5H), 7.44 (dd, J = 3.6, 1.1 Hz, 1H), 7.39 (dd, J = 5.1, 1.1 Hz, 1H), 7.21–7.11 (m, 5H), 7.02 (dd, J = 5.1, 3.6 Hz, 1H), 4.71 (s, 2H), 3.14 (s, 3H); ^{13}C NMR (101 MHz, CDCl_3): δ = 159.9 (C), 145.8 (C), 140.4 (C), 138.6 (CH), 134.5 (C), 132.9 (C), 131.5 (CH), 130.8 (2 \times CH), 130.6 (CH), 129.6 (2 \times CH), 129.2 (2 \times CH), 128.4 (2 \times CH), 128.2 (2 \times CH), 126.8 (CH), 125.1 (C), 124.9 (C), 123.8 (C), 54.9 (CH_2), 39.1 (CH_3); IR ν = 2925, 2854, 1736, 1606, 1507, 1344, 1155, 1060, 963, 760, 699; HRMS (ES): m/z calculated for $\text{C}_{24}\text{H}_{20}\text{N}_3\text{O}_3\text{S}_3$: 494.0667, found 494.0665 $[\text{M}+\text{H}]^+$.

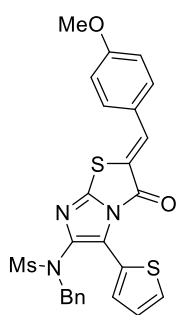
(Z)-N-Benzyl-N-(2-(2-bromobenzylidene)-3-oxo-5-phenyl-2,3-dihydroimidazo[2,1-b]thiazol-6-yl)methanesulfonamide (443)



Following **GP5** using ynamide **297** (57.1 mg, 0.20 mmol) and aminide **428** (86.5 mg, 0.24 mmol) for 22 h. Purification by flash column chromatography [hexane:EtOAc (4:1)] afforded imidazole **443** as an orange powder (43.6 mg, 38%); mp: 111–113 °C (decomp.); ^1H NMR (400 MHz, CDCl_3): δ = 8.29 (s, 1H), 7.71 (dd, J = 7.9, 0.9 Hz, 1H), 7.60 (dd, J = 7.9, 1.3 Hz, 1H), 7.47 (app. t, J = 7.9 Hz, 1H), 7.39–7.27 (m, 6H), 7.14 (t, J = 7.5 Hz, 1H), 7.09–7.02 (m, 2H), 7.01–6.95 (m, 2H), 4.62 (s, 2H), 3.19 (s, 3H); ^{13}C NMR (101 MHz, CDCl_3): δ = 159.2 (C), 145.4 (C), 140.2 (C), 137.0 (CH), 134.4 (C), 134.1 (CH), 133.23 (C),

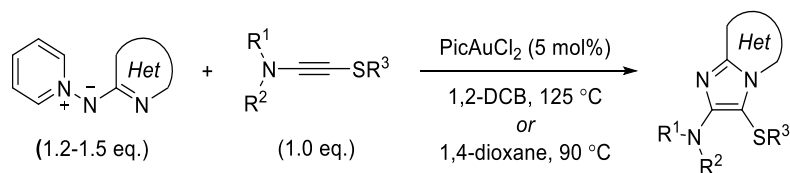
132.16 (CH), 130.4 (C), 129.8 (2×CH), 129.5 (CH), 129.2 (CH), 129.1 (2×CH), 128.3 (2×CH), 128.2 (CH), 128.0 (CH), 127.9 (2×CH), 127.3 (C), 126.7 (C), 124.8 (C), 54.9 (CH₂), 39.1 (CH₃); IR (neat): ν = 2928, 1719, 1587, 1565, 1512, 1342, 1257, 1153, 1102, 1069, 960, 830, 694; HRMS (ES): m/z calculated for C₂₆H₂₁N₃O₃S₂⁷⁹Br: 566.0208, found 566.0214 [M+H]⁺.

(Z)-N-Benzyl-N-(2-(4-methoxybenzylidene)-3-oxo-5-(thiophen-2-yl)-2,3-dihydroimidazo[2,1-b]thiazol-6-yl)methanesulfonamide (445)

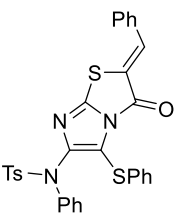


Following **GP5** using ynamide **292** (58.3 mg, 0.20 mmol) and aminide **429** (74.7 mg, 0.24 mmol) for 22 h. Purification by flash column chromatography [hexane:EtOAc (7:3)] afforded imidazole **445** as a pale yellow solid (54.0 mg, 52%); mp: 202–204 °C; ¹H NMR (400 MHz, CDCl₃): δ = 7.99 (s, 1H), 7.54 (d, J = 8.8 Hz, 2H), 7.45 (dd, J = 3.7, 1.2 Hz, 1H), 7.38 (dd, J = 5.1, 1.2 Hz, 1H), 7.22–7.10 (m, 5H), 7.04 (d, J = 8.8 Hz, 2H), 7.01 (dd, J = 5.1, 3.7 Hz, 1H), 4.71 (s, 2H), 3.89 (s, 3H), 3.14 (s, 3H); ¹³C NMR (101 MHz, CDCl₃): δ = 162.3 (C), 160.2 (C), 145.8 (C), 140.3 (C), 135.5 (CH), 134.6 (C), 133.0 (2×CH), 130.5 (CH), 129.3 (2×CH), 128.4 (2×CH), 128.13 (CH), 128.05 (CH), 126.8 (CH), 125.6 (C), 125.5 (C), 124.7 (C), 120.6 (C), 115.2 (2×CH), 55.7 (CH₃), 55.0 (CH₂), 39.1 (CH₃); IR (neat): ν = 2928, 1719, 1587, 1512, 1342, 1257, 1153, 1069, 1027, 830, 694; HRMS (ES): m/z calculated for C₂₅H₂₂N₃O₄S₃: 524.0772, found 524.0773 [M+H]⁺.

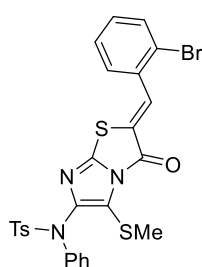
2.8. Cycloaddition products for chapter 4



(Z)-N-(2-Benzylidene-3-oxo-5-(phenylthio)-2,3-dihydroimidazo[2,1-b]thiazol-6-yl)-4-methyl-N-phenylbenzenesulfonamide (577)


 Following **GP5** using thioynamide **566** (75.9 mg, 0.20 mmol) and aminide **427** (67.5 mg, 0.24 mmol) for 1.5 h. Purification by flash column chromatography [hexane:EtOAc (4:1)] afforded imidazole **577** as a bright yellow foamy solid (116 mg, >99%); mp: 179–181 °C; ¹H NMR (400 MHz, CDCl₃): δ = 7.95 (s, 1H), 7.72 (d, *J* = 8.4 Hz, 2H), 7.57–7.45 (m, 5H), 7.44–7.37 (m, 2H), 7.33–7.12 (m, 10H), 2.43 (s, 3H); ¹³C NMR (101 MHz, CDCl₃): δ = 159.2 (C), 150.2 (C), 148.9 (C), 144.0 (C), 139.8 (C), 138.7 (CH), 136.0 (C), 134.4 (C), 132.8 (C), 131.5 (CH), 130.7 (2×CH), 129.8 (2×CH), 129.6 (2×CH), 129.4 (2×CH), 129.24 (2×CH), 129.20 (2×CH), 129.0 (2×CH), 128.9 (2×CH), 128.3 (CH), 127.3 (CH), 123.8 (C), 119.5 (C), 21.8 (CH₃); IR (neat): ν = 3060, 1737, 1483, 1350, 1305, 1164, 1060, 958, 748, 674, 570; HRMS (ES): *m/z* calculated for C₃₁H₂₄N₃O₃S₃: 582.0980, found 582.0983 [M+H]⁺.

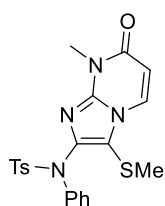
(Z)-N-(2-(2-Bromobenzylidene)-5-(methylthio)-3-oxo-2,3-dihydroimidazo[2,1-b]thiazol-6-yl)-4-methyl-N-phenylbenzenesulfonamide (578)



Following **GP5** using thioynamide **565** (47.6 mg, 0.15 mmol) and aminide **428** (64.8 mg, 0.18 mmol) for 3.5 h. Purification by flash column

chromatography [hexane:EtOAc (9:1)] afforded imidazole **578** as a bright orange solid (84.1 mg, >99%); mp: 206–208 °C; ^1H NMR (300 MHz, CDCl_3): δ = 8.37 (s, 1H), 7.75–7.66 (m, 3H), 7.59 (dd, J = 7.8, 1.6 Hz, 1H), 7.47 (app. td, J = 7.4, 0.8 Hz, 1H), 7.43–7.38 (m, 2H), 7.34 (dd, J = 7.8, 1.6 Hz, 1H), 7.31–7.22 (m, 5H), 2.45 (s, 3H); ^{13}C NMR (101 MHz, CDCl_3): δ = 159.3 (C), 148.2 (C), 147.7 (C), 144.0 (C), 139.7 (C), 137.2 (CH), 136.3 (C), 134.1 (CH), 133.2 (C), 132.2 (CH), 129.5 (CH), 129.4 (2×CH), 129.2 (2×CH), 128.8 (2×CH), 128.7 (2×CH), 128.2 (2×CH), 127.3 (C), 126.7 (C), 122.9 (C), 21.76 (CH_3), 19.3 (CH_3); IR (neat): ν = 2925, 1738, 1486, 1345, 1296, 1164, 1060, 758, 672, 570; HRMS (ES): m/z calculated for $\text{C}_{26}\text{H}_{21}\text{N}_3\text{O}_3\text{S}_3^{79}\text{Br}$: 597.9928, found 597.9924 $[\text{M}+\text{H}]^+$.

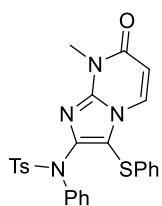
4-Methyl-N-(8-methyl-3-(methylthio)-7-oxo-7,8-dihydroimidazo[1,2-a]pyrimidin-2-yl)-N-phenylbenzenesulfonamide (579)



Following **GP6** using thioynamide **565** (63.5 mg, 0.20 mmol) and aminide **471** (60.7 mg, 0.30 mmol) for 2 h. Purification by flash column chromatography [hexane:EtOAc (1:1)] afforded imidazole **579** as a beige solid (81.0 mg, 92%); mp: 237–239 °C; ^1H NMR (300 MHz, CDCl_3): δ = 7.99 (d, J = 7.8 Hz, 1H), 7.74 (d, J = 8.3 Hz, 2H), 7.48–7.38 (m, 2H), 7.31–7.20 (m, 5H), 6.27 (d, J = 7.8 Hz, 1H), 3.61 (s, 3H), 2.44 (s, 3H), 2.20 (s, 3H); ^{13}C NMR (101 MHz, CDCl_3): δ = 159.9 (C), 144.7 (C), 143.9 (C), 143.1 (C), 140.2 (C), 136.2 (C), 131.9 (CH), 129.11 (2×CH), 129.06 (2×CH), 129.04 (2×CH), 128.7 (2×CH), 128.0 (CH), 114.4 (C), 108.2 (CH), 29.1 (CH_3), 21.8 (CH_3), 19.3 (CH_3); IR (neat): ν = 2928, 1679, 1533, 1482, 1356, 1164, 1087, 924, 815, 690, 667; HRMS (ES): m/z calculated for $\text{C}_{21}\text{H}_{21}\text{N}_4\text{O}_3\text{S}_2$: 441.1055, found 441.1053 $[\text{M}+\text{H}]^+$.

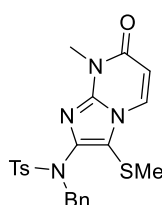
This reaction was scaled up following **GP6** using thioynamide **565** (1.11 g, 3.50 mmol), aminide **471** (1.06 g, 5.25 mmol) for 3 h. Purification by flash column chromatography [hexane:EtOAc (3:2)] afforded imidazole **579** as a beige solid (1.39 g, 90%).

4-Methyl-N-(8-methyl-7-oxo-3-(phenylthio)-7,8-dihydroimidazo[1,2-a]pyrimidin-2-yl)-N-phenylbenzenesulfonamide (581)



Following **GP6** using thioynamide **566** (75.9 mg, 0.20 mmol) and aminide **471** (60.7 mg, 0.30 mmol) for 24 h. Purification by flash column chromatography [hexane:EtOAc (3:2)] afforded imidazole **581** as a yellow solid (74.6 mg, 74%); mp: 226–228 °C; ¹H NMR (300 MHz, CDCl₃): δ = 7.78–7.69 (m, 3H), 7.41–7.33 (m, 2H), 7.28–7.11 (m, 8H), 7.05–6.97 (m, 2H), 6.16 (d, *J* = 7.8 Hz, 1H), 3.64 (s, 3H), 2.44 (s, 3H); ¹³C NMR (101 MHz, CDCl₃): δ = 159.8 (C), 146.6 (C), 143.9 (C), 143.8 (C), 140.1 (C), 136.2 (C), 133.9 (C), 131.9 (CH), 129.5 (2×CH), 129.13 (4×CH), 129.10 (2×CH), 129.06 (2×CH), 128.1 (CH), 127.5 (2×CH), 127.0 (CH), 110.2 (C), 108.4 (CH), 29.3 (CH₃), 21.8 (CH₃); IR (neat): ν = 3059, 1669, 1479, 1355, 1163, 1089, 813, 745, 696, 674; HRMS (ES): *m/z* calculated for C₂₆H₂₃N₄O₃S₂: 503.1212, found 503.1210 [M+H]⁺.

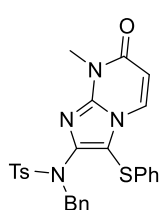
N-Benzyl-4-methyl-N-(8-methyl-3-(methylthio)-7-oxo-7,8-dihydroimidazo[1,2-a]pyrimidin-2-yl)benzenesulfonamide (582)



Following **GP6** using thioynamide **567** (66.3 mg, 0.20 mmol) and aminide **471** (60.7 mg, 0.30 mmol) for 24 h. Purification by flash column chromatography [hexane:EtOAc (7:3)] afforded imidazole **582** as a beige orange solid (38.3 mg, 42%); mp: 82–84 °C; ¹H NMR (400 MHz, CDCl₃): δ = 7.90 (d, *J* = 7.7 Hz, 1H), 7.83 (d, *J* = 8.4 Hz, 2H), 7.38–7.28 (m, 4H), 7.27–7.14 (m, 3H), 6.22 (d, *J* = 7.7 Hz, 1H), 4.61 (s, 2H),

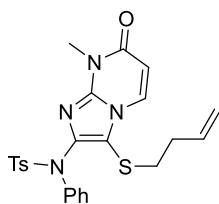
3.53 (s, 3H), 2.47 (s, 3H), 1.97 (s, 3H); ^{13}C NMR (101 MHz, CDCl_3): δ = 159.9 (C), 144.0 (C), 143.1 (C), 142.2 (C), 136.0 (C), 135.7 (C), 131.9 (CH), 129.6 (2 \times CH), 128.8 (2 \times CH), 128.6 (2 \times CH), 128.4 (2 \times CH), 127.9 (CH), 116.1 (C), 108.0 (CH), 53.4 (CH_2), 29.0 (CH_3), 21.8 (CH_3), 19.1 (CH_3); IR (neat): ν = 2923, 1672, 1538, 1483, 1347, 1161, 1090, 812, 734, 664; HRMS (ES): m/z calculated for $\text{C}_{22}\text{H}_{23}\text{N}_4\text{O}_3\text{S}_2$: 455.1212, found 455.1211 $[\text{M}+\text{H}]^+$.

***N*-Benzyl-4-methyl-*N*-(8-methyl-7-oxo-3-(phenylthio)-7,8-dihydroimidazo[1,2-*a*]pyrimidin-2-yl)benzenesulfonamide (583)**



Following **GP6** using thioynamide **563** (78.7 mg, 0.20 mmol) and aminide **471** (48.5 mg, 0.24 mmol) for 24 h. Purification by flash column chromatography [hexane:EtOAc (7:3)] afforded imidazole **583** as a beige solid (28.3 mg, 27%); mp: 209–211 °C; ^1H NMR (300 MHz, CDCl_3): δ = 7.82 (d, J = 8.3 Hz, 2H), 7.53 (d, J = 7.7 Hz, 1H), 7.37–7.25 (m, 4H), 7.17–7.02 (m, 6H), 6.65–6.58 (m, 2H), 6.06 (d, J = 7.7 Hz, 1H), 4.68 (s, 2H), 3.56 (s, 3H), 2.47 (s, 3H); ^{13}C NMR (101 MHz, CDCl_3): δ = 159.7 (C), 144.1 (C), 143.6 (C), 135.9 (C), 135.5 (C), 134.1 (C), 132.0 (CH), 129.7 (2 \times CH), 129.4 (2 \times CH), 129.0 (2 \times CH), 128.56 (2 \times CH), 128.53 (2 \times CH), 128.0 (CH), 127.0 (2 \times CH), 126.5 (CH), 111.8 (C), 108.0 (CH), 53.3 (CH_2), 29.1 (CH_3), 21.8 (CH_3) *one resonance for a quaternary carbon was not observed*; IR (neat): ν = 2924, 1666, 1541, 1479, 1350, 1162, 819, 735, 666; HRMS (ES): m/z calculated for $\text{C}_{27}\text{H}_{24}\text{N}_4\text{O}_3\text{NaS}_2$: 539.1188, found 539.1190 $[\text{M}+\text{Na}]^+$.

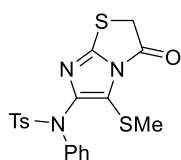
***N*-(3-(But-3-en-1-ylthio)-8-methyl-7-oxo-7,8-dihydroimidazo[1,2-*a*]pyrimidin-2-yl)-4-methyl-*N*-phenylbenzenesulfonamide (584)**



Following **GP6** using thioynamide **575** (69.8 mg, 0.20 mmol) and aminide **471** (59.1 mg, 0.29 mmol) for 5.5 h. Purification by flash column

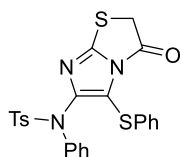
chromatography [hexane:EtOAc (7:3)] afforded imidazole **584** as a pale yellow solid (71.0 mg, 76%); mp: 154–156 °C; ^1H NMR (400 MHz, CDCl_3): δ = 8.00 (d, J = 7.8 Hz, 1H), 7.74 (d, J = 8.3 Hz, 2H), 7.45–7.39 (m, 2H), 7.29–7.22 (m, 5H), 6.25 (d, J = 7.8 Hz, 1H), 5.72 (ddt, J = 16.4, 9.8, 6.6 Hz, 1H), 5.07–4.99 (m, 2H), 3.62 (s, 3H), 2.71 (t, J = 7.2 Hz, 2H), 2.43 (s, 3H), 2.25 (q, J = 7.2 Hz, 2H); ^{13}C NMR (101 MHz, CDCl_3): δ = 159.9 (C), 145.4 (C), 143.9 (C), 143.1 (C), 140.3 (C), 136.0 (C), 135.8 (CH), 132.1 (CH), 129.13 (2 \times CH), 129.05 (2 \times CH), 129.01 (2 \times CH), 128.6 (2 \times CH), 127.9 (CH), 116.8 (CH₂), 113.1 (C), 108.0 (CH), 35.9 (CH₂), 33.9 (CH₂), 29.1 (CH₃), 21.8 (CH₃); IR (neat): ν = 2936, 1668, 1534, 1481, 1342, 1160, 1093, 813, 713, 663; HRMS (ES): m/z calculated for $\text{C}_{24}\text{H}_{25}\text{N}_4\text{O}_3\text{S}_2$: 481.1368, found 481.1372 $[\text{M}+\text{H}]^+$.

4-Methyl-N-(5-(methylthio)-3-oxo-2,3-dihydroimidazo[2,1-b]thiazol-6-yl)-N-phenylbenzenesulfonamide (590)



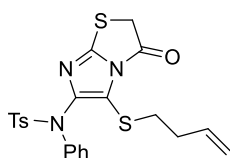
Following **GP6** using thioynamide **565** (31.7 mg, 0.10 mmol) and aminide **422** (23.2 mg, 0.12 mmol) and DTBPAu(NCMe)SbF₆ for 24 h. Purification by flash column chromatography [toluene:EtOAc (9:1)] afforded imidazole **590** as a beige powder (33.6 mg, 78%); mp: 217–219 °C; ^1H NMR (300 MHz, CDCl_3): δ = 7.70 (d, J = 8.3 Hz, 2H), 7.42–7.34 (m, 2H), 7.31–7.21 (m, 5H), 4.24 (s, 2H), 2.42 (s, 3H), 2.38 (s, 3H); ^{13}C NMR (101 MHz, CDCl_3): δ = 165.6 (C), 152.8 (C), 149.5 (C), 144.0 (C), 139.6 (C), 136.2 (C), 129.4 (2 \times CH), 129.2 (2 \times CH), 128.8 (2 \times CH), 128.7 (2 \times CH), 128.2 (CH), 121.8 (C), 38.1 (CH₂), 21.8 (CH₃), 19.5 (CH₃); IR (neat): ν = 2924, 1754, 1485, 1344, 1290, 1163, 1091, 815, 693, 570; HRMS (ES): m/z calculated for $\text{C}_{20}\text{H}_{22}\text{N}_3\text{O}_4\text{S}_3$: 464.0772, found 464.0771 $[\text{M}+\text{CH}_3\text{OH}+\text{H}]^+$.

4-Methyl-N-(3-oxo-5-(phenylthio)-2,3-dihydroimidazo[2,1-b]thiazol-6-yl)-N-phenylbenzenesulfonamide (593)



Following **GP6** using thioynamide **566** (75.9 mg, 0.20 mmol) and aminide **422** (46.4 mg, 0.24 mmol) and DTBPAu(NCMe)SbF₆ for 24 h. Purification by flash column chromatography [hexane:EtOAc (2:1)] afforded imidazole **593** as a pale orange powder (49.1 mg, 50%); mp: 235–237 °C; ¹H NMR (300 MHz, CDCl₃): δ = 7.69 (d, *J* = 8.3 Hz, 2H), 7.41–7.31 (m, 2H), 7.30–7.12 (m, 10H), 4.14 (s, 2H), 2.42 (s, 3H); ¹³C NMR (101 MHz, CDCl₃): δ = 164.7 (C), 153.8 (C), 151.4 (C), 144.0 (C), 139.7 (C), 136.0 (C), 134.3 (C), 129.8 (2×CH), 129.4 (2×CH), 129.20 (2×CH), 129.17 (2×CH), 129.0 (2×CH), 128.9 (2×CH), 128.3 (CH), 127.4 (CH), 118.6 (C), 38.0 (CH₂), 21.8 (CH₃); IR (neat): ν = 2987, 1755, 1480, 1344, 1292, 1162, 1088, 754, 689; HRMS (ES): *m/z* calculated for C₂₅H₂₄N₃O₄S₃: 526.0929, found 526.0928 [M+CH₃OH+H]⁺.

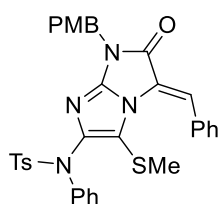
N-(5-(But-3-en-1-ylthio)-3-oxo-2,3-dihydroimidazo[2,1-b]thiazol-6-yl)-4-methyl-N-phenylbenzenesulfonamide (594)



Following **GP6** using thioynamide **575** (74.8 mg, 0.21 mmol) and aminide **422** (48.5 mg, 0.25 mmol) and DTBPAu(NCMe)SbF₆ for 18 h. Purification by flash column chromatography [hexane:EtOAc (4:1)] afforded imidazole **594** as a dark orange solid (33.5 mg, 34%); mp: 115–118 °C; ¹H NMR (300 MHz, CDCl₃): δ = 7.68 (d, *J* = 8.6 Hz, 2H), 7.41–7.35 (m 2H), 7.29–7.21 (m, 5H), 5.82–5.70 (ddt, *J* = 16.9, 10.4, 6.5 Hz, 1H), 5.07–4.97 (m, 2H), 4.24 (s, 2H), 2.87 (t, *J* = 7.4 Hz, 2H), 2.41 (s, 3H), 2.27 (q, *J* = 7.4 Hz, 2H); ¹³C NMR (125 MHz, CDCl₃): δ = 165.6 (C), 153.0 (C), 150.4 (C), 144.0 (C), 139.7 (C), 136.1 (CH), 136.0 (C), 129.4 (2×CH), 129.1 (2×CH), 128.8 (2×CH), 128.8 (2×CH), 128.1 (CH), 120.3 (C), 116.4 (CH₂), 38.1 (CH₂), 35.6

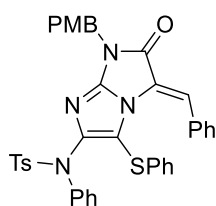
(CH₂), 33.5 (CH₂), 21.8 (CH₃); IR (neat): ν = 2924, 1752, 1484, 1344, 1292, 1163, 1089, 916, 708, 692, 667; HRMS (ES): m/z calculated for C₂₂H₂₂N₃O₃S₃: 472.0823, found 472.0822 [M+H]⁺.

(Z)-N-(3-Benzylidene-1-(4-methoxybenzyl)-5-(methylthio)-2-oxo-2,3-dihydro-1H-imidazo[1,2-a]imidazol-6-yl)-N-phenylmethanesulfonamide (595)



Following **GP6** using thioynamide **565** (31.7 mg, 0.10 mmol) and aminide **460** (35.6 mg, 0.09 mmol) for 18 h. Purification by flash column chromatography [hexane:EtOAc (4:1)] afforded imidazole **595** as a yellow fluffy solid (51.0 mg, 88%); mp: 199–201 °C; ¹H NMR (400 MHz, CDCl₃): δ = 7.69 (d, J = 8.3 Hz, 2H), 7.47 (d, J = 8.8 Hz, 2H), 7.44–7.30 (m, 8H), 7.25–7.20 (m, 5H), 6.92 (d, J = 8.8 Hz, 2H), 4.86 (s, 2H), 3.82 (s, 3H), 2.45 (s, 3H), 1.61 (s, 3H); ¹³C NMR (101 MHz, CDCl₃): δ = 164.1 (C), 159.8 (C), 147.5 (C), 144.2 (C), 143.6 (C), 140.4 (C), 136.5 (C), 132.7 (C), 130.8 (2×CH), 130.2 (2×CH), 129.6 (CH), 129.1 (2×CH), 129.0 (4×CH), 128.5 (2×CH), 127.8 (2×CH), 127.7 (CH), 127.6 (C), 125.7 (C), 120.9 (CH), 119.0 (C), 114.1 (2×CH), 55.5 (CH₃), 43.9 (CH₂), 21.8 (CH₃), 19.4 (CH₃); IR (neat): ν = 2920, 1737, 1610, 1514, 1453, 1347, 1247, 1164, 1090, 1028, 696; HRMS (ES): m/z calculated for C₃₄H₃₁N₄O₄S₂: 623.1787, found 623.1788 [M+H]⁺.

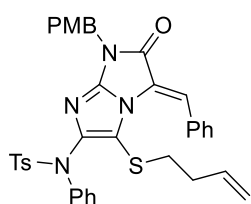
(Z)-N-(3-Benzylidene-1-(4-methoxybenzyl)-2-oxo-5-(phenylthio)-2,3-dihydro-1H-imidazo[1,2-a]imidazol-6-yl)-N-phenylmethanesulfonamide (596)



Following **GP6** using thioynamide **566** (75.9 mg, 0.20 mmol) and aminide **460** (92.3 mg, 0.24 mmol) for 22 h. Purification by flash column chromatography [hexane:EtOAc (4:1)] afforded imidazole **596** as an

orange solid (61.7 mg, 45%); mp: 88–91 °C; ^1H NMR (300 MHz, CDCl_3): δ = 7.68 (d, J = 8.4 Hz, 2H), 7.49 (d, J = 8.7 Hz, 2H), 7.36–7.27 (m, 3H), 7.26–7.11 (m, 10H), 6.97–6.82 (m, 5H), 6.30–6.21 (m, 2H), 4.90 (s, 2H), 3.83 (s, 3H), 2.45 (s, 3H); ^{13}C NMR (101 MHz, CDCl_3): δ = 164.2 (C), 159.8 (C), 148.4 (C), 146.4 (C), 143.6 (C), 140.1 (C), 136.4 (C), 135.1 (C), 132.2 (C), 130.7 (2 \times CH), 130.6 (2 \times CH), 129.5 (CH), 129.1 (2 \times CH), 129.0 (2 \times CH), 128.94 (2 \times CH), 128.89 (2 \times CH), 128.6 (2 \times CH), 127.9 (CH), 127.6 (2 \times CH), 127.5 (C), 126.0 (2 \times CH), 125.6 (CH), 124.7 (C), 122.0 (CH), 114.2 (2 \times CH), 114.1 (C), 55.5 (CH_3), 44.0 (CH_2), 21.8 (CH_3); IR (neat): ν = 2928, 1735, 1606, 1514, 1448, 1354, 1247, 1164, 1090, 684, 568; HRMS (ES): m/z calculated for $\text{C}_{39}\text{H}_{33}\text{N}_4\text{O}_4\text{S}_2$: 685.1943, found 685.1946 $[\text{M}+\text{H}]^+$.

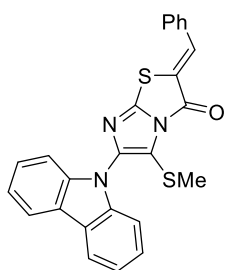
***(Z)*-N-(3-Benzylidene-5-(but-3-en-1-ylthio)-1-(4-methoxybenzyl)-2-oxo-2,3-dihydro-1H-imidazo[1,2-a]imidazol-6-yl)-N-phenylmethanesulfonamide (597)**



Following **GP6** using thioynamide **575** (86.2 mg, 0.24 mmol) and aminide **460** (111 mg, 0.29 mmol) for 24 h. Purification by flash column chromatography [hexane:EtOAc (4:2)] afforded imidazole **597** as a yellow solid (70.5 mg, 44%); mp: 55–58 °C; ^1H NMR (300 MHz, CDCl_3): δ = 7.69 (d, J = 8.3 Hz, 2H), 7.51–7.30 (m, 10H), 7.29–7.18 (m, 5H), 6.90 (d, J = 8.6 Hz, 2H), 5.41 (ddt, J = 16.9, 10.5, 6.5 Hz, 1H), 4.87 (s, 2H), 4.85–4.72 (m, 2H), 3.82 (s, 3H), 2.45 (s, 3H), 2.00 (t, J = 7.3 Hz, 2H), 1.75–7.64 (m, 2H); ^{13}C NMR (101 MHz, CDCl_3): δ = 164.2 (C), 159.8 (C), 147.5 (C), 144.6 (C), 143.6 (C), 140.6 (C), 136.4 (C), 136.1 (CH), 132.5 (C), 130.7 (2 \times CH), 130.6 (2 \times CH), 129.7 (CH), 129.0 (4 \times CH), 128.9 (2 \times CH), 128.6 (2 \times CH), 127.8 (2 \times CH), 127.7 (CH), 127.5 (C), 125.3 (C), 120.8 (CH), 117.7 (C), 115.9 (CH_2), 114.1 (2 \times CH), 55.5 (CH_3), 43.9 (CH_2), 35.2 (CH_2), 32.8 (CH_2), 21.8 (CH_3); IR (neat): ν = 2928, 1735, 1608,

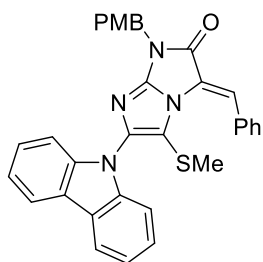
1450, 1355, 1248, 1165, 733, 693, 568; HRMS (ES): m/z calculated for $C_{37}H_{35}N_4O_4S_2$: 663.2100, found 663.2102 $[M+H]^+$.

(Z)-2-Benzylidene-6-(9H-carbazol-9-yl)-5-(methylthio)imidazo[2,1-b]thiazol-3(2H)-one (598)



Following **GP5** using thioynamide **568** (47.5 mg, 0.20 mmol) and aminide **427** (67.5 mg, 0.24 mmol) for 45 min. Purification by flash column chromatography [hexane:EtOAc (9:1)] afforded imidazole **598** as an orange solid (78.6 mg, 89%); mp: 221–223 °C; 1H NMR (300 MHz, $CDCl_3$): δ = 8.18 (s, 1H), 8.12 (app. dt, J = 7.7, 0.8 Hz, 2H), 7.69–7.62 (m, 2H), 7.61–7.51 (m, 3H), 7.50–7.39 (m, 4H), 7.32 (ddd, J = 7.8, 6.8, 1.5 Hz, 2H), 2.32 (s, 3H); ^{13}C NMR (101 MHz, $CDCl_3$): δ = 160.0 (C), 149.0 (C), 144.9 (C), 140.5 (2×C), 138.8 (CH), 132.9 (C), 131.6 (CH), 130.8 (2×CH), 129.6 (2×CH), 126.3 (2×CH), 124.2 (C), 124.0 (2×C), 120.9 (2×CH), 120.4 (2×CH), 118.3 (C), 111.0 (2×CH), 19.3 (CH_3); IR (neat): ν = 2929, 1728, 1607, 1548, 1480, 1445, 1345, 1330, 1225, 1062, 752, 743, 680, 643; HRMS (ES): m/z calculated for $C_{25}H_{18}N_3OS_2$: 440.0891, found 440.0895 $[M+H]^+$.

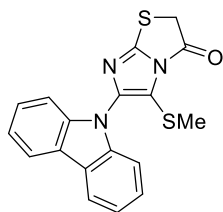
(Z)-3-Benzylidene-6-(9H-carbazol-9-yl)-1-(4-methoxybenzyl)-5-(methylthio)-1H-imidazo[1,2-a]imidazol-2(3H)-one (599)



Following **GP5** using thioynamide **568** (47.5 mg, 0.20 mmol) and aminide **460** (92.2 mg, 0.24 mmol) for 24 h. Purification by flash column chromatography [hexane:EtOAc (4:1)] afforded imidazole **599** as a yellow solid (27.8 mg, 26%); mp: 187–189 °C; 1H NMR (400 MHz, $CDCl_3$): δ = 8.09 (d, J = 7.4 Hz, 2H), 7.62–7.50 (m, 4H), 7.48–7.24 (m, 10H), 6.91 (d, J

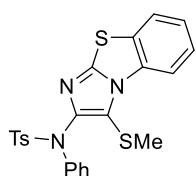
= 8.7 Hz, 2H), 4.97 (s, 2H), 3.82 (s, 3H), 1.36 (s, 3H); ^{13}C NMR (101 MHz, CDCl_3): δ = 164.4 (C), 159.8 (C), 148.3 (C), 140.7 (2×C), 140.3 (C), 132.9 (C), 131.0 (2×CH), 130.0 (2×CH), 129.8 (CH), 128.2 (2×CH), 127.5 (C), 126.1 (2×CH), 125.6 (C), 123.8 (2×C), 120.6 (CH), 120.5 (2×CH), 120.3 (2×CH), 115.0 (C), 114.2 (2×CH), 111.0 (2×CH), 55.5 (CH_3), 44.0 (CH_2), 19.5 (CH_3); IR (neat): ν = 2921, 1749, 1555, 1478, 1446, 1333, 1293, 1228, 1199, 1052, 906, 749, 722; HRMS (ES): m/z calculated for $\text{C}_{33}\text{H}_{27}\text{N}_4\text{O}_2\text{S}$: 543.1855, found 543.1860 $[\text{M}+\text{H}]^+$.

6-(9H-Carbazol-9-yl)-5-(methylthio)imidazo[2,1-b]thiazol-3(2H)-one (600)



Following **GP6** using thioynamide **568** (47.5 mg, 0.20 mmol) and aminide **422** (46.4 mg, 0.24 mmol) for 24 h. Purification by flash column chromatography [heane:EtOAc (7:3)] afforded imidazole **600** as a pale yellow oil (34.3 mg, 49%); mp: 49–52 °C (decomp); ^1H NMR (400 MHz, CDCl_3): δ = 7.68 (d, J = 7.5 Hz, 2H), 7.45 (app. td, J = 7.8, 1.1 Hz, 2H), 7.39 (d, J = 7.8 Hz, 2H), 7.32 (app. td, J = 7.5, 1.1 Hz, 2H), 4.36 (s, 2H), 2.26 (s, 3H); ^{13}C NMR (101 MHz, CDCl_3): δ = 166.5 (C), 154.0 (C), 146.2 (C), 140.3 (2×C), 126.3 (2×CH), 124.0 (2×C), 121.0 (2×CH), 120.4 (2×CH), 117.2 (C), 111.0 (2×CH), 38.4 (CH_2), 19.4 (CH_3); IR (neat): ν = 2921, 1749, 1555, 1478, 1446, 1333, 1293, 1228, 1199, 1052, 906, 749, 722; HRMS (ES): m/z calculated for $\text{C}_{18}\text{H}_{14}\text{N}_3\text{OS}_2$: 352.0578, found 352.0580 $[\text{M}+\text{H}]^+$.

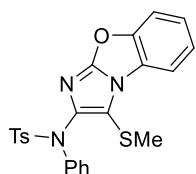
4-Methyl-N-(3-(methylthio)benzo[d]imidazo[2,1-b]thiazol-2-yl)-N-phenylbenzenesulfonamide (601)



Following **GP5** using thioynamide **565** (317 mg, 1.00 mmol) and aminide **267** (273 mg, 1.20 mmol) for 1.5 h. Purification by flash column

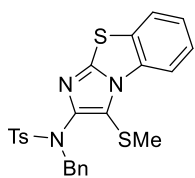
chromatography [hexane:EtOAc (4:1)] afforded imidazole **601** as an orange powder (424 mg, 91%); mp: 204–206 °C; ^1H NMR (300 MHz, CDCl_3): δ = 8.54 (dd, J = 8.1, 0.8 Hz, 1H), 7.76 (d, J = 8.4 Hz, 2H), 7.72 (dd, J = 8.1, 1.1 Hz, 1H), 7.54–7.44 (m, 3H), 7.37 (td, J = 7.8, 1.1 Hz, 1H), 7.31–7.19 (m, 5H), 2.43 (s, 3H), 2.40 (s, 3H); ^{13}C NMR (101 MHz, CDCl_3): δ = 147.5 (C), 146.7 (C), 143.7 (C), 140.5 (C), 136.5 (C), 133.8 (C), 129.6 (C), 129.4 (2×CH), 129.1 (2×CH), 128.8 (2×CH), 128.7 (2×CH), 127.8 (CH), 126.6 (CH), 125.3 (CH), 124.0 (CH), 118.6 (C), 114.3 (CH), 21.8 (CH_3), 20.0 (CH_3); IR (neat): ν = 2920, 1477, 1354, 1166, 1092, 970, 815, 751, 693, 660, 565; HRMS (ES): m/z calculated for $\text{C}_{23}\text{H}_{20}\text{N}_3\text{O}_2\text{S}_3$: 466.0718, found 466.0721 $[\text{M}+\text{H}]^+$.

4-Methyl-N-(3-(methylthio)benzo[d]imidazo[2,1-b]oxazol-2-yl)-N-phenylbenzenesulfonamide (602)



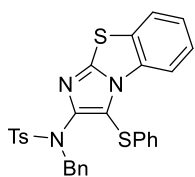
Following **GP5** using thioynamide **565** (476 mg, 1.50 mmol) and aminide **268** (380 mg, 1.80 mmol) for 1 h. Purification by flash column chromatography [hexane:EtOAc (4:1)] afforded imidazole **602** as a pale beige solid (629 mg, 93%); mp: 214–216 °C; ^1H NMR (300 MHz, CDCl_3): δ = 7.92–7.84 (m, 1H), 7.75 (d, J = 8.3 Hz, 2H), 7.57–7.46 (m, 3H), 7.41–7.32 (m, 2H), 7.32–7.19 (m, 5H), 2.43 (s, 6H); ^{13}C NMR (101 MHz, CDCl_3): δ = 152.6 (C), 149.9 (C), 143.7 (C), 143.7 (C), 140.5 (C), 136.3 (C), 129.4 (2×CH), 129.1 (2×CH), 128.8 (2×CH), 128.7 (2×CH), 127.8 (CH), 126.9 (C), 125.0 (CH), 124.7 (CH), 113.8 (C), 112.5 (CH), 111.9 (CH), 21.8 (CH_3), 19.9 (CH_3); IR (neat): ν = 2920, 1626, 1570, 1351, 1164, 1090, 814, 749, 696, 567; HRMS (ES): m/z calculated for $\text{C}_{23}\text{H}_{20}\text{N}_3\text{O}_2\text{S}_2$: 450.0946, found 450.0947 $[\text{M}+\text{H}]^+$.

***N*-Benzyl-4-methyl-*N*-(3-(methylthio)benzo[d]imidazo[2,1-*b*]thiazol-2-yl)benzenesulfonamide (603)**



Following **GP5** using thioynamide **567** (66.3 mg, 0.20 mmol) and aminide **267** (54.5 mg, 0.24 mmol) for 1 h. Purification by flash column chromatography [hexane:EtOAc (4:1)] afforded imidazole **603** as an orange solid (92.1 mg, 96%); mp: 194–197 °C; ¹H NMR (300 MHz, CDCl₃): δ = 8.42 (dd, *J* = 8.1, 0.8 Hz, 1H), 7.81 (d, *J* = 8.3 Hz, 2H), 7.69 (dd, *J* = 7.9, 0.8 Hz, 1H), 7.45 (app. td, *J* = 7.5, 1.3 Hz, 1H), 7.40–7.30 (m, 5H), 7.25–7.13 (m, 3H), 4.66 (s, 2H), 2.46 (s, 3H), 2.06 (s, 3H); ¹³C NMR (101 MHz, CDCl₃): δ = 146.6 (C), 145.3 (C), 143.9 (C), 136.0 (C), 135.9 (C), 133.7 (C), 129.8 (2×CH), 129.6 (C), 129.1 (2×CH), 128.43 (2×CH), 128.36 (2×CH), 127.8 (CH), 126.6 (CH), 125.3 (CH), 124.0 (CH), 120.0 (C), 114.3 (CH), 54.0 (CH₂), 21.8 (CH₃), 19.7 (CH₃); IR (neat): ν = 2923, 1479, 1348, 1163, 1090, 867, 739, 663; HRMS (ES): *m/z* calculated for C₂₄H₂₂N₃O₂S₃: 480.0874, found 480.0876 [M+H]⁺.

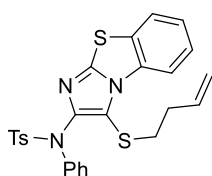
***N*-Benzyl-4-methyl-*N*-(3-(phenylthio)benzo[d]imidazo[2,1-*b*]thiazol-2-yl)benzenesulfonamide (604)**



Following **GP5** using thioynamide **563** (78.7 mg, 0.20 mmol) and aminide **267** (54.5 mg, 0.24 mmol) for 1 h. Purification by flash column chromatography [hexane:EtOAc (4:1)] afforded imidazole **604** as a white-off foamy solid (96.2 mg, 89%); mp: 200–202 °C; ¹H NMR (300 MHz, CDCl₃): δ = 7.91 (dd, *J* = 7.1, 1.6 Hz, 1H), 7.79 (d, *J* = 8.2 Hz, 2H), 7.64 (dd, *J* = 7.1, 1.6 Hz, 1H), 7.34 (d, *J* = 8.2 Hz, 2H), 7.31–7.24 (m, 4H), 7.21 (app. td, *J* = 7.7, 1.6 Hz, 1H), 7.11–6.96 (m, 6H), 6.65–6.58 (m, 2H), 4.71 (s, 2H), 2.46 (s, 3H); ¹³C NMR (101 MHz, CDCl₃): δ = 147.7 (C), 147.1 (C), 144.0 (C), 135.9 (C), 135.8 (C), 135.5 (C), 133.2 (C), 129.8 (2×CH), 129.4 (C), 129.3 (2×CH),

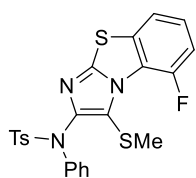
129.1 (2×CH), 128.5 (2×CH), 128.4 (2×CH), 127.8 (CH), 126.5 (CH), 126.1 (2×CH), 125.8 (CH), 125.3 (CH), 123.7 (CH), 115.1 (C), 114.8 (CH), 53.8 (CH₂), 21.8 (CH₃); IR (neat): ν = 2923, 1517, 1484, 1347, 1163, 868, 743, 665; HRMS (ES): m/z calculated for C₂₉H₂₄N₃O₂S₃: 542.1031, found 542.1033 [M+H]⁺.

***N*-(3-(*But-3-en-1-ylthio*)benzo[*d*]imidazo[2,1-*b*]thiazol-2-yl)-4-methyl-*N*-phenylbenzenesulfonamide (605)**



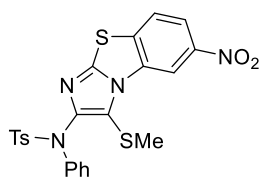
Following **GP5** using thioynamide **575** (75.5 mg, 0.21 mmol) and aminide **267** (57.6 mg, 0.25 mmol) for 2.5 h. Purification by flash column chromatography [hexane:EtOAc (9:1)] afforded imidazole **605** as an orange solid (83.5 mg, 78%); mp: 182–184 °C; ¹H NMR (300 MHz, CDCl₃): δ = 8.56 (dd, J = 8.2, 0.8 Hz, 1H), 7.76 (d, J = 8.3 Hz, 2H), 7.70 (dd, J = 7.8, 0.8 Hz, 1H), 7.55–7.48 (m, 2H), 7.45 (app. td, J = 8.2, 1.2 Hz, 1H), 7.35 (app. td, J = 7.8, 1.2 Hz, 1H), 7.30–7.21 (m, 5H), 5.77 (ddt, J = 16.9, 10.4, 6.5 Hz, 1H), 5.07–4.94 (m, 2H), 2.90 (t, J = 7.3 Hz, 2H), 2.42 (s, 3H), 2.35 (q, J = 7.3 Hz, 2H); ¹³C NMR (101 MHz, CDCl₃): δ = 148.0 (C), 146.7 (C), 143.7 (C), 140.5 (C), 136.3 (C), 136.1 (CH), 133.8 (C), 129.6 (C), 129.3 (2×CH), 129.0 (2×CH), 128.9 (2×CH), 128.5 (2×CH), 127.7 (CH), 126.3 (CH), 125.3 (CH), 124.0 (CH), 117.4 (C), 116.6 (CH₂), 114.5 (CH), 36.4 (CH₂), 33.7 (CH₂), 21.8 (CH₃); IR (neat): ν = 2926, 1753, 1480, 1351, 1290, 1164, 1091, 915, 812, 754, 694; HRMS (ES): m/z calculated for C₂₆H₂₄N₃O₂S₃: 506.1031, found 506.1028 [M+H]⁺.

***N*-(5-Fluoro-3-(methylthio)benzo[d]imidazo[2,1-*b*]thiazol-2-yl)-4-methyl-*N*-phenylbenzenesulfonamide (606)**



Following **GP5** using thioynamide **565** (63.4 mg, 0.20 mmol) and aminide **346** (58.8 mg, 0.24 mmol) for 1 h. Purification by flash column chromatography [hexane:EtOAc (4:1)] afforded imidazole **606** as a light pink solid (94.9 mg, 98%); mp: 212–214 °C; ¹H NMR (400 MHz, CDCl₃): δ = 7.76 (d, *J* = 8.3 Hz, 2H), 7.53–7.47 (m, 3H), 7.34 (app. td, *J* = 8.0, 4.3 Hz, 1H), 7.30–7.19 (m, 6H), 2.43 (s, 3H), 2.38 (s, 3H); ¹³C NMR (101 MHz, CDCl₃): δ = 150.0 (d, *J* = 256.3 Hz, C), 148.2 (C), 146.6 (C), 143.7 (C), 140.4 (C), 136.6 (C), 132.2 (d, *J* = 3.7 Hz, C), 129.4 (2×CH), 129.1 (2×CH), 128.7 (4×CH), 127.8 (CH), 126.24 (d, *J* = 6.8 Hz, CH), 122.1 (d, *J* = 15.5 Hz, C), 120.9 (C), 119.8 (d, *J* = 4.0 Hz, CH), 114.3 (d, *J* = 20.3 Hz, CH), 21.8 (CH₃), 20.56 (d, *J* = 4.2 Hz, CH₃); IR (neat): ν = 2923, 1486, 1345, 1289, 1249, 1166, 1091, 917, 777, 709, 661; HRMS (ES): *m/z* calculated for C₂₃H₁₉N₃O₂S₃F: 484.0623, found 484.0621 [M+H]⁺.

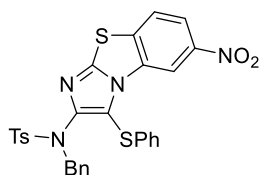
***4*-Methyl-*N*-(3-(methylthio)-6-nitrobenzo[d]imidazo[2,1-*b*]thiazol-2-yl)-*N*-phenylbenzenesulfonamide (607)**



Following **GP5** using thioynamide **565** (63.5 mg, 0.20 mmol) and aminide **344** (65.3 mg, 0.24 mmol) for 1 h. Purification by flash column chromatography [hexane:EtOAc (4:1)] afforded imidazole **607** as a light orange solid (53.0 mg, 52%); mp: 264–266 °C; ¹H NMR (300 MHz, CDCl₃): δ = 9.36 (d, *J* = 2.2 Hz, 1H), 8.30 (dd, *J* = 8.8, 2.2 Hz, 1H), 7.90 (d, *J* = 8.8 Hz, 1H), 7.74 (d, *J* = 8.3 Hz, 2H), 7.52–7.44 (m, 2H), 7.34–7.21 (m, 5H), 2.45 (s, 3H), 2.44 (s, 3H); ¹³C NMR (101 MHz, CDCl₃): δ = 148.4 (C), 146.8 (C), 146.6 (C), 144.0 (C), 140.1 (C), 137.0 (C), 136.2 (C), 133.7 (C), 129.5 (2×CH), 129.2 (2×CH), 128.89 (2×CH), 128.80 (2×CH), 128.1 (CH), 124.4

(CH), 120.2 (CH), 119.8 (C), 109.6 (CH), 21.8 (CH₃), 19.8 (CH₃); IR (neat): ν = 2921, 2851, 1520, 1482, 1342, 1163, 1092, 695, 661; HRMS (ES): m/z calculated for C₂₃H₁₉N₄O₄S₃: 511.0568, found 511.0569 [M+H]⁺.

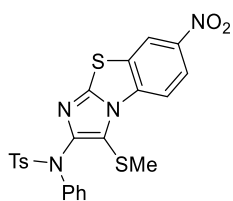
***N*-Benzyl-4-methyl-*N*-(6-nitro-3-(phenylthio)benzo[d]imidazo[2,1-*b*]thiazol-2-yl)benzenesulfonamide (608)**



Following **GP5** using thioynamide **563** (78.7 mg, 0.20 mmol) and aminide **608** (65.3 mg, 0.24 mmol) for 1 h. Purification by flash column chromatography [Et₂O:EtOAc (7:3)] afforded imidazole **608**

as a brown dark solid (98.8 mg, 84%); mp: 231–233 °C; ¹H NMR (300 MHz, CDCl₃): δ = 8.70 (d, J = 2.2 Hz, 1H), 8.12 (dd, J = 8.8, 2.2 Hz, 1H), 7.81 (d, J = 8.3 Hz, 2H), 7.76 (d, J = 8.8 Hz, 1H), 7.42–7.29 (m, 4H), 7.18–7.09 (m, 3H), 7.08–7.00 (m, 3H), 6.75–6.65 (m, 2H), 4.73 (s, 2H), 2.47 (s, 3H); ¹³C NMR (101 MHz, CDCl₃): δ = 147.5 (C), 147.3 (C), 146.3 (C), 144.2 (C), 136.5 (C), 135.6 (C), 135.3 (C), 134.0 (C), 132.8 (C), 129.9 (2×CH), 129.6 (2×CH), 129.2 (2×CH), 128.6 (2×CH), 128.4 (2×CH), 128.1 (CH), 127.4 (2×CH), 126.8 (CH), 123.9 (CH), 119.9 (CH), 117.3 (C), 110.4 (CH), 53.8 (CH₂), 21.8 (CH₃); IR (neat): ν = 3092, 2922, 1522, 1478, 1337, 1157, 1091, 878, 816, 698, 659; HRMS (ES): m/z calculated for C₂₉H₂₃N₄O₄S₃: 587.0881, found 587.0880 [M+H]⁺.

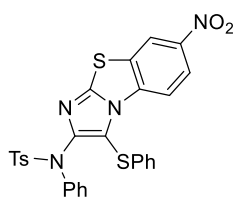
***4*-Methyl-*N*-(3-(methylthio)-7-nitrobenzo[d]imidazo[2,1-*b*]thiazol-2-yl)-*N*-phenylbenzenesulfonamide (609)**



Following **GP5** using thioynamide **565** (63.5 mg, 0.20 mmol) and aminide **343** (62.6 mg, 0.23 mmol) for 1 h. Purification by flash column chromatography [hexane:EtOAc (4:1)] afforded imidazole **609** as a

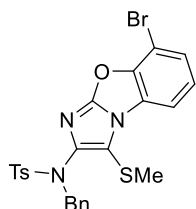
yellow powder (89.3 mg, 87%); mp: 180–182 °C; ^1H NMR (300 MHz, CDCl_3): δ = 8.74–8.64 (m, 2H), 8.40 (dd, J = 9.0, 2.4 Hz, 1H), 7.73 (d, J = 8.3 Hz, 2H), 7.53–7.43 (m, 2H), 7.34–7.21 (m, 5H), 2.44 (s, 3H), 2.42 (s, 3H); ^{13}C NMR (101 MHz, CDCl_3): δ = 148.9 (C), 147.7 (C), 144.8 (C), 144.0 (C), 140.1 (C), 137.5 (C), 136.1 (C), 130.8 (C), 129.5 (2 \times CH), 129.2 (2 \times CH), 128.82 (2 \times CH), 128.78 (2 \times CH), 128.1 (CH), 122.5 (CH), 120.2 (CH), 119.6 (C), 114.1 (CH), 21.8 (CH_3), 20.0 (CH_3); IR (neat): ν = 3109, 2925, 1522, 1482, 1342, 1290, 1164, 692, 662; HRMS (ES): m/z calculated for $\text{C}_{23}\text{H}_{19}\text{N}_4\text{O}_4\text{S}_3$: 511.0568, found 511.0570 $[\text{M}+\text{H}]^+$.

4-Methyl-N-(7-nitro-3-(phenylthio)benzo[d]imidazo[2,1-b]thiazol-2-yl)-N-phenylbenzenesulfonamide (610)



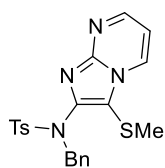
Following **GP5** using thioynamide **566** (75.9 mg, 0.20 mmol) and aminide **343** (65.3 mg, 0.24 mmol) for 1 h. Purification by flash column chromatography [hexane:EtOAc (4:1)] afforded imidazole **610** as a yellow solid (97.7 mg, 85%); ^1H NMR (400 MHz, CDCl_3): δ = 8.63 (d, J = 2.0 Hz, 1H), 8.25 (d, J = 9.0 Hz, 1H), 8.20 (dd, J = 9.0, 2.0 Hz, 1H), 7.73 (d, J = 8.31 Hz, 2H), 7.44–7.37 (m, 2H), 7.30–7.24 (m, 2H), 7.24–7.08 (m, 6H), 7.08–7.03 (m, 2H), 2.44 (s, 3H); ^{13}C NMR (101 MHz, CDCl_3): δ = 150.6 (C), 148.9 (C), 144.8 (C), 144.1 (C), 139.8 (C), 137.0 (C), 136.0 (C), 134.4 (C), 130.6 (C), 129.7 (2 \times CH), 129.5 (2 \times CH), 129.19 (2 \times CH), 129.16 (2 \times CH), 128.9 (2 \times CH), 128.3 (CH), 126.9 (CH), 126.7 (2 \times CH), 122.5 (CH), 120.0 (CH), 115.3 (C), 114.5 (CH), 21.8 (CH_3); IR (neat): ν = 3113, 1530, 1481, 1345, 1297, 1166, 713, 695; HRMS (ES): m/z calculated for $\text{C}_{28}\text{H}_{20}\text{N}_4\text{O}_4\text{NaS}_3$: 595.0544, found 595.0539 $[\text{M}+\text{Na}]^+$.

N-Benzyl-N-(8-bromo-3-(methylthio)benzo[d]imidazo[2,1-b]oxazol-2-yl)-4-methylbenzenesulfonamide (611)



Following **GP5** using thioynamide **567** (49.7 mg, 0.15 mmol) and aminide **345** (52.2 mg, 0.18 mmol) for 1 h. Purification by flash column chromatography [hexane:EtOAc (9:1)] afforded imidazole **611** as a light pink solid (81.1 mg, >99%); mp: 210–213 °C; ^1H NMR (400 MHz, CDCl_3): δ = 7.80 (d, J = 8.3 Hz, 2H), 7.74 (dd, J = 7.9, 1.0 Hz, 1H), 7.48 (dd, J = 8.2, 1.0 Hz, 1H), 7.39–7.32 (m, 4H), 7.28–7.16 (m, 4H), 4.63 (s, 2H), 2.46 (s, 3H), 2.07 (s, 3H); ^{13}C NMR (101 MHz, CDCl_3): δ = 152.0 (C), 147.8 (C), 144.0 (C), 141.8 (C), 135.9 (C), 135.7 (C), 129.8 (2 \times CH), 129.1 (2 \times CH), 128.4 (4 \times CH), 128.1 (CH), 127.8 (CH), 127.7 (C), 125.8 (CH), 115.7 (C), 110.8 (CH), 104.8 (C), 53.9 (CH_2), 21.8 (CH_3), 19.5 (CH_3); IR (neat): ν = 2921, 1626, 1576, 1461, 1390, 1352, 1164, 767, 663; HRMS (ES): m/z calculated for $\text{C}_{24}\text{H}_{20}\text{N}_3\text{O}_3\text{S}_2\text{Na}^{79}\text{Br}$: 564.0027, found 564.0031 $[\text{M}+\text{Na}]^+$.

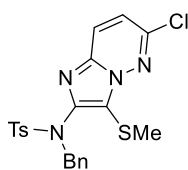
N-Benzyl-4-methyl-N-(3-(methylthio)imidazo[1,2-a]pyrimidin-2-yl)benzenesulfonamide (612)



Following **GP6** using thioynamide **567** (66.3 mg, 0.20 mmol) and aminide **214** (41.3 mg, 0.24 mmol) and DTBPAu(NCMe)SbF₆ for 4 h. Purification by flash column chromatography [hexane:EtOAc (2:3)] afforded imidazole **612** as an off-white solid (74.4 mg, 85%); mp: 155–157 °C; ^1H NMR (300 MHz, CDCl_3): δ = 8.59 (dd, J = 4.1, 1.7 Hz, 1H), 8.54 (dd, J = 6.7, 1.7 Hz, 1H), 7.81 (d, J = 8.3 Hz, 2H), 7.41–7.29 (m, 4H), 7.22–7.10 (m, 3H), 6.99 (dd, J = 6.7, 4.1 Hz, 1H), 4.76 (s, 2H), 2.44 (s, 3H), 2.00 (s, 3H); ^{13}C NMR (101 MHz, CDCl_3): δ = 151.1 (CH), 147.02 (C), 146.95 (C), 143.9 (C), 135.8 (C), 132.3 (CH), 129.8 (2 \times CH), 128.8 (2 \times CH), 128.4 (2 \times CH), 128.3 (2 \times CH), 127.7 (CH),

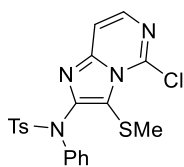
114.3 (C), 109.7 (CH), 53.8 (CH₂), 21.7 (CH₃), 17.6 (CH₃) *one resonance for a quaternary carbon was not observed*; IR (neat): ν = 3065, 2927, 1614, 1514, 1496, 1350, 1164, 1063, 787, 685; HRMS (ES): m/z calculated for C₂₁H₂₁N₄O₂S₂: 425.1106, found 425.1102 [M+H]⁺.

***N*-Benzyl-*N*-(6-chloro-3-(methylthio)imidazo[1,2-*b*]pyridazin-2-yl)-4-methylbenzenesulfonamide (613)**



Following **GP6** using thioynamide **567** (166 mg, 0.50 mmol) and aminide **262** (124 mg, 0.60 mmol) for 5.5 h. Purification by flash column chromatography [hexane:EtOAc (7:3-3:2)] afforded imidazole **613** as a pale yellow solid (164 mg, 71%); mp: 192–194 °C; ¹H NMR (300 MHz, CDCl₃): δ = 7.82–7.72 (m, 3H), 7.38–7.27 (m, 4H), 7.22–7.13 (m, 3H), 7.11 (d, J = 9.4 Hz, 1H), 4.76 (s, 2H), 2.45 (s, 3H), 2.18 (s, 3H); ¹³C NMR (101 MHz, CDCl₃): δ = 147.9 (C), 144.7 (C), 144.0 (C), 136.9 (C), 135.9 (C), 135.5 (C), 129.8 (2×CH), 128.7 (2×CH), 128.41 (2×CH), 128.37 (2×CH), 127.8 (CH), 127.0 (CH), 121.7 (C), 120.1 (CH), 53.8 (CH₂), 21.8 (CH₃), 16.3 (CH₃); IR (neat): ν = 2924, 1667, 1495, 1339, 1163, 1089, 697, 673; HRMS (ES): m/z calculated for C₂₁H₂₀N₄O₂S₂³⁵Cl: 459.0716, found 459.0715 [M+H]⁺.

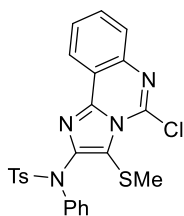
***N*-(5-Chloro-3-(methylthio)imidazo[1,2-*c*]pyrimidin-2-yl)-4-methyl-*N*-phenylbenzenesulfonamide (614)**



Following **GP6** using thioynamide **565** (63.5 mg, 0.20 mmol) and aminide **684** (49.6 mg, 0.24 mmol) for 7 h. Purification by flash column chromatography [hexane:EtOAc (4:1)] afforded imidazole **614** as a yellow solid (8.7 mg, 10%); mp: 208–210 °C; ¹H NMR (300 MHz, CDCl₃): δ = 7.87 (d, J = 6.2 Hz, 1H), 7.75 (d, J = 8.3 Hz, 2H), 7.50–7.41 (m, 3H), 7.31–7.21 (m, 5H), 2.43 (s, 3H), 2.34 (s,

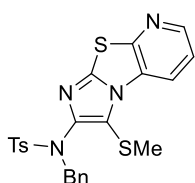
3H); ^{13}C NMR (125 MHz, CDCl_3): δ = 150.8 (C), 146.8 (C), 144.0 (C), 140.0 (CH), 139.8 (C), 138.5 (C), 136.2 (C), 129.40 (2 \times CH), 129.13 (2 \times CH), 129.11 (2CH), 128.9 (2 \times CH), 128.1 (CH), 116.4 (C), 112.2 (CH), 22.3 (CH_3), 21.8 (CH_3); IR (neat): ν = 2924, 1752, 1485, 1342, 1208, 1166, 1091, 812, 694; HRMS (ES): m/z calculated for $\text{C}_{20}\text{H}_{18}\text{N}_4\text{O}_2\text{S}_2^{35}\text{Cl}$: 445.0560, found 445.0563 $[\text{M}+\text{H}]^+$.

***N*-(5-Chloro-3-(methylthio)imidazo[1,2-*c*]quinazolin-2-yl)-4-methyl-*N*-phenylbenzenesulfonamide (615)**



Following **GP6** using thioynamide **565** (63.5 mg, 0.20 mmol) and aminide **616** (61.6 mg, 0.24 mmol) for 20 h. Purification by flash column chromatography [hexane:EtOAc (4:1)] afforded imidazole **615** as a beige solid (56.6 mg, 57%); mp: 185–187 °C; ^1H NMR (400 MHz, CDCl_3): δ = 8.43 (dd, J = 7.8, 1.3 Hz, 1H), 7.85 (dd, J = 8.0, 1.0 Hz, 1H), 7.82 (d, J = 8.3 Hz, 2H), 7.72 (app. td, J = 8.0, 1.3 Hz, 1H), 7.66 (app. td, J = 7.8, 1.0 Hz, 1H), 7.54–7.47 (m, 2H), 7.35–7.21 (m, 5H), 2.47 (s, 3H), 2.34 (s, 3H); ^{13}C NMR (101 MHz, CDCl_3): δ = 149.2 (C), 145.1 (C), 143.9 (C), 140.8 (C), 140.1 (C), 136.2 (C), 135.1 (C), 131.4 (CH), 129.2 (4 \times CH), 129.1 (2 \times CH), 129.0 (2 \times CH), 128.9 (CH), 128.0 (CH), 127.4 (CH), 123.3 (CH), 118.5 (C), 118.4 (C), 21.82 (2 \times CH_3); IR (neat): ν = 2923, 1595, 1488, 1355, 1304, 1164, 1087, 761, 693; HRMS (ES): m/z calculated for $\text{C}_{24}\text{H}_{20}\text{N}_4\text{O}_2\text{S}_2^{35}\text{Cl}$: 495.0716, found 495.0714 $[\text{M}+\text{H}]^+$.

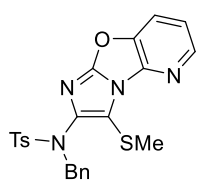
***N*-Benzyl-4-methyl-*N*-(3-(methylthio)imidazo[2',1':2,3]thiazolo[5,4-*b*]pyridin-2-yl)benzenesulfonamide (630)**



Following **GP5** using thioynamide **567** (66.3 mg, 0.20 mmol) and aminide **686** (54.8 mg, 0.24 mmol) for 1 h. Purification by flash column

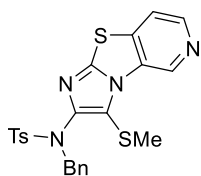
chromatography [hexane:EtOAc (7:3)] afforded imidazole **630** as a dark brown crystalline solid (93.1 mg, 97%); mp: 153–155 °C; ¹H NMR (300 MHz, CDCl₃): δ = 8.57 (dd, *J* = 8.2, 1.4 Hz, 1H), 8.49 (dd, *J* = 4.9, 1.4 Hz, 1H), 7.80 (d, *J* = 8.3 Hz, 2H), 7.40 (dd, *J* = 8.2, 4.9 Hz, 1H), 7.39–7.32 (m, 4H), 7.25–7.16 (m, 3H), 4.66 (s, 2H), 2.46 (s, 3H), 2.05 (s, 3H); ¹³C NMR (101 MHz, CDCl₃): δ = 152.9 (C), 146.3 (CH), 145.1 (C), 145.0 (C), 144.0 (C), 135.9 (C), 135.7 (C), 129.8 (2×CH), 129.12 (C), 129.08 (2×CH), 128.4 (4×CH), 127.9 (CH), 121.1 (CH), 120.8 (CH), 120.3 (C), 53.9 (CH₂), 21.8 (CH₃), 19.4 (CH₃); IR (neat): ν = 2922, 1480, 1414, 1346, 1299, 1163, 1088, 801, 695, 661; HRMS (ES): *m/z* calculated for C₂₃H₂₀N₄O₂S₃Na: 503.0646, found 503.0650 [M+Na]⁺.

***N*-Benzyl-4-methyl-*N*-(3-(methylthio)imidazo[2',1':2,3]oxazolo[4,5-*b*]pyridin-2-yl)benzenesulfonamide (631)**



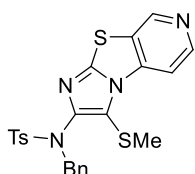
Following **GP5** using thioynamide **567** (66.3 mg, 0.20 mmol) and aminide **700** (50.9 mg, 0.24 mmol) for 1 h. Purification by flash column chromatography [hexane:EtOAc (4:2-7:3)] afforded imidazole **631** as an off-white solid (82.4 mg, 87%); mp: 208–210 °C; ¹H NMR (300 MHz, CDCl₃): δ = 8.38 (dd, *J* = 5.1, 1.2 Hz, 1H), 7.82 (d, *J* = 8.3 Hz, 2H), 7.78 (dd, *J* = 8.2, 1.2 Hz, 1H), 7.41–7.27 (m, 5H), 7.25–7.16 (m, 3H), 4.65 (s, 2H), 2.46 (s, 3H), 2.27 (s, 3H); ¹³C NMR (101 MHz, CDCl₃): δ = 152.7 (C), 144.5 (CH), 143.9 (C), 143.5 (C), 141.5 (C), 141.2 (C), 136.0 (C), 135.6 (C), 129.8 (2×CH), 128.9 (2×CH), 128.4 (4×CH), 127.8 (CH), 120.1 (CH), 119.7 (CH), 116.9 (C), 53.7 (CH₂), 21.8 (CH₃), 19.3 (CH₃); IR (neat): ν = 2923, 1623, 1573, 1454, 1349, 1164, 1090, 801, 661; HRMS (ES): *m/z* calculated for C₂₃H₂₀N₄O₃NaS₂: 487.0875, found 487.0876 [M+Na]⁺.

***N*-Benzyl-4-methyl-*N*-(3-(methylthio)imidazo[2',1':2,3]thiazolo[4,5-*c*]pyridin-2-yl)benzenesulfonamide (632)**



Following **GP5** using thioynamide **567** (66.3 mg, 0.20 mmol) and aminide **689** (54.8 mg, 0.24 mmol) for 8 h. Purification by flash column chromatography [hexane:EtOAc (3:2)] afforded imidazole **632** as a pale orange solid (72.0 mg, 75%); mp: 179–181 °C; ¹H NMR (300 MHz, CDCl₃): δ = 9.63 (s, 1H), 8.56 (d, *J* = 5.3 Hz, 1H), 7.81 (d, *J* = 8.3 Hz, 2H), 7.70 (d, *J* = 5.3 Hz, 1H), 7.41–7.30 (m, 4H), 7.25–7.13 (m, 3H), 4.66 (s, 2H), 2.46 (s, 3H), 2.11 (s, 3H); ¹³C NMR (101 MHz, CDCl₃): δ = 145.9 (C), 145.3 (C), 144.9 (CH), 144.0 (C), 139.2 (C), 135.9 (C), 135.6 (C), 135.5 (CH), 130.9 (C), 129.8 (2×CH), 129.0 (2×CH), 128.39 (2×CH), 128.37 (2×CH), 127.9 (CH), 120.8 (C), 118.8 (CH), 54.0 (CH₂), 21.8 (CH₃), 19.2 (CH₃); IR (neat): ν = 2922, 1480, 1445, 1350, 1153, 1090, 830, 740, 677, 658; HRMS (ES): *m/z* calculated for C₂₃H₂₁N₄O₂S₃: 481.0827, found 481.0828 [M+H]⁺.

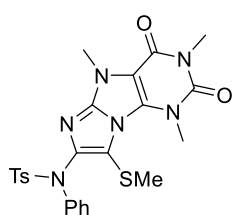
***N*-Benzyl-4-methyl-*N*-(3-(methylthio)imidazo[2',1':2,3]thiazolo[5,4-*c*]pyridin-2-yl)benzenesulfonamide (633)**



Following **GP5** using thioynamide **567** (33.1 mg, 0.10 mmol) and aminide **627** (27.4 mg, 0.12 mmol) for 22 h. Purification by flash column chromatography [hexane:EtOAc (1:1)] afforded imidazole **633** as a light brown solid (27.8 mg, 58%); mp: 179–181 °C; ¹H NMR (400 MHz, CDCl₃): δ = 8.96 (s, 1H), 8.65 (d, *J* = 5.5 Hz, 1H), 8.28 (d, *J* = 5.5 Hz, 1H), 7.80 (d, *J* = 8.3 Hz, 2H), 7.39–7.31 (m, 4H), 7.24–7.14 (m, 3H), 4.65 (s, 2H), 2.46 (s, 3H), 2.08 (s, 3H); ¹³C NMR (101 MHz, CDCl₃): δ = 147.4 (C), 146.8 (CH), 146.8 (C), 145.1 (CH), 144.1 (C), 139.1 (C), 135.8 (C), 135.6 (C), 129.9 (2×CH), 129.0 (2×CH), 128.5 (2×CH), 128.4 (2×CH), 127.9 (CH), 127.0

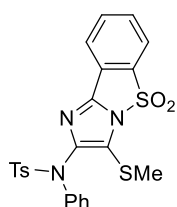
(C), 120.9 (C), 108.8 (CH), 53.9 (CH₂), 21.8 (CH₃), 19.7 (CH₃); IR (neat): ν = 2915, 1560, 1524, 1484, 1341, 1160, 1090, 872, 739, 714, 662; HRMS (ES): m/z calculated for C₂₃H₂₁N₄O₂S₃: 481.0827, found 481.0834 [M+H]⁺.

4-Methyl-N-phenyl-N-(1,3,5-trimethyl-8-(methylthio)-2,4-dioxo-1,3,4,5-tetrahydro-2H-imidazo[1,2-e]purin-7-yl)benzenesulfonamide (636)



Following **GP6** using thioynamide **565** (63.5 mg, 0.20 mmol) and aminide **685** (68.7 mg, 0.24 mmol) for 1.5 h. Purification by flash column chromatography [hexane:EtOAc (7:3)] afforded imidazole **636** as a beige powder (94.0 mg, 90%); mp: 235–237 °C (decomp); ¹H NMR (300 MHz, CDCl₃): δ = 7.78 (d, J = 8.3 Hz, 2H), 7.52–7.44 (m, 2H), 7.30–7.18 (m, 5H), 4.22 (s, 3H), 3.96 (s, 3H), 3.46 (s, 3H), 2.43 (s, 3H), 2.23 (s, 3H); ¹³C NMR (101 MHz, CDCl₃): δ = 155.6 (C), 150.6 (C), 150.4 (C), 146.7 (C), 143.7 (C), 140.3 (C), 136.3 (C), 131.8 (C), 129.2 (2×CH), 129.0 (2×CH), 129.0 (2×CH), 128.4 (2×CH), 127.7 (CH), 111.2 (C), 107.0 (C), 36.0 (CH₃), 31.3 (CH₃), 28.6 (CH₃), 21.7 (CH₃), 20.9 (CH₃); IR (neat): ν = 2922, 1662, 1638, 1345, 1310, 1163, 700, 663; HRMS (ES): m/z calculated for C₂₄H₂₅N₆O₄S₂: 525.1379, found 525.1378 [M+H]⁺.

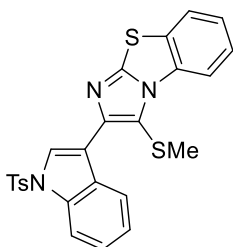
4-Methyl-N-(3-(methylthio)-5,5-dioxidobenzo[d]imidazo[1,2-b]isothiazol-2-yl)-N-phenylbenzenesulfonamide (639)



Following **GP6** using thioynamide **565** (31.7 mg, 0.10 mmol) and aminide **637** (31.1 mg, 0.12 mmol) for 21 h. Purification by flash column chromatography [hexane:EtOAc (4:1)] afforded imidazole **639** as a beige crystalline solid (23.3 mg, 47%); mp: 174–176 °C; ¹H NMR (400 MHz, CDCl₃): δ = 7.90 (d, J = 7.8 Hz, 1H), 7.82 (d, J = 7.8 Hz, 1H), 7.77–7.71 (m, 3H), 7.62 (app. td, J = 7.7, 1.0 Hz,

¹H), 7.45–7.40 (m, 2H), 7.32–7.23 (m, 5H), 2.49 (s, 3H), 2.44 (s, 3H); ¹³C NMR (101 MHz, CDCl₃): δ = 147.6 (C), 144.0 (C), 142.1 (C), 139.7 (C), 138.8 (C), 136.1 (C), 135.0 (CH), 131.2 (CH), 129.4 (2×CH), 129.2 (2×CH), 128.8 (2×CH), 128.7 (2×CH), 128.2 (CH), 125.2 (C), 123.0 (C), 122.7 (CH), 122.3 (CH), 21.8 (CH₃), 20.4 (CH₃); IR (neat): ν = 2921, 2850, 1597, 1489, 1354, 1165, 1091, 817, 693, 571; HRMS (ES): *m/z* calculated for C₂₃H₂₀N₃O₄S₃: 498.0616, found 498.0618 [M+H]⁺.

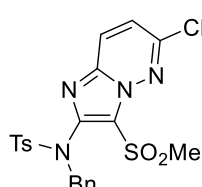
3-(Methylthio)-2-(1-tosyl-1H-indol-3-yl)benzo[d]imidazo[2,1-b]thiazole (642)



Following **GP5** using thioynamide **640** (102 mg, 0.30 mmol) and aminide **267** (81.8 mg, 0.36 mmol) for 24 h. Purification by flash column chromatography [hexane:EtOAc (9:1)] afforded imidazole **642** as a light brown powder (19.6 mg, 13%); mp: 222–225 °C; ¹H NMR (300 MHz, CDCl₃): δ = 8.66 (dd, *J* = 8.2, 0.7 Hz, 1H), 8.46–8.36 (m, 2H), 8.07–8.01 (m, 1H), 7.82 (d, *J* = 8.4 Hz, 2H), 7.73 (dd, *J* = 8.0, 0.7 Hz, 1H), 7.51 (app. td, *J* = 7.5, 1.3 Hz, 1H), 7.43–7.28 (m, 3H), 7.21 (d, *J* = 8.4 Hz, 2H), 2.39 (s, 3H), 2.32 (s, 3H); ¹³C NMR (101 MHz, CDCl₃): δ = 149.7 (C), 145.9 (C), 145.1 (C), 135.3 (C), 135.1 (C), 133.7 (C), 130.4 (C), 130.1 (C), 130.0 (2×CH), 127.0 (2×CH), 126.6 (CH), 125.0 (2×CH), 124.6 (CH), 124.3 (CH), 123.9 (CH), 123.0 (CH), 115.9 (C), 115.6 (C), 114.1 (CH), 113.5 (CH), 21.7 (CH₃), 20.1 (CH₃); IR (neat): ν = 2920, 2851, 1475, 1440, 1364, 1168, 1132, 735, 654, 578; HRMS (ES): *m/z* calculated for C₂₅H₂₀N₃O₂S₃: 490.0718, found 490.0720 [M+H]⁺.

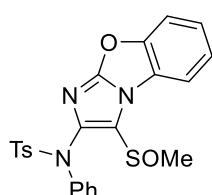
2.9. Post catalysis modification products

N-Benzyl-*N*-(6-chloro-3-(methylsulfonyl)imidazo[1,2-*b*]pyridazin-2-yl)-4-methylbenzenesulfonamide (**644**)



To a solution of sulfide **613** (0.1 mmol, 45.9 mg, 1.0 eq.) in CH₂Cl₂ (1 mL) at 0 °C was added *m*CPBA (77% in water) (0.2 mmol, 49.3 mg, 2.2 eq.) portionwise. The resulting reaction mixture was allowed to warm up to room temperature and was stirred for 17 h. The mixture was quenched with Na₂S₂O₃(sat sol) (10 mL) and washed with NaHCO₃(sat sol) (10 mL). The aqueous phase was extracted with CH₂Cl₂ (3×10 mL). The combined organic phases were dried over Na₂SO₄, filtered off and concentrated under reduced pressure. Purification by flash column chromatography [hexane:EtOAc (3:2)] gave sulfone **644** as a white powder (43 mg, 88%); mp: 220–221 °C; ¹H NMR (300 MHz, CDCl₃): δ = 7.88 (d, *J* = 9.5 Hz, 1H), 7.79 (d, *J* = 8.4 Hz, 2H), 7.37–7.31 (m, 4H), 7.29 (d, *J* = 9.5 Hz, 1H), 7.21–7.09 (m, 3H), 4.75 (s, 2H), 3.39 (s, 3H), 2.46 (s, 3H); ¹³C NMR (101 MHz, CDCl₃): δ = 149.0 (C), 144.5 (C), 144.2 (C), 136.7 (C), 135.3 (C), 134.5 (C), 129.9 (2×CH), 128.9 (2×CH), 128.6 (2×CH), 128.5 (2×CH), 128.0 (CH), 127.3 (CH), 123.0 (CH), 122.3 (C), 53.5 (CH₂), 43.0 (CH₃), 21.8 (CH₃); IR (neat): ν = 2923, 1507, 1356, 1318, 1163, 1089, 812, 728, 670; HRMS (ES): *m/z* calculated for C₂₁H₁₉N₄O₄S₂ClNa: 513.0434, found 513.0440 [M+Na]⁺.

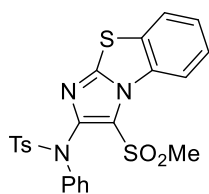
4-Methyl-*N*-(3-(methylsulfinyl)benzo[*d*]imidazo[2,1-*b*]oxazol-2-yl)-*N*-phenylbenzenesulfonamide (**645**)



To a solution of sulfide **602** (0.2 mmol, 89.9 mg, 1.0 eq.) in CH₂Cl₂ (2 mL) at 0 °C was added *m*CPBA (77% in water) (0.2 mmol, 53.8 mg, 2.2 eq.)

portionwise. The resulting reaction mixture was allowed to warm up to room temperature and was stirred for 4 h. The mixture was quenched with $\text{Na}_2\text{S}_2\text{O}_3(\text{sat sol})$ (4 mL) and washed with $\text{NaHCO}_3(\text{sat sol})$ (4 mL). The aqueous phase was extracted with CH_2Cl_2 (3×5 mL). The combined organic phases were dried over Na_2SO_4 , filtered off and concentrated under reduced pressure. Purification by flash column chromatography [hexane:EtOAc (3:2)] gave sulfoxide **645** as a white foam (52 mg, 56%); mp: 242–244 °C; ^1H NMR (400 MHz, CDCl_3): δ = 8.23–8.15 (m, 1H), 7.62–7.55 (m, 3H), 7.48–7.39 (m, 4H), 7.33–7.24 (m, 5H), 3.20 (s, 3H), 2.44 (s, 3H); ^{13}C NMR (101 MHz, CDCl_3): δ = 153.8 (C), 150.1 (C), 144.4 (C), 140.0 (C), 139.2 (C), 135.3 (C), 129.6 (2×CH), 129.3 (2×CH), 129.1 (2×CH), 128.7 (3×CH), 126.2 (C), 125.9 (CH), 125.4 (CH), 122.3 (C), 116.0 (CH), 112.5 (CH), 40.0 (CH_3), 21.8 (CH_3); IR (neat): ν = 2922, 1687, 1472, 1349, 1164, 961, 815, 751, 692, 664, 571; HRMS (ES): m/z calculated for $\text{C}_{23}\text{H}_{19}\text{N}_3\text{O}_4\text{S}_2\text{Na}$: 488.0715, found 488.0719 $[\text{M}+\text{Na}]^+$.

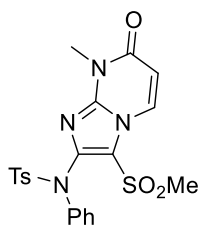
4-Methyl-N-(3-(methylsulfonyl)benzo[d]imidazo[2,1-b]thiazol-2-yl)-N-phenylbenzenesulfonamide (646)



To a solution of sulfide **601** (0.2 mmol, 93.1 mg, 1.0 eq.) in CH_2Cl_2 (2 mL) at 0 °C was added *m*CPBA (77% in water) (0.9 mmol, 197 mg, 4.4 eq.) portionwise. The resulting reaction mixture was allowed to warm up to room temperature and was stirred for 20 h. The mixture was quenched with $\text{Na}_2\text{S}_2\text{O}_3(\text{sat sol})$ (5 mL) and washed with $\text{NaHCO}_3(\text{sat sol})$ (5 mL). The aqueous phase was extracted with CH_2Cl_2 (3×10 mL). The combined organic phases were dried over Na_2SO_4 , filtered off and concentrated under reduced pressure. Purification by flash column chromatography [hexane:EtOAc (7:3)] gave sulfone **646** as a white powder (31 mg, 31%); mp: >250 °C; ^1H NMR (400 MHz, CDCl_3): δ = 8.67 (d, J = 8.5 Hz, 1H), 7.77 (dd, J = 8.0, 1.0 Hz, 1H), 7.64 (d,

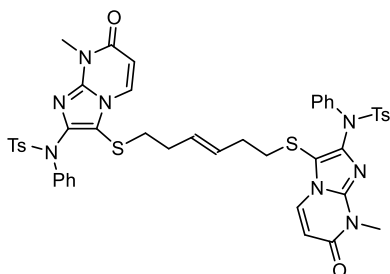
$J = 8.3$ Hz, 2H), 7.60–7.51 (m, 3H), 7.46 (app. td, $J = 8.0, 1.0$ Hz, 1H), 7.32–7.23 (m, 5H), 3.54 (s, 3H), 2.43 (s, 3H); ^{13}C NMR (101 MHz, CDCl_3): $\delta = 149.3$ (C), 147.1 (C), 144.1 (C), 139.2 (C), 135.9 (C), 133.0 (C), 129.52 (C), 129.47 (4 \times CH), 129.1 (2 \times CH), 128.8 (2 \times CH), 128.4 (CH), 127.5 (CH), 126.4 (CH), 124.3 (CH), 123.5 (C), 116.9 (CH), 45.3 (CH_3), 21.8 (CH_3); IR (neat): $\nu = 2913, 1682, 1478, 1347, 1329, 1161, 1088, 758, 693, 665, 567$; HRMS (ES): m/z calculated for $\text{C}_{23}\text{H}_{19}\text{N}_3\text{O}_4\text{NaS}_3$: 520.0435, found 520.0433 $[\text{M}+\text{H}]^+$.

4-Methyl-N-(8-methyl-3-(methylsulfonyl)-7-oxo-7,8-dihydroimidazo[1,2-a]pyrimidin-2-yl)-N-phenylbenzenesulfonamide (647)



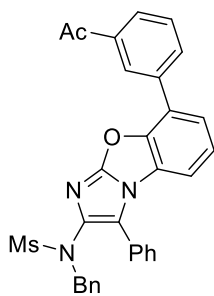
To a solution of sulfide **579** (0.2 mmol, 88.1 mg, 1.0 eq.) in CH_2Cl_2 (2 mL) at 0 °C was added *m*CPBA (77% in water) (0.9 mmol, 197 mg, 4.4 eq.) portionwise. The resulting reaction mixture was allowed to warm up to room temperature and was stirred for 5 h. The mixture was quenched with saturated $\text{Na}_2\text{S}_2\text{O}_3(\text{aq})$ (10 mL) and washed with saturated $\text{NaHCO}_3(\text{aq})$ (10 mL). The aqueous phase was extracted with CH_2Cl_2 (3 \times 10 mL). The combined organic phases were dried over Na_2SO_4 , filtered off and concentrated under reduced pressure. Purification by flash column chromatography [hexane:EtOAc (3:2)] gave sulfone **647** as a white-off solid (39 mg, 42%); mp: >250 °C; ^1H NMR (400 MHz, CDCl_3): $\delta = 8.53$ (d, $J = 8.0$ Hz, 1H), 7.61 (d, $J = 8.3$ Hz, 2H), 7.50–7.40 (m, 2H), 7.33–7.20 (m, 5H), 6.34 (d, $J = 8.0$ Hz, 1H), 3.62 (s, 3H), 3.41 (s, 3H), 2.44 (s, 3H); ^{13}C NMR (101 MHz, CDCl_3): $\delta = 158.8$ (C), 144.5 (C), 144.4 (C), 143.8 (C), 138.8 (C), 135.0 (C), 133.2 (CH), 129.4 (2 \times CH), 129.2 (4 \times CH), 129.1 (2 \times CH), 128.7 (CH), 117.8 (C), 110.0 (CH), 46.1 (CH_3), 29.7 (CH_3), 21.8 (CH_3); IR (neat): $\nu = 1687, 1526, 1475, 1357, 1325, 1159, 1117, 1090, 817, 666, 561$; HRMS (ES): m/z calculated for $\text{C}_{21}\text{H}_{20}\text{N}_4\text{O}_5\text{NaS}_2$: 495.0773, found 495.0772 $[\text{M}+\text{Na}]^+$.

(Z)-N,N'-((Hex-3-ene-1,6-diylbis(sulfanediyl))bis(8-methyl-7-oxo-7,8-dihydroimidazo[1,2-a]pyrimidine-3,2-diyl))bis(4-methyl-N-phenylbenzenesulfonamide) (654)



To a heat-gun dried Schlenk tube containing a solution of imidazole **584** (0.06 mmol, 30.0 mg, 1.0 eq.) in dry CH₂Cl₂ (0.4 mL) was added Grubbs II catalyst (0.004 mmol, 3.7 mg, 0.07 eq.). The mixture was stirred at room temperature for 18 h. The crude reaction mixture was concentrated under reduced pressure. Purification by flash column chromatography [hexane:EtOAc (3:2)] afforded dimer **654** as a pale grey powder (24 mg, 82%); mp: 246–248 °C; ¹H NMR (400 MHz, CDCl₃): δ = 7.99 (d, *J* = 7.8 Hz, 2H), 7.73 (d, *J* = 8.5 Hz, 4H), 7.43–7.37 (m, 4H), 7.29–7.20 (m, 10H), 6.22 (d, *J* = 7.8 Hz, 2H), 5.41 (t, *J* = 3.7 Hz, 2H), 3.61 (s, 6H), 2.69 (t, *J* = 7.3 Hz, 4H), 2.43 (s, 6H), 2.26–2.17 (m, 4H); ¹³C NMR (125 MHz, CDCl₃): δ = 159.9 (2×C), 145.3 (2×C), 143.9 (2×C), 143.1 (2×C), 140.2 (2×C), 136.0 (2×C), 132.1 (2×CH), 129.8 (2×CH), 129.1 (4×CH), 129.1 (4×CH), 129.0 (4×CH), 128.6 (4×CH), 127.9 (2×CH), 113.1 (2×C), 108.1 (2×CH), 36.3 (2×CH₂), 32.8 (2×CH₂), 29.2 (2×CH₃), 21.8 (2×CH₃); IR (neat): ν = 2924, 1679, 1530, 1476, 1347, 1160, 1088, 939, 813, 693, 565; HRMS (ES): *m/z* calculated for C₄₆H₄₄N₈O₆NaS₄: 955.2164, found 955.2169 [M+Na]⁺. The stereochemistry of **654** could not be assigned as yet a single crystal has not been successfully grown.

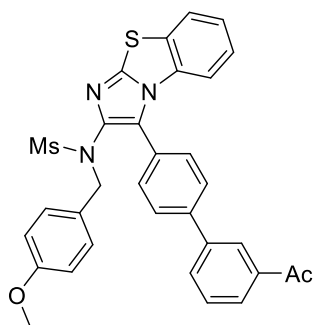
N-(8-(3-Acetylphenyl)-3-phenylbenzo[d]imidazo[2,1-b]oxazol-2-yl)-N-benzylmethanesulfonamide (664)



Following a reported procedure,¹¹¹ a heat-gun dried Schlenk tube was charged with bromide **352** (0.1 mmol, 49.6 mg, 1.0 eq.), boronic acid **663**

(0.2 mmol, 24.6 mg, 1.5 eq.), K₂CO₃ (0.3 mmol, 41.5 mg, 3.0 eq.) and Pd(PPh₃)₄ (0.005 mmol, 5.8 mg, 0.05 eq.). It was evacuated and back-filled with argon (3 cycles). Degassed 1,4-dioxane (1.4 mL) and H₂O (0.5 mL) were added and the mixture was stirred at 83 °C for 23 h. The crude mixture was allowed to cool down to room temperature, diluted with EtOAc (10 mL) and washed with KHSO₄ [1 M] (10 mL), brine (10 mL) and saturated NaHCO_{3(aq)} (10 mL). The organic phases were dried over Na₂SO₄, filtered off and concentrated under vacuum. Purification by flash column chromatography [hexane:EtOAc (7:3)] afforded compound **664** as a yellow powder (36 mg, 67%); mp: 232–235 °C; ¹H NMR (300 MHz, CDCl₃): δ = 8.37 (s, 1H), 8.10–7.98 (m, 2H), 7.63 (t, *J* = 7.8 Hz, 1H), 7.50 (dd, *J* = 6.9, 2.2 Hz, 1H), 7.45–7.34 (m, 5H), 7.33–7.22 (m, 3H), 7.12–6.91 (m, 4H), 4.69 (s, 2H), 3.27 (s, 3H), 2.70 (s, 3H); ¹³C NMR (101 MHz, CDCl₃): δ = 197.8 (C), 151.8 (C), 147.5 (C), 137.9 (C), 134.9 (C), 134.8 (C), 133.7 (C), 133.3 (CH), 129.4 (CH), 129.3 (2×CH), 128.8 (2×CH), 128.7 (CH), 128.6 (3×CH), 128.3 (CH), 128.1 (3×CH), 127.8 (CH), 127.4 (C), 127.0 (C), 125.9 (C), 124.6 (2×CH), 123.7 (C), 111.6 (CH), 55.4 (CH₂), 38.4 (CH₃), 26.9 (CH₃); IR (neat): ν = 1682, 1589, 1340, 1247, 1157, 958, 783, 702, 692; HRMS (ES): *m/z* calculated for C₃₁H₂₅N₃O₄NaS: 558.1463, found 558.1472 [M+Na]⁺.

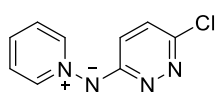
***N*-(3-(3'-Acetyl-[1,1'-biphenyl]-4-yl)benzo[d]imidazo[2,1-*b*]thiazol-2-yl)-*N*-(4-methoxybenzyl)methanesulfonamide (665)**



Following a reported procedure,¹¹¹ a heat-gun dried Schlenk tube was charged with bromide **305** (0.1 mmol, 54.2 mg, 1.0 eq.), boronic acid **663** (0.2 mmol, 24.6 mg, 1.5 eq.), K₂CO₃ (0.3 mmol, 41.5 mg, 3.0 eq.) and Pd(PPh₃)₄ (0.005 mmol, 5.8 mg, 0.05 eq.). It was evacuated and back-filled with argon (3 cycles). Degassed 1,4-

dioxane (1.4 mL) and H₂O (0.5 mL) were added and the mixture was stirred at 83 °C for 20 h. The crude mixture was allowed to cool down to room temperature, diluted with EtOAc (10 mL) and washed with KHSO₄ [1 M] (10 mL), brine (10 mL) and saturated NaHCO_{3(aq)} (10 mL). The organic phases were dried over Na₂SO₄, filtered off and concentrated under vacuum. Purification by flash column chromatography [hexane:EtOAc (13:3)] afforded compound **665** as a beige oil (54 mg, 92%); mp: 110–113 °C (decomp); ¹H NMR (300 MHz, CDCl₃): δ = 8.28 (t, *J* = 1.3 Hz, 1H), 7.99 (app. td, *J* = 7.8, 1.3 Hz, 1H), 7.89 (app. td, *J* = 7.8, 1.3 Hz, 1H), 7.69 (d, *J* = 7.8 Hz, 1H), 7.65–7.55 (m, 3H), 7.35–7.24 (m, 3H), 7.22–7.11 (m, 2H), 6.89 (d, *J* = 8.6 Hz, 2H), 6.52 (d, *J* = 8.6 Hz, 2H), 4.63 (s, 2H), 3.67 (s, 3H), 3.28 (s, 3H), 2.71 (s, 3H); ¹³C NMR (101 MHz, CDCl₃): δ = 198.2 (C), 159.3 (C), 144.9 (C), 141.1 (C), 140.6 (C), 138.5 (C), 137.9 (C), 133.1 (C), 131.8 (CH), 130.1 (2×CH), 130.6 (2×CH), 129.7 (C), 129.4 (CH), 127.7 (CH), 127.4 (C), 127.2 (C), 127.02 (CH), 126.99 (2×CH), 126.7 (C), 126.0 (CH), 125.1 (CH), 124.2 (CH), 114.2 (CH), 113.5 (2×CH), 55.3 (CH₃), 54.8 (CH₂), 38.5 (CH₃), 26.9 (CH₃); IR (neat): ν = 2926, 1682, 1487, 1331, 1237, 1147, 963, 759, 690, 563; HRMS (ES): *m/z* calculated for C₃₂H₂₈N₃O₄S₂: 582.1521, found 582.1528 [M+H]⁺.

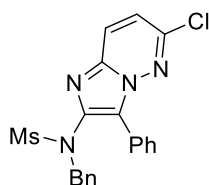
(6-Chloropyridazin-3-yl)(pyridin-1-ium-1-yl)amide (262)



Following **GP6** using *N*-aminopyridinium iodide (666 mg, 3.0 mmol), 1,4-dichlorobenzene (456 mg, 3.1 mmol) and K₂CO₃ (1.24 g, 9.0 mmol) for 24 h. Purification by flash column chromatography [EtOAc:MeOH (9:1)] afforded aminide **262** as a yellow powder (550 mg, 89%); ¹H NMR (300 MHz, CDCl₃): δ = 9.07–9.3 (m, 2H), 7.73 (tt, *J* = 7.6, 1.2 Hz 1H), 7.62–7.55 (m, 2H), 7.01 (d, *J* = 9.3 Hz, 1H), 6.74 (d, *J* = 9.3 Hz, 1H); ¹³C NMR (101 MHz, CDCl₃): δ = 162.5 (C), 145.5 (C), 142.1 (2×CH), 134.3 (CH),

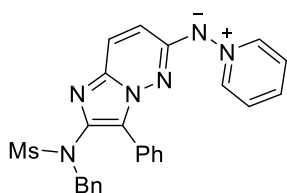
128.5 (CH), 126.4 (2×CH), 122.3 (CH); IR (neat): ν = 3029, 1579, 1473, 1412, 1339, 1147, 1004, 839, 766, 675; MS (ES): m/z 207.05 $[M+H]^+$.

N-Benzyl-N-(6-chloro-3-phenylimidazo[1,2-*b*]pyridazin-2-yl)methanesulfonamide (673)



Following **GP7** using ynamide **297** (143 mg, 0.5 mmol), aminide **262** (124 mg, 0.6 mmol) for 1 h. Purification by flash column chromatography [hexane:EtOAc (3:2)] afforded imidazole **673** as a pale yellow solid (179 mg, 87%); mp: 68–70 °C (decomp); ^1H NMR (400 MHz, CDCl_3): δ = 7.86 (d, J = 9.4 Hz, 1H), 7.59–7.54 (m, 2H), 7.41–7.36 (m, 3H), 7.15–7.08 (m, 2H), 7.06–6.96 (m, 4H), 4.75 (s, 2H), 3.25 (s, 3H); ^{13}C NMR (101 MHz, CDCl_3): δ = 147.4 (C), 140.2 (C), 135.0 (C), 134.7 (C), 129.3 (2×CH), 129.2 (2×CH), 129.1 (CH), 128.4 (2×CH), 128.3 (2×CH), 128.0 (CH), 127.0 (CH), 126.7 (C), 125.8 (C), 119.8 (CH), 55.5 (CH_2), 39.4 (CH_3); IR (neat): ν = 2926, 1489, 1343, 1296, 1152, 1097, 958, 803, 694; HRMS (ES): m/z calculated for $\text{C}_{20}\text{H}_{17}\text{N}_4\text{O}_2\text{NaS}^{35}\text{Cl}$: 435.0658, found 435.0659 $[M+\text{Na}]^+$.

(2-(N-Benzylmethylsulfonamido)-3-phenylimidazo[1,2-*b*]pyridazin-6-yl)(pyridin-1-ium-1-yl)amide (674)

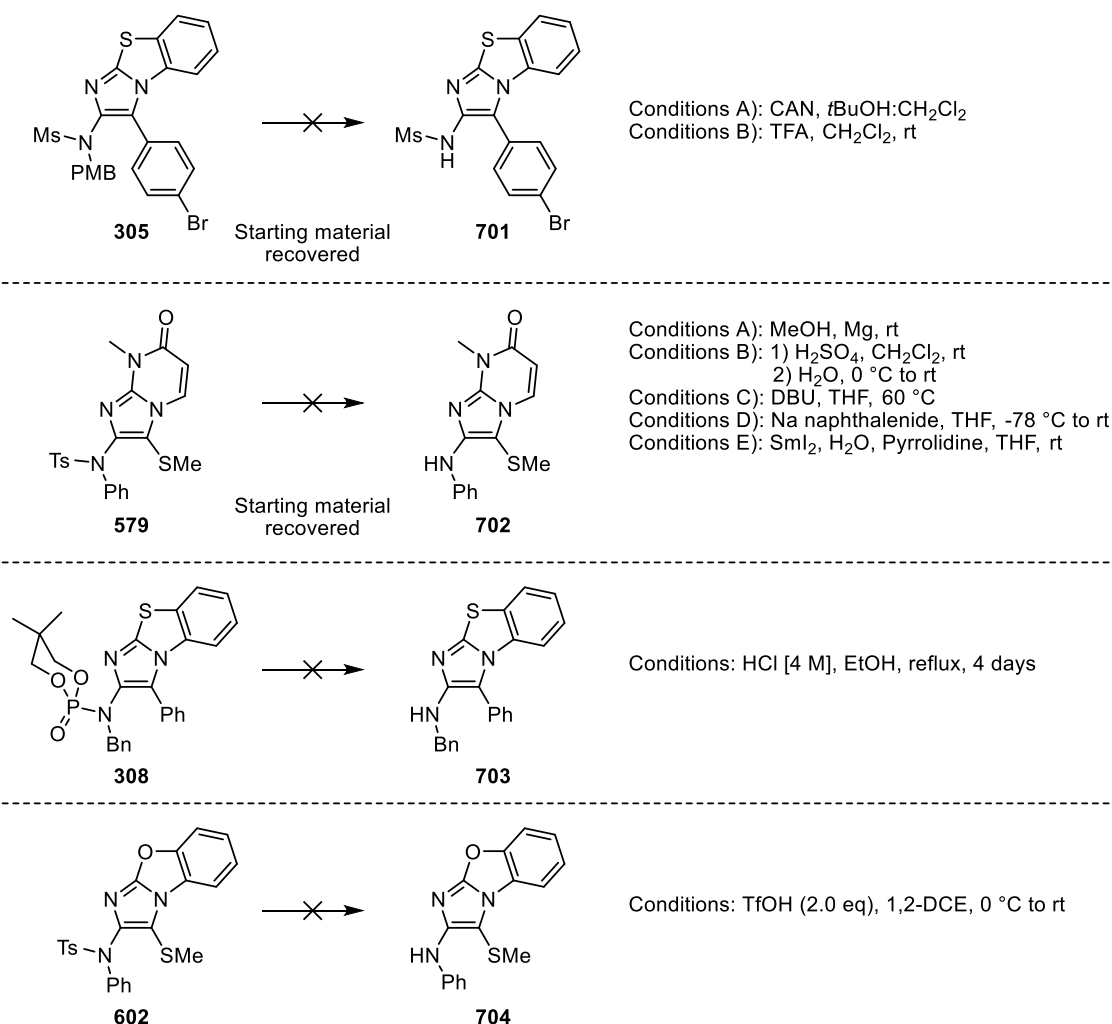


Following **GP6** using *N*-aminopyridinium iodide (111 mg, 0.3 mmol), imidazole **673** (129 mg, 0.3 mmol) and K_2CO_3 (124 mg, 0.9 mmol) for 6 h. Purification by flash column chromatography [EtOAc:MeOH (9:1)] afforded aminide **674** as a yellow solid (72 mg, 51%); mp: 198–200 °C; ^1H NMR (300 MHz, CDCl_3): δ = 9.21–9.13 (m, 2H), 7.57–7.47 (m, 4H), 7.43–7.35 (m, 2H), 7.28–7.20 (m, 3H), 7.10–6.95 (m, 5H), 6.71 (d, J = 9.8 Hz, 1H), 4.75 (s, 2H), 3.27 (s, 3H); ^{13}C NMR (101 MHz, CDCl_3) δ 157.2 (C), 140.8 (CH), 135.9 (C), 135.4 (C), 134.1 (C), 131.8

(CH), 129.3 (2×CH), 129.2 (2×CH), 128.11 (CH), 128.06 (2×CH), 127.63 (2×CH), 127.61 (2×CH), 125.7 (2×CH), 125.3 (C), 124.6 (CH), 118.9 (CH), 55.5 (CH₂), 38.9 (CH₃) *one resonance for a quaternary carbon was not observed*; IR (neat): ν = 2926, 1490, 1450, 1341, 1296, 1140, 957, 759, 697, 665; HRMS (ES): m/z calculated for C₂₅H₂₃N₆O₂S: 471.1603, found 471.1602 [M+H]⁺.

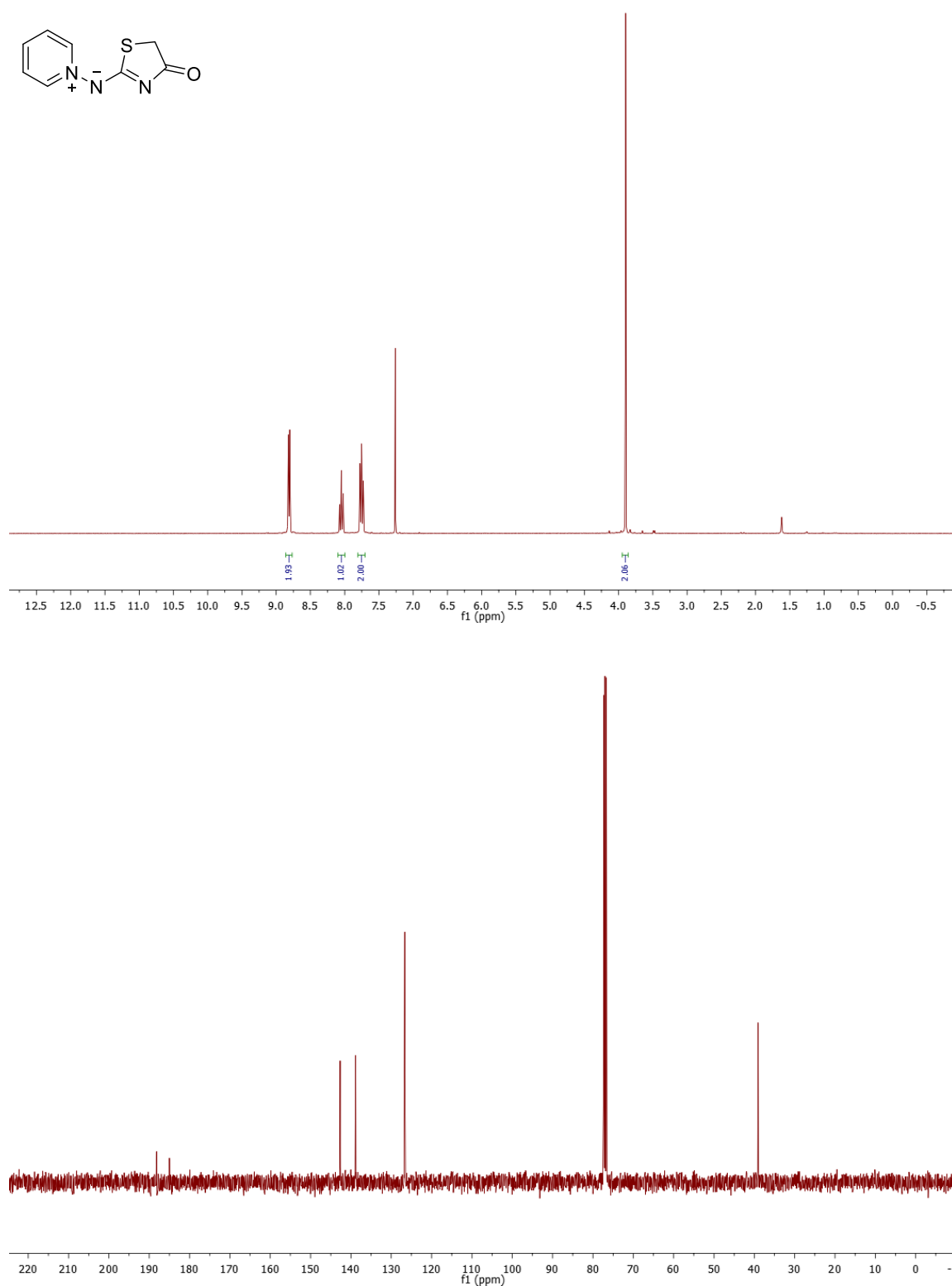
3. Attempted sulfonamide deprotections

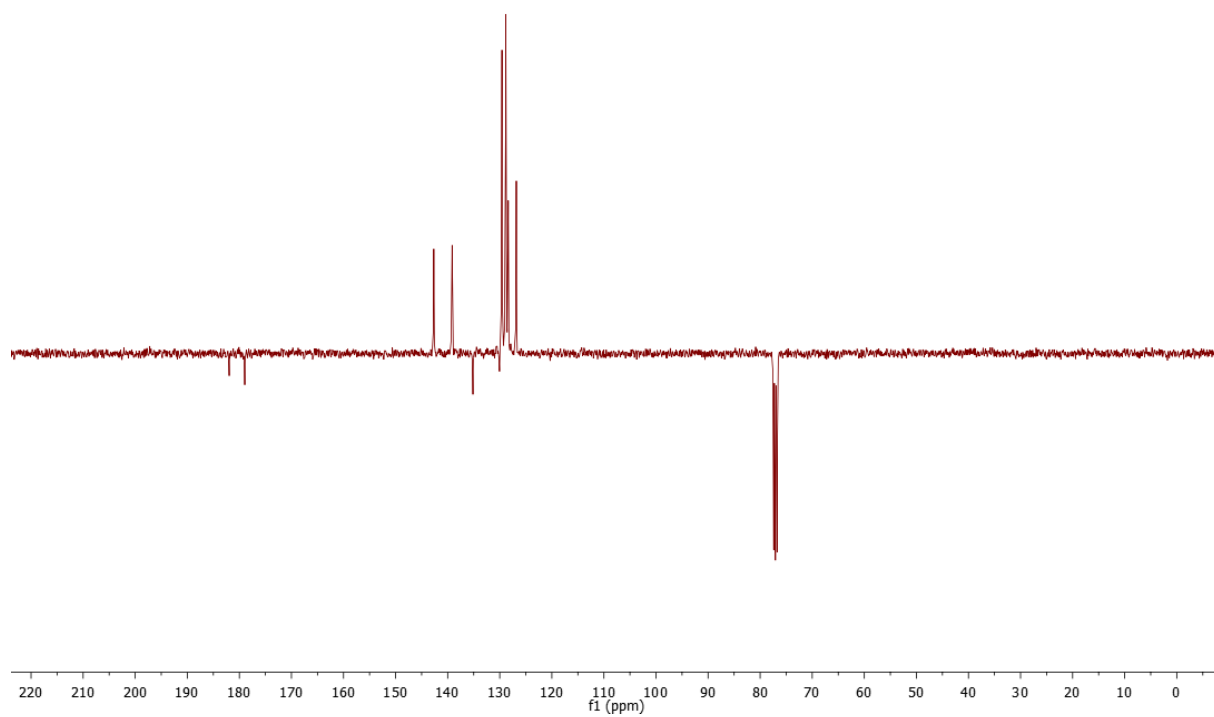
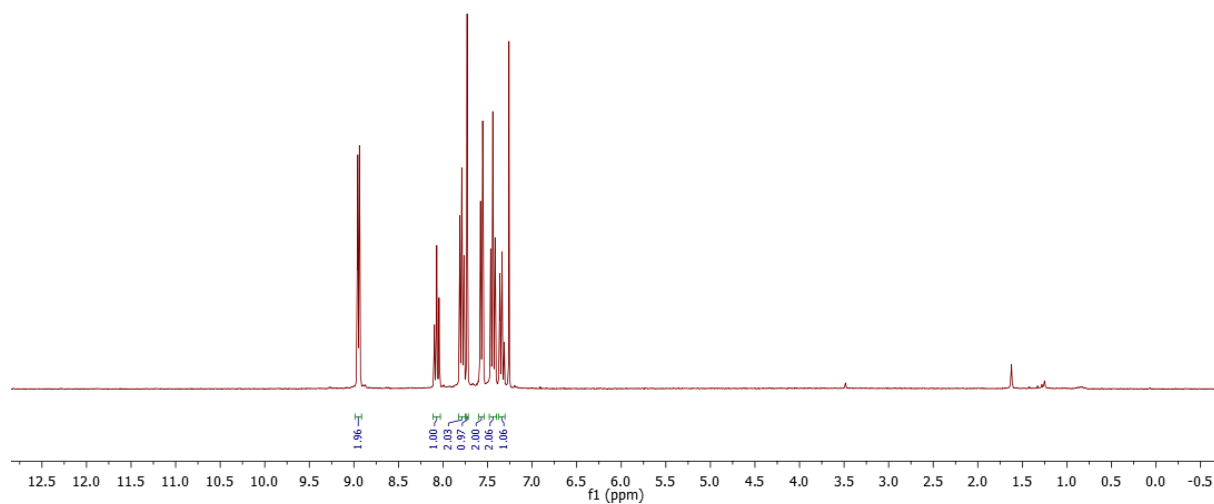
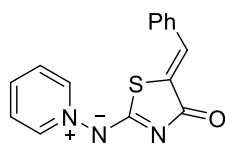
Several reaction conditions to deprotect the aminide were attempted in several protecting groups on the sulfonamide moiety. PMB removal was tried using cerium ammonium nitrate (CAN) and trifluoroacetic acid but the amine was notoriously robust. Cleavage of the tosyl group was attempted using a range of conditions, classically applied for tosyl cleavage, yet none of them proved fruitful; just starting material was recovered. Attempted cleavage of the phosphoramidite moiety also failed.

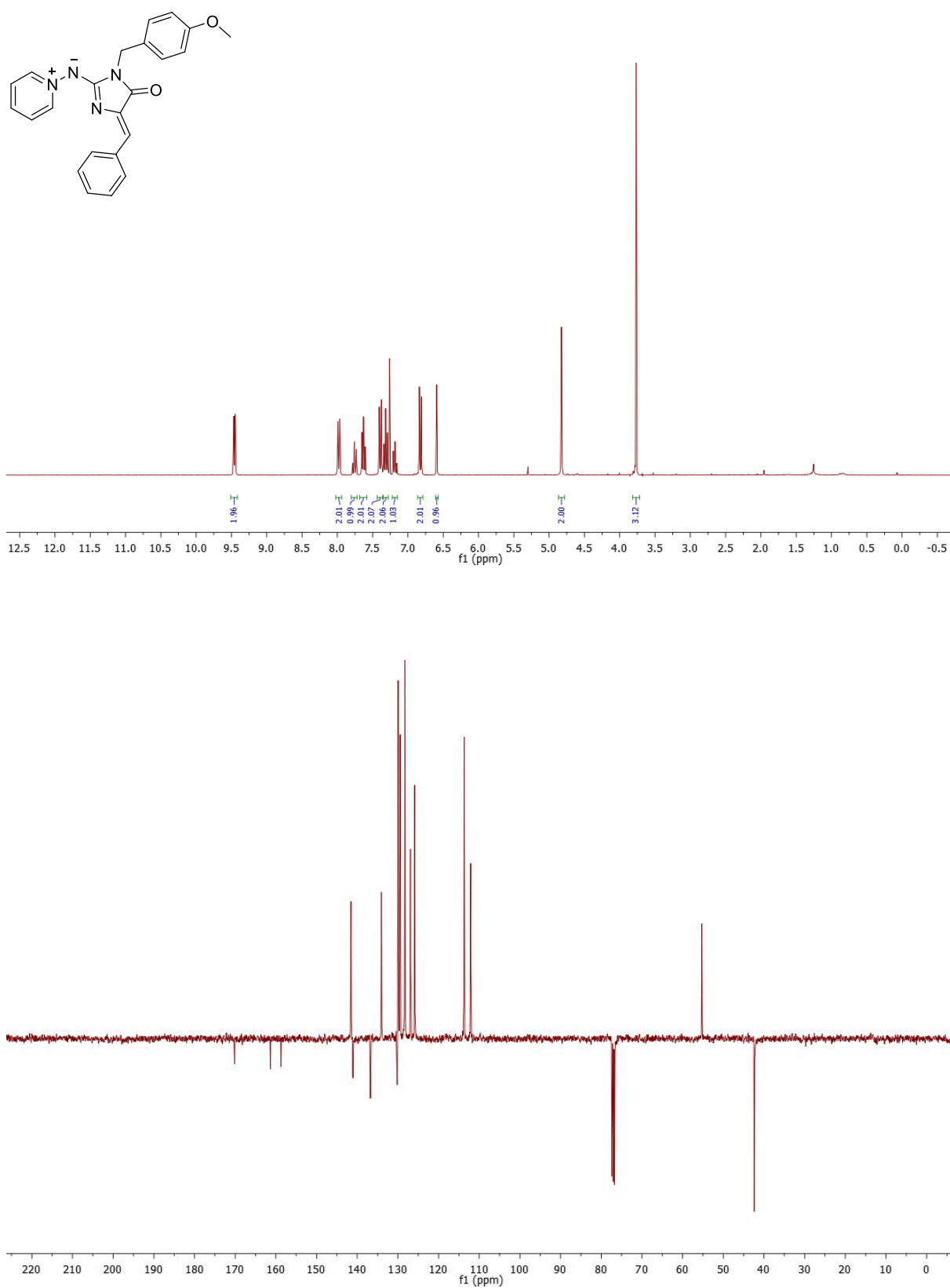


4. Selected NMR Spectra

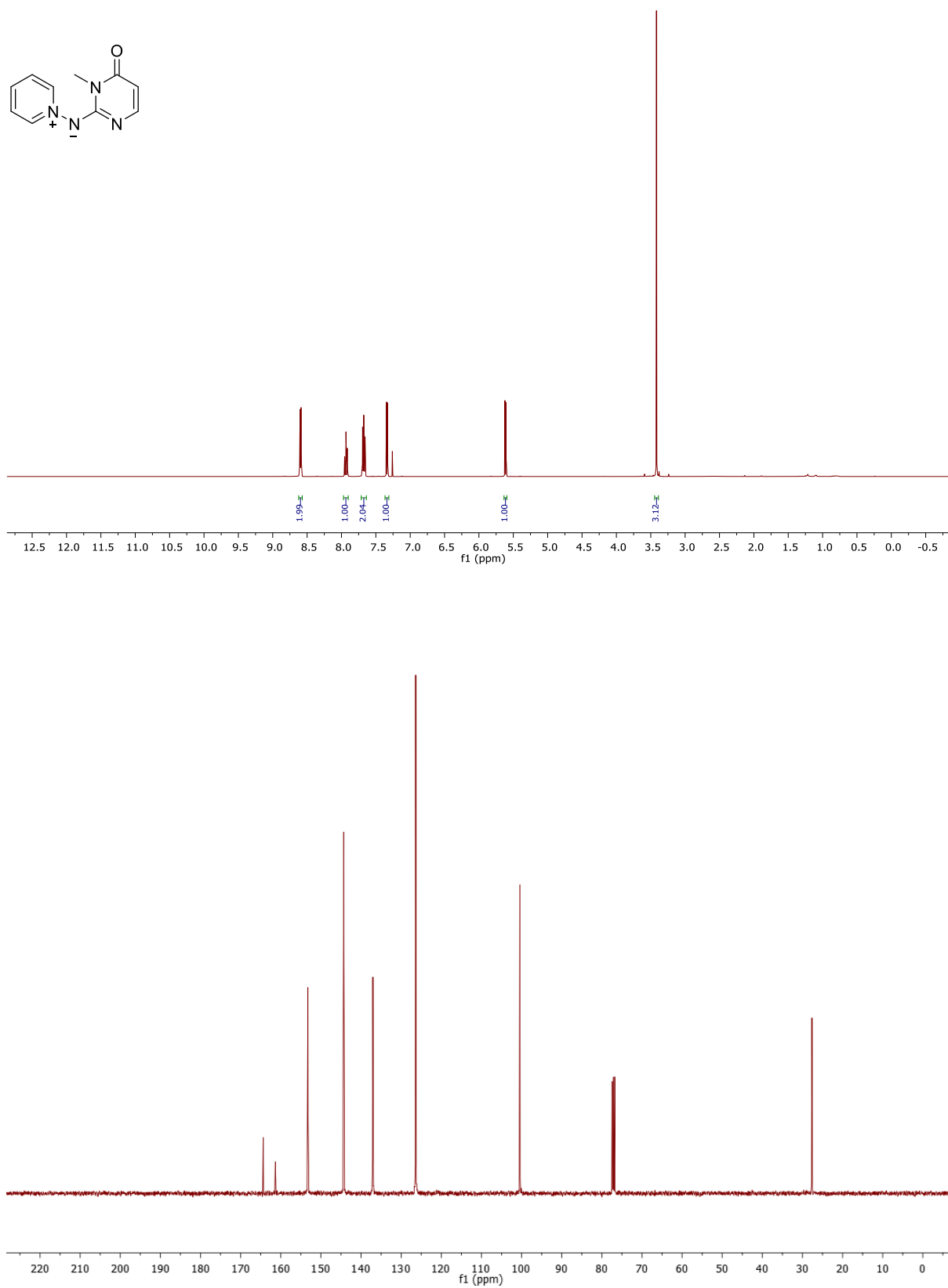
Aminide 422 – ^1H NMR (300 MHz, CDCl_3) and ^{13}C NMR (UDEFT) (101 MHz, CDCl_3)

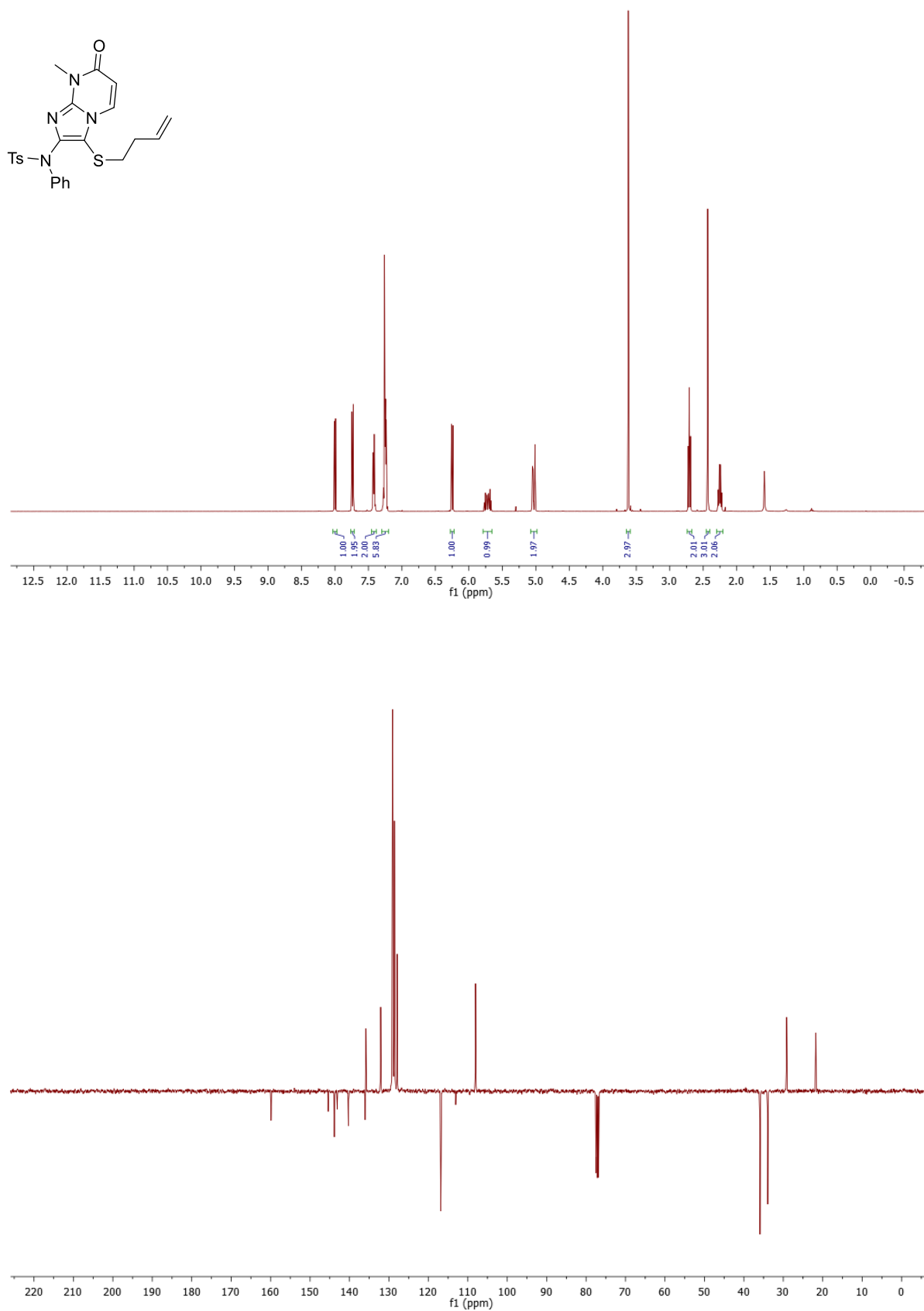


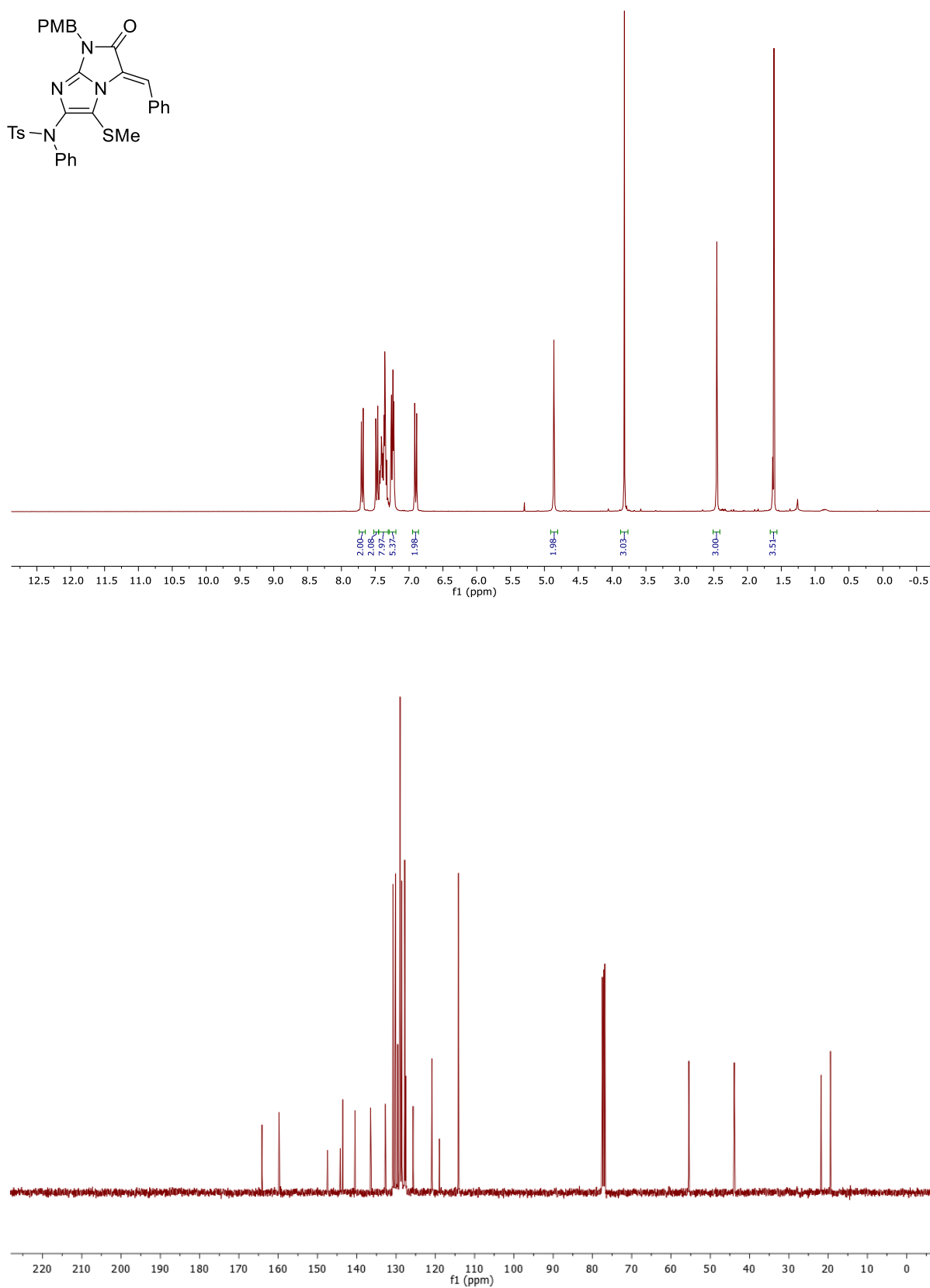
Aminide 427 – ^1H NMR (300 MHz, CDCl_3) and ^{13}C NMR (Pendant) (101 MHz, CDCl_3)

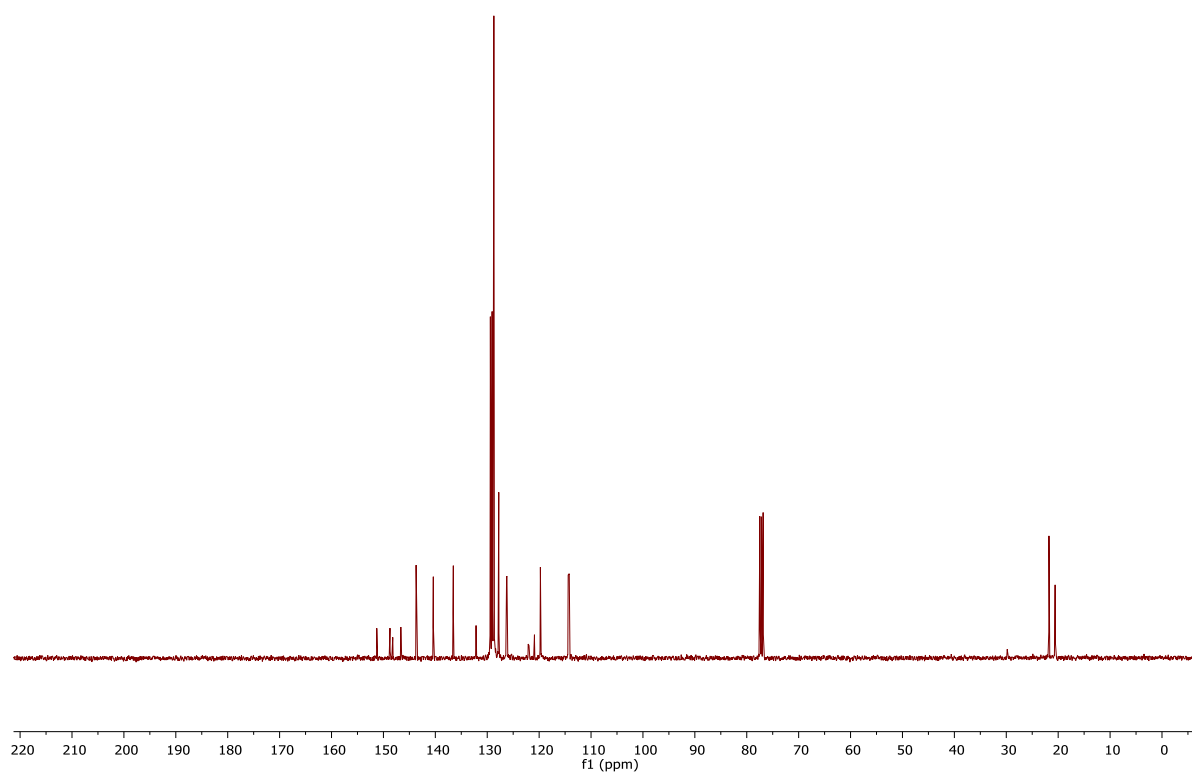
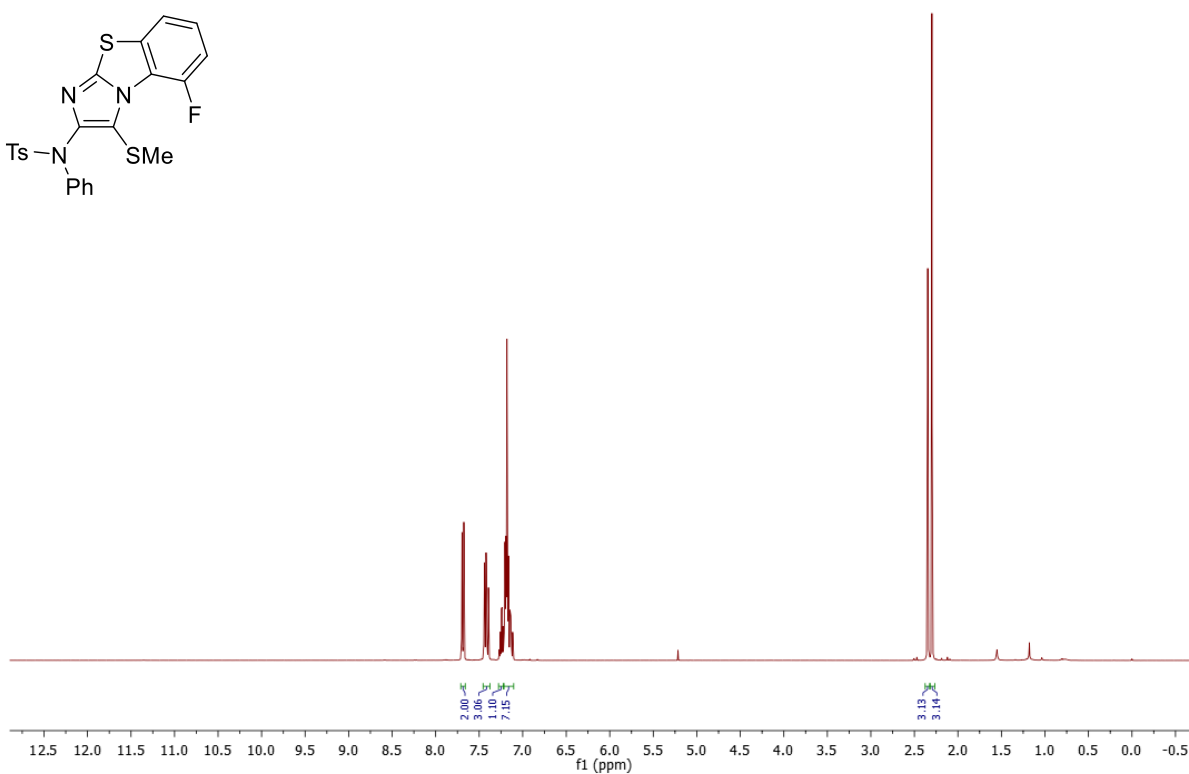
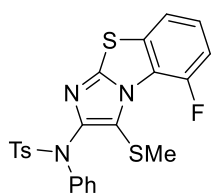
Aminide 460 – ^1H NMR (300 MHz, CDCl_3) and ^{13}C NMR (Pendant) (101 MHz, CDCl_3)

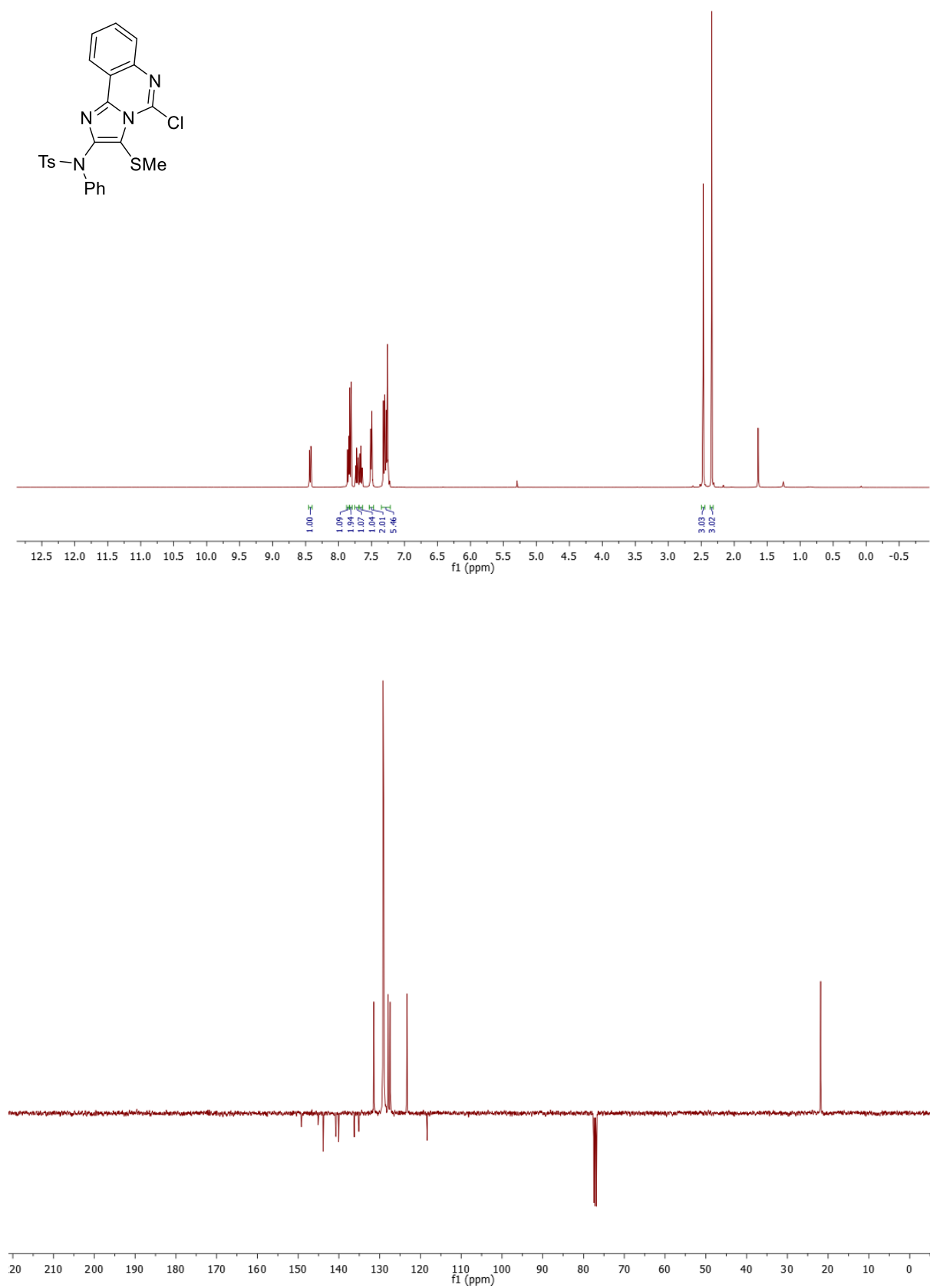
Aminide 471 – ^1H NMR (400 MHz, CDCl_3) and ^{13}C NMR (UDEFT) (101 MHz, CDCl_3)

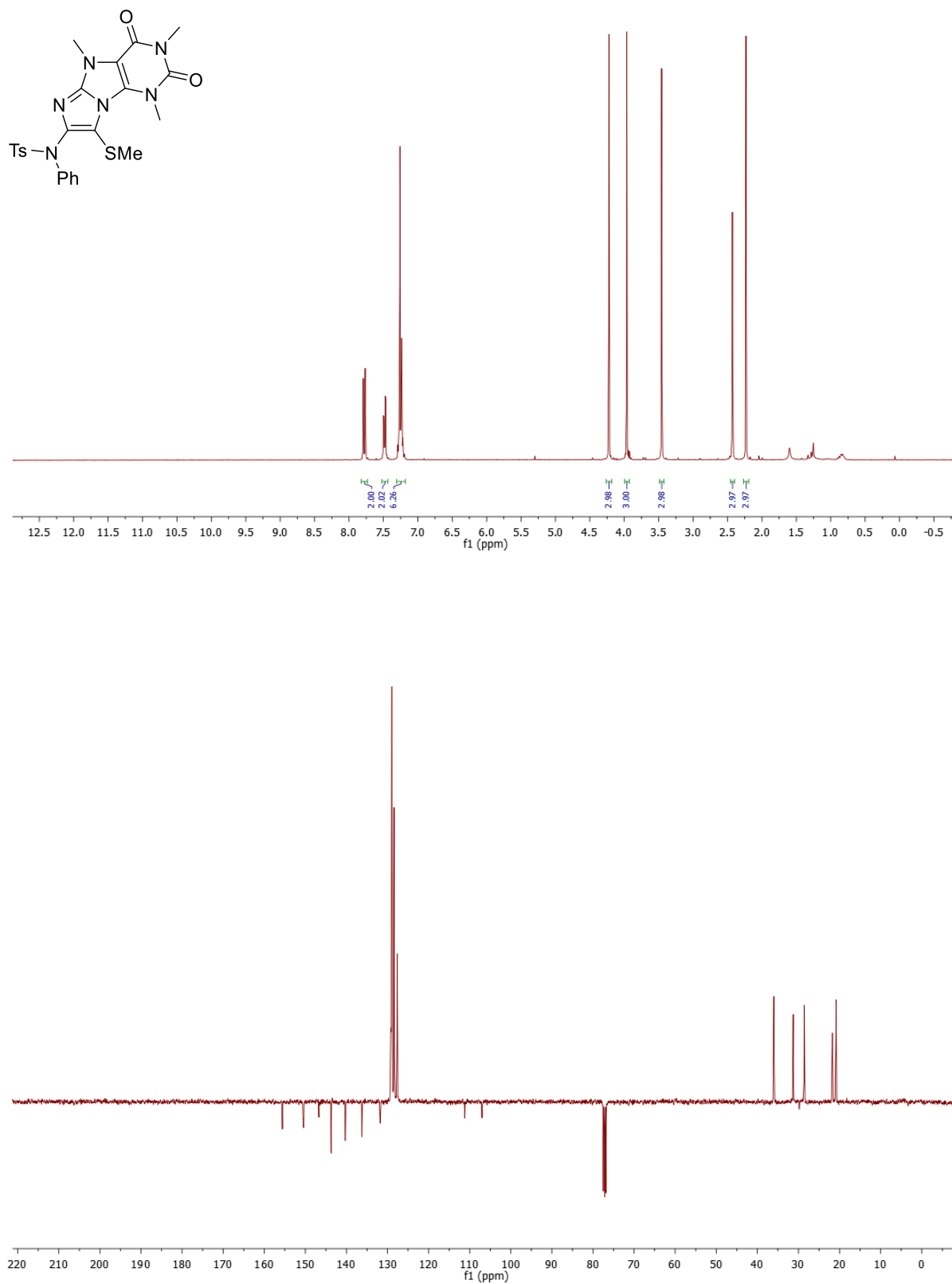


Imidazole 584 – ^1H NMR (400 MHz, CDCl_3) and ^{13}C NMR (Pendant) (101 MHz, CDCl_3)

Imidazole 595 – ^1H NMR (400 MHz, CDCl_3) and ^{13}C NMR (UDEFT) (101 MHz, CDCl_3)

Imidazole 606 – ^1H NMR (400 MHz, CDCl_3) and ^{13}C NMR (UDEFT) (101 MHz, CDCl_3)

Imidazole 615 – ^1H NMR (400 MHz, CDCl_3) and ^{13}C NMR (Pendant) (101 MHz, CDCl_3)

Imidazole 636 – ^1H NMR (400 MHz, CDCl_3) and ^{13}C NMR (Pendant) (101 MHz, CDCl_3)

5. Crystallographic Data

Aminide 422

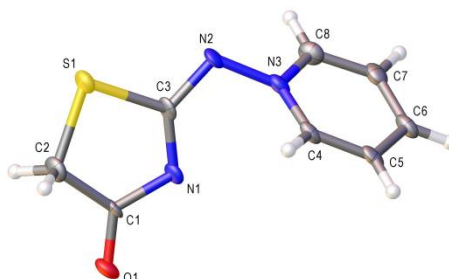
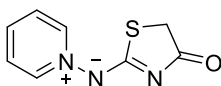


Table 1 Crystal data and structure refinement for 422.

Identification code	422
Empirical formula	C ₈ H ₇ N ₃ OS
Formula weight	193.23
Temperature/K	100.01(10)
Crystal system	orthorhombic
Space group	Pca2 ₁
a/Å	22.159(2)
b/Å	3.8818(4)
c/Å	9.3990(7)
α/°	90
β/°	90
γ/°	90
Volume/Å ³	808.49(13)
Z	4
ρ _{calc} /g/cm ³	1.587
μ/mm ⁻¹	3.224
F(000)	400.0
Crystal size/mm ³	0.218 × 0.026 × 0.021
Radiation	CuKα (λ = 1.54184)
2θ range for data collection/°	7.98 to 148.994
Index ranges	-27 ≤ h ≤ 27, -4 ≤ k ≤ 2, -11 ≤ l ≤ 11

Reflections collected	4726
Independent reflections	1530 [$R_{\text{int}} = 0.1307$, $R_{\text{sigma}} = 0.0931$]
Data/restraints/parameters	1530/163/118
Goodness-of-fit on F^2	1.115
Final R indexes [$I \geq 2\sigma(I)$]	$R_1 = 0.1219$, $wR_2 = 0.3030$
Final R indexes [all data]	$R_1 = 0.1243$, $wR_2 = 0.3045$
Largest diff. peak/hole / $e \text{ \AA}^{-3}$	1.42/-0.75
Flack parameter	0.09(4)

Table 2 Fractional Atomic Coordinates ($\times 10^4$) and Equivalent Isotropic Displacement Parameters ($\text{\AA}^2 \times 10^3$) for 422. U_{eq} is defined as 1/3 of of the trace of the orthogonalised U_{IJ} tensor.

Atom	x	y	z	$U(\text{eq})$
C1	3918(6)	4800(30)	7700(13)	14(2)
C2	4490(7)	3240(40)	8281(14)	22(3)
C3	4217(6)	2210(40)	5718(13)	16(2)
C4	3183(6)	310(30)	4079(13)	17(2)
C5	2667(6)	850(40)	3362(14)	19(3)
C6	2701(7)	2750(40)	2052(14)	21(3)
C7	3246(6)	3840(40)	1586(16)	23(3)
C8	3760(7)	3290(40)	2388(15)	22(3)
N1	3780(5)	4010(30)	6326(11)	16(2)
N2	4256(5)	980(30)	4381(12)	18(2)
N3	3711(5)	1630(30)	3641(12)	19(2)
O1	3588(5)	6600(30)	8457(11)	24(2)
S1	4862.1(14)	1217(8)	6779(3)	20.4(8)

Table 3 Anisotropic Displacement Parameters ($\text{\AA}^2 \times 10^3$) for 422. The Anisotropic displacement factor exponent takes the form: $-2\pi^2[h^2a^{*2}U_{11}+2hka^*b^*U_{12}+\dots]$.

Atom	U_{11}	U_{22}	U_{33}	U_{23}	U_{13}	U_{12}
C1	24(5)	12(5)	5(4)	-2(4)	0(4)	0(4)
C2	31(6)	22(6)	11(5)	5(5)	-3(4)	2(5)
C3	26(5)	16(5)	6(4)	5(4)	-3(4)	-3(4)
C4	30(5)	12(5)	9(5)	-1(4)	1(4)	-3(4)
C5	31(6)	13(5)	12(5)	-5(4)	2(4)	-4(5)
C6	35(5)	17(5)	10(5)	-1(4)	-1(4)	2(5)
C7	32(5)	19(5)	17(5)	-7(5)	-2(5)	4(5)
C8	30(6)	18(5)	18(5)	5(5)	3(5)	1(5)

N1	24(5)	17(5)	7(4)	2(4)	0(3)	-1(4)
N2	25(5)	17(5)	13(4)	-9(4)	0(4)	-1(4)
N3	28(5)	18(5)	11(4)	-3(4)	1(4)	-1(4)
O1	32(5)	27(6)	15(5)	-9(4)	4(4)	0(4)
S1	26.8(15)	23.4(15)	11.0(13)	0.0(15)	-2.1(12)	0.6(13)

Table 4 Bond Lengths for 422.

Atom	Atom	Length/Å	Atom	Atom	Length/Å
C1	C2	1.506(19)	C4	C5	1.34(2)
C1	N1	1.362(17)	C4	N3	1.342(18)
C1	O1	1.236(16)	C5	C6	1.44(2)
C2	S1	1.814(15)	C6	C7	1.35(2)
C3	N1	1.323(18)	C7	C8	1.38(2)
C3	N2	1.346(17)	C8	N3	1.346(19)
C3	S1	1.785(13)	N2	N3	1.417(16)

Table 5 Bond Angles for 422.

Atom	Atom	Atom	Angle/°	Atom	Atom	Atom	Angle/°
N1	C1	C2	116.2(12)	C7	C6	C5	119.0(13)
O1	C1	C2	121.0(11)	C6	C7	C8	120.7(14)
O1	C1	N1	122.8(12)	N3	C8	C7	119.0(13)
C1	C2	S1	105.9(9)	C3	N1	C1	111.4(11)
N1	C3	N2	129.5(12)	C3	N2	N3	109.9(11)
N1	C3	S1	117.3(9)	C4	N3	C8	121.4(12)
N2	C3	S1	113.2(10)	C4	N3	N2	121.7(11)
N3	C4	C5	122.0(13)	C8	N3	N2	116.5(11)
C4	C5	C6	117.7(13)	C3	S1	C2	88.7(6)

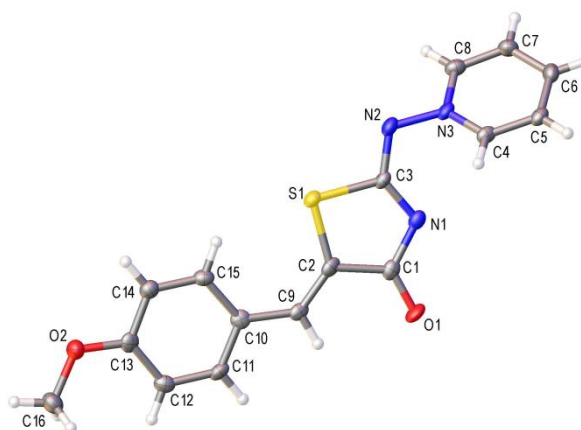
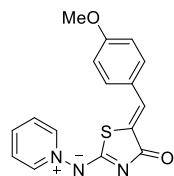
Table 6 Torsion Angles for 422.

A	B	C	D	Angle/°	A	B	C	D	Angle/°
C1	C2	S1	C3	-5.8(10)	N1	C1	C2	S1	7.8(15)
C2	C1	N1	C3	-5.4(17)	N1	C3	N2	N3	-5(2)
C3	N2	N3	C4	-61.1(16)	N1	C3	S1	C2	3.7(11)
C3	N2	N3	C8	126.6(13)	N2	C3	N1	C1	-179.1(14)
C4	C5	C6	C7	1(2)	N2	C3	S1	C2	-176.9(11)
C5	C4	N3	C8	-6(2)	N3	C4	C5	C6	3(2)
C5	C4	N3	N2	-178.2(12)	O1	C1	C2	S1	-174.3(11)
C5	C6	C7	C8	-3(2)	O1	C1	N1	C3	176.6(13)
C6	C7	C8	N3	0(2)	S1	C3	N1	C1	0.3(15)
C7	C8	N3	C4	4(2)	S1	C3	N2	N3	175.5(8)

C7 C8 N3 N2 176.7(12)

Table 7 Hydrogen Atom Coordinates ($\text{\AA} \times 10^4$) and Isotropic Displacement Parameters ($\text{\AA}^2 \times 10^3$) for 422.

Atom	<i>x</i>	<i>y</i>	<i>z</i>	U(eq)
H2A	4398.14	1550.59	9009.42	26
H2B	4744.95	5011.93	8691.25	26
H4	3173.69	-1008.61	4903.64	20
H5	2301	13.22	3701.8	22
H6	2353.38	3217.53	1533.33	25
H7	3274.98	4966.1	716.62	27
H8	4133.61	4048.75	2067.26	26

Aminide 429**Table 1 Crystal data and structure refinement for 429.**

Identification code	429
Empirical formula	C ₁₆ H ₁₃ N ₃ O ₂ S
Formula weight	311.35
Temperature/K	100.00(10)
Crystal system	monoclinic
Space group	P2 ₁ /c
a/Å	18.552(3)
b/Å	3.8518(3)
c/Å	20.943(2)
α/°	90
β/°	108.427(14)
γ/°	90
Volume/Å ³	1419.8(3)
Z	4
ρ _{calc} /cm ³	1.457
μ/mm ⁻¹	2.125
F(000)	648.0
Crystal size/mm ³	0.399 × 0.112 × 0.036
Radiation	CuKα (λ = 1.54184)
2θ range for data collection/°	8.73 to 133.136

Index ranges	$-21 \leq h \leq 22, -2 \leq k \leq 4, -24 \leq l \leq 23$
Reflections collected	4168
Independent reflections	2510 [$R_{\text{int}} = 0.0372, R_{\text{sigma}} = 0.0484$]
Data/restraints/parameters	2510/0/200
Goodness-of-fit on F^2	1.271
Final R indexes [$I \geq 2\sigma(I)$]	$R_1 = 0.0812, wR_2 = 0.1819$
Final R indexes [all data]	$R_1 = 0.0959, wR_2 = 0.1884$
Largest diff. peak/hole / $e \text{ \AA}^{-3}$	1.01/-0.45

Table 2 Fractional Atomic Coordinates ($\times 10^4$) and Equivalent Isotropic Displacement Parameters ($\text{\AA}^2 \times 10^3$) for 429. U_{eq} is defined as 1/3 of of the trace of the orthogonalised U_{ij} tensor.

Atom	<i>x</i>	<i>y</i>	<i>z</i>	$U(\text{eq})$
C1	3047(3)	1098(14)	8598(3)	20.7(12)
C2	2506(3)	1635(14)	7898(3)	20.5(12)
C3	3849(3)	3456(14)	8125(2)	17.1(11)
C4	5121(3)	6275(14)	9146(3)	19.4(11)
C5	5789(3)	6423(15)	9675(3)	21.1(11)
C6	6454(3)	5129(16)	9592(3)	23.2(12)
C7	6433(3)	3778(16)	8971(3)	24.2(12)
C8	5750(3)	3646(15)	8453(3)	22.6(12)
C9	1778(3)	682(13)	7722(3)	18.6(11)
C10	1157(3)	918(14)	7089(3)	20.2(12)
C11	462(3)	-488(14)	7063(3)	20.2(12)
C12	-177(3)	-293(15)	6495(3)	22.0(12)
C13	-113(3)	1383(15)	5927(3)	21.5(12)
C14	581(3)	2769(15)	5932(3)	22.6(12)
C15	1208(3)	2553(14)	6499(3)	20.8(12)
C16	-1427(3)	440(18)	5307(3)	31.5(14)
N1	3779(3)	2121(12)	8682(2)	19.8(10)
N2	4442(3)	4756(12)	7982(2)	20.7(10)
N3	5108(3)	4830(12)	8555(2)	19.1(10)
O1	2843(2)	-187(11)	9052.8(18)	26.5(9)
O2	-702(2)	1854(11)	5345.4(19)	26.6(9)
S1	3006.6(7)	3510(4)	7404.5(6)	19.6(3)

Table 3 Anisotropic Displacement Parameters ($\text{\AA}^2 \times 10^3$) for 429. The Anisotropic displacement factor exponent takes the form: $-2\pi^2[h^2a^{*2}U_{11}+2hka^*b^*U_{12}+\dots]$.

Atom	U ₁₁	U ₂₂	U ₃₃	U ₂₃	U ₁₃	U ₁₂
C1	29(3)	15(3)	18(3)	-2(2)	7(2)	4(2)
C2	34(3)	14(3)	16(3)	-3(2)	11(2)	2(3)
C3	24(3)	14(3)	15(2)	2(2)	8(2)	3(2)
C4	28(3)	13(3)	20(3)	-3(2)	12(2)	-1(2)
C5	30(3)	18(3)	17(3)	1(2)	10(2)	-2(3)
C6	24(3)	24(3)	19(3)	3(2)	3(2)	-2(2)
C7	22(3)	26(3)	27(3)	0(3)	12(2)	1(3)
C8	27(3)	19(3)	26(3)	-1(2)	15(2)	0(3)
C9	29(3)	11(3)	19(3)	-3(2)	12(2)	0(2)
C10	26(3)	10(3)	26(3)	-2(2)	10(2)	4(2)
C11	30(3)	16(3)	18(3)	1(2)	14(2)	2(2)
C12	23(3)	17(3)	29(3)	-3(2)	12(2)	1(2)
C13	27(3)	18(3)	20(3)	-6(2)	8(2)	3(2)
C14	26(3)	21(3)	23(3)	-1(2)	10(2)	1(2)
C15	23(3)	15(3)	28(3)	0(2)	13(2)	-1(2)
C16	23(3)	36(4)	33(3)	-2(3)	6(3)	-3(3)
N1	27(2)	16(2)	17(2)	0.0(19)	7.8(18)	4(2)
N2	28(2)	20(2)	14(2)	1.9(19)	7.2(18)	0(2)
N3	27(2)	18(2)	14(2)	3.2(19)	8.7(18)	1(2)
O1	37(2)	28(2)	17.6(19)	6.6(17)	12.8(17)	-2.3(19)
O2	23(2)	33(2)	22(2)	2.8(18)	4.9(16)	0.0(19)
S1	24.3(7)	19.3(7)	16.5(6)	2.0(5)	8.3(5)	-0.1(6)

Table 4 Bond Lengths for 429.

Atom	Atom	Length/ \AA	Atom	Atom	Length/ \AA
C1	C2	1.506(7)	C7	C8	1.384(8)
C1	N1	1.371(7)	C8	N3	1.353(7)
C1	O1	1.234(7)	C9	C10	1.459(8)
C2	C9	1.334(8)	C10	C11	1.384(8)
C2	S1	1.749(5)	C10	C15	1.416(8)
C3	N1	1.319(7)	C11	C12	1.392(8)
C3	N2	1.326(7)	C12	C13	1.390(8)
C3	S1	1.796(5)	C13	C14	1.390(8)
C4	C5	1.378(8)	C13	O2	1.368(7)
C4	N3	1.351(7)	C14	C15	1.378(8)
C5	C6	1.391(8)	C16	O2	1.430(7)
C6	C7	1.391(8)	N2	N3	1.426(6)

Table 5 Bond Angles for 429.

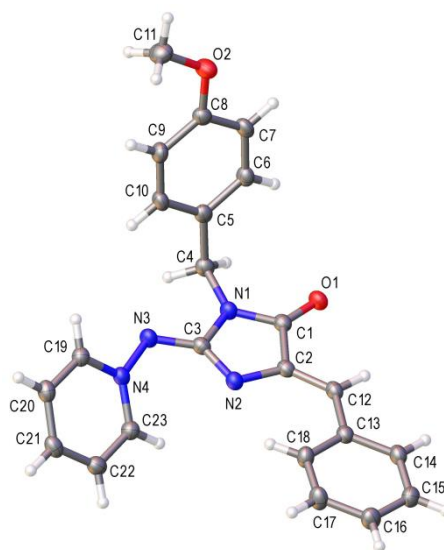
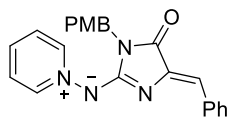
Atom	Atom	Atom	Angle/°	Atom	Atom	Atom	Angle/°
N1	C1	C2	114.4(5)	C11	C10	C15	117.4(5)
O1	C1	C2	122.3(5)	C15	C10	C9	124.7(5)
O1	C1	N1	123.3(5)	C10	C11	C12	122.9(5)
C1	C2	S1	108.5(4)	C13	C12	C11	118.5(5)
C9	C2	C1	122.4(5)	C12	C13	C14	120.1(5)
C9	C2	S1	129.1(4)	O2	C13	C12	124.2(5)
N1	C3	N2	131.9(5)	O2	C13	C14	115.6(5)
N1	C3	S1	116.4(4)	C15	C14	C13	120.7(5)
N2	C3	S1	111.7(4)	C14	C15	C10	120.5(5)
N3	C4	C5	120.2(5)	C3	N1	C1	111.7(4)
C4	C5	C6	119.6(5)	C3	N2	N3	112.2(4)
C5	C6	C7	119.1(5)	C4	N3	C8	121.5(5)
C8	C7	C6	119.6(5)	C4	N3	N2	122.6(4)
N3	C8	C7	119.9(5)	C8	N3	N2	115.7(4)
C2	C9	C10	132.3(5)	C13	O2	C16	118.2(5)
C11	C10	C9	118.0(5)	C2	S1	C3	89.0(2)

Table 6 Torsion Angles for 429.

A	B	C	D	Angle/°	A	B	C	D	Angle/°
C1	C2	C9	C10	-179.9(5)	C11	C12	C13	O2	-177.7(5)
C1	C2	S1	C3	-0.1(4)	C12	C13	C14	C15	-1.0(9)
C2	C1	N1	C3	1.5(7)	C12	C13	O2	C16	-2.1(8)
C2	C9	C10	C11	177.0(6)	C13	C14	C15	C10	-0.2(8)
C2	C9	C10	C15	-4.4(10)	C14	C13	O2	C16	179.1(5)
C3	N2	N3	C4	-52.0(7)	C15	C10	C11	C12	-1.2(8)
C3	N2	N3	C8	133.9(5)	N1	C1	C2	C9	177.8(5)
C4	C5	C6	C7	1.4(9)	N1	C1	C2	S1	-0.7(6)
C5	C4	N3	C8	-3.2(8)	N1	C3	N2	N3	-3.3(9)
C5	C4	N3	N2	-176.9(5)	N1	C3	S1	C2	1.1(5)
C5	C6	C7	C8	-2.0(9)	N2	C3	N1	C1	179.8(6)
C6	C7	C8	N3	0.0(9)	N2	C3	S1	C2	179.9(4)
C7	C8	N3	C4	2.6(8)	N3	C4	C5	C6	1.1(9)
C7	C8	N3	N2	176.8(5)	O1	C1	C2	C9	-1.6(9)
C9	C2	S1	C3	-178.5(6)	O1	C1	C2	S1	179.9(5)
C9	C10	C11	C12	177.4(5)	O1	C1	N1	C3	-179.1(5)
C9	C10	C15	C14	-177.3(5)	O2	C13	C14	C15	177.8(5)
C10	C11	C12	C13	0.1(8)	S1	C2	C9	C10	-1.7(10)
C11	C10	C15	C14	1.2(8)	S1	C3	N1	C1	-1.7(6)
C11	C12	C13	C14	1.0(8)	S1	C3	N2	N3	178.1(3)

Table 7 Hydrogen Atom Coordinates ($\text{\AA}\times 10^4$) and Isotropic Displacement Parameters ($\text{\AA}^2\times 10^3$) for 429.

Atom	<i>x</i>	<i>y</i>	<i>z</i>	U(eq)
H4	4676.38	7173.01	9196.3	23
H5	5795.47	7381.95	10083.97	25
H6	6906.94	5166.99	9948.15	28
H7	6875.7	2967.55	8903.07	29
H8	5731.87	2745.28	8036.54	27
H9	1640.03	-327.15	8069.8	22
H11	420.09	-1612.12	7443.09	24
H12	-636.29	-1261.15	6494.09	26
H14	621.5	3854.07	5548.51	27
H15	1668.82	3488.03	6494.53	25
H16A	-1779.44	858.53	4866.77	47
H16B	-1609.19	1525.85	5638.86	47
H16C	-1379.48	-2015.09	5388.65	47

Aminide 460**Table 1 Crystal data and structure refinement for 460.**

Identification code	460
Empirical formula	C ₂₃ H ₂₀ N ₄ O ₂
Formula weight	384.43
Temperature/K	100.01(10)
Crystal system	triclinic
Space group	P-1
a/Å	9.0055(3)
b/Å	10.8897(3)
c/Å	11.4185(3)
α/°	93.655(2)
β/°	111.851(3)
γ/°	111.187(3)
Volume/Å ³	943.31(5)
Z	2
ρ _{calc} /cm ³	1.353
μ/mm ⁻¹	0.717
F(000)	404.0
Crystal size/mm ³	0.331 × 0.158 × 0.077

Radiation	CuK α ($\lambda = 1.54184$)
2 Θ range for data collection/ $^{\circ}$	8.572 to 144.238
Index ranges	$-10 \leq h \leq 11$, $-13 \leq k \leq 13$, $-14 \leq l \leq 14$
Reflections collected	32837
Independent reflections	3696 [$R_{\text{int}} = 0.0327$, $R_{\text{sigma}} = 0.0166$]
Data/restraints/parameters	3696/0/263
Goodness-of-fit on F^2	1.046
Final R indexes [$I \geq 2\sigma(I)$]	$R_1 = 0.0407$, $wR_2 = 0.1030$
Final R indexes [all data]	$R_1 = 0.0463$, $wR_2 = 0.1087$
Largest diff. peak/hole / $e \text{ \AA}^{-3}$	0.29/-0.23

Table 2 Fractional Atomic Coordinates ($\times 10^4$) and Equivalent Isotropic Displacement Parameters ($\text{\AA}^2 \times 10^3$) for 460. U_{eq} is defined as 1/3 of of the trace of the orthogonalised U_{ij} tensor.

Atom	x	y	z	U(eq)
C1	2132.8(17)	7143.2(12)	5569.8(13)	22.9(3)
C2	1261.9(17)	6062.7(12)	4350.4(12)	22.0(3)
C3	3032.5(17)	5466.7(12)	5831.1(12)	22.1(3)
C4	4413.8(18)	7450.0(13)	7793.1(12)	24.8(3)
C5	6205.6(17)	8423.5(13)	7942.5(12)	23.3(3)
C6	6561.4(18)	9776.8(13)	7900.9(12)	25.2(3)
C7	8185.2(19)	10662.9(13)	8007.7(13)	26.3(3)
C8	9485.1(18)	10209.8(13)	8146.1(12)	24.9(3)
C9	9160.7(19)	8869.8(13)	8199.5(13)	27.7(3)
C10	7529.6(19)	7994.0(13)	8104.0(13)	27.0(3)
C11	12436(2)	10737.4(16)	8425.8(16)	36.5(4)
C12	117.4(17)	6168.6(13)	3229.6(13)	23.2(3)
C13	-826.5(17)	5230.4(12)	1964.9(12)	22.4(3)
C14	-2109.7(18)	5471.5(13)	967.8(13)	26.0(3)
C15	-3059.5(19)	4606.8(14)	-251.6(13)	29.1(3)
C16	-2725(2)	3496.7(14)	-507.5(13)	30.3(3)
C17	-1448(2)	3253.4(14)	461.8(14)	31.4(3)
C18	-517.0(19)	4098.6(13)	1686.4(13)	26.8(3)
C19	5175.3(18)	3391.5(13)	6241.7(12)	23.8(3)
C20	5011.0(19)	2105.4(13)	5858.2(13)	27.0(3)
C21	3359.6(19)	1058.1(13)	5184.6(13)	27.6(3)
C22	1904.2(19)	1344.3(13)	4890.3(12)	26.6(3)
C23	2100.8(18)	2634.7(13)	5283.9(13)	25.3(3)

N1	3232.0(15)	6710.8(10)	6449.0(10)	22.9(2)
N2	1866.2(14)	5057.6(10)	4593.8(10)	22.9(2)
N3	4047.1(15)	4926.7(10)	6561.6(10)	24.4(3)
N4	3736.3(14)	3638.6(10)	5969.1(10)	22.1(2)
O1	1959.2(12)	8191.9(9)	5774.4(9)	26.9(2)
O2	11022.0(13)	11137.6(10)	8179.8(10)	32.5(2)

Table 3 Anisotropic Displacement Parameters ($\text{\AA}^2 \times 10^3$) for 460. The Anisotropic displacement factor exponent takes the form: $-2\pi^2[h^2a^{*2}U_{11}+2hka^*b^*U_{12}+\dots]$.

Atom	U ₁₁	U ₂₂	U ₃₃	U ₂₃	U ₁₃	U ₁₂
C1	22.6(6)	20.0(6)	27.2(6)	6.2(5)	11.6(5)	8.8(5)
C2	22.9(6)	18.1(6)	25.8(6)	5.2(5)	11.4(5)	8.3(5)
C3	24.6(7)	18.4(6)	24.2(6)	4.1(5)	11.5(5)	8.7(5)
C4	29.4(7)	22.0(6)	21.7(6)	3.0(5)	9.7(5)	10.7(5)
C5	27.6(7)	21.0(6)	18.7(6)	2.8(5)	7.4(5)	9.9(5)
C6	30.0(7)	22.1(6)	24.9(6)	3.7(5)	10.3(5)	14.3(5)
C7	34.2(7)	17.1(6)	27.2(6)	3.8(5)	11.8(6)	11.8(5)
C8	27.0(7)	21.1(6)	22.6(6)	2.1(5)	8.3(5)	8.6(5)
C9	28.6(7)	25.3(7)	30.5(7)	7.4(5)	8.8(6)	16.3(6)
C10	32.7(7)	19.3(6)	27.8(7)	6.7(5)	9.3(6)	12.9(5)
C11	28.0(8)	34.7(8)	43.4(9)	5.4(6)	13.3(7)	11.9(6)
C12	25.6(7)	19.7(6)	27.9(7)	7.5(5)	12.9(5)	11.5(5)
C13	23.1(6)	20.5(6)	24.8(6)	7.4(5)	11.0(5)	9.2(5)
C14	28.5(7)	23.0(6)	29.6(7)	8.8(5)	12.3(6)	13.6(5)
C15	29.6(7)	28.8(7)	26.8(7)	9.6(5)	8.4(6)	13.4(6)
C16	36.8(8)	28.9(7)	22.4(6)	5.0(5)	8.6(6)	14.8(6)
C17	41.5(8)	28.2(7)	28.3(7)	5.7(6)	12.6(6)	21.1(6)
C18	30.6(7)	27.3(7)	24.9(6)	7.6(5)	9.5(5)	16.7(6)
C19	24.7(7)	24.6(6)	24.0(6)	7.4(5)	10.4(5)	11.9(5)
C20	32.2(7)	28.0(7)	28.8(7)	10.5(5)	15.2(6)	17.9(6)
C21	39.0(8)	22.2(6)	26.2(7)	7.8(5)	15.8(6)	15.4(6)
C22	29.4(7)	23.0(6)	24.0(6)	5.2(5)	10.2(5)	8.6(5)
C23	24.6(7)	24.6(6)	26.1(6)	6.2(5)	9.5(5)	10.9(5)
N1	25.4(6)	19.1(5)	23.5(5)	3.2(4)	8.6(4)	10.6(4)
N2	25.0(6)	20.0(5)	24.0(5)	5.2(4)	9.3(4)	10.7(4)
N3	27.9(6)	19.0(5)	25.3(5)	2.8(4)	8.6(5)	11.9(4)
N4	26.0(6)	19.7(5)	21.7(5)	5.3(4)	9.8(4)	11.0(4)
O1	29.8(5)	19.0(4)	31.6(5)	4.2(4)	11.5(4)	11.6(4)
O2	29.1(5)	23.9(5)	44.3(6)	6.8(4)	16.3(5)	10.3(4)

Table 4 Bond Lengths for 460.

Atom	Atom	Length/Å	Atom	Atom	Length/Å
C1	C2	1.4998(17)	C9	C10	1.391(2)
C1	N1	1.3664(16)	C11	O2	1.4288(18)
C1	O1	1.2269(16)	C12	C13	1.4568(18)
C2	C12	1.3551(18)	C13	C14	1.4066(18)
C2	N2	1.3886(16)	C13	C18	1.4008(18)
C3	N1	1.4048(16)	C14	C15	1.3860(19)
C3	N2	1.3322(16)	C15	C16	1.386(2)
C3	N3	1.3266(17)	C16	C17	1.388(2)
C4	C5	1.5141(19)	C17	C18	1.3823(19)
C4	N1	1.4640(16)	C19	C20	1.3780(18)
C5	C6	1.3984(18)	C19	N4	1.3458(17)
C5	C10	1.3874(19)	C20	C21	1.384(2)
C6	C7	1.384(2)	C21	C22	1.382(2)
C7	C8	1.389(2)	C22	C23	1.3742(18)
C8	C9	1.3910(18)	C23	N4	1.3586(17)
C8	O2	1.3721(17)	N3	N4	1.3993(14)

Table 5 Bond Angles for 460.

Atom	Atom	Atom	Angle/°	Atom	Atom	Atom	Angle/°
N1	C1	C2	103.93(10)	C18	C13	C12	123.31(12)
O1	C1	C2	130.01(12)	C18	C13	C14	118.09(12)
O1	C1	N1	126.06(12)	C15	C14	C13	121.13(12)
C12	C2	C1	121.29(11)	C16	C15	C14	119.79(13)
C12	C2	N2	129.57(12)	C15	C16	C17	119.78(13)
N2	C2	C1	109.12(11)	C18	C17	C16	120.72(13)
N2	C3	N1	113.07(11)	C17	C18	C13	120.47(12)
N3	C3	N1	115.23(11)	N4	C19	C20	120.42(12)
N3	C3	N2	131.68(12)	C19	C20	C21	120.06(13)
N1	C4	C5	112.64(11)	C22	C21	C20	118.39(12)
C6	C5	C4	120.81(12)	C23	C22	C21	120.49(13)
C10	C5	C4	120.99(12)	N4	C23	C22	119.92(13)
C10	C5	C6	118.19(13)	C1	N1	C3	108.17(10)
C7	C6	C5	120.99(13)	C1	N1	C4	124.74(11)
C6	C7	C8	120.04(12)	C3	N1	C4	127.09(11)
C7	C8	C9	119.81(13)	C3	N2	C2	105.70(10)
O2	C8	C7	116.16(11)	C3	N3	N4	114.66(10)
O2	C8	C9	124.00(13)	C19	N4	C23	120.68(11)
C8	C9	C10	119.54(13)	C19	N4	N3	115.44(11)
C5	C10	C9	121.41(12)	C23	N4	N3	123.47(11)

C2	C12	C13	128.53(12)	C8	O2	C11	117.53(11)
C14	C13	C12	118.60(12)				

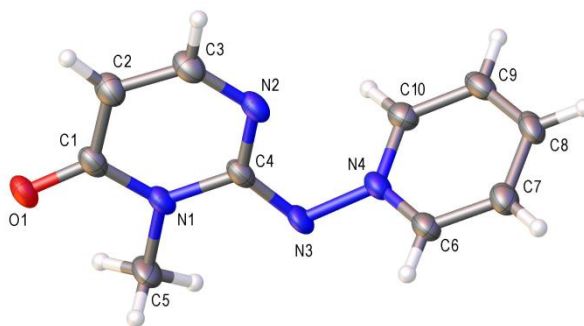
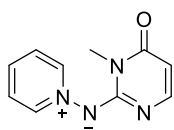
Table 6 Torsion Angles for 460.

A	B	C	D	Angle/°	A	B	C	D	Angle/°
C1	C2	C12	C13	179.40(12)	C16	C17	C18	C13	-1.1(2)
C1	C2	N2	C3	-1.29(14)	C18	C13	C14	C15	0.8(2)
C2	C1	N1	C3	-0.88(14)	C19	C20	C21	C22	1.3(2)
C2	C1	N1	C4	178.46(11)	C20	C19	N4	C23	-1.70(19)
C2	C12	C13	C14	172.70(13)	C20	C19	N4	N3	171.16(11)
C2	C12	C13	C18	-7.6(2)	C20	C21	C22	C23	-1.3(2)
C3	N3	N4	C19	142.60(12)	C21	C22	C23	N4	-0.1(2)
C3	N3	N4	C23	-44.76(17)	C22	C23	N4	C19	1.63(19)
C4	C5	C6	C7	-178.53(12)	C22	C23	N4	N3	-170.64(11)
C4	C5	C10	C9	177.87(12)	N1	C1	C2	C12	-177.10(12)
C5	C4	N1	C1	-89.35(15)	N1	C1	C2	N2	1.36(14)
C5	C4	N1	C3	89.86(15)	N1	C3	N2	C2	0.76(15)
C5	C6	C7	C8	0.6(2)	N1	C3	N3	N4	175.09(11)
C6	C5	C10	C9	-1.15(19)	N1	C4	C5	C6	92.99(14)
C6	C7	C8	C9	-1.1(2)	N1	C4	C5	C10	-86.00(15)
C6	C7	C8	O2	176.85(12)	N2	C2	C12	C13	1.3(2)
C7	C8	C9	C10	0.5(2)	N2	C3	N1	C1	0.13(15)
C7	C8	O2	C11	175.08(12)	N2	C3	N1	C4	-179.19(12)
C8	C9	C10	C5	0.7(2)	N2	C3	N3	N4	-6.5(2)
C9	C8	O2	C11	-7.06(19)	N3	C3	N1	C1	178.85(11)
C10	C5	C6	C7	0.50(19)	N3	C3	N1	C4	-0.47(19)
C12	C2	N2	C3	177.01(14)	N3	C3	N2	C2	-177.69(14)
C12	C13	C14	C15	-179.44(12)	N4	C19	C20	C21	0.2(2)
C12	C13	C18	C17	-179.43(13)	O1	C1	C2	C12	2.1(2)
C13	C14	C15	C16	-1.2(2)	O1	C1	C2	N2	-179.40(13)
C14	C13	C18	C17	0.3(2)	O1	C1	N1	C3	179.84(13)
C14	C15	C16	C17	0.4(2)	O1	C1	N1	C4	-0.8(2)
C15	C16	C17	C18	0.7(2)	O2	C8	C9	C10	-177.32(12)

Table 7 Hydrogen Atom Coordinates ($\text{\AA} \times 10^4$) and Isotropic Displacement Parameters ($\text{\AA}^2 \times 10^3$) for 460.

Atom	x	y	z	U(eq)
H4A	4556.98	6806.79	8327.63	30
H4B	3882.89	7950.78	8102.87	30
H6	5694.19	10086.2	7800	30
H7	8405.59	11562.11	7986.84	32
H9	10028.69	8561.7	8298.4	33

H10	7321.88	7101.26	8149.38	32
H11A	12102.78	10010.24	7728.01	55
H11B	12698.4	10441.32	9223.36	55
H11C	13457.83	11491.82	8491.1	55
H12	-93.21	6941.95	3273.56	28
H14	-2324.59	6223.93	1129.55	31
H15	-3918.6	4770.87	-896.03	35
H16	-3353.28	2916.91	-1325.81	36
H17	-1216.41	2513.67	285.3	38
H18	320.85	3914.49	2330.01	32
H19	6287.7	4093.23	6691.65	29
H20	6010.94	1941.15	6052.37	32
H21	3232.47	182.7	4935.93	33
H22	783.24	658.68	4422.36	32
H23	1115.46	2820.56	5081.57	30

Aminide 471**Table 1 Crystal data and structure refinement for 471.**

Identification code	471
Empirical formula	C ₁₀ H ₁₀ N ₄ O
Formula weight	202.22
Temperature/K	100.01(10)
Crystal system	monoclinic
Space group	C2/c
a/Å	18.0994(15)
b/Å	7.8972(7)
c/Å	13.9809(15)
α /°	90
β /°	111.965(11)
γ /°	90
Volume/Å ³	1853.3(3)
Z	8
$\rho_{\text{calc}}/\text{cm}^3$	1.449
μ/mm^{-1}	0.821
F(000)	848.0
Crystal size/mm ³	0.138 × 0.052 × 0.031
Radiation	CuK α (λ = 1.54184)
2 Θ range for data collection/°	10.54 to 149.544

Index ranges	$-22 \leq h \leq 21, -7 \leq k \leq 9, -10 \leq l \leq 17$
Reflections collected	3485
Independent reflections	1830 [$R_{\text{int}} = 0.0234, R_{\text{sigma}} = 0.0293$]
Data/restraints/parameters	1830/0/137
Goodness-of-fit on F^2	1.048
Final R indexes [$I \geq 2\sigma(I)$]	$R_1 = 0.0467, wR_2 = 0.1315$
Final R indexes [all data]	$R_1 = 0.0549, wR_2 = 0.1408$
Largest diff. peak/hole / $e \text{ \AA}^{-3}$	0.20/-0.22

Table 2 Fractional Atomic Coordinates ($\times 10^4$) and Equivalent Isotropic Displacement Parameters ($\text{\AA}^2 \times 10^3$) for 471. U_{eq} is defined as 1/3 of the trace of the orthogonalised U_{ij} tensor.

Atom	x	y	z	$U(\text{eq})$
C1	4194.1(10)	5702(2)	5833.9(12)	28.1(4)
C2	4906.1(10)	6680(2)	6209.3(13)	31.9(4)
C3	5618.2(10)	5861(2)	6583.2(14)	31.8(4)
C4	5064.4(9)	3221(2)	6250.6(12)	26.3(4)
C5	3600.2(10)	2905(3)	5398.2(16)	38.9(5)
C6	6110.4(9)	140(2)	7585.9(14)	29.9(4)
C7	6865.1(10)	-558(2)	8003.1(14)	32.2(4)
C8	7374.8(9)	-414(2)	7475.0(14)	32.0(4)
C9	7114.9(9)	409(2)	6531.1(14)	32.1(4)
C10	6351.1(9)	1069(2)	6134.2(14)	30.5(4)
N1	4311.1(7)	3953.0(19)	5835.6(11)	27.3(3)
N2	5721.9(8)	4173.0(19)	6632.7(11)	28.2(3)
N3	5076.1(7)	1524(2)	6250.9(12)	31.0(4)
N4	5868.7(8)	921.5(18)	6667.6(11)	28.3(3)
O1	3502.8(6)	6272.0(17)	5504.0(10)	33.6(3)

Table 3 Anisotropic Displacement Parameters ($\text{\AA}^2 \times 10^3$) for 471. The Anisotropic displacement factor exponent takes the form: $-2\pi^2[h^2a^{*2}U_{11}+2hka^*b^*U_{12}+\dots]$.

Atom	U_{11}	U_{22}	U_{33}	U_{23}	U_{13}	U_{12}
C1	20.4(7)	37.6(9)	28.8(8)	2.3(6)	11.9(6)	4.1(6)
C2	24.4(8)	33.2(9)	37.3(9)	-3.8(7)	10.8(7)	1.6(7)
C3	20.9(8)	36.4(9)	36.3(9)	-5.5(7)	8.7(6)	-2.5(6)
C4	15.8(7)	35.1(9)	29.2(8)	1.7(6)	9.7(6)	1.9(6)
C5	15.3(7)	36.0(10)	59.4(11)	4.1(8)	7.2(7)	-1.5(6)
C6	18.2(7)	30.5(9)	41.0(9)	1.7(7)	11.2(6)	-0.2(6)

C7	20.5(8)	30.8(8)	41.5(9)	0.3(7)	7.1(7)	0.4(6)
C8	15.6(7)	28.3(9)	48.2(10)	-3.4(7)	7.4(7)	1.2(6)
C9	19.2(8)	31.8(9)	47.8(10)	-3.3(7)	15.5(7)	-2.7(6)
C10	22.0(8)	30.8(8)	39.7(9)	2.1(7)	12.6(7)	-1.8(6)
N1	14.3(6)	33.3(8)	33.5(7)	2.0(6)	8.1(5)	0.7(5)
N2	16.0(6)	34.6(8)	33.1(7)	-3.3(6)	8.1(5)	0.6(5)
N3	11.9(6)	34.3(8)	44.3(8)	5.8(6)	7.8(5)	2.1(5)
N4	14.9(6)	28.4(7)	40.8(8)	0.6(6)	9.6(6)	0.0(5)
O1	18.5(5)	41.6(7)	42.3(7)	7.1(5)	13.2(5)	7.4(5)

Table 4 Bond Lengths for 471.

Atom	Atom	Length/Å	Atom	Atom	Length/Å
C1	C2	1.423(2)	C5	N1	1.458(2)
C1	N1	1.398(2)	C6	C7	1.384(2)
C1	O1	1.245(2)	C6	N4	1.342(2)
C2	C3	1.359(2)	C7	C8	1.385(3)
C3	N2	1.345(2)	C8	C9	1.386(3)
C4	N1	1.3921(19)	C9	C10	1.384(2)
C4	N2	1.338(2)	C10	N4	1.349(2)
C4	N3	1.340(2)	N3	N4	1.4136(17)

Table 5 Bond Angles for 471.

Atom	Atom	Atom	Angle/°	Atom	Atom	Atom	Angle/°
N1	C1	C2	114.81(14)	C10	C9	C8	119.38(15)
O1	C1	C2	125.93(18)	N4	C10	C9	120.12(16)
O1	C1	N1	119.25(16)	C1	N1	C5	116.81(13)
C3	C2	C1	118.79(17)	C4	N1	C1	122.36(14)
N2	C3	C2	125.82(16)	C4	N1	C5	120.81(15)
N2	C4	N1	121.29(16)	C4	N2	C3	116.75(14)
N2	C4	N3	123.35(14)	C4	N3	N4	110.51(13)
N3	C4	N1	115.36(14)	C6	N4	C10	121.46(14)
N4	C6	C7	120.25(15)	C6	N4	N3	117.81(13)
C6	C7	C8	119.47(17)	C10	N4	N3	120.67(14)
C7	C8	C9	119.31(15)				

Table 6 Torsion Angles for 471.

A	B	C	D	Angle/°	A	B	C	D	Angle/°
C1	C2	C3	N2	0.3(3)	N1	C1	C2	C3	-3.7(2)
C2	C1	N1	C4	5.0(2)	N1	C4	N2	C3	-0.8(2)
C2	C1	N1	C5	-176.29(15)	N1	C4	N3	N4	178.75(13)
C2	C3	N2	C4	2.1(3)	N2	C4	N1	C1	-2.9(2)

C4	N3	N4	C6	110.95(17)	N2	C4	N1	C5	178.46(16)
C4	N3	N4	C10	-71.8(2)	N2	C4	N3	N4	-2.2(2)
C6	C7	C8	C9	-0.8(3)	N3	C4	N1	C1	176.15(15)
C7	C6	N4	C10	-0.8(3)	N3	C4	N1	C5	-2.5(2)
C7	C6	N4	N3	176.39(15)	N3	C4	N2	C3	-
C7	C8	C9	C10	-0.1(3)	N4	C6	C7	C8	179.75(16)
C8	C9	C10	N4	0.6(3)	N4	C6	C7	C8	1.3(3)
C8	C9	C10	N4	0.6(3)	O1	C1	C2	C3	177.35(16)
C9	C10	N4	C6	-0.1(3)	O1	C1	N1	C4	-
C9	C10	N4	N3	-177.25(15)	O1	C1	N1	C5	175.97(14)
					O1	C1	N1	C5	2.7(2)

Table 7 Hydrogen Atom Coordinates ($\text{\AA} \times 10^4$) and Isotropic Displacement Parameters ($\text{\AA}^2 \times 10^3$) for 471.

Atom	x	y	z	U(eq)
H2	4884.56	7856.39	6199.05	38
H3	6074.29	6528.84	6826.44	38
H5A	3346.44	2798.25	5887.75	58
H5B	3747.69	1803.24	5239.83	58
H5C	3238.41	3423.48	4779.14	58
H6	5769.24	67.15	7943.26	36
H7	7028.96	-1119.49	8633.09	39
H8	7886.03	-864.82	7750.9	38
H9	7450.43	517.55	6167.84	38
H10	6170.29	1614.22	5498.53	37

Imidazole 382

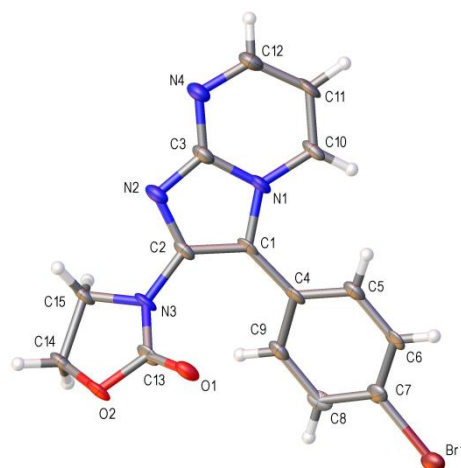
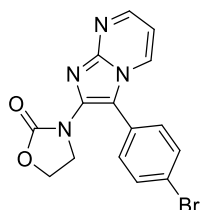


Table 1 Crystal data and structure refinement for 382.

Identification code	382
Empirical formula	C ₁₅ H ₁₁ BrN ₄ O ₂
Formula weight	359.19
Temperature/K	99.99(10)
Crystal system	monoclinic
Space group	P2 ₁ /n
a/Å	4.3065(5)
b/Å	15.0036(15)
c/Å	21.307(2)
α/°	90
β/°	91.972(10)
γ/°	90
Volume/Å ³	1375.9(3)
Z	4
ρ _{calc} /g/cm ³	1.734
μ/mm ⁻¹	4.203
F(000)	720.0
Crystal size/mm ³	0.183 × 0.035 × 0.015
Radiation	CuKα (λ = 1.54184)
2θ range for data collection/°	7.208 to 150.036

Index ranges	$-3 \leq h \leq 5, -18 \leq k \leq 17, -24 \leq l \leq 26$
Reflections collected	5027
Independent reflections	2701 [$R_{\text{int}} = 0.0784, R_{\text{sigma}} = 0.0947$]
Data/restraints/parameters	2701/211/199
Goodness-of-fit on F^2	1.209
Final R indexes [$I \geq 2\sigma(I)$]	$R_1 = 0.1313, wR_2 = 0.3747$
Final R indexes [all data]	$R_1 = 0.1457, wR_2 = 0.3834$
Largest diff. peak/hole / $e \text{ \AA}^{-3}$	3.27/-1.40

Table 2 Fractional Atomic Coordinates ($\times 10^4$) and Equivalent Isotropic Displacement Parameters ($\text{\AA}^2 \times 10^3$) for 382. U_{eq} is defined as 1/3 of the trace of the orthogonalised U_{ij} tensor.

Atom	x	y	z	U(eq)
C1	3450(30)	6149(7)	6688(6)	21(2)
C2	3000(30)	5516(8)	6220(6)	20(2)
C3	850(30)	6672(8)	5828(6)	24(2)
C4	4810(30)	6091(8)	7321(6)	22(2)
C5	3780(30)	6596(8)	7831(6)	24(2)
C6	4940(30)	6462(8)	8430(6)	24(2)
C7	7180(30)	5821(8)	8538(6)	23(2)
C8	8330(30)	5315(8)	8059(6)	20.0(19)
C9	7150(30)	5456(8)	7452(6)	23(2)
C10	1850(30)	7774(8)	6630(7)	23(2)
C11	390(30)	8374(8)	6242(7)	29(3)
C12	-810(40)	8088(9)	5657(7)	32(3)
C13	3430(30)	3974(8)	6636(6)	22(2)
C14	6080(30)	3311(8)	5841(7)	26(2)
C15	5070(30)	4238(8)	5614(6)	23(2)
Br1	8680(4)	5610.9(9)	9378.1(7)	30.6(6)
N1	2030(30)	6910(7)	6426(5)	24(2)
N2	1420(30)	5825(7)	5697(5)	24(2)
N3	4090(20)	4634(7)	6208(5)	20.8(19)
N4	-630(30)	7265(8)	5440(6)	30(2)
O1	2230(20)	4046(6)	7127(4)	28(2)
O2	4550(20)	3188(6)	6421(4)	26.5(19)

Table 3 Anisotropic Displacement Parameters ($\text{\AA}^2 \times 10^3$) for 382. The Anisotropic displacement factor exponent takes the form: $-2\pi^2[h^2a^{*2}U_{11}+2hka^*b^*U_{12}+\dots]$.

Atom	U ₁₁	U ₂₂	U ₃₃	U ₂₃	U ₁₃	U ₁₂
C1	25(6)	4(4)	34(4)	1(3)	3(4)	-3(4)
C2	18(5)	7(3)	34(5)	-1(3)	2(4)	-1(4)
C3	28(7)	10(4)	35(5)	0(3)	-2(4)	1(4)
C4	28(6)	4(5)	34(4)	1(4)	0(4)	-1(4)
C5	28(6)	8(5)	35(4)	0(4)	2(4)	-1(4)
C6	33(6)	5(5)	35(4)	-2(4)	-2(4)	-5(4)
C7	30(6)	10(5)	30(4)	1(4)	-5(4)	-8(4)
C8	6(5)	16(5)	38(4)	4(4)	2(4)	-4(4)
C9	29(6)	8(5)	34(4)	-2(4)	2(4)	-1(4)
C10	19(6)	8(4)	42(6)	-2(4)	-2(5)	2(4)
C11	36(7)	8(5)	42(6)	-2(4)	0(5)	9(5)
C12	45(8)	14(4)	37(6)	3(5)	-2(5)	8(5)
C13	22(6)	6(4)	37(5)	0(3)	3(4)	-7(4)
C14	29(7)	8(5)	40(6)	-1(4)	2(5)	4(4)
C15	28(6)	8(5)	34(5)	-1(3)	2(5)	4(4)
Br1	39.8(9)	16.3(8)	35.0(9)	3.0(5)	-9.6(6)	-2.6(6)
N1	33(6)	8(3)	32(4)	0(3)	0(4)	3(4)
N2	26(5)	10(4)	37(5)	0(3)	-3(4)	2(4)
N3	22(5)	6(3)	35(5)	1(3)	3(4)	4(3)
N4	38(7)	14(4)	37(5)	0(4)	-7(4)	5(4)
O1	37(5)	13(4)	35(4)	3(3)	5(4)	6(4)
O2	34(5)	5(3)	40(5)	1(3)	4(4)	2(3)

Table 4 Bond Lengths for 382.

Atom	Atom	Length/ \AA	Atom	Atom	Length/ \AA
C1	C2	1.386(17)	C7	Br1	1.907(13)
C1	C4	1.454(19)	C8	C9	1.390(19)
C1	N1	1.401(16)	C10	C11	1.363(19)
C2	N2	1.366(17)	C10	N1	1.370(16)
C2	N3	1.404(15)	C11	C12	1.40(2)
C3	N1	1.402(17)	C12	N4	1.322(18)
C3	N2	1.326(17)	C13	N3	1.382(16)
C3	N4	1.359(17)	C13	O1	1.187(16)
C4	C5	1.409(18)	C13	O2	1.360(15)
C4	C9	1.408(18)	C14	C15	1.532(16)
C5	C6	1.367(19)	C14	O2	1.431(17)
C6	C7	1.378(19)	C15	N3	1.474(16)
C7	C8	1.377(19)			

Table 5 Bond Angles for 382.

Atom	Atom	Atom	Angle/°	Atom	Atom	Atom	Angle/°
C2	C1	C4	131.8(11)	C8	C9	C4	121.7(12)
C2	C1	N1	103.0(11)	C11	C10	N1	117.5(12)
N1	C1	C4	125.0(11)	C10	C11	C12	119.2(12)
C1	C2	N3	128.4(12)	N4	C12	C11	124.9(13)
N2	C2	C1	114.0(11)	O1	C13	N3	128.5(12)
N2	C2	N3	117.5(11)	O1	C13	O2	123.1(11)
N2	C3	N1	111.8(11)	O2	C13	N3	108.3(11)
N2	C3	N4	125.9(12)	O2	C14	C15	104.8(10)
N4	C3	N1	122.3(11)	N3	C15	C14	100.4(10)
C5	C4	C1	123.9(12)	C1	N1	C3	107.1(10)
C9	C4	C1	119.2(11)	C10	N1	C1	132.3(12)
C9	C4	C5	116.8(12)	C10	N1	C3	120.5(11)
C6	C5	C4	121.8(12)	C3	N2	C2	104.2(11)
C5	C6	C7	119.4(12)	C2	N3	C15	120.1(10)
C6	C7	Br1	119.0(10)	C13	N3	C2	125.9(11)
C8	C7	C6	121.9(12)	C13	N3	C15	110.6(10)
C8	C7	Br1	119.1(10)	C12	N4	C3	115.5(12)
C7	C8	C9	118.4(12)	C13	O2	C14	111.1(9)

Table 6 Torsion Angles for 382.

A	B	C	D	Angle/°	A	B	C	D	Angle/°
C1	C2	N2	C3	0.2(15)	C15	C14	O2	C13	-14.6(14)
C1	C2	N3	C13	59.5(19)	Br1	C7	C8	C9	178.0(9)
C1	C2	N3	C15	-143.6(13)	N1	C1	C2	N2	-0.3(15)
C1	C4	C5	C6	174.0(12)	N1	C1	C2	N3	176.3(12)
C1	C4	C9	C8	-174.1(11)	N1	C1	C4	C5	29(2)
C2	C1	C4	C5	-146.1(14)	N1	C1	C4	C9	-155.3(13)
C2	C1	C4	C9	30(2)	N1	C3	N2	C2	-0.1(15)
C2	C1	N1	C3	0.2(14)	N1	C3	N4	C12	2(2)
C2	C1	N1	C10	-174.8(14)	N1	C10	C11	C12	-1(2)
C4	C1	C2	N2	175.6(13)	N2	C2	N3	C13	-124.0(14)
C4	C1	C2	N3	-8(2)	N2	C2	N3	C15	32.8(17)
C4	C1	N1	C3	-176.0(12)	N2	C3	N1	C1	-0.1(16)
C4	C1	N1	C10	9(2)	N2	C3	N1	C10	175.6(12)
C4	C5	C6	C7	0.6(19)	N2	C3	N4	C12	-176.8(14)
C5	C4	C9	C8	1.9(18)	N3	C2	N2	C3	-176.7(11)
C5	C6	C7	C8	0.6(19)	N3	C13	O2	C14	1.4(15)
C5	C6	C7	Br1	-178.0(10)	N4	C3	N1	C1	-178.7(13)
C6	C7	C8	C9	-0.6(18)	N4	C3	N1	C10	-3(2)

C7	C8	C9	C4	-0.8(18)	N4	C3	N2	C2	178.5(13)
C9	C4	C5	C6	-1.9(19)	O1	C13	N3	C2	-11(2)
C10	C11	C12	N4	0(3)	O1	C13	N3	C15	-170.1(14)
C11	C10	N1	C1	177.0(14)	O1	C13	O2	C14	-175.3(13)
C11	C10	N1	C3	3(2)	O2	C13	N3	C2	172.0(11)
C11	C12	N4	C3	0(2)	O2	C13	N3	C15	13.4(14)
C14	C15	N3	C2	178.9(11)	O2	C14	C15	N3	20.6(13)
C14	C15	N3	C13	-21.0(14)					

Table 7 Hydrogen Atom Coordinates ($\text{\AA} \times 10^4$) and Isotropic Displacement Parameters ($\text{\AA}^2 \times 10^3$) for 382.

Atom	<i>x</i>	<i>y</i>	<i>z</i>	U(eq)
H5	2281.79	7033.54	7759.5	28
H6	4213.62	6799.21	8760.02	29
H8	9860.18	4888.37	8140.22	24
H9	7923.01	5122.94	7124.67	28
H10	2700.71	7944.85	7019.28	28
H11	183.18	8965.03	6364.12	35
H12	-1804.43	8510.05	5400.91	39
H14A	5444.36	2857.79	5538.78	31
H14B	8320.99	3282.57	5907.18	31
H15A	6786.18	4565.41	5439.71	28
H15B	3369.92	4206.12	5304.68	28

Imidazole 579

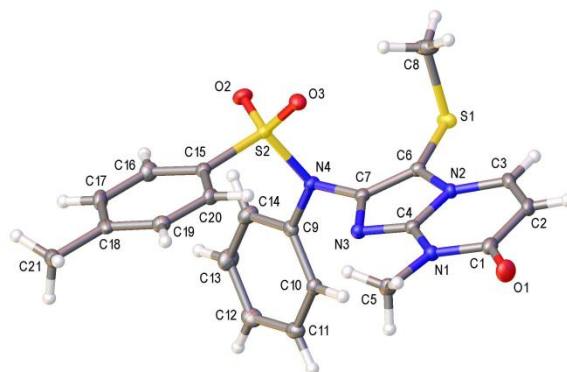
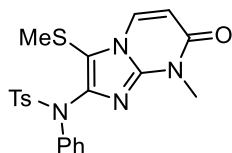


Table 1 Crystal data and structure refinement for 579.

Identification code	579
Empirical formula	C ₂₁ H ₂₀ N ₄ O ₃ S ₂
Formula weight	440.53
Temperature/K	100.00(10)
Crystal system	monoclinic
Space group	P2 ₁ /c
a/Å	12.0576(6)
b/Å	20.0021(9)
c/Å	8.7492(4)
α/°	90
β/°	109.416(5)
γ/°	90
Volume/Å ³	1990.11(17)
Z	4
ρ _{calc} /cm ³	1.470
μ/mm ⁻¹	0.300
F(000)	920.0
Crystal size/mm ³	0.225 × 0.154 × 0.110
Radiation	MoKα (λ = 0.71073)
2θ range for data collection/°	7.084 to 54.956

Index ranges	$-15 \leq h \leq 15, -25 \leq k \leq 20, -11 \leq l \leq 11$
Reflections collected	13445
Independent reflections	4464 [$R_{\text{int}} = 0.0291, R_{\text{sigma}} = 0.0325$]
Data/restraints/parameters	4464/0/274
Goodness-of-fit on F^2	1.086
Final R indexes [$I \geq 2\sigma(I)$]	$R_1 = 0.0351, wR_2 = 0.0834$
Final R indexes [all data]	$R_1 = 0.0430, wR_2 = 0.0884$
Largest diff. peak/hole / $e \text{ \AA}^{-3}$	0.36/-0.43

Table 2 Fractional Atomic Coordinates ($\times 10^4$) and Equivalent Isotropic Displacement Parameters ($\text{\AA}^2 \times 10^3$) for 579. U_{eq} is defined as 1/3 of of the trace of the orthogonalised U_{ij} tensor.

Atom	x	y	z	U(eq)
C1	7899.8(14)	6820.8(9)	4596(2)	16.8(3)
C2	8413.6(15)	6562.9(9)	3415(2)	18.1(4)
C3	8602.1(14)	5911.1(9)	3276.0(19)	15.7(3)
C4	7822.4(13)	5668.5(8)	5407.9(19)	12.7(3)
C5	7006.7(15)	6533.0(9)	6675(2)	17.4(3)
C6	8385.0(14)	4760.8(8)	4390.5(19)	13.3(3)
C7	7946.4(14)	4615.0(8)	5604.4(19)	12.8(3)
C8	7590.1(16)	4060.6(11)	1509(2)	25.7(4)
C9	8513.0(14)	3698.7(8)	7620(2)	13.5(3)
C10	9296.3(14)	4124.3(8)	8720(2)	14.7(3)
C11	10044.1(15)	3874.0(9)	10183(2)	18.0(4)
C12	9988.6(15)	3209.6(9)	10586(2)	20.4(4)
C13	9207.8(16)	2787.1(9)	9489(2)	22.7(4)
C14	8482.2(15)	3023.1(9)	8003(2)	19.7(4)
C15	5673.0(14)	3762.9(8)	6702.9(19)	13.5(3)
C16	5481.8(15)	3203.4(9)	7520(2)	18.3(4)
C17	4880.3(15)	3278.2(9)	8609(2)	19.4(4)
C18	4465.8(14)	3900.4(9)	8890(2)	16.4(3)
C19	4666.6(14)	4453.1(9)	8051(2)	16.3(3)
C20	5275.7(14)	4393.0(8)	6964(2)	15.4(3)
C21	3840.3(16)	3962.6(10)	10115(2)	20.9(4)
N1	7613.9(12)	6334.9(7)	5546.3(16)	13.5(3)
N2	8303.5(11)	5462.7(7)	4274.6(16)	12.8(3)
N3	7596.2(12)	5175.6(7)	6247.2(16)	13.6(3)
N4	7760.6(12)	3959.8(7)	6093.7(16)	13.7(3)
O1	7714.8(12)	7411.2(6)	4774.3(16)	23.3(3)

O2	6449.2(10)	2977.8(6)	4924.2(15)	19.0(3)
O3	5850.1(10)	4122.5(6)	3930.3(14)	17.2(3)
S1	8921.3(4)	4264.2(2)	3167.0(5)	16.93(11)
S2	6383.5(3)	3675.0(2)	5251.6(5)	13.26(10)

Table 3 Anisotropic Displacement Parameters ($\text{\AA}^2 \times 10^3$) for 579. The Anisotropic displacement factor exponent takes the form: $-2\pi^2[h^2a^{*2}U_{11}+2hka^*b^*U_{12}+\dots]$.

Atom	U ₁₁	U ₂₂	U ₃₃	U ₂₃	U ₁₃	U ₁₂
C1	15.6(8)	16.6(9)	16.2(8)	2.3(7)	2.6(7)	-3.0(6)
C2	19.6(8)	19.9(9)	14.8(8)	3.3(7)	5.9(7)	-5.3(7)
C3	13.9(8)	22.4(9)	11.4(8)	0.8(7)	4.9(6)	-3.6(7)
C4	10.8(7)	14.3(8)	12.3(7)	-1.9(6)	3.1(6)	-1.5(6)
C5	18.6(8)	16.2(8)	19.5(8)	-2.8(7)	9.3(7)	-0.7(7)
C6	12.4(7)	13.5(8)	13.2(8)	-1.8(6)	3.4(6)	-0.9(6)
C7	11.6(7)	13.2(8)	12.3(8)	-0.7(6)	2.2(6)	-1.1(6)
C8	17.9(9)	38.1(11)	19.3(9)	-12.6(8)	3.7(7)	0.1(8)
C9	12.1(7)	15.3(8)	14.2(8)	1.0(6)	5.8(6)	2.3(6)
C10	16.0(8)	12.9(8)	16.5(8)	-0.6(7)	7.0(7)	-0.3(6)
C11	15.2(8)	22.2(9)	16.3(8)	-2.6(7)	4.9(7)	1.2(7)
C12	15.9(8)	24.9(9)	17.9(9)	3.6(7)	2.3(7)	5.8(7)
C13	22.6(9)	15.6(9)	27.2(10)	5.2(8)	4.5(8)	1.8(7)
C14	17.6(8)	15.4(8)	23.2(9)	-0.8(7)	2.9(7)	-0.7(7)
C15	11.9(7)	14.8(8)	12.6(8)	0.4(6)	2.6(6)	-1.5(6)
C16	18.4(8)	15.0(8)	20.6(9)	3.3(7)	5.0(7)	1.7(7)
C17	19.1(8)	19.4(9)	19.4(9)	7.6(7)	5.8(7)	-2.6(7)
C18	12.6(8)	22.9(9)	11.6(8)	0.4(7)	1.3(6)	-2.9(7)
C19	15.3(8)	15.5(8)	17.2(8)	-1.4(7)	4.3(7)	1.0(6)
C20	17.0(8)	13.5(8)	14.5(8)	3.0(6)	3.9(6)	-1.4(6)
C21	20.2(9)	27.1(10)	16.3(8)	1.3(7)	7.1(7)	-3.5(7)
N1	14.7(7)	13.0(7)	13.3(7)	-0.3(5)	5.1(5)	-0.3(5)
N2	12.8(6)	14.5(7)	12.2(6)	-0.8(5)	5.6(5)	-1.3(5)
N3	15.4(7)	12.7(7)	13.0(7)	-0.7(5)	5.3(5)	-1.3(5)
N4	13.9(7)	12.5(7)	13.1(7)	-0.3(5)	2.5(5)	-2.3(5)
O1	30.4(7)	13.5(6)	27.3(7)	2.5(5)	11.4(6)	-0.1(5)
O2	21.4(6)	15.0(6)	19.4(6)	-5.1(5)	5.2(5)	-3.8(5)
O3	16.2(6)	20.3(6)	13.4(6)	1.4(5)	2.7(5)	-1.7(5)
S1	14.4(2)	21.0(2)	15.7(2)	-5.14(17)	5.36(16)	1.59(16)
S2	13.76(19)	12.8(2)	12.4(2)	-1.15(15)	3.22(15)	-2.08(15)

Table 4 Bond Lengths for 579.

Atom	Atom	Length/Å	Atom	Atom	Length/Å
C1	C2	1.464(2)	C9	N4	1.440(2)
C1	N1	1.394(2)	C10	C11	1.391(2)
C1	O1	1.221(2)	C11	C12	1.382(3)
C2	C3	1.336(2)	C12	C13	1.386(3)
C3	N2	1.381(2)	C13	C14	1.387(2)
C4	N1	1.369(2)	C15	C16	1.388(2)
C4	N2	1.368(2)	C15	C20	1.394(2)
C4	N3	1.311(2)	C15	S2	1.7608(16)
C5	N1	1.466(2)	C16	C17	1.384(2)
C6	C7	1.366(2)	C17	C18	1.393(2)
C6	N2	1.409(2)	C18	C19	1.392(2)
C6	S1	1.7352(16)	C18	C21	1.506(2)
C7	N3	1.382(2)	C19	C20	1.386(2)
C7	N4	1.419(2)	N4	S2	1.6766(14)
C8	S1	1.8162(18)	O2	S2	1.4311(12)
C9	C10	1.392(2)	O3	S2	1.4342(12)
C9	C14	1.396(2)			

Table 5 Bond Angles for 579.

Atom	Atom	Atom	Angle/°	Atom	Atom	Atom	Angle/°
N1	C1	C2	114.93(15)	C17	C16	C15	118.83(16)
O1	C1	C2	124.65(16)	C16	C17	C18	121.26(16)
O1	C1	N1	120.41(15)	C17	C18	C21	119.55(15)
C3	C2	C1	122.20(15)	C19	C18	C17	118.73(15)
C2	C3	N2	119.22(15)	C19	C18	C21	121.71(16)
N2	C4	N1	119.44(14)	C20	C19	C18	121.17(16)
N3	C4	N1	127.16(15)	C19	C20	C15	118.70(15)
N3	C4	N2	113.39(14)	C1	N1	C5	119.39(14)
C7	C6	N2	103.48(13)	C4	N1	C1	122.46(14)
C7	C6	S1	132.64(13)	C4	N1	C5	118.06(13)
N2	C6	S1	123.88(12)	C3	N2	C6	131.79(14)
C6	C7	N3	113.13(14)	C4	N2	C3	121.72(14)
C6	C7	N4	124.91(15)	C4	N2	C6	106.49(13)
N3	C7	N4	121.75(14)	C4	N3	C7	103.52(13)
C10	C9	C14	119.50(15)	C7	N4	C9	120.04(13)
C10	C9	N4	119.51(15)	C7	N4	S2	114.44(11)
C14	C9	N4	120.98(15)	C9	N4	S2	120.72(11)
C11	C10	C9	119.94(16)	C6	S1	C8	102.09(8)
C12	C11	C10	120.62(16)	N4	S2	C15	107.30(7)

C11	C12	C13	119.26(16)	O2	S2	C15	108.31(8)
C12	C13	C14	120.89(17)	O2	S2	N4	107.84(7)
C13	C14	C9	119.72(16)	O2	S2	O3	119.12(7)
C16	C15	C20	121.30(15)	O3	S2	C15	108.88(7)
C16	C15	S2	119.66(13)	O3	S2	N4	104.80(7)
C20	C15	S2	119.00(12)				

Table 6 Torsion Angles for 579.

A	B	C	D	Angle/°	A	B	C	D	Angle/°
C1	C2	C3	N2	0.1(3)	C18	C19	C20	C15	1.0(2)
C2	C1	N1	C4	1.4(2)	C20	C15	C16	C17	0.2(3)
C2	C1	N1	C5	-175.05(14)	C20	C15	S2	N4	77.60(14)
C2	C3	N2	C4	-0.2(2)	C20	C15	S2	O2	-166.23(13)
C2	C3	N2	C6	179.16(16)	C20	C15	S2	O3	-35.31(15)
C6	C7	N3	C4	0.18(18)	C21	C18	C19	C20	177.95(16)
C6	C7	N4	C9	108.45(18)	N1	C1	C2	C3	-0.6(2)
C6	C7	N4	S2	-95.91(17)	N1	C4	N2	C3	0.9(2)
C7	C6	N2	C3	-179.83(16)	N1	C4	N2	C6	-178.57(14)
C7	C6	N2	C4	-0.40(17)	N1	C4	N3	C7	178.59(16)
C7	C6	S1	C8	87.09(18)	N2	C4	N1	C1	-1.6(2)
C7	N4	S2	C15	-100.99(12)	N2	C4	N1	C5	174.90(14)
C7	N4	S2	O2	142.52(11)	N2	C4	N3	C7	-0.46(17)
C7	N4	S2	O3	14.66(13)	N2	C6	C7	N3	0.15(18)
C9	C10	C11	C12	-2.4(2)	N2	C6	C7	N4	174.92(14)
C9	N4	S2	C15	54.47(14)	N2	C6	S1	C8	-91.93(15)
C9	N4	S2	O2	-62.02(14)	N3	C4	N1	C1	179.43(15)
C9	N4	S2	O3	170.12(12)	N3	C4	N1	C5	-4.1(2)
C10	C9	C14	C13	1.8(2)	N3	C4	N2	C3	-179.93(14)
C10	C9	N4	C7	10.1(2)	N3	C4	N2	C6	0.57(18)
C10	C9	N4	S2	-143.98(13)	N3	C7	N4	C9	-77.20(19)
C10	C11	C12	C13	2.4(3)	N3	C7	N4	S2	78.44(17)
C11	C12	C13	C14	-0.3(3)	N4	C7	N3	C4	-174.78(14)
C12	C13	C14	C9	-1.8(3)	N4	C9	C10	C11	-178.65(14)
C14	C9	C10	C11	0.3(2)	N4	C9	C14	C13	-179.31(15)
C14	C9	N4	C7	-168.81(15)	O1	C1	C2	C3	179.70(17)
C14	C9	N4	S2	37.1(2)	O1	C1	N1	C4	-178.93(15)
C15	C16	C17	C18	0.2(3)	O1	C1	N1	C5	4.6(2)
C16	C15	C20	C19	-0.8(2)	S1	C6	C7	N3	-179.01(12)
C16	C15	S2	N4	-104.68(14)	S1	C6	C7	N4	-4.2(3)
C16	C15	S2	O2	11.50(16)	S1	C6	N2	C3	-0.6(2)
C16	C15	S2	O3	142.41(13)	S1	C6	N2	C4	178.85(12)

C16	C17	C18	C19	0.0(3)	S2	C15	C16	C17	-177.45(13)
C16	C17	C18	C21	-178.57(16)	S2	C15	C20	C19	176.90(12)
C17	C18	C19	C20	-0.6(2)					

Table 7 Hydrogen Atom Coordinates ($\text{\AA} \times 10^4$) and Isotropic Displacement Parameters ($\text{\AA}^2 \times 10^3$) for 579.

Atom	x	y	z	U(eq)
H2	8615.5	6862.92	2739.09	22
H3	8930.5	5761.1	2515.39	19
H5A	6523.2	6170.59	6803.14	26
H5B	6523.07	6916.6	6253.72	26
H5C	7576.24	6641.68	7706.61	26
H8A	7764.85	3731.12	824.16	39
H8B	7289.94	4456.44	889.14	39
H8C	7011.76	3886.5	1937.3	39
H10	9319.73	4575.53	8476.18	18
H11	10586.47	4156.29	10896.75	22
H12	10469.83	3047.82	11582.67	24
H13	9169.91	2339.24	9753.34	27
H14	7977.2	2732.5	7263.93	24
H16	5753.03	2785.64	7338.82	22
H17	4750.47	2906	9163.85	23
H19	4387.06	4869.95	8222.21	20
H20	5416.59	4765.78	6420.71	18
H21A	4408.75	3983.29	11184.96	31
H21B	3339.95	3581.54	10034.18	31
H21C	3373.66	4362.51	9905.24	31

Imidazole 590

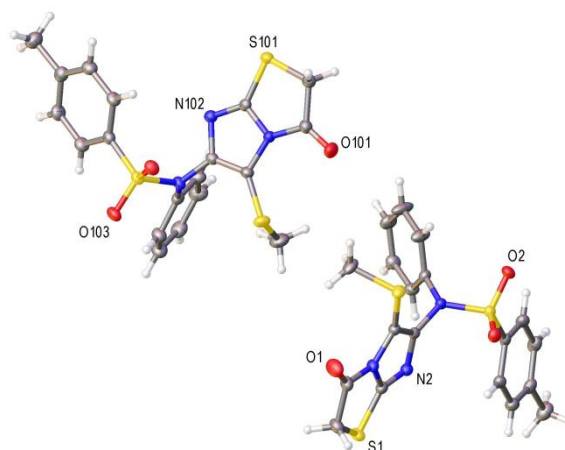
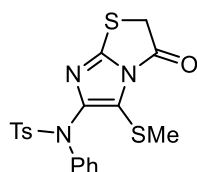


Table 1 Crystal data and structure refinement for 590.

Identification code	590
Empirical formula	C ₁₉ H ₁₇ N ₃ O ₃ S ₃
Formula weight	431.53
Temperature/K	100.01(10)
Crystal system	monoclinic
Space group	P2 ₁ /n
a/Å	10.3552(2)
b/Å	15.3465(3)
c/Å	24.9029(4)
α/°	90
β/°	101.764(2)
γ/°	90
Volume/Å ³	3874.35(13)
Z	8
ρ _{calc} /cm ³	1.480
μ/mm ⁻¹	3.729
F(000)	1792.0
Crystal size/mm ³	0.309 × 0.181 × 0.034
Radiation	CuKα (λ = 1.54184)

2 Θ range for data collection/ $^{\circ}$	6.806 to 148.934
Index ranges	$-12 \leq h \leq 8$, $-18 \leq k \leq 18$, $-27 \leq l \leq 30$
Reflections collected	21607
Independent reflections	7699 [$R_{\text{int}} = 0.0553$, $R_{\text{sigma}} = 0.0458$]
Data/restraints/parameters	7699/0/509
Goodness-of-fit on F^2	1.048
Final R indexes [$I \geq 2\sigma(I)$]	$R_1 = 0.0481$, $wR_2 = 0.1344$
Final R indexes [all data]	$R_1 = 0.0557$, $wR_2 = 0.1449$
Largest diff. peak/hole / $e \text{ \AA}^{-3}$	0.47/-0.65

Table 2 Fractional Atomic Coordinates ($\times 10^4$) and Equivalent Isotropic Displacement Parameters ($\text{\AA}^2 \times 10^3$) for 590. U_{eq} is defined as 1/3 of the trace of the orthogonalised U_{ij} tensor.

Atom	x	y	z	$U(\text{eq})$
C1	979(2)	10255.1(18)	6099.6(11)	23.3(5)
C2	183(3)	10107(2)	6540.8(12)	29.1(6)
C3	2242(2)	9188.3(16)	6656.9(10)	19.0(5)
C4	3949(2)	9023.7(16)	6326.8(9)	17.9(5)
C5	3251(2)	9633.5(16)	5993.6(10)	18.2(5)
C6	2630(3)	9785(2)	4868.9(11)	31.4(6)
C7	5233(2)	7895.9(17)	5979.8(10)	19.2(5)
C8	4841(2)	7129.0(17)	6182.5(10)	22.8(5)
C9	4781(3)	6374.3(17)	5867.3(11)	24.7(5)
C10	5123(3)	6391.6(19)	5360.1(11)	29.7(6)
C11	5536(4)	7165(2)	5163.3(12)	40.3(8)
C12	5586(3)	7924.8(19)	5471.9(11)	32.2(6)
C13	6797(2)	8422.5(16)	7286.2(9)	18.2(5)
C14	6072(2)	8593.2(17)	7689.9(10)	21.2(5)
C15	6292(3)	8081.5(18)	8159.6(10)	24.1(5)
C16	7214(3)	7409.0(17)	8234.1(10)	24.0(5)
C17	7907(3)	7243.7(18)	7819.2(11)	26.2(6)
C18	7708(2)	7750.5(17)	7346.3(10)	23.6(5)
C19	7480(3)	6880.8(19)	8758.7(11)	32.9(6)
N1	2111(2)	9745.0(14)	6212.8(8)	19.0(4)
N2	3332(2)	8742.1(14)	6743.6(8)	19.8(4)
N3	5199.2(19)	8707.1(14)	6272.6(8)	18.3(4)
O1	689(2)	10743.4(15)	5717.9(9)	37.1(5)
O2	7600.9(17)	8940.1(13)	6420.9(7)	23.7(4)
O3	6174.4(17)	9941.8(12)	6831.4(7)	22.5(4)

S1	923.1(6)	9228.1(5)	6990.6(3)	25.16(16)
S2	3697.9(6)	10234.6(4)	5469.3(2)	22.94(16)
S3	6520.9(5)	9079.3(4)	6692.2(2)	17.88(14)
C101	3938(2)	5623.4(18)	3724.2(11)	23.1(5)
C102	4617(2)	5515.1(18)	3243.7(10)	23.6(5)
C103	2582(2)	4582.9(16)	3181.1(10)	18.5(5)
C104	950(2)	4412.2(16)	3561.8(10)	18.4(5)
C105	1720(2)	4986.6(16)	3897.2(10)	19.7(5)
C106	1929(3)	4724(2)	5006.3(12)	39.2(7)
C107	-340(2)	3325.0(16)	3958.9(10)	19.7(5)
C108	655(3)	2713.0(18)	4003.4(11)	27.3(6)
C109	653(3)	1989.6(19)	4342.0(12)	32.3(6)
C110	-352(3)	1869.7(19)	4624.2(11)	30.8(6)
C111	-1348(3)	2479(2)	4573.7(12)	33.1(6)
C112	-1345(3)	3218.5(18)	4251.2(11)	25.5(5)
C113	-1794(2)	3714.8(16)	2602.9(10)	20.1(5)
C114	-1223(2)	3905.2(17)	2155.5(10)	23.0(5)
C115	-1454(3)	3347.1(18)	1707.6(11)	25.9(5)
C116	-2226(3)	2606.0(18)	1697.5(11)	25.6(5)
C117	-2747(3)	2409.9(18)	2157.6(11)	26.6(6)
C118	-2543(3)	2960.3(17)	2610.3(11)	24.5(5)
C119	-2513(3)	2030(2)	1195.1(12)	34.9(6)
N101	2810(2)	5100.1(14)	3644.5(8)	18.9(4)
N102	1484(2)	4147.8(14)	3117.0(8)	19.7(4)
N103	-295(2)	4100.1(14)	3634.8(8)	19.1(4)
O101	4314(2)	6092.3(15)	4112.2(8)	34.4(5)
O102	-1210.7(17)	5268.6(12)	2991.8(8)	23.5(4)
O103	-2728.0(17)	4358.2(12)	3401.5(8)	24.5(4)
S101	3819.8(6)	4639.8(4)	2804.0(2)	22.11(15)
S102	1444.5(7)	5534.3(5)	4475.8(3)	27.58(17)
S103	-1583.9(6)	4433.9(4)	3162.6(2)	19.30(15)

Table 3 Anisotropic Displacement Parameters ($\text{\AA}^2 \times 10^3$) for 590. The Anisotropic displacement factor exponent takes the form: $-2\pi^2[h^2a^{*2}U_{11}+2hka^*b^*U_{12}+\dots]$.

Atom	U ₁₁	U ₂₂	U ₃₃	U ₂₃	U ₁₃	U ₁₂
C1	19.3(12)	26.0(13)	23.6(12)	6.7(10)	2.1(10)	0.0(10)
C2	19.8(12)	38.2(16)	30.3(14)	6.8(12)	7.6(10)	1.3(11)
C3	21.0(12)	20.0(12)	15.6(11)	1.2(9)	2.6(9)	-2.3(9)
C4	17.5(11)	20.6(12)	15.5(10)	-1.2(9)	3.5(9)	-2.7(9)
C5	18.1(11)	19.4(12)	16.8(11)	1.2(9)	2.9(9)	-0.6(9)
C6	40.6(16)	36.8(16)	15.3(12)	2.1(11)	1.7(11)	-10.3(13)
C7	19.6(11)	21.5(12)	15.9(11)	-1.5(9)	1.9(9)	0.2(9)
C8	25.1(12)	24.3(13)	20.2(11)	1.4(10)	7.6(9)	3.1(10)

C9	25.6(12)	19.9(12)	29.3(13)	2.9(10)	7.1(10)	-0.3(10)
C10	38.9(15)	24.0(14)	26.7(13)	-7.0(11)	8.0(11)	-2.3(12)
C11	68(2)	34.3(16)	24.4(14)	-9.8(12)	23.9(14)	-17.5(15)
C12	51.3(17)	26.8(14)	22.3(13)	-3.6(11)	16.4(12)	-13.0(13)
C13	17.7(11)	17.9(11)	17.4(11)	-4.1(9)	-0.3(8)	1.0(9)
C14	20.4(11)	21.6(12)	21.3(12)	-3.6(10)	4.1(9)	0.8(10)
C15	26.3(13)	26.2(13)	20.3(12)	-0.6(10)	5.5(10)	-1.8(11)
C16	28.8(13)	20.2(12)	20.2(12)	-1.0(10)	-1.2(10)	-2.4(10)
C17	27.8(13)	22.0(13)	26.1(13)	-1.2(10)	-1.0(10)	7.0(11)
C18	23.5(12)	25.1(13)	22.2(12)	-6.1(10)	4.9(9)	1.7(10)
C19	43.5(16)	27.1(14)	24.8(13)	3.1(11)	-0.4(12)	-0.3(13)
N1	17.6(9)	22.1(11)	16.6(9)	4.4(8)	2.1(8)	-0.2(8)
N2	19.9(10)	22.4(11)	17.1(9)	1.5(8)	3.9(8)	-1.9(8)
N3	16.6(9)	21.6(10)	17.1(9)	-2.9(8)	4.2(7)	-0.9(8)
O1	28.9(10)	47.7(13)	33.9(11)	17.0(10)	4.3(9)	9.5(9)
O2	17.0(8)	30.8(10)	24.9(9)	-0.5(7)	8.5(7)	-1.4(7)
O3	22.8(9)	19.6(9)	24.6(9)	-2.7(7)	3.4(7)	-2.0(7)
S1	20.0(3)	33.5(4)	23.7(3)	6.1(3)	8.6(2)	1.0(3)
S2	25.9(3)	26.9(3)	16.1(3)	4.4(2)	4.3(2)	-5.5(2)
S3	16.5(3)	19.8(3)	17.4(3)	-1.6(2)	3.8(2)	-1.0(2)
C101	19.3(12)	26.6(13)	23.3(12)	0.6(10)	4.6(10)	-0.6(10)
C102	21.6(12)	27.5(13)	21.9(12)	1.2(10)	4.4(10)	1.0(10)
C103	17.5(11)	20.4(12)	16.8(11)	0.5(9)	1.5(9)	4.2(9)
C104	17.6(11)	18.3(12)	19.6(11)	3.5(9)	5.0(9)	2.0(9)
C105	19.8(11)	22.4(12)	18.0(11)	1.8(9)	6.4(9)	0.4(10)
C106	50.5(19)	48.2(19)	20.8(13)	2.4(13)	11.5(13)	1.3(15)
C107	23.0(12)	18.4(12)	17.2(11)	0.3(9)	2.9(9)	-2.2(10)
C108	33.4(14)	27.4(14)	22.7(12)	4.6(10)	9.4(11)	6.2(11)
C109	42.4(16)	26.2(14)	29.4(14)	7.8(11)	9.7(12)	9.5(12)
C110	39.6(15)	26.6(14)	24.0(13)	7.9(11)	1.8(11)	-1.1(12)
C111	30.8(14)	41.1(17)	28.0(13)	8.7(12)	7.6(11)	-6.0(13)
C112	23.5(12)	27.7(14)	26.0(12)	6.6(11)	6.6(10)	0.3(11)
C113	17.4(11)	20.8(12)	21.4(11)	4.5(9)	2.2(9)	0.9(9)
C114	22.4(12)	22.7(12)	24.8(12)	6.3(10)	6.8(10)	-2.8(10)
C115	27.0(13)	27.4(14)	24.5(12)	7.1(11)	7.8(10)	2.2(11)
C116	25.8(12)	24.7(13)	24.9(12)	1.5(10)	1.9(10)	3.5(11)
C117	27.0(13)	21.1(13)	31.6(14)	2.3(11)	5.5(11)	-5.8(11)
C118	25.3(12)	23.3(13)	25.8(13)	6.5(10)	7.3(10)	-2.3(10)
C119	39.8(16)	34.3(16)	29.6(14)	-1.4(12)	5.0(12)	-0.2(13)
N101	17.4(9)	22.8(10)	16.5(9)	-2.5(8)	3.6(8)	-1.2(8)
N102	20.4(10)	20.3(10)	18.8(10)	1.4(8)	4.5(8)	2.0(8)
N103	16.7(9)	19.0(10)	22.0(10)	5.0(8)	5.1(8)	1.3(8)
O101	30.4(10)	44.1(12)	28.7(10)	-12.6(9)	5.8(8)	-12.8(9)

O102	22.4(9)	19.5(9)	29.4(9)	4.7(7)	6.8(7)	1.5(7)
O103	17.6(8)	29.2(10)	28.0(9)	7.1(8)	7.5(7)	4.3(7)
S101	19.2(3)	29.5(3)	18.8(3)	-1.2(2)	6.5(2)	0.8(2)
S102	33.3(4)	29.5(4)	22.4(3)	-5.3(3)	11.6(3)	-0.2(3)
S103	16.9(3)	18.6(3)	23.0(3)	4.7(2)	5.6(2)	1.5(2)

Table 4 Bond Lengths for 590.

Atom	Atom	Length/Å	Atom	Atom	Length/Å
C1	C2	1.519(4)	C101	C102	1.515(3)
C1	N1	1.390(3)	C101	N101	1.398(3)
C1	O1	1.199(3)	C101	O101	1.204(3)
C2	S1	1.819(3)	C102	S101	1.821(3)
C3	N1	1.382(3)	C103	N101	1.380(3)
C3	N2	1.300(3)	C103	N102	1.300(3)
C3	S1	1.739(2)	C103	S101	1.739(2)
C4	C5	1.358(3)	C104	C105	1.356(4)
C4	N2	1.394(3)	C104	N102	1.395(3)
C4	N3	1.414(3)	C104	N103	1.421(3)
C5	N1	1.408(3)	C105	N101	1.411(3)
C5	S2	1.737(2)	C105	S102	1.741(3)
C6	S2	1.806(3)	C106	S102	1.809(3)
C7	C8	1.374(4)	C107	C108	1.382(4)
C7	C12	1.387(3)	C107	C112	1.397(3)
C7	N3	1.447(3)	C107	N103	1.444(3)
C8	C9	1.393(4)	C108	C109	1.394(4)
C9	C10	1.380(4)	C109	C110	1.381(4)
C10	C11	1.385(4)	C110	C111	1.378(4)
C11	C12	1.391(4)	C111	C112	1.391(4)
C13	C14	1.397(3)	C113	C114	1.395(3)
C13	C18	1.385(4)	C113	C118	1.395(4)
C13	S3	1.765(2)	C113	S103	1.756(3)
C14	C15	1.388(4)	C114	C115	1.388(4)
C15	C16	1.393(4)	C115	C116	1.388(4)
C16	C17	1.396(4)	C116	C117	1.395(4)
C16	C19	1.514(4)	C116	C119	1.511(4)
C17	C18	1.391(4)	C117	C118	1.390(4)
N3	S3	1.646(2)	N103	S103	1.669(2)
O2	S3	1.4355(17)	O102	S103	1.4275(18)
O3	S3	1.4323(19)	O103	S103	1.4347(18)

Table 5 Bond Angles for 590.

Atom	Atom	Atom	Angle/°	Atom	Atom	Atom	Angle/°
N1	C1	C2	109.2(2)	N101	C101	C102	109.5(2)
O1	C1	C2	125.6(2)	O101	C101	C102	125.0(2)
O1	C1	N1	125.3(2)	O101	C101	N101	125.5(2)
C1	C2	S1	109.51(19)	C101	C102	S101	109.25(18)
N1	C3	S1	113.69(18)	N101	C103	S101	113.77(18)
N2	C3	N1	113.5(2)	N102	C103	N101	113.2(2)
N2	C3	S1	132.78(19)	N102	C103	S101	133.00(19)
C5	C4	N2	113.6(2)	C105	C104	N102	113.6(2)
C5	C4	N3	124.2(2)	C105	C104	N103	125.1(2)
N2	C4	N3	122.1(2)	N102	C104	N103	121.3(2)
C4	C5	N1	103.4(2)	C104	C105	N101	103.2(2)
C4	C5	S2	129.44(19)	C104	C105	S102	130.41(19)
N1	C5	S2	126.86(18)	N101	C105	S102	126.21(19)
C8	C7	C12	121.0(2)	C108	C107	C112	120.1(2)
C8	C7	N3	120.9(2)	C108	C107	N103	119.8(2)
C12	C7	N3	118.0(2)	C112	C107	N103	120.0(2)
C7	C8	C9	119.2(2)	C107	C108	C109	119.8(3)
C10	C9	C8	120.6(2)	C110	C109	C108	120.5(3)
C9	C10	C11	119.7(3)	C111	C110	C109	119.4(3)
C10	C11	C12	120.2(3)	C110	C111	C112	121.1(3)
C7	C12	C11	119.3(3)	C111	C112	C107	119.1(3)
C14	C13	S3	118.48(19)	C114	C113	C118	120.8(2)
C18	C13	C14	121.1(2)	C114	C113	S103	119.9(2)
C18	C13	S3	120.43(19)	C118	C113	S103	119.36(19)
C15	C14	C13	118.7(2)	C115	C114	C113	118.8(2)
C14	C15	C16	121.5(2)	C114	C115	C116	121.6(2)
C15	C16	C17	118.6(2)	C115	C116	C117	118.7(3)
C15	C16	C19	120.7(2)	C115	C116	C119	120.7(3)
C17	C16	C19	120.7(2)	C117	C116	C119	120.7(3)
C18	C17	C16	121.0(2)	C118	C117	C116	121.0(2)
C13	C18	C17	119.2(2)	C117	C118	C113	119.1(2)
C1	N1	C5	136.8(2)	C101	N101	C105	136.8(2)
C3	N1	C1	116.9(2)	C103	N101	C101	116.4(2)
C3	N1	C5	106.3(2)	C103	N101	C105	106.6(2)
C3	N2	C4	103.1(2)	C103	N102	C104	103.4(2)
C4	N3	C7	117.39(19)	C104	N103	C107	118.85(19)
C4	N3	S3	118.62(16)	C104	N103	S103	114.98(16)
C7	N3	S3	121.09(16)	C107	N103	S103	122.32(16)
C3	S1	C2	90.29(12)	C103	S101	C102	90.33(12)
C5	S2	C6	101.97(12)	C105	S102	C106	101.81(14)
N3	S3	C13	107.81(11)	N103	S103	C113	108.55(11)

O2	S3	C13	107.50(11)	O102	S103	C113	108.95(11)
O2	S3	N3	106.05(10)	O102	S103	N103	105.02(11)
O3	S3	C13	109.32(11)	O102	S103	O103	119.53(11)
O3	S3	N3	104.92(11)	O103	S103	C113	107.39(12)
O3	S3	O2	120.60(11)	O103	S103	N103	107.00(11)

Table 6 Torsion Angles for 590.

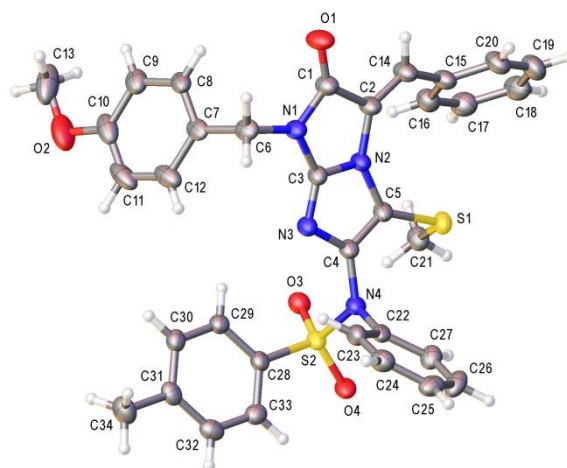
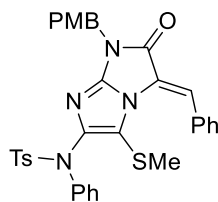
A	B	C	D	Angle/°	A	B	C	D	Angle/°
C1	C2	S1	C3	6.2(2)	C101	C102	S101	C103	8.20(19)
C2	C1	N1	C3	4.2(3)	C102	C101	N101	C103	2.9(3)
C2	C1	N1	C5	-174.7(3)	C102	C101	N101	C105	-171.2(3)
C4	C5	N1	C1	178.9(3)	C104	C105	N101	C101	174.6(3)
C4	C5	N1	C3	0.0(3)	C104	C105	N101	C103	0.1(3)
C4	C5	S2	C6	111.0(3)	C104	C105	S102	C106	83.1(3)
C4	N3	S3	C13	87.6(2)	C104	N103	S103	C113	86.3(2)
C4	N3	S3	O2	-157.50(18)	C104	N103	S103	O102	-30.1(2)
C4	N3	S3	O3	-28.8(2)	C104	N103	S103	O103	-158.07(18)
C5	C4	N2	C3	0.3(3)	C105	C104	N102	C103	-1.1(3)
C5	C4	N3	C7	-97.1(3)	C105	C104	N103	C107	-89.6(3)
C5	C4	N3	S3	101.9(3)	C105	C104	N103	S103	111.9(2)
C7	C8	C9	C10	0.7(4)	C107	C108	C109	C110	1.4(4)
C7	N3	S3	C13	-72.6(2)	C107	N103	S103	C113	-71.3(2)
C7	N3	S3	O2	42.3(2)	C107	N103	S103	O102	172.31(19)
C7	N3	S3	O3	170.94(18)	C107	N103	S103	O103	44.3(2)
C8	C7	C12	C11	0.3(5)	C108	C107	C112	C111	-1.7(4)
C8	C7	N3	C4	-65.1(3)	C108	C107	N103	C104	-26.4(3)
C8	C7	N3	S3	95.4(3)	C108	C107	N103	S103	130.4(2)
C8	C9	C10	C11	0.2(4)	C108	C109	C110	C111	-0.8(5)
C9	C10	C11	C12	-0.9(5)	C109	C110	C111	C112	-1.1(5)
C10	C11	C12	C7	0.6(5)	C110	C111	C112	C107	2.4(4)
C12	C7	C8	C9	-1.0(4)	C112	C107	C108	C109	-0.1(4)
C12	C7	N3	C4	110.7(3)	C112	C107	N103	C104	150.0(2)
C12	C7	N3	S3	-88.9(3)	C112	C107	N103	S103	-53.2(3)
C13	C14	C15	C16	0.0(4)	C113	C114	C115	C116	-0.5(4)
C14	C13	C18	C17	-0.5(4)	C114	C113	C118	C117	-1.9(4)
C14	C13	S3	N3	-81.5(2)	C114	C113	S103	N103	-94.2(2)
C14	C13	S3	O2	164.57(19)	C114	C113	S103	O102	19.6(2)
C14	C13	S3	O3	32.0(2)	C114	C113	S103	O103	150.5(2)
C14	C15	C16	C17	-1.2(4)	C114	C115	C116	C117	-1.9(4)
C14	C15	C16	C19	177.6(2)	C114	C115	C116	C119	177.3(2)
C15	C16	C17	C18	1.5(4)	C115	C116	C117	C118	2.5(4)
C16	C17	C18	C13	-0.7(4)	C116	C117	C118	C113	-0.6(4)
C18	C13	C14	C15	0.8(4)	C118	C113	C114	C115	2.4(4)

C18	C13	S3	N3	98.1(2)	C118	C113	S103	N103	86.3(2)
C18	C13	S3	O2	-15.9(2)	C118	C113	S103	O102	-159.88(19)
C18	C13	S3	O3	-148.4(2)	C118	C113	S103	O103	-29.1(2)
C19	C16	C17	C18	-177.2(2)	C119	C116	C117	C118	-176.7(3)
N1	C1	C2	S1	-6.9(3)	N101	C101	C102	S101	-7.7(3)
N1	C3	N2	C4	-0.3(3)	N101	C103	N102	C104	1.2(3)
N1	C3	S1	C2	-4.2(2)	N101	C103	S101	C102	-6.97(19)
N1	C5	S2	C6	-76.9(2)	N101	C105	S102	C106	-101.8(2)
N2	C3	N1	C1	-179.0(2)	N102	C103	N101	C101	-176.7(2)
N2	C3	N1	C5	0.2(3)	N102	C103	N101	C105	-0.9(3)
N2	C3	S1	C2	175.4(3)	N102	C103	S101	C102	173.4(3)
N2	C4	C5	N1	-0.2(3)	N102	C104	C105	N101	0.6(3)
N2	C4	C5	S2	173.32(18)	N102	C104	C105	S102	176.48(19)
N2	C4	N3	C7	84.3(3)	N102	C104	N103	C107	91.3(3)
N2	C4	N3	S3	-76.7(3)	N102	C104	N103	S103	-67.2(3)
N3	C4	C5	N1	-178.8(2)	N103	C104	C105	N101	-178.6(2)
N3	C4	C5	S2	-5.4(4)	N103	C104	C105	S102	-2.7(4)
N3	C4	N2	C3	179.0(2)	N103	C104	N102	C103	178.1(2)
N3	C7	C8	C9	174.6(2)	N103	C107	C108	C109	176.3(2)
N3	C7	C12	C11	-175.4(3)	N103	C107	C112	C111	-178.1(2)
O1	C1	C2	S1	174.1(3)	O101	C101	C102	S101	172.7(2)
O1	C1	N1	C3	-176.8(3)	O101	C101	N101	C103	-177.5(3)
O1	C1	N1	C5	4.3(5)	O101	C101	N101	C105	8.4(5)
S1	C3	N1	C1	0.7(3)	S101	C103	N101	C101	3.7(3)
S1	C3	N1	C5	179.87(16)	S101	C103	N101	C105	179.42(16)
S1	C3	N2	C4	-179.9(2)	S101	C103	N102	C104	-179.2(2)
S2	C5	N1	C1	5.2(4)	S102	C105	N101	C101	-1.5(4)
S2	C5	N1	C3	-173.72(19)	S102	C105	N101	C103	-175.97(19)
S3	C13	C14	C15	-179.60(19)	S103	C113	C114	C115	-177.10(19)
S3	C13	C18	C17	179.9(2)	S103	C113	C118	C117	177.6(2)

Table 7 Hydrogen Atom Coordinates ($\text{\AA} \times 10^4$) and Isotropic Displacement Parameters ($\text{\AA}^2 \times 10^3$) for 590.

Atom	x	y	z	U(eq)
H2A	-718.12	9957.19	6372.07	35
H2B	168.27	10636.38	6752.14	35
H6A	2855.22	10029.39	4545.18	47
H6B	1729.75	9921.58	4876.33	47
H6C	2738.98	9163.44	4865.89	47
H8	4619.42	7113.87	6525.9	27
H9	4506.59	5854.2	5999.97	30
H10	5077.5	5885.77	5151.36	36
H11	5779.19	7177.35	4824.04	48

H12	5854.27	8446.48	5339.12	39
H14	5453.16	9040.64	7644.89	25
H15	5812.66	8190.27	8430.35	29
H17	8511.08	6787.84	7859.67	31
H18	8181.25	7639.41	7073.86	28
H19A	8079.64	7193.08	9037.4	49
H19B	7861.27	6330.66	8693.43	49
H19C	6666.25	6783.65	8877.93	49
H10A	5540.99	5377.8	3376.3	28
H10B	4561.12	6054.04	3036.81	28
H10C	1563.44	4169.11	4877.08	59
H10D	1605.82	4889.43	5326.7	59
H10E	2873.12	4682.93	5096.59	59
H108	1323.88	2783.24	3808.18	33
H109	1332.83	1584.54	4378.13	39
H110	-356.58	1382.77	4846.12	37
H111	-2032.83	2393.9	4758.49	40
H112	-2004.49	3636.22	4230.38	31
H114	-697.71	4397.04	2157.2	28
H115	-1081.03	3472.78	1406.86	31
H117	-3237.84	1903.4	2161.48	32
H118	-2899.76	2827.52	2914.14	29
H11A	-3126.44	2317.84	909.01	52
H11B	-2886.81	1489.6	1284.65	52
H11C	-1708.93	1915.65	1072.37	52

Imidazole 595**Table 1 Crystal data and structure refinement for 595.**

Identification code	595
Empirical formula	C ₃₄ H ₃₀ N ₄ O ₄ S ₂
Formula weight	622.74
Temperature/K	100.00(10)
Crystal system	monoclinic
Space group	P2 ₁ /c
a/Å	19.1869(6)
b/Å	8.9727(4)
c/Å	18.1187(6)
α /°	90
β /°	102.814(3)
γ /°	90
Volume/Å ³	3041.6(2)
Z	4
$\rho_{\text{calc}}/\text{cm}^3$	1.360
μ/mm^{-1}	1.963
F(000)	1304.0
Crystal size/mm ³	0.201 × 0.181 × 0.106
Radiation	CuK α (λ = 1.54184)

2 Θ range for data collection/ $^{\circ}$	9.454 to 140.124
Index ranges	$-23 \leq h \leq 21$, $-10 \leq k \leq 10$, $-22 \leq l \leq 18$
Reflections collected	20391
Independent reflections	5751 [$R_{\text{int}} = 0.0414$, $R_{\text{sigma}} = 0.0316$]
Data/restraints/parameters	5751/0/400
Goodness-of-fit on F^2	1.045
Final R indexes [$I \geq 2\sigma(I)$]	$R_1 = 0.0432$, $wR_2 = 0.1034$
Final R indexes [all data]	$R_1 = 0.0488$, $wR_2 = 0.1076$
Largest diff. peak/hole / $e \text{ \AA}^{-3}$	0.35/-0.43

Table 2 Fractional Atomic Coordinates ($\times 10^4$) and Equivalent Isotropic Displacement Parameters ($\text{\AA}^2 \times 10^3$) for 595. U_{eq} is defined as 1/3 of the trace of the orthogonalised U_{ij} tensor.

Atom	x	y	z	U(eq)
C1	8695.8(11)	5927(3)	8281.7(11)	34.4(5)
C2	9135.1(11)	5787(3)	7686.1(11)	32.1(5)
C3	8027.3(10)	4823(2)	7244.7(10)	28.2(4)
C4	7959.1(10)	3741(2)	6213.8(10)	27.8(4)
C5	8632.5(10)	4334(2)	6373.3(10)	28.4(4)
C6	7401.3(11)	5352(3)	8296.1(11)	35.5(5)
C7	6912.8(11)	6635(3)	8010.6(11)	35.1(5)
C8	7080.7(11)	8064(3)	8276.9(11)	35.6(5)
C9	6652.6(12)	9284(3)	8004.8(12)	42.3(6)
C10	6033.4(13)	9045(4)	7448.7(13)	50.9(7)
C11	5858.9(12)	7616(4)	7175.5(13)	55.2(8)
C12	6290.6(12)	6422(4)	7452.0(12)	46.3(7)
C13	5765.2(18)	11645(5)	7399.9(16)	74.9(11)
C14	9799.5(11)	6303(3)	7813.0(12)	37.4(5)
C15	10283.4(11)	6524(3)	7296.9(12)	36.7(5)
C16	10065.4(12)	7335(3)	6635.4(12)	39.5(5)
C17	10533.7(13)	7640(3)	6174.7(13)	44.5(6)
C18	11229.5(13)	7099(3)	6371.7(13)	46.3(6)
C19	11450.0(12)	6297(3)	7027.5(14)	48.5(6)
C20	10986.2(12)	6013(3)	7498.0(13)	43.6(6)
C21	9071.1(11)	5424(3)	5115.7(11)	37.3(5)
C22	7693.0(10)	1232(2)	5684.3(10)	27.9(4)
C23	7300.8(11)	555(3)	6147.8(11)	33.4(5)
C24	7340.4(12)	-980(3)	6252.6(12)	38.2(5)
C25	7752.6(12)	-1838(3)	5881.9(11)	38.9(5)

C26	8144.5(13)	-1149(3)	5416.3(12)	42.7(6)
C27	8121.3(12)	382(3)	5323.4(11)	35.5(5)
C28	6231.2(10)	3206(2)	5031.4(10)	27.4(4)
C29	5987.6(10)	4065(2)	5564.5(11)	29.4(4)
C30	5322.1(11)	3767(3)	5702.6(11)	31.2(4)
C31	4891.3(10)	2628(3)	5322.3(11)	31.5(5)
C32	5140.6(11)	1814(3)	4779.6(11)	33.5(5)
C33	5807.8(11)	2088(2)	4635.9(11)	31.4(4)
C34	4177.1(12)	2289(3)	5500.5(14)	43.9(6)
N1	8028.9(9)	5365(2)	7958.8(9)	31.0(4)
N2	8669.4(8)	5090(2)	7064.8(9)	28.2(4)
N3	7569.4(9)	4049(2)	6759.2(9)	29.3(4)
N4	7677.8(8)	2830(2)	5578.6(8)	28.0(4)
O1	8882.7(9)	6441(2)	8909.6(8)	44.6(4)
O2	5572.6(10)	10166(3)	7138.5(10)	70.0(7)
O3	7218.4(7)	5113.3(17)	4891.7(7)	32.2(3)
O4	7138.0(7)	2704.8(19)	4202.8(7)	34.8(4)
S1	9310.3(3)	4091.2(6)	5886.2(3)	31.73(14)
S2	7088.0(2)	3544.9(6)	4863.4(2)	27.89(13)

Table 3 Anisotropic Displacement Parameters ($\text{\AA}^2 \times 10^3$) for 595. The Anisotropic displacement factor exponent takes the form: $-2\pi^2[h^2a^{*2}U_{11}+2hka^*b^*U_{12}+\dots]$.

Atom	U ₁₁	U ₂₂	U ₃₃	U ₂₃	U ₁₃	U ₁₂
C1	32.6(10)	48.8(14)	22.1(10)	-4.6(9)	7.0(8)	-4.4(9)
C2	29.6(10)	48.4(14)	18.0(9)	-5.1(9)	4.5(8)	-3.3(9)
C3	24.8(9)	42.9(12)	17.7(9)	-1.8(8)	6.3(7)	1.6(8)
C4	25.6(9)	41.2(12)	16.4(8)	-1.2(8)	4.1(7)	2.0(8)
C5	25.8(9)	43.7(12)	16.0(8)	-1.0(8)	4.8(7)	3.0(8)
C6	34.4(11)	53.9(14)	22.0(9)	-4.3(9)	14.6(8)	-6.2(10)
C7	27.8(10)	62.7(16)	18.2(9)	-5.1(9)	12.6(8)	-2.2(10)
C8	28.1(10)	59.0(15)	19.9(9)	-7.3(9)	5.5(8)	5.8(10)
C9	38.1(12)	68.2(17)	22.0(10)	-2.4(10)	9.4(9)	11.5(11)
C10	33.6(12)	96(2)	24.0(11)	7.9(13)	9.2(9)	17.8(13)
C11	27.1(11)	112(3)	24.5(11)	0.2(14)	2.1(9)	-5.7(14)
C12	31.1(11)	85(2)	24.6(11)	-6.1(11)	8.9(9)	-13.1(12)
C13	74(2)	113(3)	41.7(15)	20.3(18)	21.0(14)	55(2)
C14	31.1(10)	58.1(15)	22.7(10)	-6.4(10)	5.4(8)	-8.0(10)
C15	29.5(10)	54.3(15)	26.4(10)	-8.9(10)	6.4(8)	-8.8(10)
C16	32.8(11)	52.2(15)	33.2(11)	-1.5(10)	6.4(9)	-1.1(10)
C17	46.3(13)	56.1(16)	32.4(11)	-2.1(11)	11.6(10)	-4.6(11)
C18	39.6(12)	66.9(18)	36.9(12)	-8.3(12)	18.0(10)	-11.8(12)
C19	28.7(11)	75.3(19)	41.2(13)	-5.7(12)	6.7(9)	-4.5(11)
C20	30.5(11)	69.2(18)	28.9(11)	-3.3(11)	2.2(9)	-4.3(11)

C21	31.9(10)	55.5(15)	25.7(10)	2.8(10)	9.4(8)	3.3(10)
C22	23.8(9)	41.3(12)	16.7(8)	-3.6(8)	0.6(7)	4.2(8)
C23	26.2(10)	46.8(13)	28.1(10)	-6.1(9)	7.7(8)	0.5(9)
C24	36.5(11)	49.7(14)	28.9(11)	-1.8(10)	8.2(9)	-5.1(10)
C25	49.4(13)	41.6(13)	22.1(10)	-1.9(9)	0.3(9)	5.4(10)
C26	54.4(14)	53.8(15)	22.2(10)	1.0(10)	13.0(10)	19.4(12)
C27	37.8(11)	50.3(14)	20.4(9)	2.2(9)	10.6(8)	8.8(10)
C28	23.7(9)	37.1(11)	20.5(9)	1.5(8)	3.2(7)	3.7(8)
C29	27.3(9)	37.6(12)	21.7(9)	-2.0(8)	2.1(7)	3.4(8)
C30	29.1(10)	40.1(12)	24.3(10)	2.1(9)	5.7(8)	8.1(9)
C31	26.9(10)	38.5(12)	28.2(10)	9.2(9)	3.9(8)	2.8(8)
C32	34.8(11)	35.9(12)	27.1(10)	4.8(9)	0.8(8)	-2.8(9)
C33	35.8(11)	36.6(12)	20.8(9)	0.6(8)	4.2(8)	3.6(9)
C34	32.7(11)	56.8(16)	43.4(13)	7.2(11)	11.2(10)	-1.8(11)
N1	28.6(8)	46.5(11)	18.9(8)	-6.0(7)	7.8(6)	-2.9(8)
N2	23.8(8)	43.1(10)	17.8(7)	-3.7(7)	4.6(6)	-1.9(7)
N3	25.7(8)	43.8(11)	19.0(8)	-3.0(7)	6.5(6)	-0.3(7)
N4	26.1(8)	39.0(10)	17.6(7)	-2.6(7)	2.0(6)	2.5(7)
O1	42.6(9)	68.2(12)	23.5(7)	-13.1(7)	8.8(6)	-13.8(8)
O2	47.6(11)	123(2)	37.5(10)	13.4(12)	4.4(8)	35.7(12)
O3	30.0(7)	41.3(9)	25.2(7)	1.8(6)	5.8(5)	-0.7(6)
O4	30.8(7)	55.9(10)	17.1(6)	-4.9(6)	3.8(5)	5.0(7)
S1	25.6(2)	47.2(3)	24.1(2)	-0.6(2)	8.98(18)	4.7(2)
S2	24.7(2)	42.1(3)	16.6(2)	-1.13(19)	4.02(17)	2.40(19)

Table 4 Bond Lengths for 595.

Atom	Atom	Length/Å	Atom	Atom	Length/Å
C1	C2	1.515(3)	C15	C20	1.394(3)
C1	N1	1.379(3)	C16	C17	1.383(3)
C1	O1	1.206(3)	C17	C18	1.391(4)
C2	C14	1.328(3)	C18	C19	1.373(4)
C2	N2	1.418(2)	C19	C20	1.386(3)
C3	N1	1.382(2)	C21	S1	1.818(2)
C3	N2	1.364(2)	C22	C23	1.386(3)
C3	N3	1.298(3)	C22	C27	1.386(3)
C4	C5	1.368(3)	C22	N4	1.447(3)
C4	N3	1.393(2)	C23	C24	1.390(3)
C4	N4	1.417(2)	C24	C25	1.380(3)
C5	N2	1.413(2)	C25	C26	1.393(3)
C5	S1	1.7399(19)	C26	C27	1.384(4)
C6	C7	1.502(3)	C28	C29	1.395(3)
C6	N1	1.466(2)	C28	C33	1.386(3)

C7	C8	1.382(3)	C28	S2	1.763(2)
C7	C12	1.396(3)	C29	C30	1.381(3)
C8	C9	1.392(3)	C30	C31	1.397(3)
C9	C10	1.393(3)	C31	C32	1.392(3)
C10	C11	1.389(4)	C31	C34	1.507(3)
C10	O2	1.375(3)	C32	C33	1.384(3)
C11	C12	1.378(4)	N4	S2	1.6494(16)
C13	O2	1.429(5)	O3	S2	1.4283(16)
C14	C15	1.470(3)	O4	S2	1.4356(14)
C15	C16	1.385(3)			

Table 5 Bond Angles for 595.

Atom	Atom	Atom	Angle/°	Atom	Atom	Atom	Angle/°
N1	C1	C2	106.13(16)	C23	C22	N4	121.13(18)
O1	C1	C2	127.4(2)	C27	C22	N4	118.65(19)
O1	C1	N1	126.43(19)	C22	C23	C24	119.8(2)
C14	C2	C1	120.82(18)	C25	C24	C23	120.4(2)
C14	C2	N2	134.67(19)	C24	C25	C26	119.5(2)
N2	C2	C1	104.49(16)	C27	C26	C25	120.5(2)
N2	C3	N1	110.32(17)	C26	C27	C22	119.7(2)
N3	C3	N1	133.12(18)	C29	C28	S2	119.51(16)
N3	C3	N2	116.35(17)	C33	C28	C29	120.66(19)
C5	C4	N3	113.77(17)	C33	C28	S2	119.83(15)
C5	C4	N4	124.61(17)	C30	C29	C28	118.9(2)
N3	C4	N4	121.55(17)	C29	C30	C31	121.50(19)
C4	C5	N2	103.52(16)	C30	C31	C34	120.6(2)
C4	C5	S1	128.41(16)	C32	C31	C30	118.29(19)
N2	C5	S1	127.87(15)	C32	C31	C34	121.1(2)
N1	C6	C7	110.99(18)	C33	C32	C31	121.1(2)
C8	C7	C6	120.73(19)	C32	C33	C28	119.46(19)
C8	C7	C12	118.4(2)	C1	N1	C3	109.59(16)
C12	C7	C6	120.9(2)	C1	N1	C6	126.60(17)
C7	C8	C9	122.2(2)	C3	N1	C6	123.80(17)
C8	C9	C10	118.5(3)	C3	N2	C2	109.36(15)
C11	C10	C9	120.0(3)	C3	N2	C5	104.89(16)
O2	C10	C9	123.4(3)	C5	N2	C2	144.56(17)
O2	C10	C11	116.6(2)	C3	N3	C4	101.42(16)
C12	C11	C10	120.7(2)	C4	N4	C22	118.12(16)
C11	C12	C7	120.4(3)	C4	N4	S2	119.04(14)
C2	C14	C15	130.89(19)	C22	N4	S2	118.66(13)
C16	C15	C14	120.6(2)	C10	O2	C13	116.6(2)

C16	C15	C20	119.2(2)	C5	S1	C21	102.55(10)
C20	C15	C14	120.0(2)	N4	S2	C28	107.50(9)
C17	C16	C15	121.0(2)	O3	S2	C28	109.04(9)
C16	C17	C18	119.4(2)	O3	S2	N4	105.71(9)
C19	C18	C17	119.9(2)	O3	S2	O4	120.25(9)
C18	C19	C20	120.8(2)	O4	S2	C28	106.89(9)
C19	C20	C15	119.7(2)	O4	S2	N4	106.85(9)
C23	C22	C27	120.2(2)				

Table 6 Hydrogen Atom Coordinates ($\text{\AA} \times 10^4$) and Isotropic Displacement Parameters ($\text{\AA}^2 \times 10^3$) for 595.

Atom	x	y	z	U(eq)
H6A	7555.16	5414.72	8842.58	43
H6B	7144.08	4422.42	8172.4	43
H8	7493.31	8214.23	8650.2	43
H9	6776.96	10236.85	8189.8	51
H11	5446.51	7462.27	6802.3	66
H12	6166.8	5470.14	7265.43	56
H13A	5802.51	11692.83	7936.6	112
H13B	5405.84	12331.12	7149.95	112
H13C	6216.62	11902.51	7288.89	112
H14	9991.13	6570.11	8312.72	45
H16	9597.22	7679.21	6499.24	47
H17	10384.69	8202.1	5736.84	53
H18	11545.14	7280.2	6059.63	56
H19	11916.31	5940.33	7157.42	58
H20	11143.09	5485.23	7945.66	52
H21A	9198.49	6410.35	5303.32	56
H21B	8565.67	5378.65	4908.52	56
H21C	9322.93	5187.01	4728.33	56
H23	7012.13	1125.31	6387.83	40
H24	7087.65	-1431.81	6574.46	46
H25	7768.53	-2867.94	5942.48	47
H26	8423.79	-1722.74	5166.13	51
H27	8391.59	838.83	5020.41	43
H29	6268.89	4826.52	5822.72	35
H30	5156.98	4337.78	6056.81	37
H32	4853.81	1073.6	4508.95	40
H33	5970.8	1526.69	4276.84	38
H34A	4248.89	1849.01	5994.5	66
H34B	3918.2	1607.74	5130.87	66
H34C	3909.09	3195.64	5489.52	66

Imidazole 639

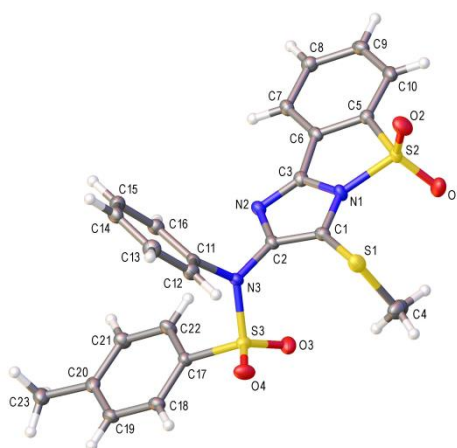
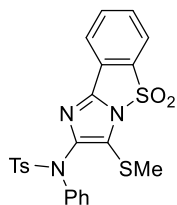


Table 1 Crystal data and structure refinement for 639.

Identification code	639
Empirical formula	C ₂₃ H ₁₉ N ₃ O ₄ S ₃
Formula weight	497.59
Temperature/K	100.00(10)
Crystal system	monoclinic
Space group	P2 ₁ /n
a/Å	11.1459(3)
b/Å	15.8489(4)
c/Å	12.5780(3)
α/°	90
β/°	100.493(2)
γ/°	90
Volume/Å ³	2184.75(10)
Z	4
ρ _{calc} /g/cm ³	1.513
μ/mm ⁻¹	3.428
F(000)	1032.0
Crystal size/mm ³	0.199 × 0.145 × 0.11
Radiation	CuKα (λ = 1.54184)
2θ range for data collection/°	9.07 to 140.098

Index ranges	$-12 \leq h \leq 13, -19 \leq k \leq 17, -10 \leq l \leq 15$
Reflections collected	6861
Independent reflections	4092 [$R_{\text{int}} = 0.0451, R_{\text{sigma}} = 0.0496$]
Data/restraints/parameters	4092/0/300
Goodness-of-fit on F^2	1.044
Final R indexes [$I \geq 2\sigma(I)$]	$R_1 = 0.0389, wR_2 = 0.1031$
Final R indexes [all data]	$R_1 = 0.0445, wR_2 = 0.1089$
Largest diff. peak/hole / $e \text{ \AA}^{-3}$	0.48/-0.45

Table 2 Fractional Atomic Coordinates ($\times 10^4$) and Equivalent Isotropic Displacement Parameters ($\text{\AA}^2 \times 10^3$) for 639. U_{eq} is defined as 1/3 of the trace of the orthogonalised U_{ij} tensor.

Atom	x	y	z	$U(\text{eq})$
C1	3369.5(18)	4334.7(13)	7589.7(15)	15.9(4)
C2	2553.2(17)	3692.3(13)	7626.1(15)	15.0(4)
C3	4178.8(18)	3062.5(13)	7434.3(15)	16.0(4)
C4	3829(2)	5641.0(16)	9018.5(19)	32.1(5)
C5	6218.6(17)	3088.0(13)	7184.8(15)	15.5(4)
C6	5232.9(17)	2563.1(13)	7269.8(15)	15.7(4)
C7	5347.5(17)	1701.2(13)	7161.1(16)	17.4(4)
C8	6453.6(18)	1381.0(14)	6964.7(16)	19.0(4)
C9	7424.4(18)	1915.3(14)	6882.9(16)	20.3(4)
C10	7321.4(18)	2782.2(14)	6990.3(16)	19.6(4)
C11	411.4(17)	3668.2(13)	6733.1(15)	15.3(4)
C12	-275.2(19)	4337.6(13)	6232.1(17)	19.4(4)
C13	-1066(2)	4196.8(14)	5257.4(17)	22.2(4)
C14	-1165.7(18)	3406.6(14)	4780.9(17)	20.8(4)
C15	-489.3(18)	2738.3(14)	5297.7(17)	19.9(4)
C16	286.5(18)	2865.9(13)	6276.0(17)	18.3(4)
C17	30.0(17)	3223.9(13)	9153.8(15)	15.3(4)
C18	-1090.5(18)	3384.9(14)	9455.4(16)	18.3(4)
C19	-1785.8(18)	2703.4(14)	9675.4(16)	19.4(4)
C20	-1391.9(18)	1877.3(14)	9603.0(15)	18.7(4)
C21	-253.4(19)	1736.8(14)	9315.3(17)	20.3(4)
C22	453.3(18)	2402.1(13)	9093.9(17)	19.4(4)
C23	-2178(2)	1138.8(14)	9794.3(17)	23.4(5)
N1	4430.3(15)	3906.8(11)	7475.8(13)	16.2(3)
N2	3048.0(14)	2901.2(11)	7531.3(13)	15.5(3)
N3	1314.1(14)	3799.9(11)	7697.7(13)	15.6(3)

O1	6493.1(13)	4529.5(10)	8300.0(13)	26.0(4)
O2	5815.0(14)	4616.4(10)	6334.0(13)	26.4(4)
O3	2061.8(14)	4098.1(10)	9615.5(12)	23.1(3)
O4	174.1(14)	4806.2(9)	8704.0(12)	24.0(3)
S1	3195.2(5)	5420.7(3)	7616.3(4)	21.39(14)
S2	5869.0(4)	4164.4(3)	7318.8(4)	16.95(14)
S3	932.1(4)	4073.2(3)	8862.4(4)	16.24(14)

Table 3 Anisotropic Displacement Parameters ($\text{\AA}^2 \times 10^3$) for 639. The Anisotropic displacement factor exponent takes the form: $-2\pi^2[h^2a^{*2}U_{11}+2hka^*b^*U_{12}+\dots]$.

Atom	U ₁₁	U ₂₂	U ₃₃	U ₂₃	U ₁₃	U ₁₂
C1	14.8(9)	18.3(10)	15.0(9)	0.4(8)	3.8(7)	1.9(8)
C2	13.9(9)	17.4(10)	14.0(9)	1.1(7)	3.5(7)	-0.9(7)
C3	16.5(9)	17.3(10)	14.0(9)	2.2(7)	2.0(7)	-1.0(8)
C4	45.5(15)	22.2(11)	31.4(13)	-4.6(10)	14.1(11)	-8.3(10)
C5	15.2(9)	16.7(10)	14.5(9)	-0.4(7)	2.3(7)	-0.3(7)
C6	12.3(9)	21.3(10)	13.3(9)	1.5(7)	1.9(7)	0.4(8)
C7	13.6(9)	20.2(10)	18.1(10)	1.6(8)	2.3(7)	-1.0(8)
C8	19.5(10)	18.9(10)	18.3(10)	-0.2(8)	2.7(8)	2.2(8)
C9	15.7(9)	27.4(11)	18.0(10)	-2.4(8)	3.9(7)	2.8(8)
C10	15.7(10)	26.7(11)	16.7(10)	-1.9(8)	3.3(7)	-3.1(8)
C11	12.0(9)	19.8(10)	15.1(9)	0.2(7)	5.2(7)	-2.0(7)
C12	20.4(10)	15.5(10)	23.0(11)	-0.2(8)	5.6(8)	0.3(8)
C13	21.0(10)	21.3(11)	23.5(11)	3.7(8)	1.5(8)	3.7(8)
C14	14.9(9)	26.6(11)	20.6(10)	-0.1(8)	2.4(8)	-0.8(8)
C15	18.4(10)	19.7(10)	22.0(11)	-3.1(8)	4.4(8)	-1.0(8)
C16	16.8(9)	17.7(10)	20.8(10)	1.5(8)	4.5(8)	2.8(8)
C17	14.9(9)	16.3(10)	15.3(9)	-0.1(7)	4.3(7)	-1.5(7)
C18	16.8(9)	21.9(10)	17.1(10)	-1.3(8)	5.7(7)	1.8(8)
C19	15.7(9)	25.4(11)	18.5(10)	-1.8(8)	6.4(7)	0.2(8)
C20	19.6(10)	23.7(11)	12.4(9)	-1.1(8)	2.2(7)	-4.6(8)
C21	20.4(10)	18.4(10)	22.8(11)	1.4(8)	5.8(8)	2.4(8)
C22	15.1(9)	20.4(11)	24.3(11)	2.5(8)	7.7(8)	2.9(8)
C23	24.2(11)	26.6(12)	20.4(11)	-0.2(9)	6.7(8)	-6.0(9)
N1	12.1(8)	15.8(8)	20.9(9)	2.2(7)	3.9(6)	-0.7(6)
N2	13.0(8)	17.7(9)	15.9(8)	1.8(6)	3.2(6)	0.4(6)
N3	12.4(8)	19.9(9)	15.4(8)	-1.5(6)	4.9(6)	0.1(6)
O1	17.6(7)	27.1(8)	32.1(9)	-8.7(7)	1.4(6)	-2.0(6)
O2	28.2(8)	22.0(8)	32.1(9)	6.0(6)	13.4(7)	-1.3(6)
O3	23.8(8)	29.5(9)	16.2(7)	-0.9(6)	4.3(6)	-8.2(6)
O4	32.1(8)	16.1(7)	27.1(8)	1.0(6)	14.5(6)	4.2(6)
S1	21.7(3)	14.7(3)	28.8(3)	2.67(19)	7.2(2)	1.80(18)
S2	13.0(2)	16.7(3)	21.8(3)	-1.27(18)	4.94(18)	-2.65(17)

S3 18.0(3) 15.9(3) 16.1(3) -0.92(17) 6.33(19) -1.63(18)

Table 4 Bond Lengths for 639.

Atom	Atom	Length/Å	Atom	Atom	Length/Å
C1	C2	1.372(3)	C12	C13	1.391(3)
C1	N1	1.393(3)	C13	C14	1.384(3)
C1	S1	1.733(2)	C14	C15	1.391(3)
C2	N2	1.383(3)	C15	C16	1.384(3)
C2	N3	1.411(2)	C17	C18	1.393(3)
C3	C6	1.462(3)	C17	C22	1.392(3)
C3	N1	1.366(3)	C17	S3	1.758(2)
C3	N2	1.313(3)	C18	C19	1.386(3)
C4	S1	1.811(2)	C19	C20	1.389(3)
C5	C6	1.398(3)	C20	C21	1.399(3)
C5	C10	1.384(3)	C20	C23	1.508(3)
C5	S2	1.765(2)	C21	C22	1.375(3)
C6	C7	1.381(3)	N1	S2	1.7007(17)
C7	C8	1.396(3)	N3	S3	1.6560(16)
C8	C9	1.392(3)	O1	S2	1.4245(16)
C9	C10	1.387(3)	O2	S2	1.4227(16)
C11	C12	1.390(3)	O3	S3	1.4317(16)
C11	C16	1.392(3)	O4	S3	1.4289(15)
C11	N3	1.443(2)			

Table 5 Bond Angles for 639.

Atom	Atom	Atom	Angle/°	Atom	Atom	Atom	Angle/°
C2	C1	N1	102.86(17)	C22	C17	S3	119.52(15)
C2	C1	S1	131.24(16)	C19	C18	C17	118.23(19)
N1	C1	S1	125.86(15)	C18	C19	C20	121.76(19)
C1	C2	N2	113.11(17)	C19	C20	C21	118.63(19)
C1	C2	N3	125.13(18)	C19	C20	C23	121.42(19)
N2	C2	N3	121.69(17)	C21	C20	C23	119.9(2)
N1	C3	C6	111.78(17)	C22	C21	C20	120.7(2)
N2	C3	C6	135.82(19)	C21	C22	C17	119.62(18)
N2	C3	N1	112.38(18)	C1	N1	S2	136.97(15)
C6	C5	S2	112.20(15)	C3	N1	C1	107.98(16)
C10	C5	C6	122.74(19)	C3	N1	S2	114.96(14)
C10	C5	S2	125.04(16)	C3	N2	C2	103.65(16)
C5	C6	C3	110.59(18)	C2	N3	C11	118.01(15)
C7	C6	C3	129.83(18)	C2	N3	S3	120.04(13)
C7	C6	C5	119.54(18)	C11	N3	S3	121.95(13)

C6	C7	C8	118.53(19)	C1	S1	C4	100.66(11)
C9	C8	C7	121.0(2)	N1	S2	C5	90.47(9)
C10	C9	C8	121.05(19)	O1	S2	C5	113.20(9)
C5	C10	C9	117.13(19)	O1	S2	N1	108.60(9)
C12	C11	C16	120.30(19)	O2	S2	C5	112.25(9)
C12	C11	N3	120.84(18)	O2	S2	N1	109.31(9)
C16	C11	N3	118.76(18)	O2	S2	O1	119.10(10)
C11	C12	C13	119.0(2)	N3	S3	C17	103.48(9)
C14	C13	C12	121.0(2)	O3	S3	C17	110.53(9)
C13	C14	C15	119.51(19)	O3	S3	N3	104.81(9)
C16	C15	C14	120.1(2)	O4	S3	C17	107.79(9)
C15	C16	C11	120.00(19)	O4	S3	N3	109.27(9)
C18	C17	S3	119.44(16)	O4	S3	O3	119.75(10)
C22	C17	C18	121.04(19)				

Table 6 Torsion Angles for 639.

A	B	C	D	Angle/°	A	B	C	D	Angle/°
C1	C2	N2	C3	-0.1(2)	C16	C11	C12	C13	-1.4(3)
C1	C2	N3	C11	104.0(2)	C16	C11	N3	C2	64.2(2)
C1	C2	N3	S3	-75.8(2)	C16	C11	N3	S3	-116.10(18)
C1	N1	S2	C5	-176.1(2)	C17	C18	C19	C20	0.1(3)
C1	N1	S2	O1	69.1(2)	C18	C17	C22	C21	1.2(3)
C1	N1	S2	O2	-62.3(2)	C18	C17	S3	N3	-131.56(16)
C2	C1	N1	C3	1.0(2)	C18	C17	S3	O3	116.70(17)
C2	C1	N1	S2	177.21(16)	C18	C17	S3	O4	-15.88(19)
C2	C1	S1	C4	100.3(2)	C18	C19	C20	C21	1.0(3)
C2	N3	S3	C17	-118.97(16)	C18	C19	C20	C23	-177.18(19)
C2	N3	S3	O3	-3.10(18)	C19	C20	C21	C22	-0.9(3)
C2	N3	S3	O4	126.41(16)	C20	C21	C22	C17	-0.2(3)
C3	C6	C7	C8	177.38(19)	C22	C17	C18	C19	-1.2(3)
C3	N1	S2	C5	-0.09(15)	C22	C17	S3	N3	49.30(18)
C3	N1	S2	O1	-114.83(15)	C22	C17	S3	O3	-62.44(18)
C3	N1	S2	O2	113.75(15)	C22	C17	S3	O4	164.98(16)
C5	C6	C7	C8	-0.2(3)	C23	C20	C21	C22	177.26(19)
C6	C3	N1	C1	177.65(15)	N1	C1	C2	N2	-0.6(2)
C6	C3	N1	S2	0.5(2)	N1	C1	C2	N3	-177.55(17)
C6	C3	N2	C2	-177.7(2)	N1	C1	S1	C4	-82.62(19)
C6	C5	C10	C9	-0.2(3)	N1	C3	C6	C5	-0.7(2)
C6	C5	S2	N1	-0.36(15)	N1	C3	C6	C7	-178.5(2)
C6	C5	S2	O1	110.16(15)	N1	C3	N2	C2	0.8(2)
C6	C5	S2	O2	-111.50(15)	N2	C2	N3	C11	-72.8(2)

C6	C7	C8	C9	0.2(3)	N2	C2	N3	S3	107.47(19)
C7	C8	C9	C10	-0.2(3)	N2	C3	C6	C5	177.7(2)
C8	C9	C10	C5	0.2(3)	N2	C3	C6	C7	-0.1(4)
C10	C5	C6	C3	-177.80(18)	N2	C3	N1	C1	-1.2(2)
C10	C5	C6	C7	0.2(3)	N2	C3	N1	S2	-178.31(13)
C10	C5	S2	N1	178.08(18)	N3	C2	N2	C3	177.01(17)
C10	C5	S2	O1	-71.40(19)	N3	C11	C12	C13	174.91(18)
C10	C5	S2	O2	66.94(19)	N3	C11	C16	C15	-173.97(18)
C11	C12	C13	C14	-0.6(3)	S1	C1	C2	N2	176.99(15)
C11	N3	S3	C17	61.29(17)	S1	C1	C2	N3	0.0(3)
C11	N3	S3	O3	177.16(16)	S1	C1	N1	C3	-176.75(15)
C11	N3	S3	O4	-53.33(18)	S1	C1	N1	S2	-0.5(3)
C12	C11	C16	C15	2.5(3)	S2	C5	C6	C3	0.7(2)
C12	C11	N3	C2	-112.3(2)	S2	C5	C6	C7	178.70(15)
C12	C11	N3	S3	67.5(2)	S2	C5	C10	C9	-178.51(15)
C12	C13	C14	C15	1.7(3)	S3	C17	C18	C19	179.69(15)
C13	C14	C15	C16	-0.6(3)	S3	C17	C22	C21	-179.63(16)
C14	C15	C16	C11	-1.4(3)					

Table 7 Hydrogen Atom Coordinates ($\text{\AA} \times 10^4$) and Isotropic Displacement Parameters ($\text{\AA}^2 \times 10^3$) for 639.

Atom	x	y	z	U(eq)
H4A	4699.18	5572.2	9136.99	48
H4B	3488.76	5257.63	9474.55	48
H4C	3636.06	6210.08	9187.47	48
H7	4702.19	1342.07	7217.55	21
H8	6543.3	802.09	6887.28	23
H9	8153.46	1687.33	6754.29	24
H10	7965.74	3142.21	6934.03	24
H12	-207.25	4871.54	6543.92	23
H13	-1533.71	4640.32	4920.95	27
H14	-1681.51	3323.16	4120.01	25
H15	-558.51	2204.58	4985.25	24
H16	724.5	2415.59	6628.07	22
H18	-1364.75	3934.89	9507.62	22
H19	-2536.04	2801.88	9876.83	23
H21	28.13	1187.61	9273.49	24
H22	1209.99	2303.66	8905.13	23
H23A	-2813.45	1329.1	10159.68	35
H23B	-1687.12	725.64	10231.57	35
H23C	-2535.66	891.51	9113.27	35

REFERENCES

- [1] a) A. Fürstner, P. W. Davies, *Angew. Chem. Int. Ed.* **2007**, *46*, 3410-3449, b) G. Dequierez, V. Pons, P. Dauban, *Angew. Chem. Int. Ed.* **2012**, *51*, 7384-7395.
- [2] a) C. G. Espino, P. M. Wehn, J. Chow, J. Du Bois, *J. Am. Chem. Soc.* **2001**, *123*, 6935-6936, b) C. G. Espino, J. Du Bois, *Angew. Chem. Int. Ed.* **2001**, *40*, 598-600.
- [3] a) H. Lebel, K. Huard, S. Lectard, *J. Am. Chem. Soc.* **2005**, *127*, 14198-14199, b) K. Huard, H. Lebel, *Chem-Eur. J.* **2008**, *14*, 6222-6230.
- [4] K. A. Parker, W. Chang, *Org. Lett.* **2005**, *7*, 1785-1788.
- [5] A. R. Thornton, S. B. Blakey, *J. Am. Chem. Soc.* **2008**, *130*, 5020-5021.
- [6] A. R. Thornton, V. I. Martin, S. B. Blakey, *J. Am. Chem. Soc.* **2009**, *131*, 2434-2435.
- [7] N. Mace, A. R. Thornton, S. B. Blakey, *Angew. Chem.* **2013**, *125*, 5948-5951.
- [8] C.-Q. Wang, Y. Zhang, C. Feng, *Angew. Chem. Int. Ed.* **2017**, *56*, 14918-14922.
- [9] D. J. Gorin, F. D. Toste, *Nature* **2007**, *446*, 395-403.
- [10] a) E. Jiménez-Núñez, A. M. Echavarren, *Chem. Rev.* **2008**, *108*, 3326-3350, b) V. Michelet, P. Y. Toullec, J.-P. Genêt, *Angew. Chem. Int. Ed.* **2008**, *47*, 4268-4315, c) A. Corma, A. Leyva-Pérez, M. J. Sabater, *Chem. Rev.* **2011**, *111*, 1657-1712, d) F. López, J. L. Mascareñas, *Beilstein. J. Org. Chem.* **2011**, *7*, 1075-1094, e) H. C. Shen, *Tetrahedron* **2008**, *64*, 7847-7870.
- [11] a) D. Garayalde, C. Nevado, *ACS. Catal.* **2012**, *2*, 1462-1479, b) W. Debrouwer, T. S. A. Heugebaert, B. I. Roman, C. V. Stevens, *Adv. Synth. Catal.* **2015**, *357*, 2975-3006, c) F. López, J. L. Mascareñas, *Beilstein. J. Org. Chem.* **2013**, *9*, 2250-2264, d) B. Ranieri, I. Escofet, A. M. Echavarren, *Org. Biomol. Chem.* **2015**, *13*, 7103-7118.
- [12] a) D. Pflästerer, A. S. K. Hashmi, *Chem. Soc. Rev.* **2016**, *45*, 1331-1367, b) R. Dorel, A. M. Echavarren, *Chem. Rev.* **2015**, *115*, 9028-9072, c) Y. Zhang, T. Luo, Z. Yang, *Nat. Prod. Rep.* **2014**, *31*, 489-503, d) B. Alcaide, P. Almendros, *Accounts. Chem. Res.* **2014**, *47*, 939-952, e) L. Zhang, *Accounts. Chem. Res.* **2014**, *47*, 877-888, f) A. Fürstner, *Accounts. Chem. Res.* **2014**, *47*, 925-938, g) C. Obradors, A. M. Echavarren, *Chem. Commun.* **2014**, *50*, 16-28, h) A. S. K. Hashmi, M. Rudolph, *Chem. Soc. Rev.* **2008**, *37*, 1766-1775, i) Z. Zhang, M. Shi, *Chem-Eur. J.* **2010**, *16*, 7725-7729.
- [13] D. J. Gorin, N. R. Davis, F. D. Toste, *J. Am. Chem. Soc.* **2005**, *127*, 11260-11261.
- [14] Z.-Y. Yan, Y. Xiao, L. Zhang, *Angew. Chem. Int. Ed.* **2012**, *51*, 8624-8627.
- [15] C. Gronnier, G. Boissonnat, F. Gagosz, *Org. Lett.* **2013**, *15*, 4234-4237.
- [16] Y. Tokimizu, S. Oishi, N. Fujii, H. Ohno, *Org. Lett.* **2014**, *16*, 3138-3141.

- [17] A. Wetzel, F. Gagosz, *Angew. Chem. Int. Ed.* **2011**, *50*, 7354-7358.
- [18] B. Lu, Y. Luo, L. Liu, L. Ye, Y. Wang, L. Zhang, *Angew. Chem. Int. Ed.* **2011**, *50*, 8358-8362.
- [19] N. Li, T.-Y. Wang, L.-Z. Gong, L. Zhang, *Chem-Eur. J.* **2015**, *21*, 3585-3588.
- [20] C. Li, L. Zhang, *Org. Lett.* **2011**, *13*, 1738-1741.
- [21] P. W. Davies, A. Cremonesi, L. Dumitrescu, *Angew. Chem. Int. Ed.* **2011**, *50*, 8931-8935.
- [22] A. D. Gillie, R. J. Reddy, P. W. Davies, *Adv. Synth. Catal.* **2016**, *358*, 226-239.
- [23] a) G. Evano, B. Michelet, C. Zhang, *CR. Chim.* **2017**, *20*, 648-664, b) F. Pan, C. Shu, L.-W. Ye, *Org. Biomol. Chem.* **2016**, *14*, 9456-9465, c) G. Evano, N. Blanchard, G. Compain, A. Coste, C. S. Demmer, W. Gati, C. Guissart, J. Heimbürger, N. Henry, K. Jouvin, G. Karthikeyan, A. Laouiti, M. Lecomte, A. Martin-Mingot, B. Métayer, B. Michelet, A. Nitelet, C. Theunissen, S. Thibaudeau, J. Wang, M. Zarca, C. Zhang, *Chem. Lett.* **2016**, *45*, 574-585, d) X.-N. Wang, H.-S. Yeom, L.-C. Fang, S. He, Z.-X. Ma, B. L. Kedrowski, R. P. Hsung, *Accounts. Chem. Res.* **2014**, *47*, 560-578, e) G. Evano, A. Coste, K. Jouvin, *Angew. Chem. Int. Ed.* **2010**, *49*, 2840-2859, f) K. A. DeKorver, H. Li, A. G. Lohse, R. Hayashi, Z. Lu, Y. Zhang, R. P. Hsung, *Chem. Rev.* **2010**, *110*, 5064-5106.
- [24] M. Garzón, P. W. Davies, *Org. Lett.* **2014**, *16*, 4850-4853.
- [25] a) S. K. Pawar, R. L. Sahani, R.-S. Liu, *Chem-Eur. J.* **2015**, *21*, 10843-10850, b) Y. Wu, L. Zhu, Y. Yu, X. Luo, X. Huang, *J. Org. Chem.* **2015**, *80*, 11407-11416, c) C. Shu, Y.-H. Wang, B. Zhou, X.-L. Li, Y.-F. Ping, X. Lu, L.-W. Ye, *J. Am. Chem. Soc.* **2015**, *137*, 9567-9570, d) L. Zhu, Y. Yu, Z. Mao, X. Huang, *Org. Lett.* **2015**, *17*, 30-33.
- [26] A.-H. Zhou, Q. He, C. Shu, Y.-F. Yu, S. Liu, T. Zhao, W. Zhang, X. Lu, L.-W. Ye, *Chem. Sci.* **2015**, *6*, 1265-1271.
- [27] H. Jin, L. Huang, J. Xie, M. Rudolph, F. Rominger, A. S. K. Hashmi, *Angew. Chem. Int. Ed.* **2016**, *55*, 794-797.
- [28] R. L. Sahani, R.-S. Liu, *Angew. Chem. Int. Ed.* **2017**, *56*, 12736-12740.
- [29] J. González, J. Santamaría, Á. L. Suárez-Sobrino, A. Ballesteros, *Adv. Synth. Catal.* **2016**, *358*, 1398-1403.
- [30] M. Chen, N. Sun, H. Chen, Y. Liu, *Chem. Commun.* **2016**, *52*, 6324-6327.
- [31] Z. Zeng, H. Jin, J. Xie, B. Tian, M. Rudolph, F. Rominger, A. S. K. Hashmi, *Org. Lett.* **2017**, *19*, 1020-1023.
- [32] W. Xu, G. Wang, N. Sun, Y. Liu, *Org. Lett.* **2017**, *19*, 3307-3310.
- [33] a) Z. Jin, *Nat. Prod. Rep.* **2011**, *28*, 1143-1191, b) L. Costantino, D. Barlocco, *Curr. Med. Chem.* **2006**, *13*, 65-85.

- [34] a) M. M. Heravi, M. Daraie, V. Zadsirjan, *Mol. Divers.* **2015**, *19*, 577-623, b) J. C. Lee, J. T. Laydon, P. C. McDonnell, T. F. Gallagher, S. Kumar, D. Green, D. McNulty, M. J. Blumenthal, J. R. Keys, S. W. Land vatter, J. E. Strickler, M. M. McLaughlin, I. R. Siemens, S. M. Fisher, G. P. Livi, J. R. White, J. L. Adams, P. R. Young, *Nature* **1994**, *372*, 739-746, c) M. Antolini, A. Bozzoli, C. Ghiron, G. Kennedy, T. Rossi, A. Ursini, *Bioorg. Med. Chem. Lett.* **1999**, *9*, 1023-1028, d) H. J. Cho, H. Y. Gee, K.-H. Baek, S.-K. Ko, J.-M. Park, H. Lee, N.-D. Kim, M. G. Lee, I. Shin, *J. Am. Chem. Soc.* **2011**, *133*, 20267-20276.
- [35] J.-H. Choi, N. Abe, H. Tanaka, K. Fushimi, Y. Nishina, A. Morita, Y. Kiriwa, R. Motohashi, D. Hashizume, H. Koshino, H. Kawagishi, *J. Agr. Food. Chem.* **2010**, *58*, 9956-9959.
- [36] J. Dupont, R. F. de Souza, P. A. Z. Suarez, *Chem. Rev.* **2002**, *102*, 3667-3692.
- [37] W. Lin, L. Long, L. Yuan, Z. Cao, B. Chen, W. Tan, *Org. Lett.* **2008**, *10*, 5577-5580.
- [38] W. A. Herrmann, *Angew. Chem. Int. Ed.* **2002**, *41*, 1290-1309.
- [39] R. Carceller, J. L. García-Navío, M. L. Izquierdo, J. Alvarez-Builla, *Tetrahedron. Lett.* **1993**, *34*, 2019-2020.
- [40] a) Q. Chao, K. G. Sprankle, R. M. Grotzfeld, A. G. Lai, T. A. Carter, A. M. Velasco, R. N. Gunawardane, M. D. Cramer, M. F. Gardner, J. James, P. P. Zarrinkar, H. K. Patel, S. S. Bhagwat, *J. Mater. Chem.* **2009**, *52*, 7808-7816, b) A. Furlan, F. Colombo, A. Kover, N. Issaly, C. Tintori, L. Angeli, V. Leroux, S. Letard, M. Amat, Y. Asses, B. Maigret, P. Dubreuil, M. Botta, R. Dono, J. Bosch, O. Piccolo, D. Passarella, F. Maina, *Eur. J. Med. Chem.* **2012**, *47*, 239-254, c) X. Zhang, J. Jia, C. Ma, *Org. Biomol. Chem.* **2012**, *10*, 7944-7948, d) M. S. Christodoulou, F. Colombo, D. Passarella, G. Ieronimo, V. Zuco, M. De Cesare, F. Zunino, *Bioorgan. Med. Chem.* **2011**, *19*, 1649-1657.
- [41] a) T. H. Al-Tel, R. A. Al-Qawasmeh, R. Zaarour, *Eur. J. Med. Chem.* **2011**, *46*, 1874-1881, b) M. Palkar, M. Noolvi, R. Sankangoud, V. Maddi, A. Gadad, G. Nargund Laxmi Venkat, *Arch. Pharm.* **2010**, *343*, 353-359.
- [42] G. Trapani, M. Franco, A. Latrofa, A. Reho, G. Liso, *Eur. J. Pharm. Sci.* **2001**, *14*, 209-216.
- [43] a) B. H. Yousefi, A. Drzezga, B. von Reutern, A. Manook, M. Schwaiger, H.-J. Wester, G. Henriksen, *ACS. Med. Chem. Lett.* **2011**, *2*, 673-677, b) B. H. Yousefi, A. Manook, A. Drzezga, B. v. Reutern, M. Schwaiger, H.-J. Wester, G. Henriksen, *J. Mater. Chem.* **2011**, *54*, 949-956.
- [44] B. A. Chalmers, S. Saha, T. Nguyen, J. McMurtrie, S. T. Sigurdsson, S. E. Bottle, K.-S. Masters, *Org. Lett.* **2014**, *16*, 5528-5531.
- [45] J. Wang, J. Li, Q. Zhu, *Org. Lett.* **2015**, *17*, 5336-5339.
- [46] S. Mishra, K. Monir, S. Mitra, A. Hajra, *Org. Lett.* **2014**, *16*, 6084-6087.
- [47] S. K. Guchhait, V. Chaudhary, *Org. Biomol. Chem.* **2014**, *12*, 6694-6705.
- [48] M. José Reyes, C. Burgos, M. Luisa Izquierdo, J. Alvarez-Builla, *Tetrahedron* **2004**, *60*, 1093-1097.

- [49] a) L. Li, X.-M. Chen, Z.-S. Wang, B. Zhou, X. Liu, X. Lu, L.-W. Ye, *ACS. Catal.* **2017**, *7*, 4004-4010, b) T. Wezeman, S. Zhong, M. Nieger, S. Bräse, *Angew. Chem. Int. Ed.* **2016**, *55*, 3823-3827, c) L. Chen, Y.-M. Cui, Z. Xu, J. Cao, Z.-J. Zheng, L.-W. Xu, *Chem. Commun.* **2016**, *52*, 11131-11134, d) R. Rey-Rodriguez, G. Grelhier, L. Habert, P. Retailleau, B. Darses, I. Gillaizeau, P. Dauban, *J. Org. Chem.* **2017**, *82*, 11897-11902, e) S. Suzuki, T. Asako, K. Itami, J. Yamaguchi, *Org. Biomol. Chem.* **2018**, *16*, 3771-3776, f) C. Theunissen, B. Métayer, M. Lecomte, N. Henry, H.-C. Chan, G. Compain, P. Gérard, C. Bachmann, N. Mokhtari, J. Marrot, A. Martin-Mingot, S. Thibaudeau, G. Evano, *Org. Biomol. Chem.* **2017**, *15*, 4399-4416, g) G. Duret, R. Quinlan, R. E. Martin, P. Bissere, M. Neuburger, V. Gandon, N. Blanchard, *Org. Lett.* **2016**, *18*, 1610-1613, h) G. Wang, X. You, Y. Gan, Y. Liu, *Org. Lett.* **2017**, *19*, 110-113.
- [50] Y. Zhang, R. P. Hsung, M. R. Tracey, K. C. M. Kurtz, E. L. Vera, *Org. Lett.* **2004**, *6*, 1151-1154.
- [51] J. R. Dunetz, R. L. Danheiser, *Org. Lett.* **2003**, *5*, 4011-4014.
- [52] A. Coste, G. Karthikeyan, F. Couty, G. Evano, *Angew. Chem. Int. Ed.* **2009**, *48*, 4381-4385.
- [53] T. Hamada, X. Ye, S. S. Stahl, *J. Am. Chem. Soc.* **2008**, *130*, 833-835.
- [54] S. J. Mansfield, C. D. Campbell, M. W. Jones, E. A. Anderson, *Chem. Commun.* **2015**, *51*, 3316-3319.
- [55] Y. Tu, X. Zeng, H. Wang, J. Zhao, *Org. Lett.* **2018**, *20*, 280-283.
- [56] H. Harkat, S. Borghèse, M. D. Nigris, S. Kiselev, V. Bénéteau, P. Pale, *Adv. Synth. Catal.* **2014**, *356*, 3842-3848.
- [57] K. Jouvin, F. Couty, G. Evano, *Org. Lett.* **2010**, *12*, 3272-3275.
- [58] B. Witulski, T. Stengel, *Angew. Chem. Int. Ed.* **1998**, *37*, 489-492.
- [59] N. B. Desai, N. McKelvie, F. Ramirez, *J. Am. Chem. Soc.* **1962**, *84*, 1745-1747.
- [60] a) X.-N. Wang, G. N. Winston-McPherson, M. C. Walton, Y. Zhang, R. P. Hsung, K. A. DeKorver, *J. Org. Chem.* **2013**, *78*, 6233-6244, b) K. A. DeKorver, W. L. Johnson, Y. Zhang, R. P. Hsung, H. Dai, J. Deng, A. G. Lohse, Y.-S. Zhang, *J. Org. Chem.* **2011**, *76*, 5092-5103, c) K. A. DeKorver, X.-N. Wang, M. C. Walton, R. P. Hsung, *Org. Lett.* **2012**, *14*, 1768-1771.
- [61] a) S. Couty, C. Meyer, J. Cossy, *Tetrahedron* **2009**, *65*, 1809-1832, b) S. Couty, C. Meyer, J. Cossy, *Angew. Chem. Int. Ed.* **2006**, *45*, 6726-6730.
- [62] N. S. Nandurkar, M. D. Bhor, S. D. Samant, B. M. Bhanage, *Ind. Eng. Chem. Res.* **2007**, *46*, 8590-8596.
- [63] Y. Yu, G. Chen, L. Zhu, Y. Liao, Y. Wu, X. Huang, *J. Org. Chem.* **2016**, *81*, 8142-8154.
- [64] M. Garzón, P. W. Davies, *Org. Lett.* **2014**, *16*, 4850-4853.
- [65] M. Garzón, E. M. Arce, R. J. Reddy, P. W. Davies, *Adv. Synth. Catal.* **2017**, *359*, 1837-1843.

- [66] a) A. Ziyaei Halimehjani, M. A. Alaei, F. Soleymani Movahed, N. Jomeh, M. R. Saidi, *J. Sulfur. Chem.* **2016**, *37*, 529-536, b) S. Golota, I. Sydorenko, R. Surma, O. Karpenko, A. Gzella, R. Lesyk, *Synthetic Communications*. **2017**, *47*, 1071-1076, c) M. Sarkis, D. N. Tran, S. Kolb, M. A. Miteva, B. O. Villoutreix, C. Garbay. E. Braud, *Bioorg. Med. Chem. Lett* **2012**, *22*, 7345-7350, d) G. Solene, P. Ludovic, C. Francois, D. Emilie, B. Helene, G. Remy Le, C. Anne, M. Laurent, B. Jean-Pierre, *Current Microwave Chemistry* **2014**, *1*, 33-40, e) L.-F. Yu, Y.-Y. Li, M.-B. Su, M. Zhang, W. Zhang, L.-N. Zhang, T. Pang, R.-T. Zhang, B. Liu, J.-Y. Li, J. Li, F.-J. Nan, *ACS. Med. Chem. Lett.* **2013**, *4*, 475-480, f) N. G. Aher, B. Kafle, H. Cho, *B. Kor. Chem. Soc.* **2013**, *34*, 1275-1277.
- [67] a) J. Senkiv, N. Finiuk, D. Kaminsky, D. Havrylyuk, M. Wojtyra, I. Kril, A. Gzella, R. Stoika, R. Lesyk, *Eur. J. Med. Chem.* **2016**, *117*, 33-46, b) I. Stawoska, W. Tejchman, O. Mazuryk, A. Lyčka, P. Nowak-Sliwinska, E. Żesławska, W. Nitek, A. Kania, *J. Heterocyclic. Chem.* **2017**, *54*, 2889-2897, c) D. Havrylyuk, B. Zimenkovsky, O. Vasylenko, L. Zaprutko, A. Gzella, R. Lesyk, *Eur. J. Med. Chem.* **2009**, *44*, 1396-1404.
- [68] M. M. M. El-Miligy, A. A. Hazzaa, H. El-Messmary, R. A. Nassra, S. A. M. El-Hawash, *Bioorg. Chem.* **2017**, *72*, 102-115.
- [69] a) H. Kim, S. J. Cho, M. Yoo, S. K. Kang, K. R. Kim, H. H. Lee, J. S. Song, S. D. Rhee, W. H. Jung, J. H. Ahn, J.-K. Jung, K.-Y. Jung, *Bioorg. Med. Chem. Lett.* **2017**, *27*, 5213-5220, b) D. D. Subhedar, M. H. Shaikh, B. B. Shingate, L. Nawale, D. Sarkar, V. M. Khedkar, F. A. Kalam Khan, J. N. Sangshetti, *Eur. J. Med. Chem.* **2017**, *125*, 385-399.
- [70] M. Krátký, J. Vinšová, J. Stolaříková, *Bioorgan. Med. Chem.* **2017**, *25*, 1839-1845.
- [71] M. J. Robertson, A. Horatscheck, S. Sauer, L. von Kleist, J. R. Baker, W. Stahlschmidt, M. Nazare, A. Whiting, N. Chau, P. J. Robinson, V. Haucke, A. McCluskey, *Org. Biomol. Chem.* **2016**, *14*, 11266-11278.
- [72] J. Huang, R. Sun, S. Feng, J. He, F. Fei, H. Gao, Y. Zhao, Y. Zhang, H. Gu, J. Aa, G. Wang, *J. Chromatogr. B.* **2017**, *1055-1056*, 98-103.
- [73] a) P. Naik, A. Planchat, Y. Pellegrin, F. Odobel, A. Vasudeva Adhikari, *Sol. Energy.* **2017**, *157*, 1064-1073, b) S. S. Soni, K. B. Fadadu, J. V. Vaghasiya, B. G. Solanki, K. K. Sonigara, A. Singh, D. Das, P. K. Iyer, *J. Mater. Chem. A.* **2015**, *3*, 21664-21671, c) G. Saritha, J. J. Wu, S. Anandan, *Org. Electron.* **2016**, *37*, 326-335.
- [74] M. Yan, J. Zhao, D. Sun, W. Sun, B. Zhang, W. Deng, D. Zhang, L. Wang, *Tetrahedron* **2017**, *73*, 3355-3362.
- [75] a) C. A. McLellan, B. M. Vincent, N. V. Solis, A. K. Lancaster, L. B. Sullivan, C. L. Hartland, W. Youngsaye, S. G. Filler, L. Whitesell, S. Lindquist, *Nat. Chem. Biol.* **2017**, *14*, 135-141, b) C. Bathula, S. Ghosh, S. Hati, S. Tripathy, S. Singh, S. Chakrabarti, S. Sen, *RSC. Adv.* **2017**, *7*, 3563-3572, c) F. Song, L. Cui, J. Piao, H. Liang, H. Si, Y. Duan, H. Zhai, *Chem. Biol. Drug. Des.* **2017**, *90*, 535-544, d) F. Wu, H. Jiang, B. Zheng, M. Kogiso, Y. Yao, C. Zhou, X.-N. Li, Y. Song, *J. Mater. Chem.* **2015**, *58*, 6899-6908, e) M. K. Thorson, R. M. Van Wagoner, M. K. Harper, C. M. Ireland, T. Majtan, J. P. Kraus, A. M. Barrios, *Bioorg. Med. Chem. Lett.* **2015**, *25*, 1064-1066, f) Y. Zheng, J. Zhou, S. M. Cooper, C. Opoku-Temeng, A. M. De Brito, H. O. Sintim, *Tetrahedron* **2016**, *72*, 3554-3558, g) M. R. Bull, J. A. Spicer, K. M. Huttunen, W. A. Denny, A. Ciccone, K. A. Browne, J. A. Trapani, N. A. Helsby, *Eur. J. Drug. Metab. Ph.* **2015**, *40*, 417-425, h) Y. Zheng, J. Zhou, D. A. Sayre, H. O. Sintim, *Chem. Commun.*

- 2014**, 50, 11234-11237, i) H. R. Kim, H. J. Lee, Y. J. Choi, Y. J. Park, Y. Woo, S. J. Kim, M. H. Park, H. W. Lee, P. Chun, H. Y. Chung, H. R. Moon, *MedChemComm* **2014**, 5, 1410-1417.
- [76] a) V. Singh, A. Singh, G. Singh, R. K. Verma, R. Mall, *Med. Chem. Res.* **2018**, 27, 735-743, b) H. Abe, Y. Yamazaki, C. Sakashita, I. Momose, T. Watanabe, M. Shibasaki, *Chem. Pharm. Bull.* **2016**, 64, 982-987, c) S. Q. Tang, Y. Y. I. Lee, D. S. Packiaraj, H. K. Ho, C. L. L. Chai, *Chem. Res. Toxicol.* **2015**, 28, 2019-2033, d) F. Erben, D. Michalik, H. Feist, D. Kleeblatt, M. Hein, A. Matin, J. Iqbal, P. Langer, *RSC. Adv.* **2014**, 4, 10879-10893, e) H. Yoshino, H. Sato, T. Shiraishi, K. Tachibana, T. Emura, A. Honma, N. Ishikura, T. Tsunenari, M. Watanabe, A. Nishimoto, R. Nakamura, T. Nakagawa, M. Ohta, N. Takata, K. Furumoto, K. Kimura, H. Kawata, *Bioorgan. Med. Chem.* **2010**, 18, 8150-8157.
- [77] a) B. Tang, A. Guan, Y. Zhao, J. Jiang, M. Wang, L. Zhou, *Chinese. J. Chem.* **2017**, 35, 1133-1140, b) Z. Yu, T. Bo, G. Aiying, W. Weiwei, Z. Zhenhua, W. Mingan, *Synthesis* **2017**, 49, 4663-4669, c) B. Tang, M. Yang, Y. Zhao, L. Kong, W. Wang, M. Wang, *Molecules* **2015**, 20, 13740-13752, d) J. Thanusu, V. Kanagarajan, M. Gopalakrishnan, *Bioorg. Med. Chem. Lett.* **2010**, 20, 713-717.
- [78] A. O. Yüce, G. Kardaş, *Corros. Sci.* **2012**, 58, 86-94.
- [79] L. Birzan, M. Cristea, C. C. Draghici, V. Tecuceanu, M. Maganu, A. Hanganu, A. C. Razus, G. O. Buica, E. M. Ungureanu, *Dyes. Pigments.* **2016**, 131, 246-255.
- [80] C. Li, M.-A. Plamont, I. Aujard, T. Le Saux, L. Jullien, A. Gautier, *Org. Biomol. Chem.* **2016**, 14, 9253-9261.
- [81] a) B. Rajarathinam, K. Kumaravel, G. Vasuki, *ACS. Comb. Sci.* **2017**, 19, 455-463, b) P. K. Chrysanthopoulos, P. Mujumdar, L. A. Woods, O. Dolezal, B. Ren, T. S. Peat, S.-A. Poulsen, *J. Mater. Chem.* **2017**, 60, 7333-7349, c) E. A. Lafayette, S. M. V. de Almeida, R. V. Cavalcanti Santos, J. F. de Oliveira, C. A. d. C. Amorim, R. M. F. da Silva, M. G. d. R. Pitta, I. d. R. Pitta, R. O. de Moura, L. B. de Carvalho Júnior, M. J. B. de Melo Rêgo, M. d. C. A. de Lima, *Eur. J. Med. Chem.* **2017**, 136, 511-522.
- [82] B. Zhong, L. Sun, H. Shi, J. Li, C. Chen, Z. Chen, *WO/2017/176812*, A61K 31/665 (2006.01), A61K 39/39 (2006.01), C07D 417/14 (2006.01) ed., **2006**.
- [83] N. Y. Bamaung, R. L. Bell, R. F. Clark, S. A. Erickson, S. D. Fidanze, R. D. Hubbard, R. A. Mantei, G. S. Sheppard, B. K. Sorensen, G. T. Wang, J. Wang, K. Sarris, *A61K31/425*, *A61P35/00*, *C07D513/04* ed., **2009**.
- [84] a) D. Zuev, V. M. Vrudhula, J. A. Michne, B. Dasgupta, S. S. Pin, X. S. Huang, D. Wu, Q. Gao, J. Zhang, M. T. Taber, J. E. Macor, G. M. Dubowchik, *Bioorganic Accounts of Chemical Research& Medicinal Chemistry Letters* **2010**, 20, 3669-3674, b) S. Grosse, C. Pillard, S. Massip, M. Marchivie, C. Jarry, P. Bernard, G. Guillaumet, *J. Org. Chem.* **2015**, 80, 8539-8551.
- [85] J.-P. Wu, J. Emeigh, D. A. Gao, D. R. Goldberg, D. Kuzmich, C. Miao, I. Potocki, K. C. Qian, R. J. Sorcek, D. D. Jeanfavre, K. Kishimoto, E. A. Mainolfi, G. Nabozny, C. Peng, P. Reilly, R. Rothlein, R. H. Sellati, J. R. Woska, S. Chen, J. A. Gunn, D. O'Brien, S. H. Norris, T. A. Kelly, *J. Mater. Chem.* **2004**, 47, 5356-5366.

- [86] a) J. Sire, G. Quérat, C. Esnault, S. Priet, *Retrovirology* **2008**, 5, 45, b) R. Olinski, M. Jurgowiak, T. Zaremba, *Mutat. Res-Rev. Mutat.* **2010**, 705, 239-245, c) R. L. Somerville, in *Encyclopedia of Genetics* (Ed.: J. H. Miller), Academic Press, New York, **2001**, pp. 2100-2101.
- [87] a) H. E. Krokan, P. Sætrom, P. A. Aas, H. S. Pettersen, B. Kavli, G. Slupphaug, *DNA Repair* **2014**, 19, 38-47, b) D. Saftic, M. Radic Stojkovic, B. Zinic, L. Glavas-Obrovac, M. Jukic, I. Piantanida, L.-M. Tumir, *New. J. Chem.* **2017**, 41, 13240-13252, c) E. C. Friedberg, *DNA Repair* **2016**, 37, A35-A39, d) T. V. Mishanina, E. M. Koehn, A. Kohen, *Bioorg. Chem.* **2012**, 43, 37-43, e) G. Burnstock, U. Krügel, M. P. Abbracchio, P. Illes, *Prog. Neurobiol.* **2011**, 95, 229-274.
- [88] a) K. Miura, H. Shima, N. Takebe, J. Rhie, K. Satoh, Y. Kakugawa, M. Satoh, M. Kinouchi, K. Yamamoto, Y. Hasegawa, M. Kawai, K. Kanazawa, T. Fujiya, M. Unno, R. Katakura, *Expert. Opin. Drug. Del.* **2017**, 14, 1355-1366, b) N. F. Smith, W. D. Figg, A. Sparreboom, *Drug. Develop. Res.* **2004**, 62, 233-253.
- [89] W. B. Parker, *Chem. Rev.* **2009**, 109, 2880-2893.
- [90] S. Jun, K. Yoshihiro, I. Eitatsu, N. Tsutomu, K. Chiaki, A01N43/90, C07D487/04, C07D498/04, C07D513/04, C07F7/08, (IPC1-7): A01N43/54, A01N43/90, C07D487/04, C07D498/04, C07D513/04 ed., **2000**.
- [91] I. Khodair Ahmed, *J. Heterocyclic. Chem.* **2009**, 39, 1153-1160.
- [92] A. Shaabani, A. Sarvary, S. Keshipour, A. H. Rezayan, R. Ghadari, *Tetrahedron* **2010**, 66, 1911-1914.
- [93] a) P. Chen, C.-X. Song, W.-S. Wang, X.-L. Yu, Y. Tang, *RSC. Adv.* **2016**, 6, 80055-80058, b) W.-S. Wang, P. Chen, Y. Tang, *Tetrahedron* **2017**, 73, 2731-2739, c) Y. Zhao, Y. Hu, X. Li, B. Wan, *Org. Biomol. Chem.* **2017**, 16, 3413-3417, d) Y. Zhao, Y. Hu, C. Wang, X. Li, B. Wan, *J. Org. Chem.* **2017**, 3935-3942, e) Y. Wang, L.-J. Song, X. Zhang, J. Sun, *Angew. Chem. Int. Ed.* **2016**, 55, 9704-9708.
- [94] F. Tibiletti, M. Simonetti, K. M. Nicholas, G. Palmisano, M. Parravicini, F. Imbesi, S. Tollari, A. Penoni, *Tetrahedron* **2010**, 66, 1280-1288.
- [95] E. Chatzopoulou, P. W. Davies, *Chem. Commun.* **2013**, 49, 8617-8619.
- [96] R. J. Reddy, M. P. Ball-Jones, P. W. Davies, *Angew. Chem. Int. Ed.* **2017**, 56, 13310-13313.
- [97] S. Ding, G. Jia, J. Sun, *Angew. Chem. Int. Ed.* **2014**, 53, 1877-1880.
- [98] X. Ye, J. Wang, S. Ding, S. Hosseyni, L. Wojtas, N. G. Akhmedov, X. Shi, *Chem-Eur. J.* **2017**, 23, 10506-10510.
- [99] I. Costa, M. Marín-Luna, M. G. Comesaña, O. N. Faza, C. Silva López, *ChemCatChem* **2016**, 8, 2387-2392.
- [100] G. Hilt, S. Lüers, K. Harms, *J. Org. Chem.* **2004**, 69, 624-630.

- [101] a) C. Savarin, J. Srogl, L. S. Liebeskind, *Org. Lett.* **2001**, 3, 91-93, b) A. Henke, J. Srogl, *Chem. Commun.* **2011**, 47, 4282-4284, c) L. Melzig, A. Metzger, P. Knochel, *Chem-Eur. J.* **2011**, 17, 2948-2956.
- [102] a) N. Riddell, W. Tam, *J. Org. Chem.* **2006**, 71, 1934-1937, b) S. You, W. Hao, M. Cai, *Synthetic Communications*. **2010**, 40, 1830-1836, c) Z. Yang, X. Chen, W. Kong, S. Xia, R. Zheng, F. Luo, G. Zhu, *Org. Biomol. Chem.* **2013**, 11, 2175-2185.
- [103] S. Y. Delavarenne, H. G. Viehe, *Tetrahedron. Lett.* **1969**, 10, 4761-4764.
- [104] a) T. Nakai, K. Tanaka, H. Setoi, N. Ishikawa, *B. Chem. Soc. Jpn.* **1977**, 50, 3069-3070, b) K. T. T. Nakai, N. Ishikawa, *Chem. Lett.* **1976**, 1263-1266.
- [105] T. Nakai, H. Setoi, Y. Kageyama, *Tetrahedron. Lett.* **1981**, 22, 4097-4100.
- [106] a) C. Jenny, H. Heimgartner, *Helv. Chim. Acta.* **1986**, 69, 174-183, b) K. Nørkjær, A. Senning, *Chem. Ber.* **1993**, 126, 73-77, c) R. Gompper, S. Mensch, G. Seybold, *Angew. Chem.* **1975**, 87, 711-712.
- [107] V. Girijavallabhan, C. Alvarez, F. G. Njoroge, *J. Org. Chem.* **2011**, 76, 6442-6446.
- [108] A. C. Oehlschlager, S. M. Singh, S. Sharma, *J. Org. Chem.* **1991**, 56, 3856-3861.
- [109] A. Gandini, *Prog. Polym. Sci.* **2013**, 38, 1-29.
- [110] G. Sabitha, B. V. S. Reddy, S. Abraham, J. S. Yadav, *Tetrahedron. Lett.* **1999**, 40, 1569-1570.
- [111] C. Kusturin, L. S. Liebeskind, H. Rahman, K. Sample, B. Schweitzer, J. Srogl, W. L. Neumann, *Org. Lett.* **2003**, 5, 4349-4352.
- [112] G. R. Fulmer, A. J. M. Miller, N. H. Sherden, H. E. Gottlieb, A. Nudelman, B. M. Stoltz, J. E. Bercaw, K. I. Goldberg, *Organometallics* **2010**, 29, 2176-2179.
- [113] B. T. Burlingham, T. S. Widlanski, *J. Am. Chem. Soc.* **2001**, 123, 2937-2945.
- [114] D. C. Johnson, T. S. Widlanski, *Org. Lett.* **2004**, 6, 4643-4646.
- [115] K. A. DeKorver, M. C. Walton, T. D. North, R. P. Hsung, *Org. Lett.* **2011**, 13, 4862-4865.
- [116] K. K. Park, J. J. Lee, J. Ryu, *Tetrahedron* **2003**, 59, 7651-7659.
- [117] E. J. Corey, P. L. Fuchs, *Tetrahedron. Lett.* **1972**, 13, 3769-3772.
- [118] A. Rosiak, W. Frey, J. Christoffers, *Eur. J. Org. Chem.* **2006**, 2006, 4044-4054.
- [119] J.-C. Poupon, A. A. Boezio, A. B. Charette, *Angew. Chem. Int. Ed.* **2006**, 45, 1415-1420.
- [120] E. N. Jacobsen, L. Deng, Y. Furukawa, L. E. Martínez, *Tetrahedron* **1994**, 50, 4323-4334.

- [121] K. C. Nicolaou, A. A. Shah, H. Korman, T. Khan, L. Shi, W. Worawalai, E. A. Theodorakis, *Angew. Chem. Int. Ed.* **2015**, *54*, 9203-9208.
- [122] C. D. Campbell, R. L. Greenaway, O. T. Holton, P. R. Walker, H. A. Chapman, C. A. Russell, G. Carr, A. L. Thomson, E. A. Anderson, *Chem-Eur. J.* **2015**, *21*, 12627-12639.
- [123] Y.-S. Feng, Z.-Q. Xu, L. Mao, F.-F. Zhang, H.-J. Xu, *Org. Lett.* **2013**, *15*, 1472-1475.
- [124] D. P. Gamblin, P. Garnier, S. J. Ward, N. J. Oldham, A. J. Fairbanks, B. G. Davis, *Org. Biomol. Chem.* **2003**, *1*, 3642-3644.
- [125] M. J. Barrett, G. F. Khan, P. W. Davies, R. S. Grainger, *Chem. Commun.* **2017**, *53*, 5733-5736.
- [126] X. Jin, K. Yamaguchi, N. Mizuno, *Chem. Commun.* **2012**, *48*, 4974-4976.
- [127] A. Mukherjee, R. B. Dateer, R. Chaudhuri, S. Bhunia, S. N. Karad, R.-S. Liu, *J. Am. Chem. Soc.* **2011**, *133*, 15372-15375.
- [128] K. H. Oh, J. G. Kim, J. K. Park, *Org. Lett.* **2017**, *19*, 3994-3997.
- [129] M. Betou, N. Kerisit, E. Meledje, Y. R. Leroux, C. Katan, J.-F. Halet, J.-C. Guillemin, Y. Trolez, *Chem-Eur. J.* **2014**, *20*, 9553-9557.
- [130] E. Rolli, M. Incerti, F. Brunoni, P. Vicini, A. Ricci, *Phytochemistry* **2012**, *74*, 159-165.
- [131] P. C. Fritch, G. McNaughton-Smith, G. S. Amato, J. F. Burns, C. W. Eargle, R. Roeloffs, W. Harrison, L. Jones, A. D. Wickenden, *J. Mater. Chem.* **2010**, *53*, 887-896.
- [132] A. Costales, M. Mathur, S. Ramurthy, J. Lan, S. Subramanian, R. Jain, G. Atallah, L. Setti, M. Lindvall, B. A. Appleton, E. Ornelas, P. Feucht, B. Warne, L. Doyle, S. E. Basham, I. Aronchik, A. B. Jefferson, C. M. Shafer, *Bioorg. Med. Chem. Lett.* **2014**, *24*, 1592-1596.
- [133] M. Córdoba, M. Galájov, M. L. Izquierdo, J. Alvarez-Builla, *Tetrahedron* **2013**, *69*, 2484-2493.
- [134] G. Burgy, T. Tahtouh, E. Durieu, B. Foll-Josselin, E. Limanton, L. Meijer, F. Carreaux, J.-P. Bazureau, *Eur. J. Med. Chem.* **2013**, *62*, 728-737.
- [135] V. Chazeau, M. Cussac, A. Boucherle, *Eur. J. Med. Chem.* **1992**, *27*, 615-625.
- [136] N. D. D'Angelo, S. F. Bellon, S. K. Booker, Y. Cheng, A. Coxon, C. Dominguez, I. Fellows, D. Hoffman, R. Hungate, P. Kaplan-Lefko, M. R. Lee, C. Li, L. Liu, E. Rainbeau, P. J. Reider, K. Rex, A. Siegmund, Y. Sun, A. S. Tasker, N. Xi, S. Xu, Y. Yang, Y. Zhang, T. L. Burgess, I. Dussault, T.-S. Kim, *J. Mater. Chem.* **2008**, *51*, 5766-5779.